APPENDIX B
Photochemical Modeling

Table of Contents

Table of Figures

Table of Tables

B Photochemical Modeling

B.1 Modeling Protocol and Attainment Demonstration

Modeling Protocol & Attainment Demonstration for the Sacramento Regional 2015 NAAQS 8-Hour Ozone Attainment and Reasonable Further Progress Plan

Prepared by
California Air Resources Board
Sacramento Metropolitan Air Quality Management District

Prepared for
United States Environmental Protection Agency Region IX

March 2023

Acronyms

ACM2 – Asymmetric Convective Model version 2

ADAM – Aerometric Data Analysis and Management

AQMIS – Air Quality and Meteorological Information System

ARB – Air Resources Board

BCs – Boundary Conditions

Calex – Research at the Nexus of Air Quality and Climate Change conducted in 2010

CAM-Chem – Community Atmosphere Model with Chemistry

CARB – California Air Resources Board

CARES – Carbonaceous Aerosols and Radiative Effects Study in 2010

CEPAM – California Emissions Projection Analysis Model

CESM2 – Community Earth System Model version 2

CMAQ Model – Community Multi-scale Air Quality Model

CTM – Chemical Transport Model

DV – Design Value

ICs – Initial Conditions

IOA – Index of Agreement

LAI – Leaf Area Index

MB – Mean Bias

MCIP – Meteorology-Chemistry Interface Processor

MCAB – Mountain Counties Air Basin

MDA8 – Maximum Daily Average 8-hour Ozone

ME – Mean Error

MEGAN – Model of Emissions of Gases and Aerosols

MFB – Mean Fractional Bias

MFE – Mean Fractional Error

MODIS – Moderate Resolution Imaging Spectroradiometer

NAAQS – National Ambient Air Quality Standards

NASA – National Aeronautics and Space Administration

NARR - North American Regional Reanalysis

NCAR – National Center for Atmospheric Research

NMB – Normalized Mean Bias

NME – Normalized Mean Error

NOAA - National Oceanic and Atmospheric Administration

NO_X – Oxides of nitrogen

OGV – Ocean Going Vessels

R – Correlation coefficient

R^2 – R-squared/Coefficient of determination

RH – Relative Humidity

RMSE – Root Mean Square Error

ROG – Reactive Organic Gases

RRF – Relative Response Factor

SAPRC – Statewide Air Pollution Research Center

SIP – State Implementation Plan

SJV – San Joaquin Valley

SJVAB – San Joaquin Valley Air Basin

SFNA – Sacramento Federal 8-hour ozone Non-attainment Area

SVAB – Sacramento Valley Air Basin

U.S. EPA – United States Environmental Protection Agency

VOCs – Volatile Organic Compounds

WRF Model – Weather and Research Forecast Model

B.1.1 Introduction

The Sacramento Federal 8-hour ozone Nonattainment Area (SFNA) is located in the northern part of California's Central Valley (Figure B-1), which is a 500-mile long northwest-southeast oriented valley encompassing two of the worst polluted air basins in the nation, the San Joaquin Valley and Sacramento Valley air basins. The SFNA is home to more than 2 million residents with an area of 5600 square miles and is geographically located in two different air basins including the southern portion of the Sacramento Valley Air Basin (SVAB) and the north central portion of the Mountain Counties Air Basin (MCAB) (Figure B-1). The SFNA area occupies the southern portion of the Sacramento Valley, extending to the inland side of the California Coastal Range on the westernmost edge, and continues to the border of the Lake Tahoe air basin to the east, encompassing portions of the Sierra Nevada Mountain Range. It extends southward to the Sacramento Delta Region and northward to include the southern portion of Sutter County. In total, the SFNA comprises all of Sacramento and Yolo counties, the eastern portion of Solano County, the southern portion of Sutter County, and the portions of El Dorado and Placer counties that are not part of the Lake Tahoe Air Basin.

Due to its inland location, the climate of the Sacramento region is more extreme than that of most coastal regions, such as the San Francisco Bay Area. The winters are generally cool and wet, while the summers are hot and dry and both seasons can experience periods of high pressure and stagnation which are conducive to pollutant buildup. These climate conditions result in seasonal patterns where ozone levels are highest during the summer, while $PM_{2.5}$ concentrations are highest during the winter. The lack of summertime precipitation, coupled with the large extent of forested land surrounding the Central Valley, also creates conditions highly conducive to wildfires during the summer months.

The worst ozone air quality in the SFNA typically occurs during summer months, where the interaction between geography, climate, and a mix of natural (biogenic) and anthropogenic emissions poses significant challenges to air quality progress. A combination of stable wind fields and recirculation patterns generated by daytime upslope and nighttime downslope flows from the mountains located to the west (Coast Range) and east (Sierra Nevada), tend to confine and trap emissions and the pollutants near the surface. The anthropogenic NO_X and ROG emissions from the urban Sacramento area and biogenic ROG emissions from the Sierra foothills coupled with the hot and dry summertime weather conditions facilitate rapid ozone production in the region. During ozone episodes within the SFNA, the most important transport pattern is toward the northeast and the foothills within the Sacramento area itself. Due to the general daytime flow pattern from west to east, as well as the time needed for photochemical processes to occur, the highest ozone mixing ratios in the Sacramento region generally occur in the afternoon in the downwind, eastern portion of the region.

Figure B-1. Map of California (top) along with the location of SFNA in magenta. The shaded and gray line contours denote the gradients in topography (km). The outer box of the top panel is the California statewide 12 km modeling domain, while the inner box shows the 4 km modeling domain covering Central California. The insert on the bottom shows a zoomed-in view of the spatial extent (magenta lines), approximate regional boundaries of the Western, Central and Eastern sub-regions (dashed black lines) and the location of ozone monitoring sites (circle markers) in the SFNA.

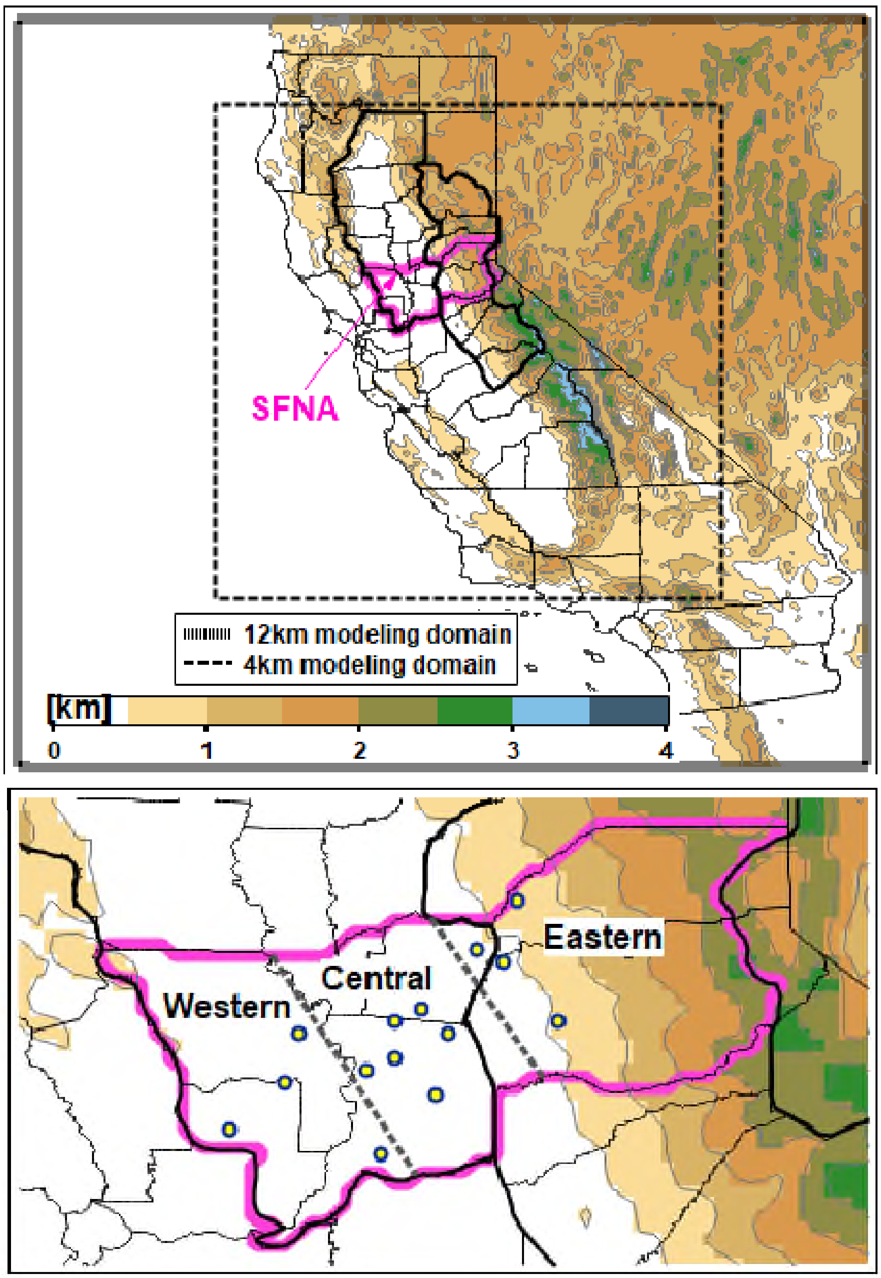

The air quality planning in the SFNA is led by the Sacramento Metropolitan Air Quality Management District (www.AirQuality.org). Four other air districts also participate in the planning and management in the area. The Yolo-Solano Air Quality Management District (AQMD) (www.ysaqmd.org) has jurisdiction over Yolo County and the SFNA portion of Solano County. Feather River AQMD (www.fraqmd.org) has jurisdiction over Sutter and Yuba counties, including the south Sutter County portion of the SFNA. Placer County Air Pollution Control District (APCD) (www.placer.ca.gov/apcd) has jurisdiction over Placer County, as does El Dorado County AQMD (www.edcgov.us/AirQualityManagement) over its county.

For purposes of model evaluation and analysis, the SFNA is divided into three sub regions that are characterized by distinct geography, meteorology, emissions characteristics, transport patterns, and air quality: 1) Western SFNA comprising Yolo, Solano and the southwest portion of Sacramento counties, which lies upwind of the Sacramento urban emission sources and is impacted by pollutant transport from the surrounding Bay Area and SJV located on the west/southwest, 2) Central SFNA including the inland urban core, and the metropolitan areas of Sacramento county and the westernmost portion of Placer county, and 3) Eastern SFNA comprising Placer and El Dorado counties in the Sierra Nevada foothills area that is located downwind of urban Sacramento. The geographical extent of the sub-regions in SFNA and their approximate regional boundaries are shown in the bottom panel of Figure B-1.

Anthropogenic sources of the oxides of nitrogen (NO_X) and reactive organic gases (ROG) are the major precursors that lead to ozone formation in the SFNA. Biogenic hydrocarbons are also important contributors to ozone precursors in the region and are projected to play an even more important role in the future as emission controls reduce anthropogenic ROG. Summer emission trends from 2000 to 2020 in the SFNA are shown in Figure B-2 for anthropogenic NO_X and ROG, along with summer biogenic ROG emissions in the SFNA averaged from May to October 2018 (magenta triangle marker). Figure B-2 clearly shows a large decrease in both local anthropogenic NO_X (from ~175 tpd to ~58 tpd) and ROG (from ~165 tpd to ~91.5 tpd) emissions from 2000 to 2020. In 2018, biogenic ROG emissions (~163 tpd) are estimated to be ~1.7 times higher than the corresponding anthropogenic emissions (~94 tpd) in the SFNA.

Figure B-2. Trend in summer emissions of NO_X and ROG (tons per day), Maximum Daily Average 8-hour Ozone Design Value (ppb) and 70 ppb 8-hour Ozone NAAQS exceedance days between 2000 and 2020 in the SFNA. Note that O_3 design site may vary from year to year. Anthropogenic Emissions estimates are from the California Emission Projection Model (CEPAM) 2019 Ozone SIP Baseline Projection Version 1.04 with 2017 base year. 2018 biogenic ROG emissions are from MEGAN 3.0 biogenic model calculations.

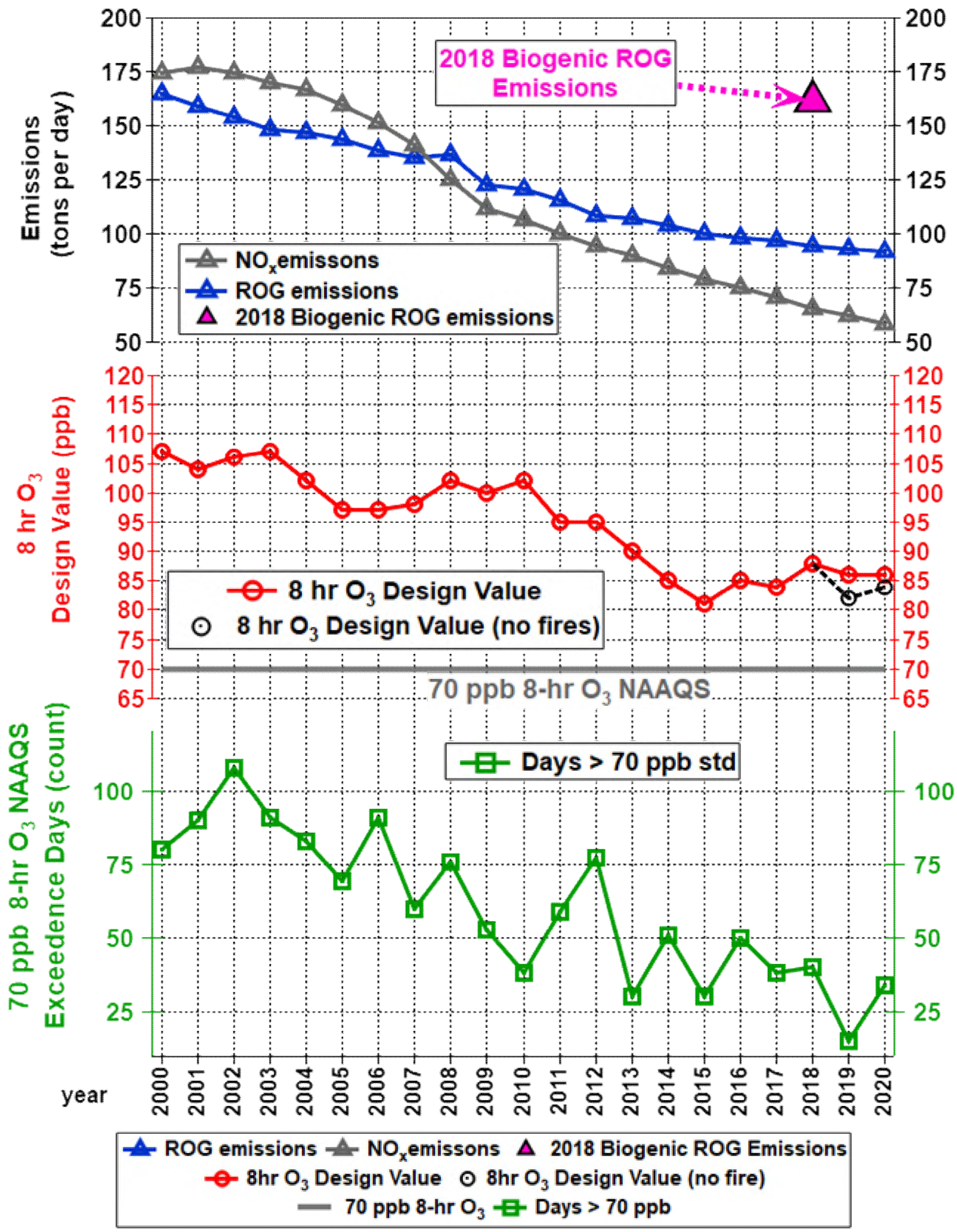

Over the same 2000 to 2020 time period, the ozone design value within the SFNA declined steadily (Figure B-2, middle panel), but did also exhibit a fair amount of variability due to year-to-year variability in meteorology and the associated changes in biogenic emissions. Overall, the region-wide design values (DVs) have declined from 107 ppb in 2000 to 86 ppb in 2020. However, these DVs are still substantially higher than the current 70 ppb standard. Exceedance days in the region (Figure B-2, bottom panel) have substantially decreased over time from 80 days in 2000 to 34 days in 2020, indicating significant improvements in ozone air quality across the entire region. In recent years, the prevalence of forest fires during the summer ozone season significantly impacted the air quality in the SFNA. High ozone concentrations were observed at several SFNA sites on days impacted by forest fires. Weight of Evidence of this SIP document focused on the days with ozone values that significantly affected the design values at Auburn site, which is one of the two high ozone sites in the SFNA. Excluding the fire impact days (7/31/2018, 8/1/2018,8/2/2018, 8/8/2018, 8/9/2018 and 8/10/2018) at Auburn site, ozone DVs would be 82 ppb in 2019 and 84 ppb in 2020 denoted by black circle markers in middle panel of Figure B-2.

The SFNA is designated as serious nonattainment for the 2015 70 ppb O_3 standard with a 2026 attainment deadline. However, it is very unlikely that SFNA would have a design value of 0.070 ppm or lower by 2026. Therefore, as part of this State Implementation Plan (SIP), SFNA is seeking to voluntarily reclassify as a severe nonattainment area with a 2032 attainment deadline. This document serves as the modeling protocol and attainment demonstration for the 2015 standard in the SFNA. The modeling analysis uses 2018 as the base year for the attainment demonstration. The year 2018 was chosen based on preliminary analysis that showed 2018 exhibiting superior model performance for O_3 in Northern California compared to adjacent years.

B.1.2 Methodology

United States Environmental Protection Agency (EPA) modeling guidance (EPA, 2018) outlines the approach for utilizing regional chemical transport models (CTMs) to predict future attainment of the 2015 (70 ppb) 8-hour ozone standard. This model attainment demonstration requires that CTMs be used in a relative sense, where the relative change in ozone to a given set of emission reductions (i.e., predicted change in future anthropogenic emissions) is modeled, and then used to predict how current/present-day ozone levels would change under the future emissions scenario.

The starting point for the attainment demonstration is the observational based design value (DV), which is used to determine compliance with the ozone standards. The DV for a specific monitor and year represents the three-year average of the annual 4th highest 8-hour ozone mixing ratio observed at the monitor. For example, the 8-hour O_3 DV for 2018 is the average of the observed 4th highest 8-hour O_3 mixing ratio from 2016, 2017, and 2018 (Table B-1). The EPA recommends using an average of three DVs to better account for the year-to-year variability in ozone levels due to meteorology. This average DV is called the weighted DV (in the context of this SIP document, the weighted DV will also be referred to as the reference year DV or DV_R). Since 2018 represents the reference year for projecting DVs to the future, site-specific DVs should be calculated for the three-year periods ending in 2018, 2019, and 2020, and then these three DVs are averaged. However, 2020 was an atypical year with large societal changes in response to the COVID19 pandemic and is not suitable for use in the DV_R calculation. To remove the impact from 2020 observations, we utilize an alternative methodology for calculating the average DVs by excluding year 2020. In this method, the 8-hour O_3 DV for 2020 was replaced by the two-year average of the 4^{th} highest 8-hour O_3 concentrations from 2018 and 2019. Table B-1 illustrates the observational data from each year that goes into the average DV_R and Equation 1 shows how the DV_R is calculated.

Table B-1 Data from each year that are utilized in the Design Value calculation for a specific year (DV Year), and the yearly weighting of data for the average Design Value calculation (or DVR).

DV Year	Years Averaged for the Design Value (4th highest observed 8-hr O_3)			
2018	2016	2017	2018	
2019		2017	2018	2019
2020			2018	2019

$$DV_R = \frac{DV_{2018} + DV_{2019} + \frac{4th\ highest\ MDA8\ O_3\ (2018 + 2019)}{2}}{3} \quad (1)$$

Table B-2 lists the design values for the sites within the three sub-regions of the SFNA that were used in the model attainment demonstration. Note that the average DVs are listed in descending order for sites within each sub-region except that at the Auburn-Atwood site, which has two average DVs due to one excluding wildfire impacted days in the DV calculation. The ozone data collected at the Colfax and Auburn sites in Placer County between January 2015 to May 2019 were deemed invalid after a technical systems audit by EPA. The audit revealed that the calibration procedures did not follow EPA regulation and guidance. Since Colfax and Auburn are two of the high ozone sites in the SFNA, it is important to examine their air quality trends to ensure these two sites will also attain the 70 ppb ozone standard by 2032. Therefore, this attainment demonstration also utilized the invalidated monitoring data in the analyses. The Placerville-Gold monitoring site, located in the Eastern SFNA, has the highest average DV in the SFNA with an average DV of 84.0 ppb if only DVs excluding wildfire days at Auburn-Atwood are considered.

Table B-2. Year-specific 8-hour ozone design values for 2018, 2019 and 2020, and the average baseline design value (DVR, represented as the average of three design values) for 2018 at the monitoring sites in the SFNA. The 2020 DV is the two-year average of the 4th highest 8-hour O_3 concentrations from 2018 and 2019.

Sub-region	Site	2018 DV (ppb)	2019 DV (ppb)	2020 DV (ppb)	2018-2020 Average DV (ppb)
Eastern SFNA	Placerville-Gold	88	81	83	84.0
Eastern SFNA	Colfax-CityHall	85	82	84	83.7
Eastern SFNA	Cool-Hwy193	84	80	81	81.7
Eastern SFNA	Auburn-Atwood, fire days excluded	83	81	81	81.7
Eastern SFNA	Auburn-Atwood, all days	88	86	88	87.3
Central SFNA	Folsom-Natoma	82	75	73	76.7
Central SFNA	Roseville-NSunrise	81	75	73	76.3
Central SFNA	N_Highlands-Blackfoot	78	74	72	74.7
Central SFNA	Sacramento-DelPas	75	71	70	72.0
Central SFNA	Sloughhouse	75	70	69	71.3
Central SFNA	Sacramento-TStreet	67	67	65	66.3
Western SFNA	Elk_Grove-Bruceville	67	68	68	67.7
Western SFNA	Woodland-Gibson	68	66	66	66.7
Western SFNA	Vacaville-Ulatis	65	64	63	64.0
Western SFNA	Davis-UCD	62	62	63	62.3

Projecting the reference DVs to the future requires three photochemical model simulations, described below:

1. Base Year Simulation

The base year simulation for 2018 is used to assess model performance (i.e., to ensure that the model is reasonably able to reproduce the observed ozone mixing ratios). Since this simulation will be used to assess model performance, it is essential to include as much day-specific detail as possible in the emissions inventory, including, but not limited to hourly adjustments to the motor vehicle and biogenic inventories based on local meteorological conditions, known wildfire and agricultural burning events, and any exceptional events such as refinery fires.

2. Reference Year Simulation

The reference year simulation was identical to the base year simulation, except that certain emissions events which are either random and/or cannot be projected to the future are removed from the emissions inventory. For 2018, the only difference between the base and reference year simulations was that wildfires were excluded from the reference year simulation.

3. Future Year Simulation

The future year simulation (2032) was identical to the reference year simulation, except that the projected future year anthropogenic emission levels were used rather than the reference year emission levels. All other model inputs (e.g., meteorology, chemical boundary conditions, biogenic emissions, and calendar for day-of-week specifications in the inventory) are the same as those used in the reference year simulation.

Projecting the reference DVs to the future is done by first calculating the fractional change in ozone between the modeled future and reference years for each monitor location. These ratios, called "relative response factors" or RRFs, are calculated based on the ratio of the modeled future year ozone to the corresponding modeled reference year ozone (Equation 2).

$$\text{RRF} = \frac{\frac{1}{N}\sum_{d=1}^{N}(MDA8\ O_3)_{future}^{d}}{\frac{1}{N}\sum_{d=1}^{N}(MDA8\ O_3)_{reference}^{d}} \quad (2)$$

here, MDA8 O_3 refers to the maximum daily average 8-hour ozone, d refers to the day (chosen from the reference year), and N is the total number of days used in the RRF calculation. These MDA8 ozone values are based on the maximum simulated ozone within a 3x3 array of cells surrounding the monitor (Figure B-3). Not all modeled days are used to calculate the average MDA8 ozone from the reference and future year simulations. The form of the 8-hour ozone NAAQS is such that it is focused on the days with the highest mixing ratios in any ozone season (i.e., the 4th highest MDA8 ozone). Therefore, the modeled days used in the RRF calculation also reflect days with the highest ozone levels. As a result, the current EPA modeling guidance (EPA, 2018) recommends using the 10 days with the highest modeled MDA8 ozone at each monitor location, where the 10 days are chosen from the reference year simulation and then the same corresponding days are selected from the future year simulation. Since the relative sensitivity to emissions changes (in both the model and real world) can vary from day-to-day due to meteorology and emissions (e.g., temperature dependent emissions or day-of-week variability) using the top 10 days ensures that the calculated RRF is not overly sensitive to any single day. Note that the MDA8 ozone from the reference and future year simulations are paired in both time (the same days are selected from each simulation) and space (the location of the peak MDA8 ozone within the 3x3 array of grid cells surrounding the monitor is selected from the reference year simulation and the same location is used when selecting the corresponding data from the future year simulation).

Figure B-3. Example showing how the location of the MDA8 ozone for the top ten days in the reference and future years are chosen.

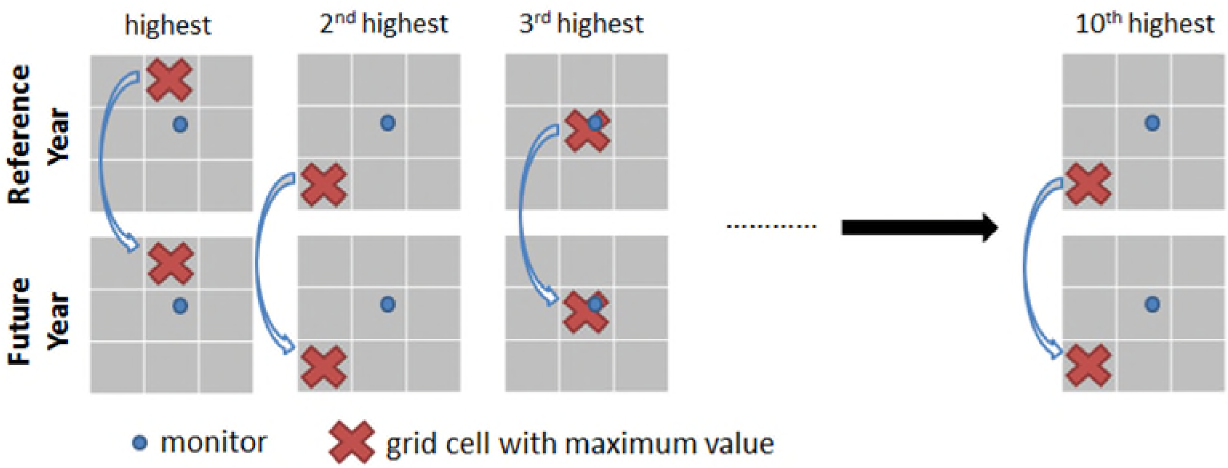

When choosing the top 10 days, the EPA recommends beginning with all days in which the simulated reference year MDA8 ozone is ≥ 60 ppb and then calculating RRFs based on the 10 days with the highest ozone in the reference simulation. If there are fewer than 10 days with MDA8 ozone ≥ 60 ppb then all days ≥ 60 ppb are used in the RRF calculation, as long as there are at least 5 days used in the calculation. If there are fewer than 5 days ≥ 60 ppb, an RRF cannot be calculated for that monitor. To ensure that only modeled days which are consistent with the observed ozone levels are used in the RRF calculation, the modeled days are further restricted to days in which the reference MDA8 ozone is within ± 20% of the observed value at the monitor location.

Future year DVs at each monitor are then calculated by multiplying the corresponding reference year DV by the site-specific RRF.

$$DV_F = DV_R \times RRF \qquad (3)$$

where, DV_F is the future year design value, DV_R is the reference year design value, and RRF is the site-specific RRF from Equation 2. The resulting future year DVs are then compared to the 8-hour ozone NAAQS to demonstrate whether attainment will be reached under the emissions scenario utilized in the future year modeling. A monitor is considered to be in attainment of the 8-hour ozone standard if the estimated future year DV does not exceed the level of the standard.

B.1.2.1 Meteorological Modeling

California's proximity to the ocean, complex terrain, and diverse climate represents a unique challenge for reproducing meteorological fields that adequately represent the synoptic and mesoscale features of the regional meteorology. In summertime, the majority of the storm tracks are far to the north of the state and a semi-permanent Pacific high pressure system typically sits off the California coast. Interactions between this eastern Pacific subtropical high pressure system and the thermal low pressure further inland over the Central Valley or South Coast lead to conditions conducive to pollution buildup over large portions of the state (Bao et al., 2008; Fosberg et al., 1966).

The state-of-the-science Weather Research and Forecasting (WRF) prognostic model (Skamarock, Klemp and Dudhia) version 4.2.1 was employed in the modeling. Its domain consisted of three nested Lambert projection grids of 36 km (D01), 12 km (D02), and 4 km (D03) uniform horizontal grid spacing as shown in Figure B-4. The 4 km innermost domain has 427x427 grid points and spans 1748 km in the east-west and the north-south directions. All three domains utilized 30 vertical sigma layers with the lowest layer extending to 30 m above the surface (Table B-3). The North America Regional Reanalysis (NARR) fields, enhanced with surface and upper-air observations, were used for initial and boundary conditions as well as Four Dimension Data Assimilation (FDDA) on the outermost (36 km) domain. The horizontal spatial resolution of the NARR data is 32 km. The major physics options for each domain are listed in Table B-4, which include the Yon-Sei University (YSU) planetary boundary layer (PBL) scheme, Kain-Fritsch cumulus parameterization for the outer two domains, and 5-layer thermal diffusion land-surface option.

Figure B-4. WRF modeling domains (D01 36 km; D02 12 km; and D03 4 km).

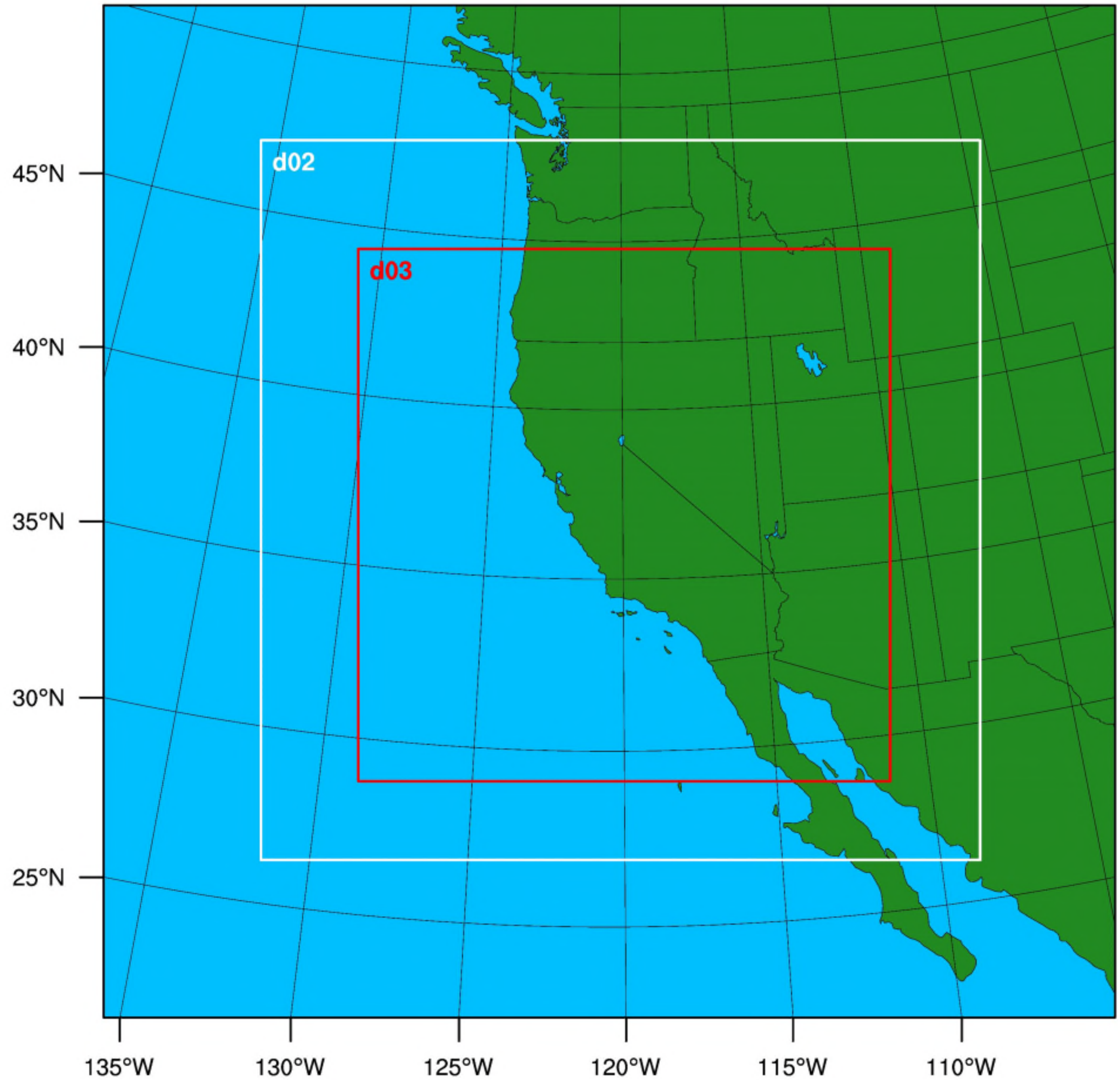

Table B-3. WRF vertical layer structure.

Layer Number	Height (m)	Layer Thickness (m)	Layer Number	Height (m)	Layer Thickness (m)
30	16082	1192	15	2262	403
29	14890	1134	14	1859	334
28	13756	1081	13	1525	279

Layer Number	Height (m)	Layer Thickness (m)	Layer Number	Height (m)	Layer Thickness (m)
27	12675	1032	12	1246	233
26	11643	996	11	1013	194
25	10647	970	10	819	162
24	9677	959	9	657	135
23	8719	961	8	522	113
22	7757	978	7	409	94
21	6779	993	6	315	79
20	5786	967	5	236	66
19	4819	815	4	170	55
18	4004	685	3	115	46
17	3319	575	2	69	38
16	2744	482	1	31	31

To prevent any large deviations from the reanalysis data, analysis nudging was applied to the outermost domain (D01) above the planetary boundary layer (PBL) for moisture and above 2 km for wind and temperature. No nudging was used on the two inner domains to allow the model physics to work fully without externally imposed forcing. Boundary conditions on the outermost domain were updated every 6 hours, while WRF was reinitialized every 6 days with one day overlap, where the first day after being reinitialized was discarded as model spin-up. The Meteorology-Chemistry Interface Processor (MCIP) version 5.1 was used to process the 12 km (D02) and 4 km (D03) WRF output for use in the CTM simulations.

Table B-4. WRF Physics options.

Physics Option	D01 (36 km)	D02 (12 km)	D03 (4 km)
Microphysics	WSM 6-class	WSM 6-class	WSM 6-class
Longwave Radiation	RRTM	RRTM	RRTM
Shortwave Radiation	Dudhia	Dudhia	Dudhia
Surface Layer	Revised MM5 Monin-Obukhov	Revised MM5 Monin-Obukhov	Revised MM5 Monin-Obukhov
Land Surface	5-layer Thermal Diffusion	5-layer Thermal Diffusion	5-layer Thermal Diffusion
Planetary Boundary Layer	YSU	YSU	YSU
Cumulus Parameterization	Kain-Fritsch Scheme	Kain-Fritsch Scheme	No

B.1.2.2 Emissions

The anthropogenic emissions inventory used in this modeling was based on the California Emissions Projection Analysis Model (CEPAM) v1.03 augmented with updates consistent with CEPAM v1.04 for select source categories. These sources are described in *http://outapp.arb.ca.gov/cefs/2019ozsip/CEPAM2019_key_updates_chron.pdf* under version "March 29, 2022 Release of Version 1.04 Planning Projections", except for emissions from Ocean Going Vessels (OGV). For a detailed description of the anthropogenic emissions inventory, updates to the inventory, and how it was processed from the planning totals to a gridded inventory for modeling, see the Modeling Emissions Inventory Appendix B.2.

Table B-5 summarizes the 2018 and 2032 SFNA anthropogenic emissions. Overall, anthropogenic NO_X emissions in CEPAM v1.04 were projected to decrease by ~48% between 2018 and 2032 from 65.6 tpd to 34.2 tpd with the bulk of the reductions coming from on-road mobile sources. In contrast, anthropogenic ROG was projected to decrease by ~15% from 94.1 tpd to 79.9 tpd with the bulk of those reductions coming from all mobile sources including on-road and other mobile sources. The right two columns in Table B-5 show the 2032 emissions after incorporating additional CARB commitments from the State SIP Strategy that will increase the overall reduction in NO_X and ROG emissions to ~57% and 16.5%, respectively, between 2018 and 2032. In addition, the emission inventory for 2032 includes an additional 2.81 tpd and 3.63 tpd of NO_X and ROG emissions, respectively, from Emission Reduction Credits (ERCs). Details on these rules/adjustments can be found in the Modeling Emissions Inventory Appendix B.2.

Table B-5. SFNA Summer Planning Emissions for 2018 and 2032 (tons/day).

	CEPAM v1.04						With CARB Commitments			
Source Category	2018 NO_X (tpd)	2032 NO_X (tpd)	NO_X diff	2018 ROG (tpd)	2032 ROG (tpd)	ROG diff	2032 NO_X (tpd)	NO_X diff	2032 ROG (tpd)	ROG diff
Stationary	6.6	6.0	-9.7%	22.7	23.9	5.5%	6.0	-9.7%	23.9	5.5%
Area	2.3	2.2	-4.4%	27.3	31.7	16.2%	2.2	-4.4%	31.7	16.2%
On-road Mobile	32.9	9.9	-69.9%	17.9	9.7	-45.8%	8.6	-73.7%	9.1	-49.3%
Other Mobile	23.9	16.1	-32.4%	26.3	14.6	-44.4%	11.3	-52.5%	13.9	-47.1%
Total	65.6	34.2	-47.9%	94.1	79.9	-15.1%	28.1	-57.2%	78.6	-16.5%

* Note that rounding errors may result in emissions totals that do not exactly match the sum of the individual categories.

Biogenic emissions were generated using the Model of Emissions of Gases and Aerosols from Nature (MEGAN3.0) biogenic emissions model (*https://bai.ess.uci.edu/megan*). MEGAN3.0 incorporates a new pre-processor (MEGAN-EFP) for estimating biogenic emission factors based on available landcover and emissions data. The MEGAN3.0 default datasets for plant growth form, eco-type, and emissions were utilized. Leaf Area Index (LAI) for non-urban grid cells was based on the 8-day 500 m resolution Moderate Resolution Imaging Spectroradiometer (MODIS) Terra/Aqua combined product

(MCD15A2H) for 2018 (*https://earthdata.nasa.gov/*). The LAI data was converted to LAIv, which represents the LAI for the vegetated fraction within each grid cell, by dividing the gridded MODIS LAI values by the Maximum Green Vegetation Fraction for each grid cell (*https://archive.usgs.gov/archive/sites/landcover.usgs.gov/green_veg.html*). The MODIS LAI product does not provide information on LAI in urban regions, so urban LAIv was estimated from the US Forest Service's Forest Inventory and Analysis urban tree plot data, processed through the i-Tree v6 software (*https://www.itreetools.org/tools/i-tree-eco*). Hourly meteorology for MEGAN was provided by the 4 km WRF simulation described above, with all stress factor adjustments turned off.

Monthly biogenic ROG totals for 2018 within the SFNA are shown in Figure B-5 (note that the same biogenic emissions were used in the 2018 and 2032 modeling). Throughout the summer, biogenic ROG emissions ranged from ~100 tpd in May to 308 tpd in July and ~215 tpd in August, with the difference in emissions primarily due to monthly differences in temperature, insolation, and leaf area from month-to-month.

Figure B-5. Monthly average biogenic ROG emissions for 2018 in the SFNA.

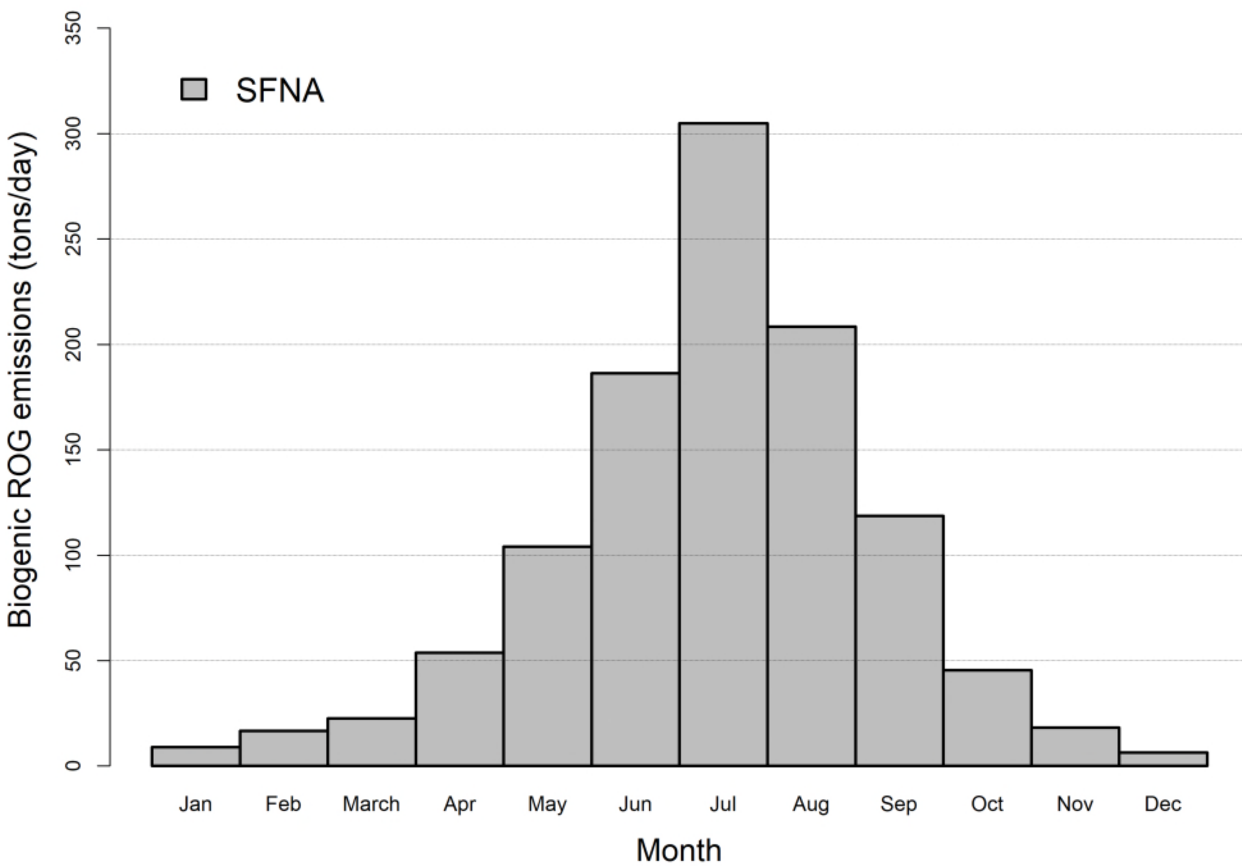

In addition to biogenic ROG emissions, the MEGAN model also estimates NO_X emissions from soils using the Yienger and Levy scheme (Yienger and Levy, 1995) that accounts for natural emissions from soils as well as enhanced emissions from managed crop lands.

Figure B-6 shows the monthly average soil NO_X emissions for 2018 from MEGAN. Soil NO_X emissions are highest during summer months where the emissions peak at 7.5 tpd in July.

Figure B-6. Monthly average soil NO_X emissions for 2018 in the SFNA

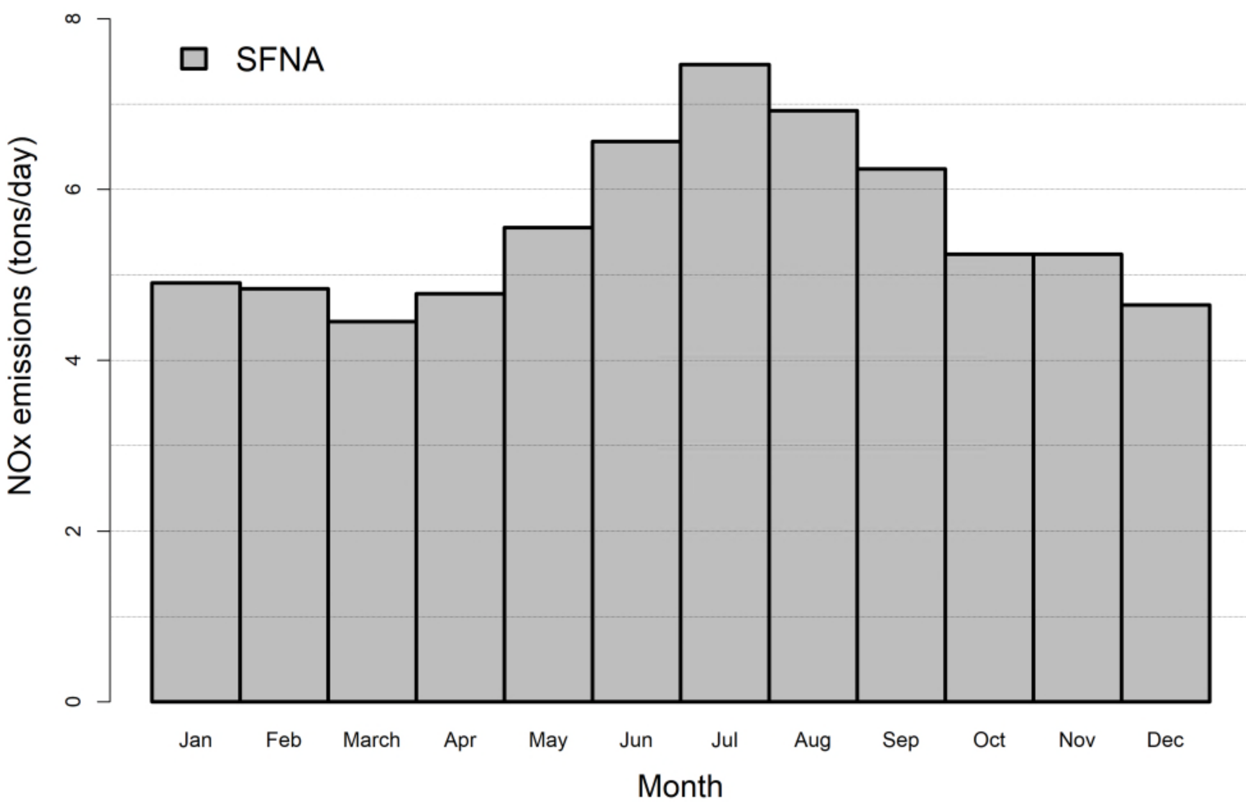

B.1.2.3 Air Quality Modeling

Figure B-1 shows the Community Multiscale Air Quality (CMAQ) modeling domains used in this work. The larger domain covering all of California has a horizontal grid size resolution of 12 km with 107x97 lateral grid cells for each vertical layer and extends from the Pacific Ocean in the west to Eastern Nevada in the east and runs from the U.S.-Mexico border in the south to the California-Oregon border in the north. The smaller nested domain (dashed black outline) covering the SFNA including the San Joaquin Valley (SJV), Sacramento Valley (SV), Mountain Counties (MC) air basin, has a finer scale 4 km grid resolution and includes 192x192 lateral grid cells.

The 12 km and 4 km domains are based on a Lambert Conformal Conic projection with reference longitude at -120.5°W, reference latitude at 37°N, and two standard parallels at 30°N and 60°N, which is consistent with the WRF domain settings. The CMAQ vertical layer structure is based on the WRF sigma-pressure coordinates, and the exact layer structure used can be found in Table B-3. The original 30 vertical layers from WRF were used for the CMAQ simulations, extending from the surface to 100 mb such that the majority of the vertical layers fall within the planetary boundary layer.

The CTM utilized in the modeling is the CMAQ model version 5.2.1 (EPA, 2018). CMAQ is the EPA's open-source regional air quality model, which is widely used in the regulatory and scientific communities and represents the current state-of-the-science. CMAQ has been utilized for studying ozone and $PM_{2.5}$ formation in California for over a decade (e.g., Cai et al., 2016, 2019; Jin et al., 2008, 2010; Kelly et al., 2010, 2014; Livingstone et al., 2009; Pun et al., 2009; Tonse et al., 2008; Vijayaraghavan et al., 2006; Zhang et al., 2010), and has been the primary CTM used in California SIPs since 2008 (SJV, 2008), having been used in over a dozen ozone and $PM_{2.5}$ SIPs (Eastern Kern, 2017; Imperial, 2017, 2018; Sacramento, 2017; SJV, 2012, 2013, 2016a,b, 2018; South Coast, 2012, 2016; Ventura, 2016; Western Mojave, 2016; Western Nevada, 2018).

Table B-6 lists the CMAQ configuration and settings used in the modeling. The SAPRC07tic chemical mechanism (Carter, 2010a,b) was chosen to represent the gas-phase photochemistry in the atmosphere, along with the aero6 aerosol module for simulating aerosol dynamics and chemistry. Photolysis rates were calculated in-line to better represent changes in photolysis rates due to meteorological conditions and gaseous and particulate pollutant levels in the atmosphere.

Table B-6. CMAQ configuration and settings.

Process	Scheme
Advection	Yamo module for horizontal and WRF module for vertical
Horizontal diffusion	Multi-scale
Vertical diffusion	ACM2 (Asymmetric Convective Model version 2)
Gas-phase chemical mechanism	SAPRC version 07tc gas-phase mechanism with extended isoprene chemistry
Chemical solver	EBI (Euler Backward Iterative solver)
Aerosol module	Aero6 (the sixth generation CMAQ aerosol mechanism)
Cloud module	ACM_AE6 (ACM cloud processor that uses the ACM methodology to compute convective mixing with heterogeneous chemistry for AERO6)
Photolysis rate	Phot/inline (calculating photolysis rates inline)

Global chemical transport Community Atmosphere Model with Chemistry (CAM-Chem) coupled to the Community Earth System Model (CESM2) (Emmons, 2020; Lamarque et al., 2012) was developed by the National Center for Atmospheric Research (NCAR) and used for simulations of global tropospheric and stratospheric atmospheric compositions. CAM-Chem modeling outputs have been widely used to provide chemical boundary conditions for various regional air quality models (Yan et al., 2021; He et al., 2018; Shahrokhishahraki et al., 2022; Wang et al., 2022). In this work, chemical boundary conditions for the outer 12-km domain were extracted from the CAM-Chem output based on the vertical and horizontal grid structure in CMAQ, processed into CMAQ model ready format and mapped to CMAQ chemical species. The CAM-chem data for 2018 was obtained from the National Center for Atmospheric Research (https://www.acom.ucar.edu/cam-chem/cam-chem.shtml) (Buchholz, 2019) and processed using the mozart2camx preprocessor version 3.2.3 (https://www.camx.com/download/support-software/). The same CAM-chem derived BCs for the 12 km outer domain were used for both base year, reference year and future year simulations. The inner 4 km domain simulations utilized BCs that were based on the output from the corresponding 12 km domain simulations.

The extended ozone season (April – October) was simulated through parallel individual monthly simulations for the base year, reference year and future year. For each month, the CMAQ simulations included a seven-day spin-up period (i.e., the last seven days of the previous month) for the outer 12 km domain where initial conditions were set to the default initial conditions included with the CMAQ release. The 4 km inner domain simulations utilized a three-day spin-up period, where the initial conditions for the start day were based on output from the corresponding day of the 12 km domain simulation. These spin-up periods were chosen based on previous testing, which showed that influence from the initial conditions was negligible after the seven- and three-day spin-up periods for the 12 km and 4 km simulations, respectively.

B.1.3 Results

B.1.3.1 Meteorological Model Evaluation

Simulated surface wind speed, temperature, and relative humidity from the 4 km domain were validated against hourly observations from 37 surface stations in the region (Figure B-7). Considering the geographical and meteorological differences, the area covered by these sites was divided into two regions: the lower elevation (Valley) and higher elevation mountain (Mountain) areas. Among the 37 surface sites used in this analysis, 21 of them are located in the valley zone with the remaining 16 sites located in the mountain region. The observational data for the surface stations were obtained from the CARB archived meteorological database available at http://www.arb.ca.gov/aqmis2/aqmis2.php. Table B-7 lists the monitoring stations and the meteorological parameters that are measured at each station, including wind speed and direction (wind), temperature (T) and relative humidity (RH). Several quantitative performance metrics were used to compare hourly surface observations and modeled estimates: mean bias (MB), mean error (ME) and index of agreement (IOA) based on the recommendations from Simon et al. (2012). The model performance statistical metrics were calculated using the available data at all the sites. A summary of these statistics is shown in Table B-8.

The average hourly wind speed bias for April-October 2018 is 0.61 m/s and 0.69 m/s for valley and mountain stations, respectively; while the average mean error is 0.73 m/s and 0.75 m/s for valley and mountain stations, respectively. The index of agreement for the wind speed in this period is 0.79 (0.69) for valley (mountain) stations. Temperature is biased low with an average bias of -1.05 K for valley stations and -1.62 for mountain stations, while the IOA for temperature is 0.97 for both valley and mountain stations. Consistent with the negative temperature bias, relative humidity has a positive bias of 12.61% and 13.19% for valley and mountain stations, respectively. The distribution of daily mean bias and mean error for wind speed, temperature and relative humidity are shown in Figure B-8. The spatial distributions of the mean bias and mean error of modeled surface wind, temperature and relative humidity are shown in Figure B-9. Observed vs. modeled scatter plots of hourly wind speed, temperature, and relative humidity are shown in Figure B-10. These results are comparable to other WRF modeling efforts in California investigating ozone formation in the Central California (e.g., Hu et al., 2012) and modeling analysis for the CalNex, CARES and Discover-AQ field studies (e.g. Fast et al., 2012; Baker et al., 2013; Kelly et al., 2014; Angevine et al., 2012; Chen et al., 2020). Detailed hourly time-series of surface temperature, relative humidity, wind speed, and wind direction can be found in the supplemental materials.

Table B-7. Meteorological site location and parameter measured.

Site Number (Figure B-7)	Site ID	Site Name	Region	Parameter(s) Measured
1	3290	Lincoln (RAWS)	Valley	Wind, T, RH
2	3397	Brooks	Valley	Wind, T, RH
3	5370	Sacramento International Airport	Valley	T, RH
4	3187	Folsom-Natoma Street	Valley	Wind, T, RH
5	5012	McClellan Air Force Base	Valley	T
6	6180	Woodland-CIMIS	Valley	Wind, T, RH
7	5776	Fair Oaks #2	Valley	Wind, T, RH
8	2731	Sacramento-Del Paso Manor	Valley	Wind, T, RH
9	5799	Bryte	Valley	Wind, T, RH
10	3011	Sacramento-T Street	Valley	Wind, T, RH
11	5319	Sacramento Mather Airport	Valley	T, RH
12	5710	Davis #2	Valley	Wind, T, RH
13	2143	Davis-UCD Campus	Valley	Wind, T, RH
14	2432	Sacramento-Executive Airport	Valley	T, RH
15	5784	Winters	Valley	Wind, T, RH
16	3209	Sloughhouse	Valley	Wind
17	5767	Dixon	Valley	Wind, T, RH
18	5384	Nut Tree Airport	Valley	T, RH
19	7232	Hastings Tract East	Valley	Wind, T, RH
20	5785	Twitchell Island	Valley	Wind, T, RH
21	3297	Briones	Valley	Wind, T, RH
22	6001	Lincoln Municipal Airport	Mountain	T

Site Number (Figure B-7)	Site ID	Site Name	Region	Parameter(s) Measured
23	5290	Blue Canyon Nyack Airport	Mountain	T, RH
24	3288	Hell Hole	Mountain	Wind, T, RH
25	2948	South Lake Tahoe-Sandy Way	Mountain	Wind, T, RH
26	3289	Bald Mountain Location	Mountain	Wind, T, RH
27	2527	South Lake Tahoe-Airport Met	Mountain	T, RH
28	3196	Cool-Highway 193	Mountain	Wind, T, RH
29	5832	Auburn #3	Mountain	Wind, T, RH
30	3291	Pilot Hill Station	Mountain	Wind, T, RH
31	3487	Echo Summit	Mountain	Wind, T, RH
32	2956	Roseville-N Sunrise Blvd	Mountain	Wind, T, RH
33	5714	Camino #2	Mountain	Wind, T, RH
34	3017	Placerville-Gold Nugget Way	Mountain	Wind, T, RH
35	3292	Owens Camp	Mountain	Wind, T, RH
36	6025	Diamond Springs-CIMIS	Mountain	Wind, T, RH
37	3293	Ben Bolt	Mountain	Wind, T, RH

Figure B-7. Meteorological monitoring sites utilized in the model evaluation for SFNA. Numbers reflect the sites listed in Table B-7.

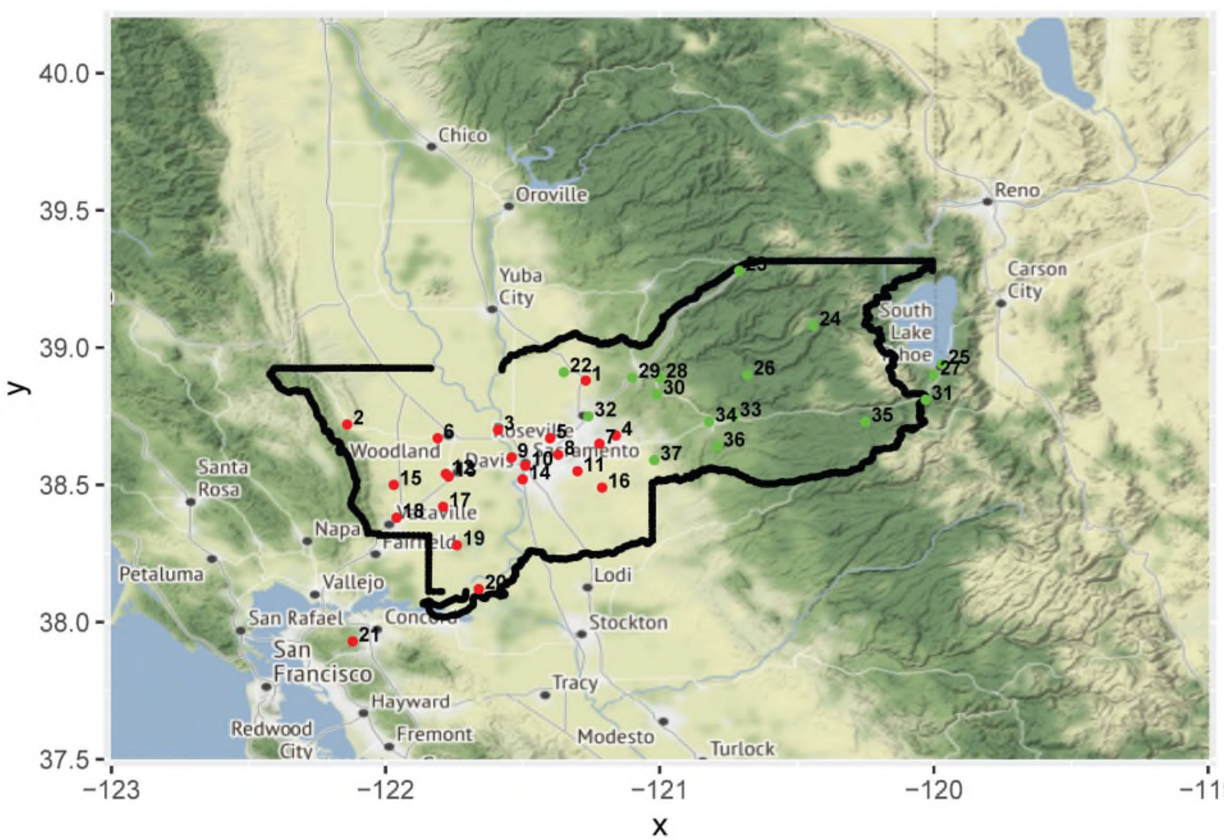

Table B-8. Hourly surface wind speed, temperature and relative humidity statistics for April through October 2018. IOA denotes index of agreement.

Parameter	Region	Obs. Mean	Mod. Mean	Mean Bias	Mean Error	IOA
Wind Speed (m/s)	Valley	2.29	2.91	0.61	0.73	0.79
Wind Speed (m/s)	Mountain	1.62	2.31	0.69	0.75	0.69
Temperature (K)	Valley	293.56	292.51	-1.05	1.84	0.97
Temperature (K)	Mountain	291.25	289.64	-1.62	1.87	0.97
Relative Humidity (%)	Valley	55.66	67.42	11.76	12.61	0.86
Relative Humidity (%)	Mountain	48.23	59.9	11.67	13.19	0.81

Figure B-8. Distribution of daily mean bias (left) and mean error (right) for Valley and Mountain sites from April – October 2018. Results are shown for wind speed (top), temperature (middle), and RH (bottom).

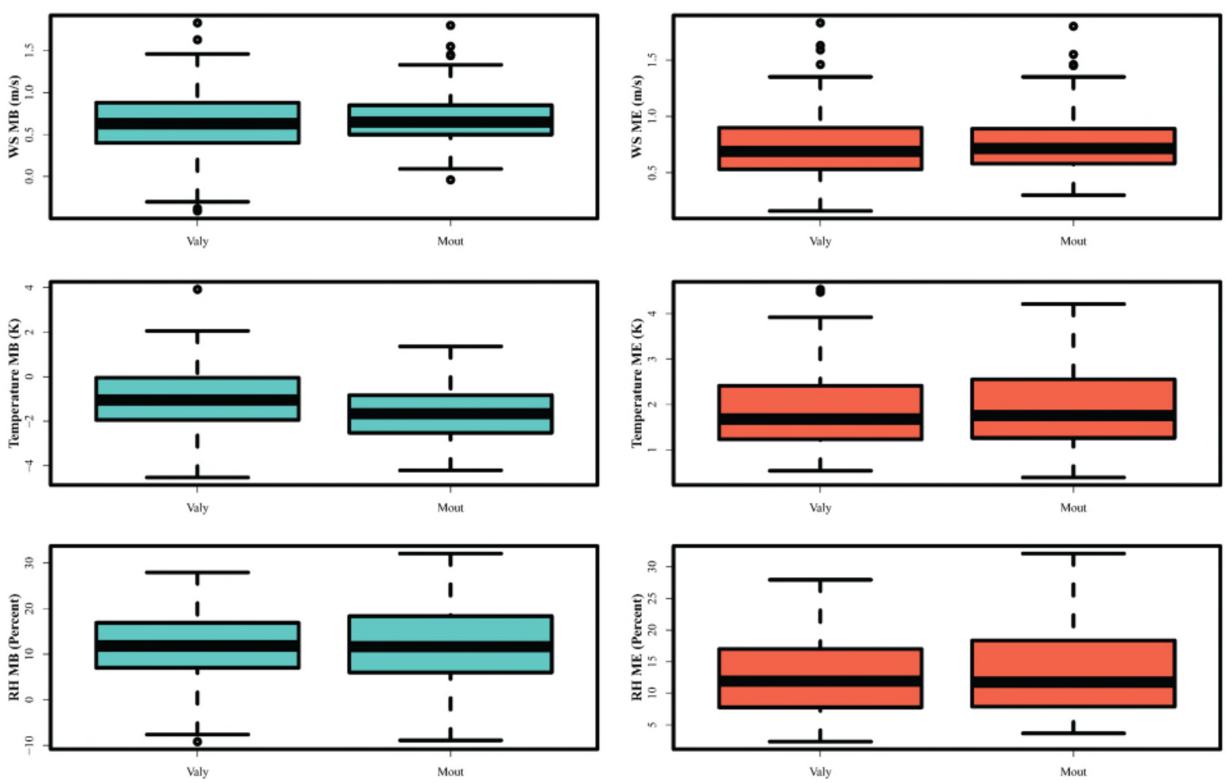

Figure B-9. Spatial distribution of mean bias (left) and mean error (right) for April-October 2018. Results are shown for wind speed (top), temperature (middle), and RH (bottom).

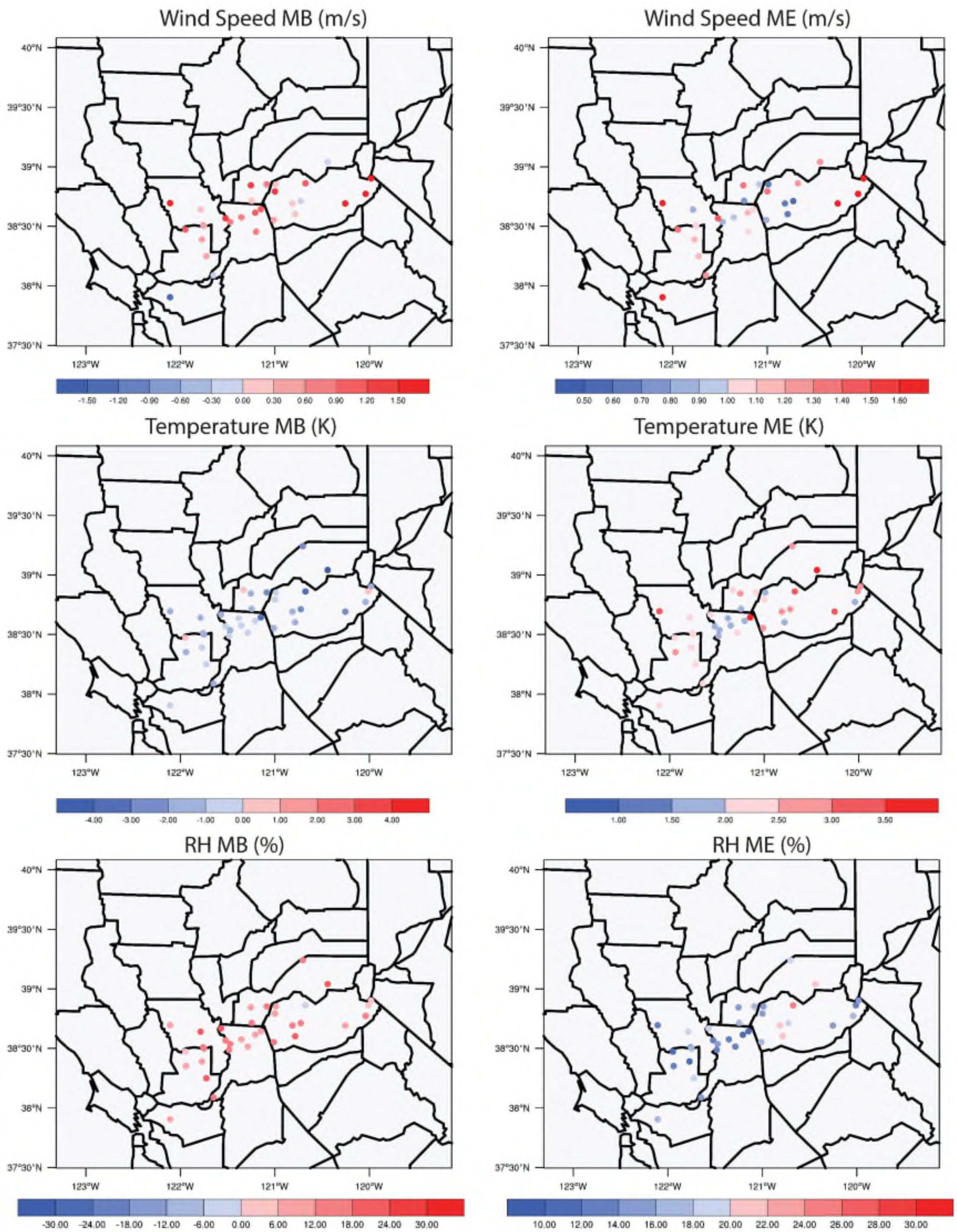

Figure B-10. Comparison of modeled and observed hourly wind speed (left), 2-meter temperature (center), and relative humidity (right) for valley stations (top) and mountain stations (bottom) for April – October 2018.

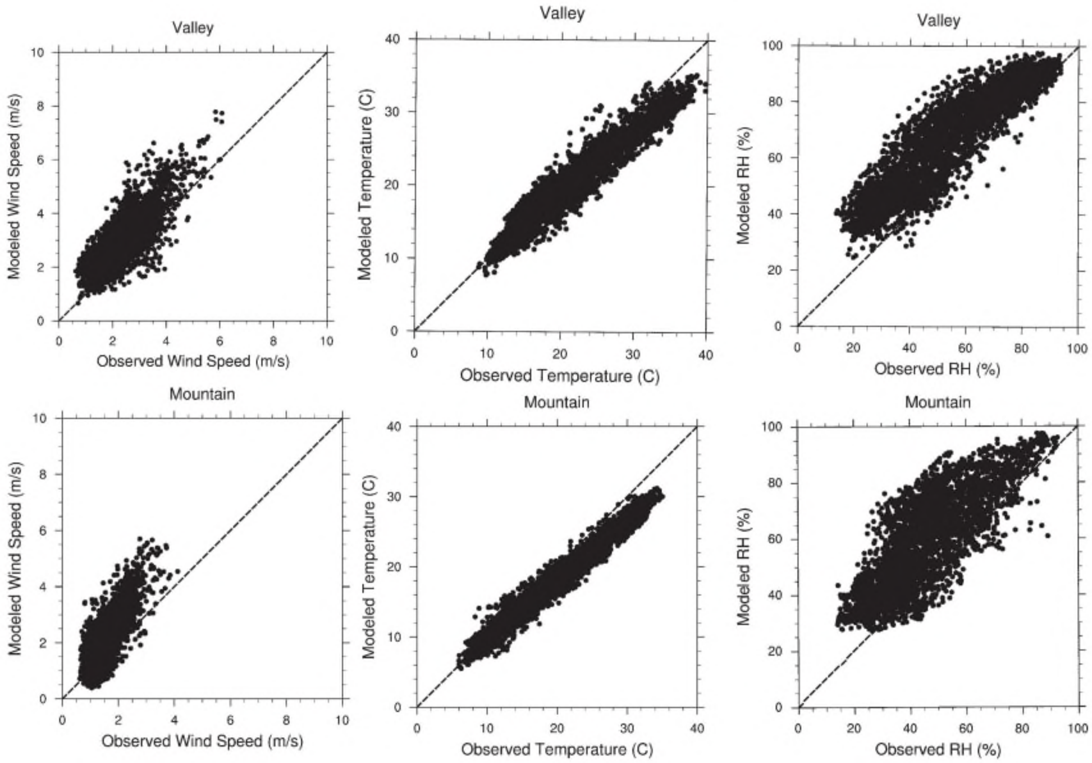

B.1.3.2 Phenomenological Evaluation

Conducting a detailed phenomenological evaluation for all modeled days can be resource intensive given that the entire ozone season (April – October) was modeled for the attainment demonstration. However, some insight and confidence that the model is able to reproduce the meteorological conditions leading to elevated ozone can be gained by investigating the meteorological conditions during peak ozone days within the SFNA in more detail.

As described in B.1.2, the Placerville-Gold monitoring site located in Sacramento Valley has the highest average DV in SFNA (Table B-2). Meteorological conditions that produced peak ozone levels in the area occurred on August 2, 2018, with a daily maximum 8-hour ozone mixing ratio of 99 ppb observed at the Placerville-Gold monitoring site. The upper-air weather charts showed that a 500 mb high pressure system was observed over California. The pressure gradient of this system was weak and the daytime temperature at the Placerville-Gold monitoring site reached 93 ˚F. Figure B-11 shows the surface wind fields in the early afternoon (13:00 PST) and the evening (20:00 PST) on the highest ozone day (August 2, 2018) at the Placerville-Gold site with the observed and modeled values denoted by red and black arrows, respectively. Overall, modeled winds compare relatively well with the observed values. The model was able to capture many of the important features of the wind fields in the SFNA. For most summer days, marine air penetrates inland through the Carquinez Strait, and then the marine air flow splits into northward flows up in the Sacramento Valley and southward flows down in the SJV due to the blocking effect of the Sierra mountain range. The daytime southwesterly wind in the Sacramento Valley was well reproduced by the model on August 2, 2018. The changes of the up-slope wind in the early afternoon and down-slope wind in the evening are also reproduced reasonably well in the model over the western slope of the Sierras.

Since RRF calculations in the model attainment test described previously are based on the top 10 peak ozone days, the modeled and measured winds in the region were examined in further detail for the top 10 ozone days observed at the Placerville-Gold monitor in 2018. The ten highest maximum daily average 8-hour ozone mixing ratios observed at the Placerville-Gold site in 2018 occurred on August 2, August 9, August 10, August 8, August 5, August 1, September 21, July 31, August 25, July 28, respectively. Figure B-12 shows the mean wind field (vector average) for the top 10 ozone days at 05:00 PST and 13:00 PST, respectively. Overall, the surface wind distribution indicates that the model is in general agreement with the observations and is able to capture important features of the observed meteorological fields, such as the daytime southwesterly winds in the valley associated with the marine air penetration as well as the daytime up-slope and nighttime down-slope wind over the western side of the Sierras, on those days when elevated ozone levels occurred.

Figure B-11 Surface wind field at 13:00 PST (top) and 20:00 PST (bottom) on August 02, 2018. The modeled wind field is shown with black wind vectors, while observations are shown in red.

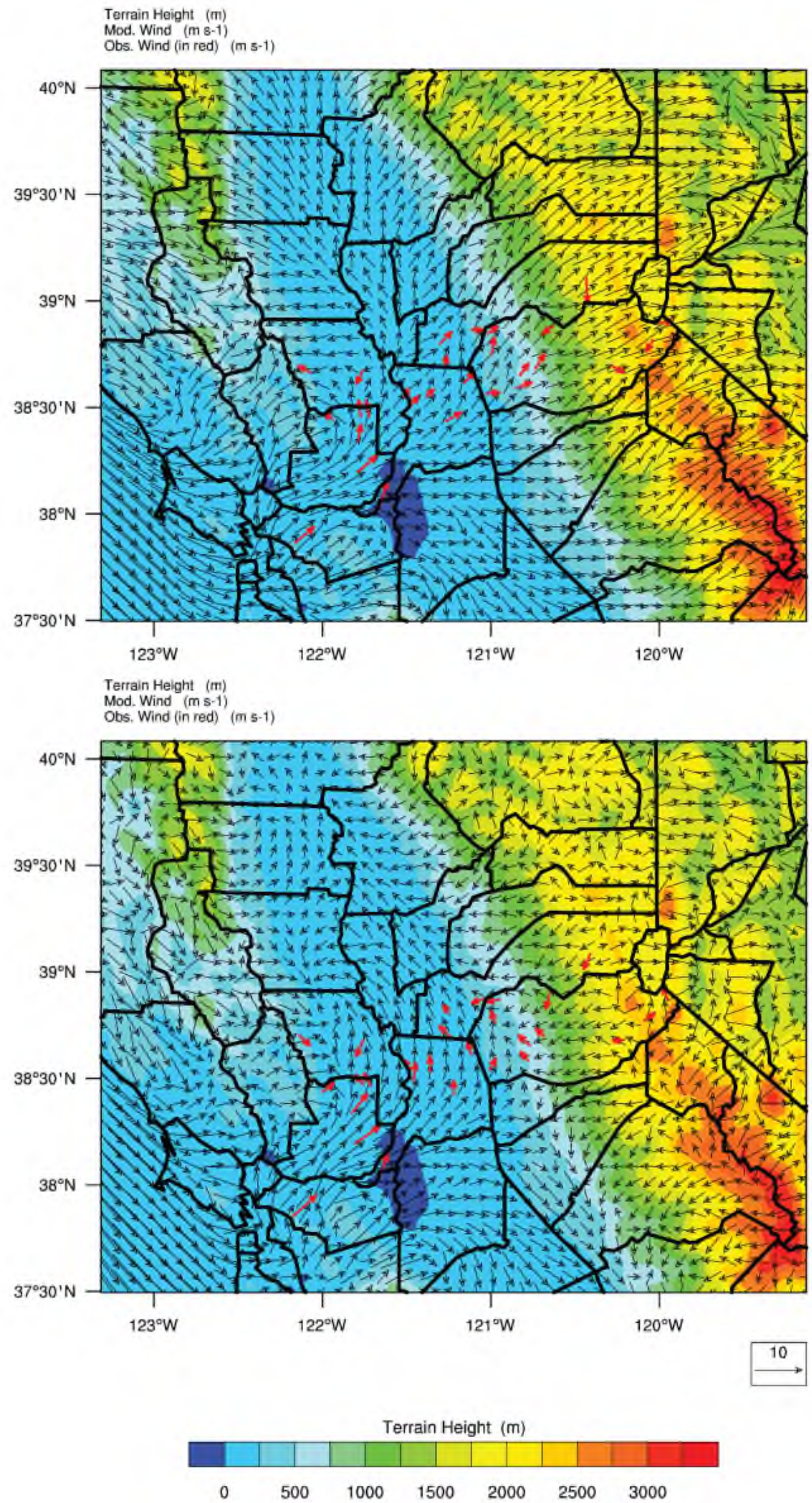

Figure B-12. Average wind field at 5:00 PST (top) and 13:00 PST (bottom) for the top 10 observed ozone days at Placerville-Gold monitor in 2018. Modeled wind field is shown with black wind vectors, while observations are shown in red.

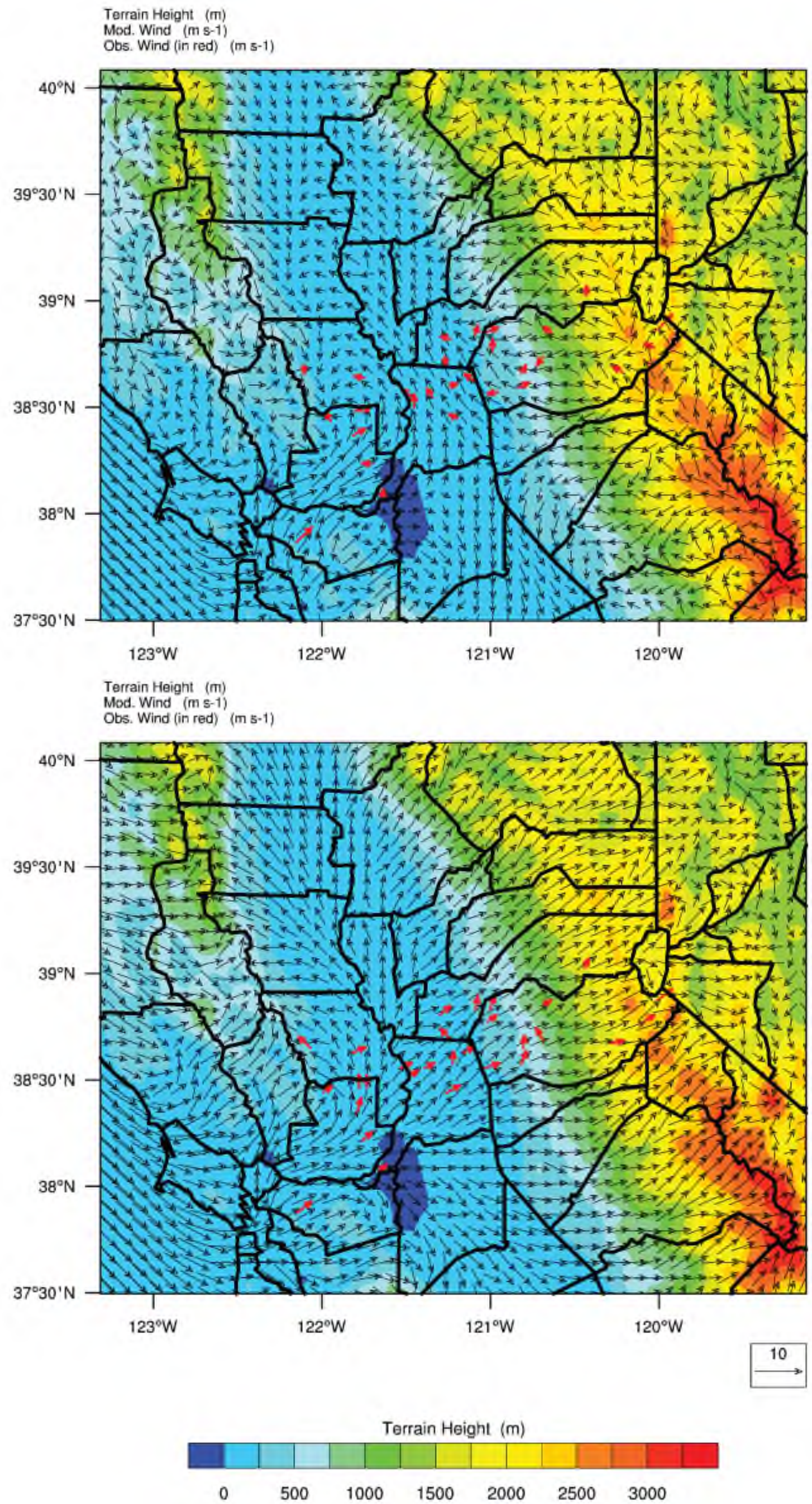

In addition, it is useful to examine the direction of predominant wind flow, through wind rose plots, on peak ozone days to ensure the same transport patterns from source to receptor observed in the atmosphere are also captured in the model. Figure B-13 shows the observed and simulated wind speed frequency and direction at the Placerville-Gold site for the top 10 ozone days in 2018. The Placerville-Gold site is located at the foothills of the western slope of the Sierras. From Figure B-13, it is clear that the dominant observed wind flow pattern on peak ozone days shows daytime up-slope wind (wind from the west/south-west and wind from the west) and nighttime down-slope wind (wind from the north/north-east and wind from the east). The model predicted higher occurrences of winds from the west, and lower occurrences of winds from the west/south-west compared to observations. It is more difficult for the model to reproduce wind fields at mountain sites due to limitations in representing unresolved topographical features and their affects on land surface process and the momentum flux. Despite a little discrepancy (~30 deg) in the dominant wind direction, the model was generally able to reproduce the wind directions and wind speeds at Placerville-Gold for the top 10 ozone days in 2018.

Figure B-13. Observed (left) and modeled (right) wind roses at the Placerville-Gold site for the top 10 observed ozone days in 2018.

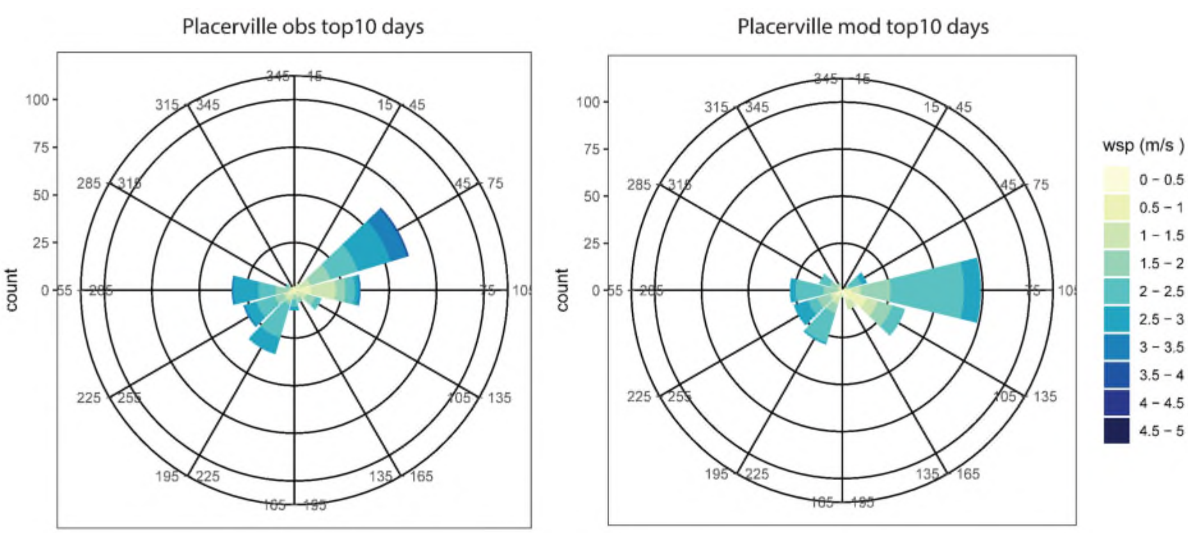

Figure B-14 shows the 500 hPa geopotential height at 12:00 UTC and 00:00 UTC for the top 10 ozone days in 2018 at the Placerville-Gold site. These times were chosen to coincide with timing of the upper-air observations. In this figure, the North American Regional Reanalysis (NARR) data is used to represent the observations. The NARR dataset is a product of observational data assimilated into some of the NOAA model products for the purpose of producing a snapshot of the weather over North America at any given time. The 500 hPa geopotential height is a useful metric to evaluate, because most weather systems follow the winds at this level. It can be seen from Figure B-14 that on average the 500 hPa geopotential height is ~5800 m above sea level and the modeled 500 hPa geopotential height closely matches the observed values.

Although a phenomenological evaluation of only a subset of peak ozone days does not necessarily mean the model performs equally well on all days, the fact that the model can adequately reproduce wind flows consistent with the ozone conceptual model, combined with reasonable performance statistics over the ozone season (Table B-8), provides added confidence in the meteorological fields utilized for this attainment demonstration modeling.

Figure B-14. Modeled and observed at 12:00 UTC (top) and 00:00 UTC (bottom) 500 hPa geopotential height for the top 10 observed ozone days at the Placerville-Gold site in 2018.

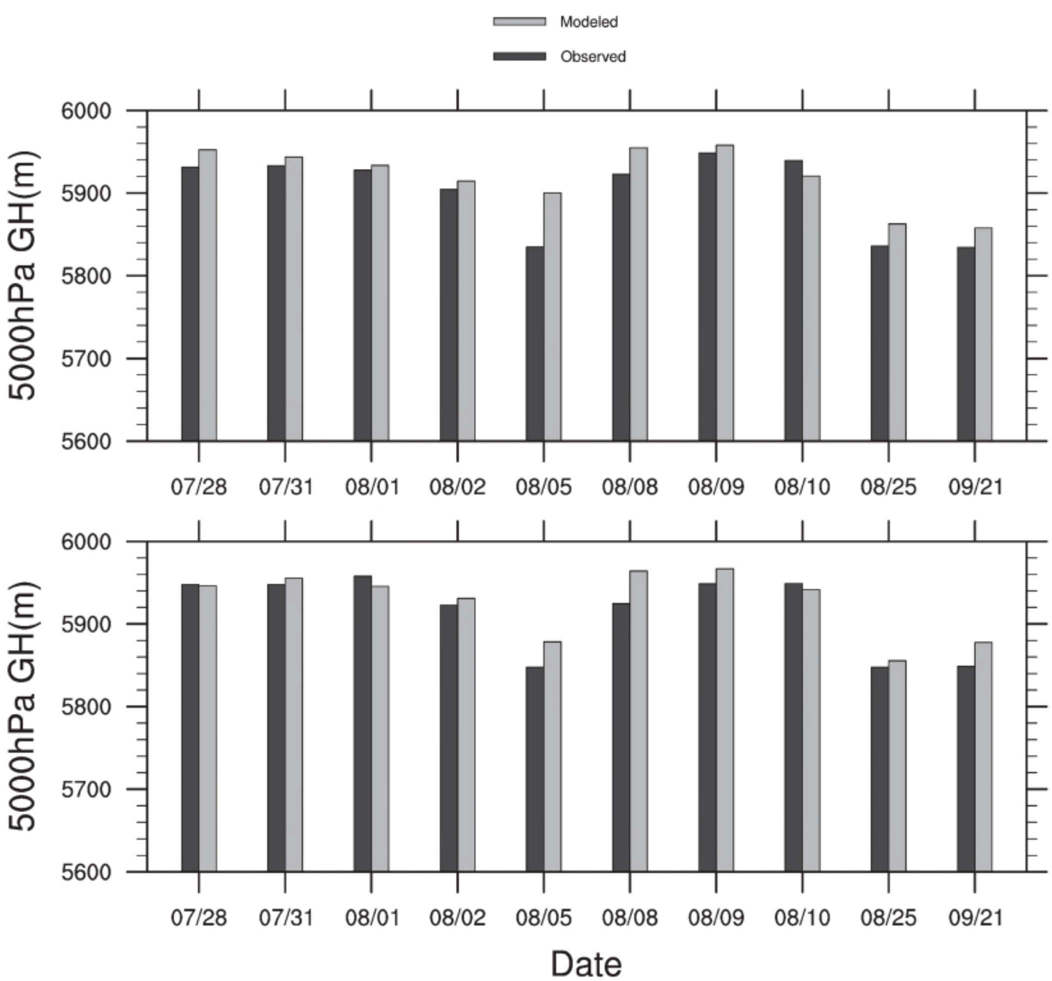

B.1.3.3 Air Quality Model Evaluation

Observed ozone data from CARB's Air Quality and Meteorological Information System (AQMIS) database (www.arb.ca.gov/airqualitytoday/) and Aerometric Data Analysis and Management (ADAM) database (www.arb.ca.gov/adam/) were used to evaluate the accuracy of the 4 km CMAQ modeling for all ozone monitors listed in Table B-2. The EPA modeling guidance (EPA, 2018) recommends using the grid cell value where the monitor is located, to pair observations with simulated values in operational evaluation of model predictions. Since the future year design value calculations are based on simulated values near the monitor (i.e., the maximum simulated ozone within a 3x3 array of grid cells with the grid cell containing the monitor located at the center of the array), model performance was evaluated by comparing observations against the simulated values at the monitored grid cell as well as the peak grid cell within the 3x3 grid array centered on the monitor (i.e., the 3x3 maximum). While different cutoff criteria have be used in different model evaluation studies (Emery et al., 2017), EPA suggests the days with simulated values > 60 ppb should receive higher priority in evaluation to give more attention to the model outputs that could potentially impact the outcome of the attainment test. Model performance is further summarized separately for the three sub-regions in the SFNA due to their distinct geographical, meteorological and air quality patterns.

As recommended by EPA modeling guidance, a number of statistical metrics have been used to evaluate the model performance for ozone. These metrics include mean bias (MB), mean error (ME), mean fractional bias (MFB), mean fractional error (MFE), normalized mean bias (NMB), normalized mean error (NME), root mean square error (RMSE), and correlation coefficient (R^2). In addition, the following plots were used in evaluating the modeling with all available data: time-series plots comparing the predictions and observations, scatter plots for comparing the magnitude of the simulated and observed concentrations, as well as frequency distributions.

The model performance evaluation is presented for the entire SFNA region and also disaggregated for the three sub regions. Performance statistics for modeling scenarios with data above 60 ppb are reported separately for different ozone metrics including maximum daily average 8-hour (MDA8) ozone, maximum daily average 1-hour (MDA1) ozone, and hourly ozone (all hours of the day) for the monitored grid cell as well as the 3x3 maximum. Performance statistics for MDA8 ozone are shown in Table B-9 and Table B-10. Overall, when simulated data extracted at the grid cell is used for comparison with observations (as shown in Table B-9), the model shows a negative bias of -3.36 ppb in MDA8 O_3 greater than 60 ppb in the entire region, with the smallest bias occurring in the central SFNA (0.40 ppb) and the largest bias occurring in the eastern SFNA (-5.85 ppb). However, when the 3x3 maximum is used instead, positive bias in the model results increases to 2.65 ppb in central SFNA and the bias in eastern SFNA reduces to -4.14 ppb. Mean error shows a consistent trend with the error getting smaller from 7.98 ppb to 7.84 ppb for the entire SFNA when the 3x3 maximum is considered. Similar statistics for maximum daily average 1-hour ozone (monitor grid cell and 3x3 maximum) and hourly ozone can be found in Table B-11and Table B-12, respectively.

Model performance statistics with the range of values shown in Table B-9 to Table B-13 are consistent with previous studies in California and studies elsewhere in the U.S. Hu et al. (2012) simulated an ozone episode in central California (July 27 – August 2, 2000) using the SAPRC07 chemical mechanism and found a model bias of -10.8 ppb for maximum daily average 8-hour ozone with 60 ppb cutoff (compared to -3.36 ppb for the entire SFNA of this work). Hu et al. also showed a model bias of -12.7 ppb for maximum daily average 1-hour ozone in Central California with 60 ppb cutoff (compared to -2.64 ppb in this work).

Similarly, Shearer et al. (2012) compared model performance in Central California during two episodes in 2000 (July 24 – 26 and July 31 – August 2) for two different chemical mechanisms and found that normalized bias for maximum daily average 8-hour ozone ranged from -7% to -14% with hourly peak ozone showing a range of -7% to -18%. These values are greater than the statistics found in this work, which were calculated as -4.86% for MDA8 ozone and -3.66% for MDA1 ozone. Jin et al. (2010) conducted a longer term simulation over Central California (summer 2000) and found a RMSE for MDA8 ozone of 14 ppb, which is greater than the 11.08 ppb found in this work. Jin et al. (2010) also showed an overall negative bias of -2 ppb, which is in the similar range of -3.36 ppb (-1.47 ppb with 3x3 maximum values) found in this work. Zhu et al. (2019) shows hourly O_3 NMB of 8.2% and NME of 11.3% for July and August 2012 with 20 ppb cutoff, both are similar to the NMB and NME shown in Table B-13.

Table B-9. Maximum daily average 8-hour ozone performance statistics by modeling subregions and entire SFNA region for the 2018 ozone season (April - October). Maximum daily average 8-hour ozone (>60ppb) with simulated data extracted at grid cell where the monitor is located.

Parameter	Western SFNA	Central SFNA	Eastern SFNA	Entire SFNA
Number of data points	44	208	329	581
Mean obs (ppb)	64.68	67.26	70.77	69.05
Mean Bias (ppb)	-2.46	0.40	-5.85	-3.36
Mean Error (ppb)	6.09	6.53	9.16	7.98
RMSE (ppb)	7.76	8.15	12.91	11.08
Mean Fractional Bias (%)	-3.95	0.42	-8.45	-4.93
Mean Fractional Error (%)	9.54	9.66	13.28	11.70
Normalized Mean Bias (%)	-3.81	0.59	-8.26	-4.86
Normalized Mean Error (%)	9.42	9.71	12.94	11.56
R-squared	0.05	0.12	0.09	0.08

Table B-10. Maximum daily average 8-hour ozone performance statistics by modeling subregions and entire SFNA region for the 2018 ozone season (April - October). Maximum daily average 8-hour ozone (>60ppb) with simulated data extracted from the 3x3 grid cell array maximum centered at the monitor.

Parameter	Western SFNA	Central SFNA	Eastern SFNA	Entire SFNA
Number of data points	44	208	329	581
Mean obs (ppb)	64.68	67.26	70.77	69.05
Mean Bias (ppb)	-1.04	2.65	-4.14	-1.47
Mean Error (ppb)	5.81	7.03	8.63	7.84
RMSE (ppb)	7.49	8.58	12.00	10.59
Mean Fractional Bias (%)	-1.71	3.69	-5.88	-2.14
Mean Fractional Error (%)	9.01	10.21	12.36	11.33
Normalized Mean Bias (%)	-1.61	3.93	-5.84	-2.13
Normalized Mean Error (%)	8.98	10.45	12.19	11.36
R-squared	0.06	0.14	0.12	0.10

Table B-11. Maximum daily average 1-hour ozone performance statistics by modeling subregions and entire SFNA region for the 2018 ozone season (April - October). Maximum daily average 1-hour ozone (>60ppb) with simulated data extracted at grid cell where the monitor is located.

Parameter	Western SFNA	Central SFNA	Eastern SFNA	Entire SFNA
Number of data points	192	431	437	1060
Mean obs (ppb)	68.07	71.69	74.29	72.10
Mean Bias (ppb)	-1.44	-0.49	-5.29	-2.64
Mean Error (ppb)	7.66	8.57	9.78	8.90
RMSE (ppb)	9.59	10.96	13.53	11.87
Mean Fractional Bias (%)	-2.55	-0.78	-7.34	-3.81
Mean Fractional Error (%)	11.43	11.89	13.48	12.46
Normalized Mean Bias (%)	-2.12	-0.68	-7.12	-3.66
Normalized Mean Error (%)	11.25	11.95	13.17	12.35
R-squared	0.12	0.20	0.20	0.19

Table B-12. Maximum daily average 1-hour ozone performance statistics by modeling subregions and entire SFNA region for the 2018 ozone season (April - October). Maximum daily average 1-hour ozone (>60ppb) with simulated data extracted from the 3x3 grid cell array maximum centered at the monitor.

Parameter	Western SFNA	Central SFNA	Eastern SFNA	Entire SFNA
Number of data points	192	431	437	1060
Mean obs (ppb)	68.07	71.69	74.29	72.10
Mean Bias (ppb)	0.71	2.81	-2.77	0.13
Mean Error (ppb)	7.72	9.15	9.41	9.00
RMSE (ppb)	9.63	11.64	12.66	11.75
Mean Fractional Bias (%)	0.62	3.64	-3.84	0.01
Mean Fractional Error (%)	11.27	12.35	12.73	12.31
Normalized Mean Bias (%)	1.04	3.92	-3.73	0.18
Normalized Mean Error (%)	11.34	12.76	12.67	12.48
R-squared	0.12	0.21	0.23	0.20

Table B-13. Hourly ozone performance statistics by modeling subregions and entire SFNA region for the 2018 ozone season (April - October). Hourly ozone (>60ppb) with simulated data extracted at grid cell where the monitor is located. Note that only statistics for the grid cell in which the monitor is located were calculated for hourly ozone.

Parameter	Western SFNA	Central SFNA	Eastern SFNA	Entire SFNA
Number of data points	648	1940	3435	6023
Mean obs (ppb)	66.70	69.20	70.69	69.78
Mean Bias (ppb)	-3.84	-1.85	-9.61	-6.49
Mean Error (ppb)	8.58	8.63	12.53	10.85
RMSE (ppb)	11.06	11.12	16.43	14.39
Mean Fractional Bias (%)	-6.57	-3.15	-15.30	-10.45
Mean Fractional Error (%)	13.52	12.70	19.43	16.62
Normalized Mean Bias (%)	-5.76	-2.68	-13.59	-9.30
Normalized Mean Error (%)	12.87	12.47	17.72	15.54
R-squared	0.04	0.12	0.09	0.08

Simon et al. (2012) conducted a review of photochemical model performance statistics published between 2006 and 2012 for North America (from 69 peer-reviewed articles). Figure B-15 illustrates the range of various statistical performance metrics presented in Simon et al. (2012), where we have overlayed the same statistical metrics calculated from the modeling used for this attainment demonstration. The box-and-whisker plots (colored in black) displayed in Figure B-15 were reproduced using data extracted from Figure 4 of Simon et al. (2012). The red dot and blue triangle in each of the panels in Figure B-15 denote the model performance statistics from the current modeling work, calculated using the simulated monitor grid cell and the 3x3 maximum, respectively.

Figure B-15. Comparison of various statistical metrics from the attainment demonstration modeling to the range of statistics from the 69 peer-reviewed studies summarized in Simon et al (2012). (MDA denotes Maximum Daily Average). Red circular markers show statistics calculated from modeled ozone at the monitor location, while blue triangular markers show statistics calculated from the maximum ozone in the 3x3 array of grid cells surrounding the monitor. Statistics for hourly ozone were only calculated from data over 60 ppb.

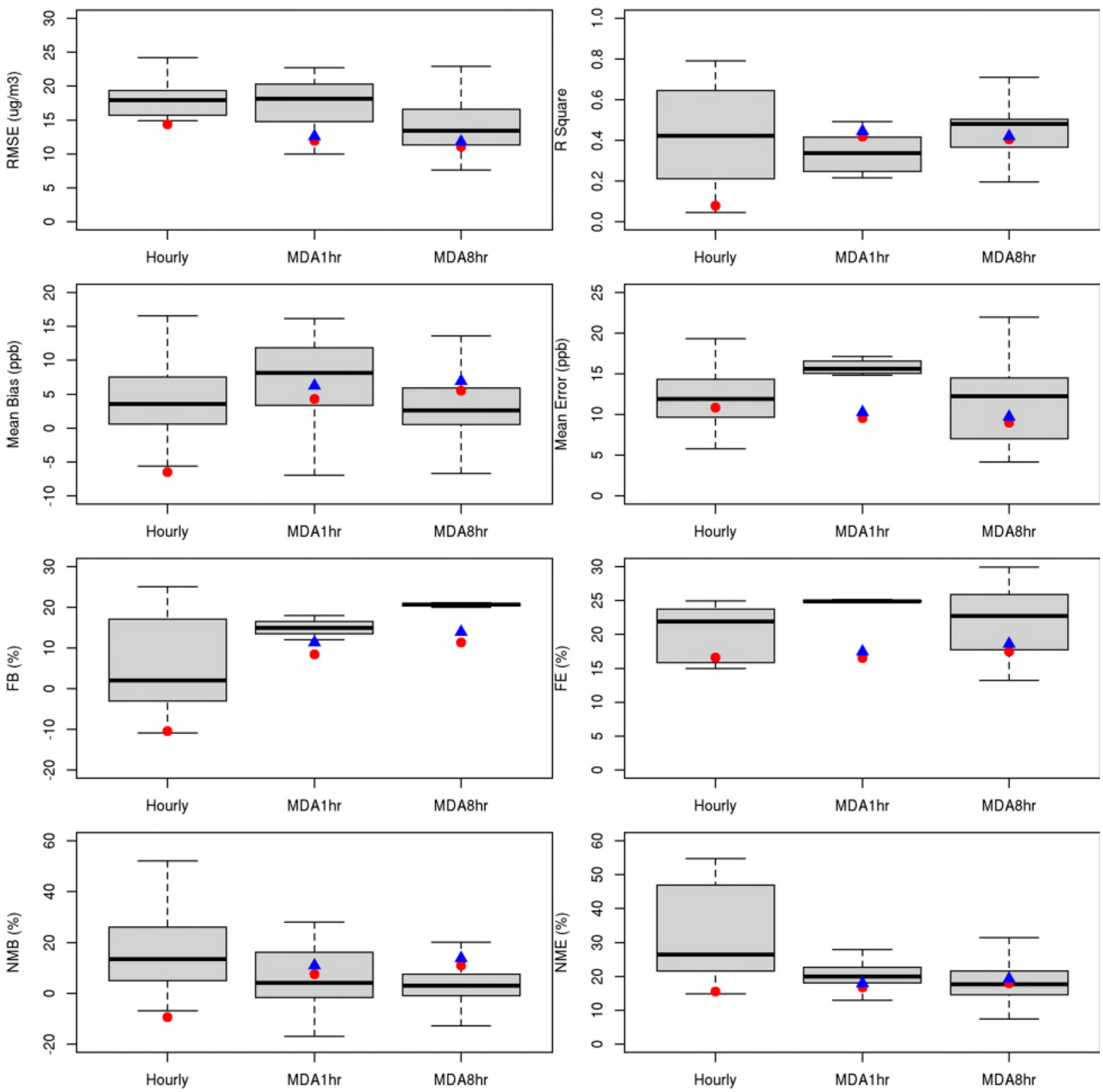

Figure B-15 clearly shows that the model performance statistical metrics for hourly, maximum daily average 8-hour and maximum daily 1-hour ozone from this work are consistent with previous modeling studies reported in the scientific literature, and in most cases are better than those statistics. In particular, the Simon et al. (2012) study found that mean bias for maximum daily average 8-hour ozone ranged from approximately -7 ppb to 13 ppb, while mean error ranged from around 4 ppb to 22 ppb, and RMSE varied from approximately 8 ppb to 23 ppb; all of which are similar in magnitude to the statistics presented in Table B-9 and Table B-10.

Spatial distributions of modeled and observed average maximum daily average 8-hour ozone for the top 10 O_3 days at the Placerville-Gold site are displayed in Figure B-16. The model is able to capture the observed spatial gradient of ozone in the modeling domain with reasonable agreement between the model and observation. Additional analysis including frequency analysis, time series plots and scatter plots of the hourly, maximum daily average 1-hr and maximum daily average 8-hour ozone at sites in the SFNA can be found in the supplemental materials. The model performance shown in these plots is consistent with the statistical analysis above. Observed and modeled daily average NO_X scatter plot for the SFNA is also shown in Figure S 60 in the supplemental materials which demonstrates decent agreement between modeled and observed NO_X concentrations.

Figure B-16. Average MDA8 ozone for the top 10 ozone days excluding fire days that impacted Auburn in 2018 from the model simulations overlaid with observation data (marked as circle) where the top 10 days from the observations were chosen based on the Placerville-Gold site.

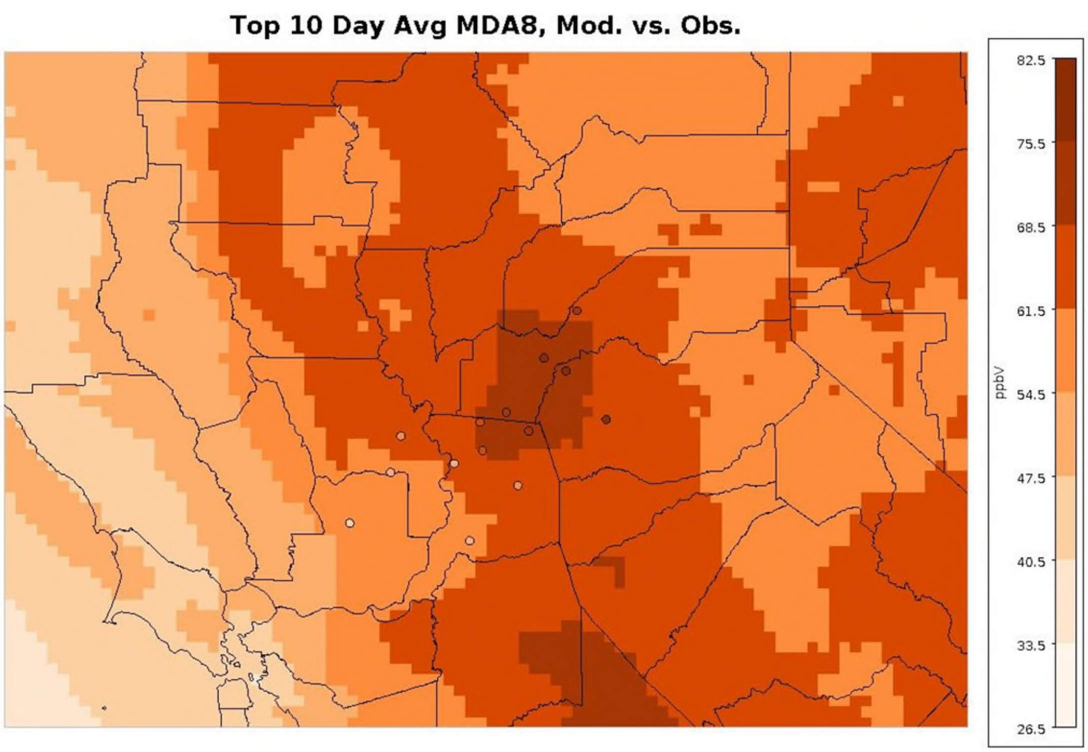

B.1.3.4 Air Quality Model Diagnostic Evaluation

In addition to the statistical evaluation presented above, since the modeling is utilized in a relative sense, it is also useful to consider whether the model is able to reproduce observable relationships between changes in emissions and ozone. One approach to this would be to conduct a retrospective analysis where additional years are modeled (e.g., 2000 or 2005) and then investigate the ability of the modeling system to reproduce the observed changes in ozone over time. Since this approach is extremely time consuming and resource intensive, it is generally not feasible to perform such an analysis under the constraints of a typical SIP modeling application. An alternative approach for investigating the ozone response to changes in emissions is through the so called “weekend effect”.

The “weekend effect” is a well-known phenomenon in some major urbanized areas where emissions of NO_X are substantially lower on weekends than on weekdays, but measured levels of ozone are higher on weekends than on weekdays. This is due to the complex and non-linear relationship between NO_X and ROG precursors and ozone (e.g., Sillman, 1999).

In general terms, under ambient conditions of high-NO_X and low-ROG (NO_X-disbenefit region in Figure B-17) ozone formation tends to exhibit a disbenefit to reductions in NO_X emissions (i.e., ozone increases with decreases in NO_X) and a benefit to reductions in ROG emissions (i.e., ozone decreases with decreases in ROG). In contrast, under ambient conditions of low-NO_X and high-ROG (NO_X-limited region in Figure B-17), ozone formation shows a benefit to reductions in NO_X emissions, while reducing ROG emissions results in only minor decreases in ozone. These two distinct “ozone chemical regimes” are illustrated in Figure B-17 along with a transitional regime that can exhibit characteristics of both the NO_X-disbenefit and NO_X-limited regimes. Note that Figure B-17 is shown for illustrative purposes only and does not represent the actual ozone sensitivity within the SFNA for a given combination of NO_X and ROG (VOC) emissions.

In this context, the prevalence of a weekend effect in a region suggests that the region is in a NO_X-disbenefit regime (Heuss et al., 2003). A lack of a weekend effect (i.e., no pronounced high O_3 occurrences during weekends) would suggest that the region is in a transition regime and moving between exhibiting a NO_X-disbenefit and being NO_X-limited. A reverse weekend effect (i.e., lower O_3 during weekends) would suggest that the region is NO_X-limited.

Investigating the “weekend effect” and how it has changed over time is a useful real-world metric for evaluating the ozone chemistry regime in the SFNA and how well it is represented in the modeling. The trend in day-of-week dependence of SFNA’s sub-regions was analyzed using the ozone observations between 2000 and 2020 and the average site-specific weekday (Wednesday and Thursday) and weekend (Sunday) observed summertime (June through September) average MDA8 ozone values by year

(2000 to 2020) are compared (Figure B-18). Different definitions of weekday and weekend days were also investigated and did not show appreciable differences from the Wednesday/Thursday and Sunday definitions.

Figure B-17. Illustration of a typical ozone isopleth plot, where each line represents ozone mixing ratio, in 10 ppb increments, as a function of initial NO_X and VOC (or ROG) mixing ratio (adapted from Seinfeld and Pandis. 1998, Figure 5.15). General chemical regimes for ozone formation are shown as NO_X-disbenefit (red circle), transitional (blue circle), and NO_X-limited (green circle).

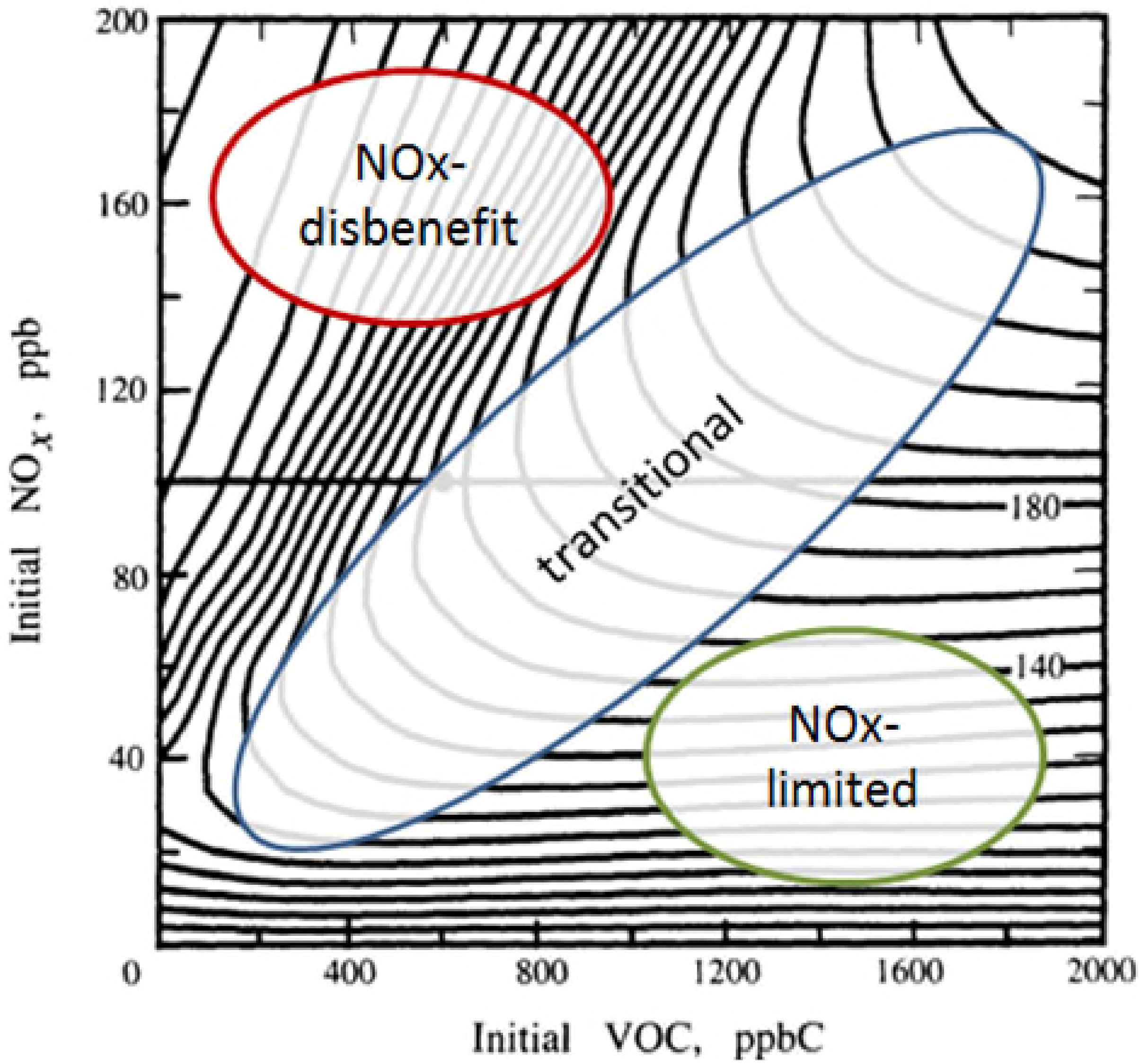

In Figure B-18, it can be seen that ozone levels are highest in the eastern (bottom left panel) and central (middle left panel) regions of the SFNA consistent with their location downwind to and within the urban core of the SFNA. The lowest ozone levels are seen in the western SFNA region, which is located upwind of the urban Sacramento emissions source. A key observation in left panels of Figure B-18 is that the summertime average weekday and weekend MDA8 ozone levels have steadily declined between 2000 and 2020.

Along with the declining ozone, there was a shift in the relative difference between weekday and weekend ozone from 2000 to 2020. In the early 2000's, the central region of the SFNA exhibited a roughly equal number sites with weekend ozone greater than weekday ozone as sites with weekday ozone greater than weekend ozone, which suggests that the region may have been in a transitional chemistry regime for ozone formation. By the mid-2000's, the majority of sites were showing weekday ozone greater than weekend ozone, which is consistent with a shift into NO_X-limited chemistry. However, some of the sites had shifted back towards a more equal distribution between weekday and weekend ozone in recent years, likely due to variability in the biogenic emissions and meteorology that can shift the ozone chemistry between NO_X-limited and NO_X-disbenefit regimes in the Sacramento area (LaFranchi et al., 2011; Wu, et al, 2022).

The Western SFNA region clearly experienced a greater NO_X-disbenefit in the early 2000's and then moved into a transitional chemical regime in the mid-2000's and transitioned into the NO_X-limited regime around the 2010/2011 timeframe. There was a shift back towards a more equal distribution between weekday and weekend ozone in some years after 2010, similar to the Central sub-region. However, this shift occurred at very low ozone levels (below 50 ppb) that are well below the 70 ppb 8-hour ozone standard.

In contrast to the central and western regions described above, the eastern portion of SFNA has been in a NO_X-limited regime since before 2000, which can be seen from the greater weekday ozone when compared to the weekend ozone. This region is in close proximity to large biogenic ROG emission sources and farther away from the anthropogenic NO_X sources in the urban Sacramento Metropolitan Area (SMA), which are conditions (i.e., low NO_X and high ROG) that place the region in a NO_X-limited regime.

The right panels of Figure B-18 show that all three sub-regions had almost fully transitioned to the NO_X-limited regime by 2018 except for some sites in the Central and Eastern regions, which continue to oscillate (middle and bottom right panels) falling above, close to or below the 1:1 dashed line depending on the year, and likely due to the year-to-year variability in meteorology and associated changes in biogenic ROG emissions. The simulated baseline 2018 weekday/weekend values (black open square markers shown in right panels of Figure B-18) from the attainment demonstration modeling fall above the 1:1 dashed line in the Western, Central and Eastern SFNA and are generally consistent with observed findings that show a shift into NO_X-limited chemistry in the SFNA.

The predicted future 2032 values (light gray open triangle markers in right panels of Figure B-18) clearly show that weekday and weekend ozone decline significantly (all values are below 60 ppb) and all three sub-regions show a shift to a NO_X-limited regime with values falling closer to but above the 1:1 dashed line, which is generally consistent with a study from UC Berkeley researchers that predicted the future cumulative NO_X controls over time will likely transition the entire SFNA (including the urban core) to a NO_X limited regime (LaFranchi et al., 2011).

Figure B-18. Site-specific average weekday and weekend maximum daily average 8-hour ozone for each year from 2000 to 2020 in the Western (top), Central (middle), and Eastern (bottom) sub-regions of SFNA. The colored circle markers denote observed values while the open black square, and gray triangle markers denote the simulated baseline 2018 and future year 2032 values. Points falling below the 1:1 dashed line represent a NO_X-disbenefit regime, those on the 1:1 dashed line represent a transitional regime, and those above the 1:1 dashed line represent a NO_X-limited regime.

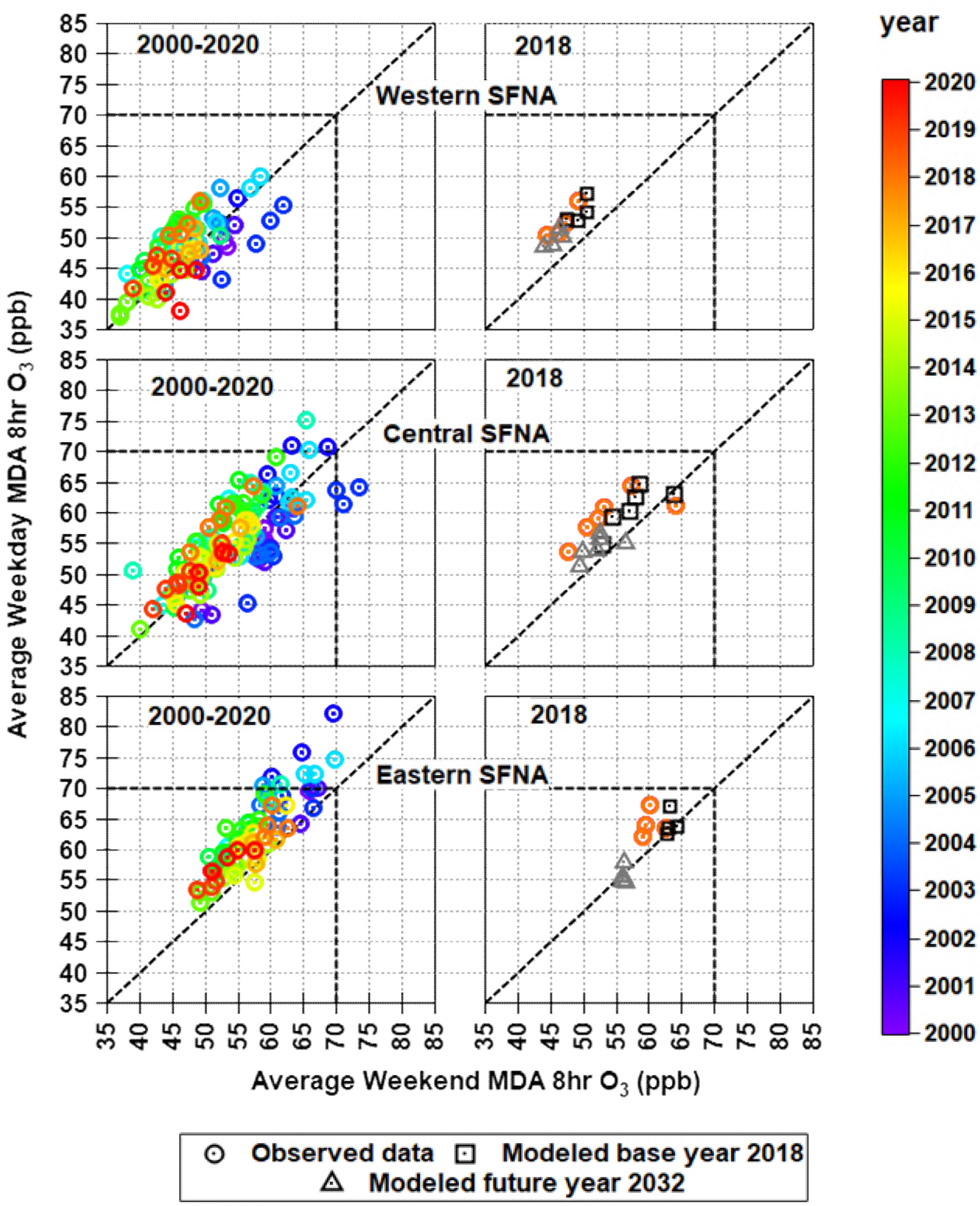

B.1.3.5 Future Design Values in 2032

The RRFs and the 2032 future ozone design values for the monitoring sites in the western, central, and eastern regions of the SFNA were calculated using the procedures outlined in the Methodology section of this document and are summarized in Table B-14. Note that the results shown in the table are ordered by each sub-region in descending order of the average reference year 2018 DVs except for the Auburn-Atwood site.

The results in Table B-14 show that all monitoring sites in the SFNA have a future DV less than 70 ppb based on the 2032 emissions inventory when fire days are excluded in the Auburn-Atwood site DV calculation. The Colfax-CityHall site in the eastern SFNA has the highest predicted future design value of 69.8 ppb and truncated value of 69 ppb in 2032. Therefore, the attainment demonstration modeling predicts that the entire SFNA will attain the 70 ppb 8-hour O_3 standard by 2032 with the commitments outlined in the SIP.

Table B-14. Summary of key parameters related to the future year 2032 ozone design value (DV) calculation.

Sub-region	Site	RRF	2018 Average DV (ppb)	2032 DV (ppb)	2032 Truncated DV (ppb)
Eastern SFNA	Placerville-Gold	0.8283	84.0	69.6	69
Eastern SFNA	Colfax-CityHall	0.8334	83.7	69.8	69
Eastern SFNA	Cool-Hwy193	0.8353	81.7	68.2	68
Eastern SFNA	Auburn-Atwood,fire days excluded	0.8356	81.7	68.3	68
Eastern SFNA	Auburn-Atwood, all days	0.8356	87.3	72.9	72
Central SFNA	Folsom-Natoma	0.8433	76.7	64.7	64
Central SFNA	Roseville-NSunrise	0.8408	76.3	64.2	64
Central SFNA	N_Highlands-Blackfoot	0.8674	74.7	64.8	64
Central SFNA	Sacramento-DelPas	0.8662	72.0	62.4	62
Central SFNA	Sloughhouse	0.8708	71.3	62.1	62
Central SFNA	Sacramento-TStreet	0.9053	66.3	60.0	60
Western SFNA	Elk_Grove-Bruceville	0.9127	67.7	61.8	61
Western SFNA	Woodland-Gibson	0.8750	66.7	58.4	58
Western SFNA	Vacaville-Ulatis	0.9100	64.0	58.2	58
Western SFNA	Davis-UCD	0.9063	62.3	56.5	56

B.1.3.6 NO_X/VOC Sensitivity Analysis for Reasonable Further Progress (RFP)

For the Clean Air Act 182(c)(2)(B) Reasonable Further Progress (RFP) requirement for areas classified as Serious nonattainment and above, EPA guidance allows for NO_X substitution to demonstrate the annual 3 percent reduction of ozone precursors if it can be demonstrated that substitution of NO_X emission reductions (for ROG reductions) yield equivalent decreases in ozone. Additional EPA guidance states that certain conditions are needed to use NO_X substitution in an RFP demonstration (EPA 1993). First, an equivalency demonstration must show that cumulative RFP emission reductions are consistent with the NO_X and ROG emission reductions determined in the ozone attainment demonstration. Second, the reductions in NO_X and ROG emissions should be consistent with the continuous RFP emission reduction requirement.

For the equivalency demonstration, ROG and NO_X emissions within the nonattainment area boundary were reduced by 45% (3% for each of the 15 years between the designation year of 2017 and attainment year of 2032) independently from the baseline modeling year of 2018. These sensitivity simulations were used to develop RRFs and design values following the same methodology utilized in the attainment demonstration, where the sensitivity simulation was treated analogous to the future year. Table B-15 summarizes the design values calculated for the 45% NO_X and ROG sensitivity simulations. At all sites except for Davis-UCD in the SFNA, the ratios of the change in ozone design value to the NO_X emissions change ($\Delta O_3/\Delta NO_X$) are greater than those of the ROG emissions change ($\Delta O_3/\Delta ROG$). Davis-UCD site has the lowest 2018 average DV (62.3 ppb) in the SFNA. When ozone concentrations are this low, the ozone-NO_X-VOC sensitivity becomes more meteorology dependent. In fact, for the sites with 2018 average DV greater than 65 ppb, most of $\Delta O_3/\Delta NO_X$ can be an order of magnitude larger than $\Delta O_3/\Delta ROG$. Since the ozone improvement from NO_X reductions is greater than that for ROG reductions, the use of NO_X substitution will result in improved ozone air quality.

Table B-15. Summary of the ozone improvement from the 45% emissions reductions at the monitoring sites in the SFNA.

Sub-region	Site	2018 Average DV (ppb)	DV After 45% NO_X Reductions (ppb)	$\Delta O_3/\Delta NO_X$ (ppb/tpd)	DV After 45% ROG Reductions (ppb)	$\Delta O_3/\Delta ROG$ (ppb/tpd)
Eastern SFNA	Placerville-Gold	84.0	76.1	0.2675	83.2	0.0189
Eastern SFNA	Colfax-CityHall	83.7	76.4	0.2472	83.2	0.0118
Eastern SFNA	Cool-Hwy193	81.7	74.8	0.2336	81.0	0.0165
Eastern SFNA	Auburn-Atwood	87.3	80.0	0.2472	85.8	0.0354
Central SFNA	Folsom-Natoma	76.7	70.8	0.1998	75.3	0.0330
Central SFNA	Roseville-NSunrise	76.3	70.8	0.1862	75.2	0.0260
Central SFNA	N_Highlands-Blackfoot	74.7	71.1	0.1219	73.2	0.0354
Central SFNA	Sacramento-DelPas	72.0	68.6	0.1151	70.7	0.0307
Central SFNA	Sloughhouse	71.3	67.6	0.1253	70.0	0.0307
Central SFNA	Sacramento-TStreet	66.3	65.2	0.0372	65.2	0.0260
Western SFNA	Elk_Grove-Bruceville	67.7	66.4	0.0440	67.5	0.0047
Western SFNA	Woodland-Gibson	66.7	63.7	0.1016	65.9	0.0189
Western SFNA	Vacaville-Ulatis	64.0	63.4	0.0203	63.7	0.0071
Western SFNA	Davis-UCD	62.3	61.9	0.0135	61.4	0.0212

B.1.3.7 Unmonitored Area Analysis

The unmonitored area analysis is used to ensure that no regions outside of the existing monitoring network would exceed the NAAQS if a monitor was present (EPA, 2018). EPA recommends combining spatially interpolated design value fields with modeled ozone gradients and grid-specific RRFs in order to generate gridded future year gradient adjusted design values.

This analysis can be done using SMAT-CE (Software for the Modeled Attainment Test – Community Edition, https://www.epa.gov/scram/photochemical-modeling-tools).

However, this software is not open source and comes as a precompiled software package. To maintain transparency and flexibility in the analysis, in-house R codes developed at CARB, were utilized in this analysis.

The unmonitored area analysis was conducted using the 8-hr O_3 weighted DVs from all the available sites that fall within the 4 km inner modeling domain along with the reference year 2018 and future years 2032 4 km CMAQ model output. The steps in the unmonitored area analysis are described below:

> **Step 1**: At each grid cell, the top 10 modeled maximum daily average 8-hour ozone mixing ratios from the reference year simulation were averaged, and a gradient in this top 10 day average between each grid cell and grid cells which contain a monitor was calculated.
> **Step 2**: A single set of spatially interpolated 8-hour ozone DV fields was generated based on the observed 5-year weighted base year 8-hour ozone DVs from the available monitors. The interpolation is done using normalized inverse distance squared weightings from each monitor within the Voronoi regions that boarder that of the grid cell (calculated with the R tripack library), and adjusted based on the gradients between the grid cell and the corresponding monitor from Step 1.
> **Step 3**: At each grid cell, the RRFs are calculated based on the reference- and future-year modeling following the same approach outlined in the Methodology section of this document, except that the +/- 20% limitation on the simulated and observed maximum daily average 8-hour ozone was not applied because observed data do not exist for grid cells in unmonitored areas.
> **Step 4**: The future year gridded 8-hour ozone DVs were calculated by multiplying the gradient-adjusted interpolated 8-hour ozone DVs from Step 2 with the gridded RRFs from Step 3
> **Step 5**: The future-year gridded 8-hour ozone DVs (from Step 4) were examined to determine if there are any peak values higher than those at the monitors, which could potentially cause violations of the applicable 8-hour ozone NAAQS.

Under the Voronoi diagram method, each monitoring site was assigned to a Voronoi region based on location and the distance to each grid cell (Sen 2016), and the interpolations were done between each grid cell and all the monitors in surrounding Voronoi regions. Voronoi diagram with inverse distance weighting method has been used in various 2-D data analysis areas, including air quality measurements interpolations (Atsuyuki, et al., 2009; Deligiorgi and Philippopoulos 2011).

Figure B-19 shows the spatial distribution of gridded DVs in 2032 for the SFNA based on the unmonitored area analysis (described above). The black star markers denote the monitoring sites, which had valid reference year 2018 DVs and were used in the analysis. Gridded DVs are below the 70 ppb standard in all areas within the nonattainment region, except at sparsely populated elevated locations over the Sierra Nevada Mountains.

Figure B-19. Spatial distribution of the future 2032 DVs based on the unmonitored area analysis in the SFNA.

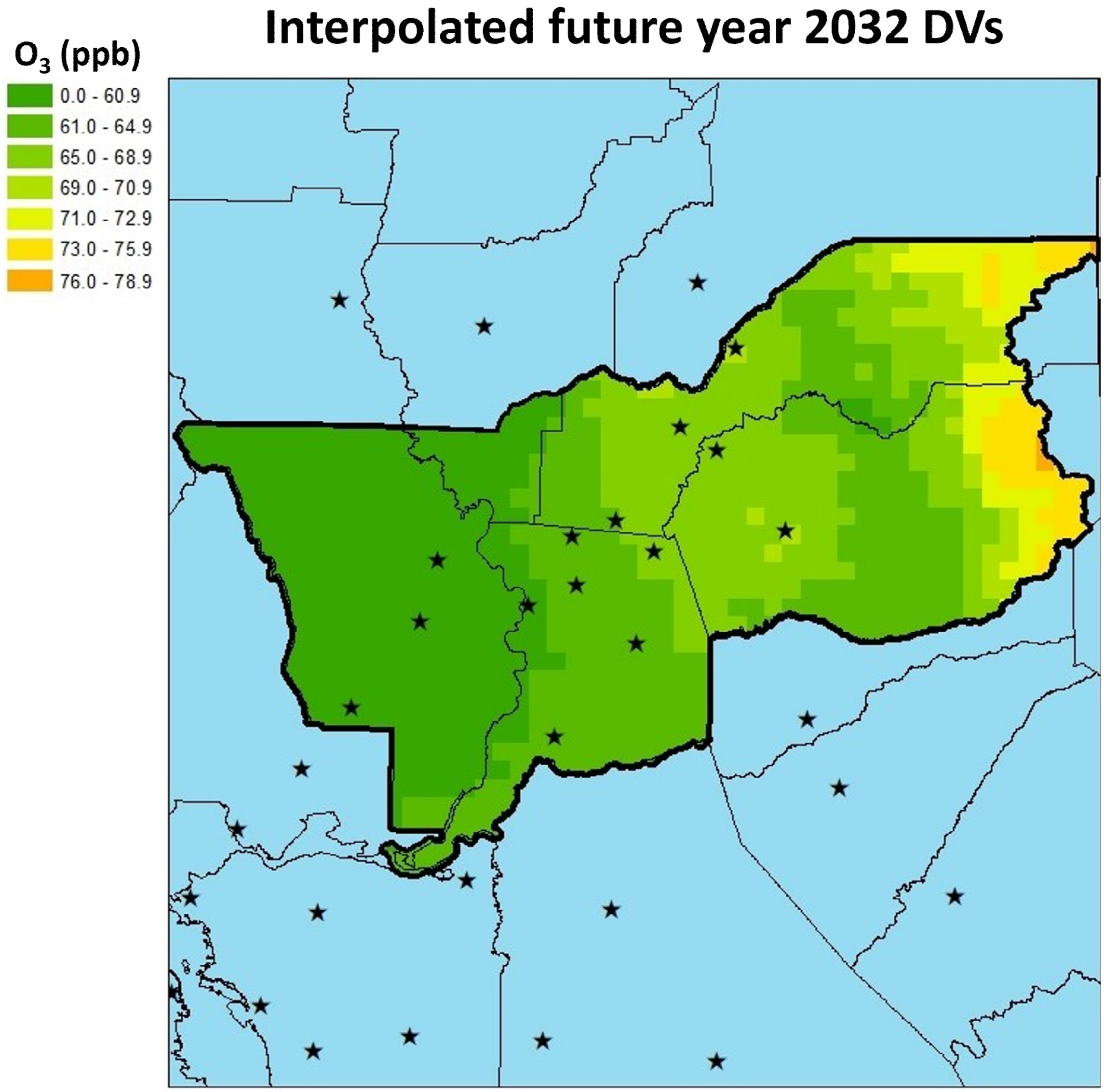

Figure B-20 shows the spatially interpolated base year DV from Step 2 above (left panel), and the RRF value at each model grid from Step 3 above (right panel). The RRF calculation is based on the top 10 days from the 2018 reference year model simulations for each grid cell. In 2018, the interpolated DVs exhibit high levels of ozone in the middle foothills region that is downwind of the Sacramento Metro region. In contrast, RRF values over the mountain regions are generally close to 1.0 while the RRF values in the foothills are mostly below 0.9, which indicates that the remote mountain regions in the east part are not responsive to the emission reductions within SFNA.

Figure B-20. Spatially interpolated 2018 base year DVs with gradient adjustment based on the unmonitored area analysis (left), and the RRF calculated for each grid (right).

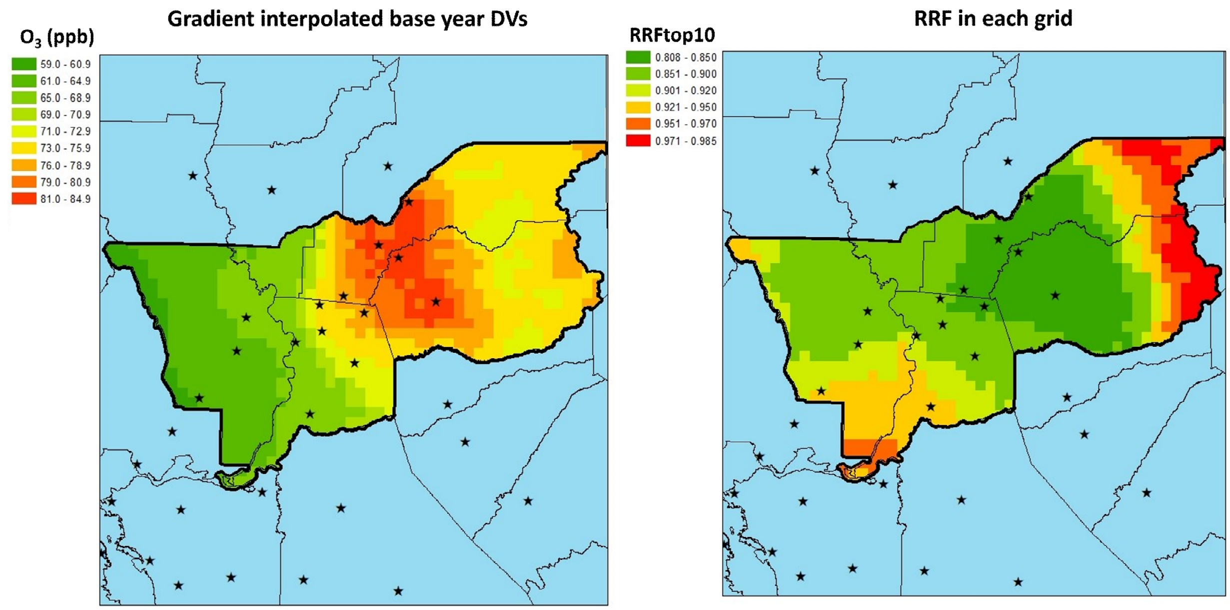

Further analysis of the modeling results shows there is a disconnect between the timing of the ozone peaks in the foothills and over the elevated mountain regions. Within the mountain regions, high O_3 concentrations occur in the springtime from April to June, while the high O_3 concentrations in the foothills region occur during the peak summer ozone season from July to September. Figure S 61 shows an east-west cross sectional curtain plot of monthly average 8-hour O_3 in May 2018 and 2032 at row 127 of the model domain, which crosses through the Cool-Hwy193 monitor site. From the figure, it is clearly seen that O_3 concentrations over the top of the mountains are significantly impacted by transport from aloft, including the impact of stratospheric intrusion of O_3, which is strongest during the spring season. Figure S 62 shows a similar curtain plot, but for August, which clearly shows that even during the peak ozone summer season, ozone pollution in the foothills does not strongly affect ozone levels at elevations above 2500 m. When spring months are excluded from the unmonitored area analysis (only data from July to October is used), the interpolated O_3 DVs in the mountain regions for 2032 are reduced significantly and the unmonitored peaks disappear (Figure B-21), while the DVs within other regions only exhibit very minor changes.

Figure B-21. Spatial distribution of the future 2032 DVs based on the unmonitored area analysis in the SFNA using modeling data of July - October.

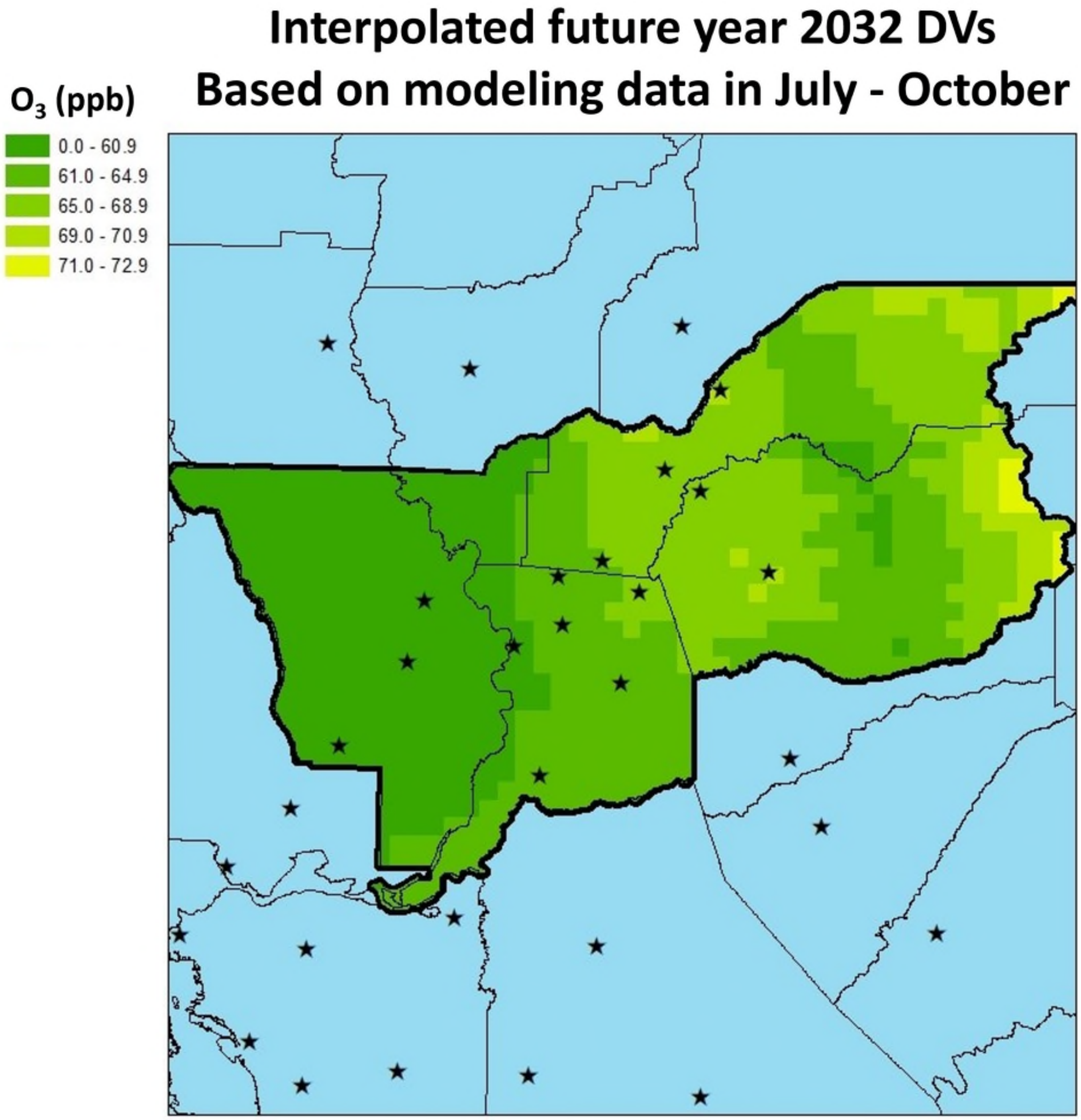

Our modeling based analysis shows that the high ozone levels within the Sierra Nevada Mountains predicted by the unmonitored area analysis are likely due to the impacts from higher ozone aloft and stratospheric influences in springtime, and are not influenced by pollution emitted and formed within the region during the peak ozone season summer months. This means that reducing anthropogenic emissions in the SFNA would not likely affect ozone levels within elevated regions of the Sierra Nevada Mountains. These unmonitored peaks are consistent with our understanding of the physical processes in the atmosphere and the role of stratospheric ozone influences in the spring (e.g., Jeanne et al., 2013, Lin et al., 2012, Ricardo et al., 2010).

The Echo Summit monitor, situated in the eastern part of SFNA with an elevation of 2250m, is considered a seasonal site, and does not meet the regulatory requirements set by the EPA and, as a result, was not included in the aforementioned analysis. To gain a better understanding of O_3 levels in the unmonitored area, additional analysis was conducted on the O_3 trend at the non-regulatory Echo Summit monitor using the available data from the site. Figure S 63 illustrates the time series of MDA8 O_3 levels at Echo Summit from April to October between 2016 and 2020. It is evident that the majority of MDA8 O_3 values at Echo Summit fall below or near 70 ppb. There were a few instances of higher MDA8 O_3 levels observed in 2018 and 2020, which can be attributed to the impact of wildfires. By utilizing the available data and following the methodology outlined in Section B.1.2, a base year O_3 DV of 67.7 ppb was derived for Echo Summit. This value is notably lower than the interpolated DV of 75.6 ppb shown in Figure B-20 from the unmonitored area analysis. These findings suggest that the peak in the unmonitored eastern region of SFNA is likely an artifact of the methodology used in the analysis of unmonitored areas. This discrepancy can be attributed to the sparse monitoring network and complex topography characteristics of the region. Taking into account the available data from the Echo Summit monitor, it is reasonable to conclude that this particular area is likely already in attainment of the 70 ppb O_3 standard.

B.1.4 References

AMSS. 2020. *Spatial Surrogate Methodology Document SNP2020-10-01.* Sacramento: INTERNAL DRAFT CARB.

AMSS. 2021. *Spatial Surrogate Methodology Document SNP2021-10-01.* Sacramento: INTERNAL DRAFT CARB.

Angevine, W. M., L. Eddington, K. Durkee, C. Fairall, L. Bianco, and J. Brioude. 2012. "Meteorological model evaluation for CalNex 2010." *Monthly Weather Review* (140): 3885-3906.

Atsuyuki, O., B. Boots, K. Sugihara, and S. N. Chiu. 2009. *Spatial tessellations: concepts and applications of Voronoi diagrams.* Second. John Wiley & Sons.

Baker, K. R., C. Misenis, M. D. Obland, R. A. Ferrare, A. J. Scarino, and J. T. Kelly. 2013. "Evaluation of surface and upper air fine scale WRF meteorological modeling of the May and June 2010 CalNex period in California." *Atmospheric Environment* (80): 299-309.

Bao, J.W., S.A. Michelson, P.O.G. Persson, I.V. Djalalova, and J.M. Wilczak. 2008. "Observed and WRF-simulated low-level winds in a high-ozone episode during the Central California ozone study." *Journal of Applied Meteorology and Climatology* 47: 2372-2394.

Beaver, S., and A. Palazoglu. 2009. "Influence of synoptic and mesoscale meteorology on ozone pollution potential for San Joaquin Valley of California." *Atmospheric Environment* 43 (10).

Blanchard, C.L., S. Tanenbaum, E.M. Fujita, D. Campbell, and J. Wilkinson. 2008. *Understanding Relationships between Changes in Ambient Ozone and Precursor Concentrations and Changes in VOC and NOx Emissions from 1990 to 2004 in Central California.* Report prepared for the California Air Resources Board, Envair, DRI and Alpine Geophysics.

Buchholz, R. R., L. K. Emmons, S. Tilmes, and & The CESM2 Development Team. 2019. "CESM2.1/CAM-chem Instantaneous Output for Boundary Conditions." UCAR/NCAR - Atmospheric Chemistry Observations and Modeling Laboratory. https://doi.org/10.5065/NMP7-EP60.

Cai, C., J. C. Avise, A. Kaduwela, J. DaMassa, C. Warneke, J. B. Gilman, W. Kuster, et al. 2019. "Simulating the Weekly Cycle of NOx-VOC-HOx-O3Photochemical System in the South Coast ofCalifornia During CalNex-2010 Campaign." *Journal of Geophysical Research: Atmospheres* 3532–3555.

Cai, C., S. Kulkarni, Z. Zhao, A. Kaduwela, J. C. Avise, and J. A. DaMassa. 2016. "Simulating Reactive Nitrogen, Carbon Monoxide, and Ozone in California During ARCTAS-CARB 2008 with High Wildfire Activity." *Atmospheric Environment* 28-44.

Caltrans. 2020. *Statewide Modeling.* https://dot.ca.gov/programs/transportation-planning/multi-modal-system-planning/statewide-modeling.

CARB. 1990. *Assessment and Mitigation of the Impacts of Transported Pollutants on Ozone Concentrations within California, Staff Report prepared by the Technical Support Division and the Office of Air Quality Planning and Liaison of the California Air Resources Board.* available at https://www.arb.ca.gov/aqd/transport/assessments/1990.pdf.

CARB. 2020. *2017 Baseline Inventory and Vehicle Miles Traveled Offset Demonstration for the 2015 70 ppb 8-hour Ozone Standard available at https://ww2.arb.ca.gov/resources/documents/2017-baseline-inventory-and-vehicle-miles-traveled-offset-demonstration-2015-70.* Accessed Jan 2022.

CARB. 2018. "2018 Western Nevada County Planning Area Ozone Attainment Plan available at https://ww3.arb.ca.gov/planning/sip/planarea/wnc/carb_staff_report.pdf." Staff Report. Accessed Jan 2022.

—. 2020. *Advanced Clean Trucks.* 02 07. https://ww2.arb.ca.gov/our-work/programs/advanced-clean-trucks.

—. 2021. *Heavy-Duty Inspection and Maintenance Regulation.* https://ww2.arb.ca.gov/rulemaking/2021/hdim2021.

—. 2020. "Heavy-Duty Low NOx." February 07. https://ww2.arb.ca.gov/our-work/programs/heavy-duty-low-nox.

CARB. 2021. *Report on Updates to the California Integrated Transportation Network (ITN).* INTERNAL DRAFT.

Carter, W.P.L. 2010b. "Development of a condensed SAPRC-07 chemical mechanism." *Atmospheric Environment* 5336-5345.

Carter, W.P.L. 2010a. "Development of the SAPRC-07 chemical mechanism." *Atmospheric Environment* 5324-5335.

Chen, J., D. Yin, Z. Zhao, A. P. Kaduwela, J. C. Avise, J. A. DaMassa, A. Beyersdorf, and S. Burton et al. 2020. "Modeling air quality in the San Joaquin Valley of California during the 2013 DISCOVER-AQ field campaign." *Atmospheric Environment* (5): 100067.

Clinton, N., P. Gong, and K. Scott. 2006. "Quantification of pollutants emitted from very large wildland fires in Southern California." *Atmospheric Environment* Volume 40, pp. 3686-3695.

Deligiorgi, D., and K. Philippopoulos. 2011. "Spatial Interpolation Methodologies in Urban Air Pollution Modeling: Application for the Greater Area of Metropolitan Athens, Greece." In *Advanced Air Pollution*. doi:10.5772/17734.

EasternKern. 2017. "2017 Ozone Attainment Plan, available at: http://www.kernair.org/Documents/Announcements/Attainment/2017%20Ozone%20Plan_EKAPCD_Adopted_7-27-17.pdf."

EKAPCD. 2003. "East Kern County Ozone Attainment Demonstration, Maintenance Plan, and Redesignation Request." available at https://www.arb.ca.gov/planning/sip/planarea/easternkern/2003kernplan.pdf.

Emery, C., Z. Liu, A. M. Russell, T. Odman, G. Yarwood, and N. Kumar. 2017. "Recommendations on statistics and benchmarks to assess photochemical model performance." *Journal of the Air & Waste Management Association* 582-598.

Emmons, L. K., R. H. Schwantes, J. J. Orlando, G. Tyndall, D. Kinnison, and J.-F. Lamarque et al. 2020. "The Chemistry Mechanism in the Community Earth System Model version 2 (CESM2)." *Journal of Advances in Modeling Earth Systems.* https://doi.org/10.1029/2019MS001882.

EPA. 2014. *Draft Modeling Guidance for Demonstrating Attainment of Air Quality Goals for Ozone, PM2.5, and RegionalHaze.* Modeling guidance, Research Triangle Park, United States Environmental Protection Agency, North Carollina: U.S. EPA. Accessed July 10, 2015. http://www.epa.gov/ttn/scram/guidance/guide/Draft_O3-PM-RH_Modeling_Guidance-2014.pdf.

—. 2016. *https://www3.epa.gov/ttn/emc/cem.html.* Accessed August 16, 2016. https://www3.epa.gov/ttn/emc/cem.html.

—. 2018. *Modeling Guidance for Demonstrating Attainment of Air Quality Goals for Ozone, PM2.5, and Regional Haze.* 11 29. https://www.epa.gov/scram/sip-modeling-guidance-documents.

EPA. 1993. "NOx Substitution Guidance, available at https://www3.epa.gov/ttn/naaqs/aqmguide/collection/cp2/19931201_oaqps_nox_substitution_guidance.pdf."

EPA. 2008. "Technical Support Document for 2008 Ozone NAAQS Designation." https://19january2017snapshot.epa.gov/www3/region9/air/ozone/pdf/R9_CA_NevadaCounty_FINAL.pdf.

EPA, U.S. 2017. "Ozone Designations - 2015 Standards accessible at https://www.epa.gov/sites/default/files/2018-05/documents/ca_tsd_combined_final_0.pdf." Accessed Jan 2022. https://www.epa.gov/sites/default/files/2018-05/documents/ca_tsd_combined_final_0.pdf.

ERG. 2019. "2014 Northern Baja California Emissions Inventory Project."

Fast, J. D., W. I. Gustafson Jr, L. K. Berg, W. J. Shaw, M. Pekour, and M. Shrivastava et al. 2012. "Transport and mixing patterns over Central California during the carbonaceous aerosol and radiative effects study (CARES)." *Atmospheric Chemistry and Physics* (12): 1759-1783.

Fosberg, M.A., and M.J. Schroeder. 1966. "Marine air penetration in Central California." *Journal of Applied Meteorology* (5): 573-589.

Fujita, E. M., R. E. Keislar, D. L. Freeman, J. Watson, A. J. Ranzieri, S. Tanrikulu, and K. Magliano. 1999. *Field study plan for the Central California Ozone Study.*

Gkatzelis, G, M. Coggon, M McDonald, J Peischl, K Aikin, J Gilman, M Trainer, and C Warneke. 2021. "Identifying Volatile Chemical Product Tracer Compounds in U.S. Cities." *Environmental Science & Technology* 55 (1): 188-199.

Gong, P., N. Clinton, and R. T. Y. a. S. J. Pu. 2003. *Extension and input refinement to the ARB wildland fire emissions estimation model Final report, contract number 00-729.* Sacramento, CA: Air Resources Board.

He, H., X-Z. Liang, and D. J. Wuebbles. 2018. "Effects of emissions change, climate change and long-range transport on regional modeling of future U.S. particulate matter pollution and speciation." *Atmospheric Environment*, 166-176. doi:https://doi.org/10.1016/j.atmosenv.2018.02.020.

Heuss, J. M., D. F. Kahlbaum, and G. T. Wolff. 2003. "Weekday/Weekend Ozone Differences: What Can We Learn from Them?" *Journal of the Air & Waste Management Association* 53 (7): 772-788.

Hu, J., C. J. Howard, F. Mitloehner, P. G. Green, and M. J. Kleeman. 2012. "Mobile Source and Livestock Feed Contributions to Regional Ozone Formation in Central California." *Environmental Science and Technology* (46): 2781-2789.

Imperial. 2017. " Imperial County 2017 State Implementation Plan for the 2008 8-Hour Ozone Standard, available at: https://ww3.arb.ca.gov/planning/sip/planarea/imperial/2017o3sip_final.pdf ."

Imperial. 2018. " Imperial County 2018 Annual Particulate Matter Less than 2.5 Microns in Diameter State Implementation Plan, available at: https://ww3.arb.ca.gov/planning/sip/planarea/imperial/final_2018_ic_pm25_sip.pdf ."

Jeanne, P., Saah, D., Esperanza, A., Bytnerowicz, A., Fraczek, W., and Cisneros, R. 2013. "Ozone Distribution in Remote Ecologically Vulnerable Terrain of the Southern Sierra Nevada, Ca." *Environmental Pollution* 182: 343-56.

Jin, L., N. J. Brown, R. A. Harley, J-W. Bao, S. A. Michelson, and J. M. Wilczak. 2010. "Seasonal versus episodic performance evaluation for an Eulerian photochemical air quality model." *Journal of Geophysical Research: Atmospheres* 115, D09302.

Jin, L., S. Tonse, D. S. Cohan, X Mao, R. A. Harley, and N. J. Brown. 2008. "Sensitivity analysis of ozone formation and transport for a central California air pollution episode." *Environmental Science and Technology* 3683-3689.

Kelly, J. T., K. R. Baker, J. B. Nowak, J. G. Murphy, Z. M. Milos, T. C. VandenBoer, R. A. Ellis, et al. 2014. "Fine-scale simulation of ammonium and nitrate over the South Coast Air Basin and San Joaquin Valley of California during CalNex-2010." *Journal of Geophysical Research* (119): 3600-3614. doi:doi:10.1002/2013JD021290.

Kelly, J.T., J. Avise, C. Cai, and A. Kaduwela. 2010. "Simulating particle size distributions over California and impact on lung deposition fraction." *Aerosol Science and Technology* 148-162.

Kelly, J.T., K.R Baker, J.B. Nowak, and J.G Murphy et al. 2014. "Fine-scale simulation of ammonium and nitrate over the South Coast Air Basin and San Joaquin Valley of California during CalNex-2010." *Journal of Geophysical Research: Atmosphere* 3600–3614.

Kulkarni, S., A. P. Kaduwela, J. C. Avise, J. A. DaMassa, and D. Chau. 2014. "An extended approach to calculate the ozone relative response factors used in the attainment demonstration for the National Ambient Air Quality Standards." *Journal of the Air and Waste Management Association* 1204-1213.

Kwok, Roger. 2016. *Meteorology-adjusted Temporal Profiles for Agricultural and Residential Wood Combustion Sectors Using Smoke Gentpro Utility Program.* Sacramento: INTERNAL DRAFT CARB.

Kwok, Roger. 2015. *Modeling Plume Rise of Ocean-going Vessel Emissions.* Sacramento: INTERNAL DRAFT CARB.

LaFranchi, B. W., A. H. Goldstein, and R. C and Cohen. 2011. "Observations of the temperature dependent response of ozone to NOx reductions in the Sacramento, CA urban plume." *Atmospheric Chemistry and Physics* 6945-6960.

Lamarque, J.-F., L. K. Emmons, P. G. Hess, D. E. Kinnison, S. Tilmes, F. Vitt, C. L. Heald, et al. 2012. "CAM-chem: description and evaluation of interactive atmospheric chemistry in the Community Earth System Model." *Geoscientific Model Development* 369-411.

Lehrman, D. 2001. *Characterization of the 2000 Measurement Period.* Interim Report prepared for California Air Resources Board, Technical and Business Systems, Inc.,.

Lehrman, D., D. Bush, B. Knuth, D. Fairley, and C. Blanchard. 2004. *Characterization of the CCOS 2000 measurement period.* Final Report prepared for California Air Resources Board, Technical and Business Systems, Inc.

Lin, M., A. M. Fiore, O. R. Cooper, L. W. Horowitz, A. O. Langford, H. Levy II, B. J. Johnson, V. Naik, and S. J. Oltmans. 2012. "Springtime high surface ozone events over the western United States: Quantifying the role of stratospheric." *Journal of Geophysical Research* D00V22, doi:10.1029/2012JD018151.

Livingstone, P.L., K. Magliano, K. Gurer, P.D. Allen, K.M. Zhang, Q. Ying, and , B.S. Jackson et al. 2009. "Simulating PM concentration during a winter episode in a subtropical valley: Sensitivity simulations and evaluation methods." *Atmospheric Environment* 5971-5977.

Mills, S., S. Weiss, and C. Liang. 2013. "VIIRS day/night band (DNB) stray light characterization and correction." *SPIE Proceedings* Vol. 8866.

Pun, B. K., J. F. Loius, and C. Seigneur. 2008. *A conceptual model of ozone formation in the San Joaquin Valley.* CP049-1-98, Atmospheric and Environmental Research Inc., San Ramon, CA.

Pun, B.K., R.T.F. Balmori, and C. Seigneur. 2009. "Modeling wintertime particulate matter formation in central California." *Atmospheric Environment* 402-409.

Pusede, S. E., and R. C. Cohen. 2012. "On the observed response of ozone to NOx and VOC reactivity reductions in San Joaquin Valley California 1995–present." *Atmospheric Chemistry and Physics* 8323-8339.

Pusede, S. E., D. R. Gentner, P. J. Wooldridge, E. C. Browne, A. W. Rollins, K. E. Min, A. R. Russell, et al. 2014. "On the temperature dependence of organic reactivity, nitrogen oxides, ozone production, and the impact of emission controls in San Joaquin Valley, California." *Atmospheric Chemistry and Physics* 3373-3395.

Ricardo, C., A. Bytnerowicz, D. Schweizer, S. Zhong, S. Traina, and D.H. and Bennett. 2010. "Ozone, Nitric Acid, and Ammonia Air Pollution Is Unhealthy for People and Ecosystems in Southern Sierra Nevada, California." *Environmental Pollution* 158 (10): 3261-71.

Sacramento. 2017. "Sacramento Regional 2008 NAAQS 8-Hour Ozone Attainment And Reasonable Further Progress Plan, available at http://www.airquality.org/ProgramCoordination/Documents/Sac%20Regional%20 2008%20NAAQS%20Attainment%20and%20RFP%20Plan.pdf."

Seinfeld, J. H., and S. N. Pandis. 1998. *Atmospheric Chemistry and Physics: From Air Pollution to Climate Change.* Edited by 1. New York: J. Wiley.

Sen, Zekai. 2016. "2.8.1 Delaney, Varoni, and Thiessen Polygons." In *Spatial Modeling Principles in Earth Sciences*, 57. Springer.

Shahrokhishahraki, N., P. J. Rayner, J. D. Silver, S. Thomas, and R. Schofield. 2022. "High-resolution modeling of gaseous air pollutants over Tehran and validation with surface and satellite data." *Atmospheric Environment.* doi:https://doi.org/10.1016/j.atmosenv.2021.118881.

Shearer, S.M, R.A. Harley, L. Jin, and N.J. Brown. 2012. "Comparison of SAPRC99 and SAPRC07 mechanisms in photochemical modeling for central California." *Atmospheric Environment* 205-216.

Sillman, S. 1999. "The relation between ozone, NOx and hydrocarbons in urban and polluted rural environments." *Atmospheric Environment* 33 (12): 1821-1845.

Simon, H., K. R. Baker, and S. Phillips. 2012. "Compilation and interpretation of photochemical model performance statistics published between 2006 and 2012." *Atmospheric Environment* (61): 124-139.

SJV. 2018. " 2018 PM2.5 Plan for the San Joaquin Valley, available at: http://valleyair.org/pmplans/ ."

SJV. 2008. "2008 PM2.5 Plan, available at: http://www.valleyair.org/Air_Quality_Plans/AQ_Proposed_PM25_2008.htm."

SJV. 2012. "2012 PM2.5 Plan, available at: http://www.valleyair.org/Air_Quality_Plans/PM25Plans2012.htm ."

SJV. 2013. "2013 Plan for the Revoked 1-Hour Ozone Standard, available at: http://valleyair.org/Air_Quality_Plans/Ozone-OneHourPlan-2013.htm ."

SJV. 2016a. "2016 Moderate Area Plan for the 2012 PM2.5 Standard, available at: http://www.valleyair.org/Air_Quality_Plans/docs/PM25-2016/2016-Plan.pdf ."

SJV. 2016b. "2016 Plan for the 2008 8-Hour Ozone Standard, available at: http://valleyair.org/Air_Quality_Plans/Ozone-Plan-2016.htm ."

Skamarock, W. C., J. B. Klemp, J. Dudhia, D. O. Gill, D. M. Barker, M. G. Duda, X.-Y. Huang, W. Wang, and J. G. Powers. 2008. "Description ofthe Advanced Research WRF version 4,Rep. NCAR/TN-475++STR,Natl. Cent. for Atmos. Res." Boulder, Colo.

SouthCoast. 2012. "Final 2012 Air Quality Management Plan, available at: http://www.aqmd.gov/home/air-quality/clean-air-plans/air-quality-mgt-plan/final-2012-air-quality-management-plan ."

SouthCoast. 2016. "Final 2016 Air Quality Management Plan, available at: http://www.aqmd.gov/docs/default-source/clean-air-plans/air-quality-management-plans/2016-air-quality-management-plan/final-2016-aqmp/cover-and-opening.pdf?sfvrsn=6."

Stein, A.F., R.R Draxler, G.D. Rolph, B.J.B. Stunder, M.D. Cohen, and F. Ngan. 2015 . " NOAA's HYSPLIT atmospheric transport and dispersion modeling system." *Bulletin of the American Meteorological Society* 2059-2077.

Tonse, S. R., N. J. Brown, R. A. Harley, and L. Jin. 2008. "A process-analysis based study of the ozone weekend effect." *Atmospheric Environment* 7728-7736.

UNC Chapel Hill - The Institute for the Environment. 2016. "SMOKE v4.0 User's Manual." September 30. Accessed 02 07, 2020. https://www.cmascenter.org/smoke/documentation/4.0/manual_smokev40.pdf.

Van Ooy, D.J., and J.J. Carroll. 1995. "The spatial variation of ozone climatology on the western slope of the Sierra Nevada." *Atmospheric Environment* 1319-1330.

Ventura. 2016. "Final 2016 Ventura County Air Quality Management Plan, available at: http://www.vcapcd.org/pubs/Planning/AQMP/2016/Final/Final-2016-Ventura-County-AQMP.pdf ."

Vijayaraghavan, K., P. Karamchadania, and C. Seigneur. 2006. "Plume-in-grid modeling of summer air pollution in Central California." *Atmospheric Environment* 5097-5109.

Wang, P., P. Wang, K. Chen, J. Du, and H Zhang. 2022. "Ground-level ozone simulation using ensemble WRF/Chem predictions over the Southeast United States." *Chemosphere.* doi:https://doi.org/10.1016/j.chemosphere.2021.132428.

WesternMojave. 2016. "2016 8-Hour Ozone SIP: Western Mojave Desert Nonattainment Area, available at: https://ww3.arb.ca.gov/planning/sip/planarea/mojavesedsip.htm#2016."

WesternNevada. 2018. "Western Nevada County 8-hour Ozone Attainment Plan, available at: https://ww3.arb.ca.gov/planning/sip/planarea/wncsip.htm."

Wu, Shenglun, Hyung Joo Lee, Andrea Anderson, Shang Liu, Toshihiro Kuwayama, Joh H Seinfeld, and Michael J Kleeman. 2022. "Direct measurements of ozone response to emissions perturbations in California." *Atompheric Chemistry and Phtsics* (Copernicus Publications on behalf of the European Geosciences Union) 4929-4949. doi:10.5194.

Yan, F., Y. Gao, M. Ma, C. Liu, X. Ji, F. Zhao, X. Yao, and H. Gao. 2021. "Revealing the modulation of boundary conditions and governing processes on ozone formation over northern China in June 2017." *Environmental Pollution* 272. doi:https://doi.org/10.1016/j.envpol.2020.115999.

Yienger, J. J., and H. Levy II. 1995. "Empirical model of global soil-biogenic NO_χ emissions." *Journal of Geophysical Research: Atmospheres* 11447-11464.

Zhang, Y., P. Liu, X. Liu, B. Pun, C. Seigneur, M.Z. Jacobson, and W. Wang. 2010. "Fine scale modeling of wintertime aerosol mass, number, and size distributions in

Central California." *Journal of Geophysical Research* D15207, doi:10.1029/2009JD012950.

Zhu, S., Horne, J. R., Kinnon, M. M., Samuelsen, G. S., Dabdub, D. 2019. "Comprehensively assessing the drivers of future air quality in California." *Environment International* 386-398.

B.1.5 Supplemental Materials

Supplemental Materials List of Figures

Figure S 1. Time series of average temperature, relative humidity, wind speed, and direction of all valley sites in April 2018.

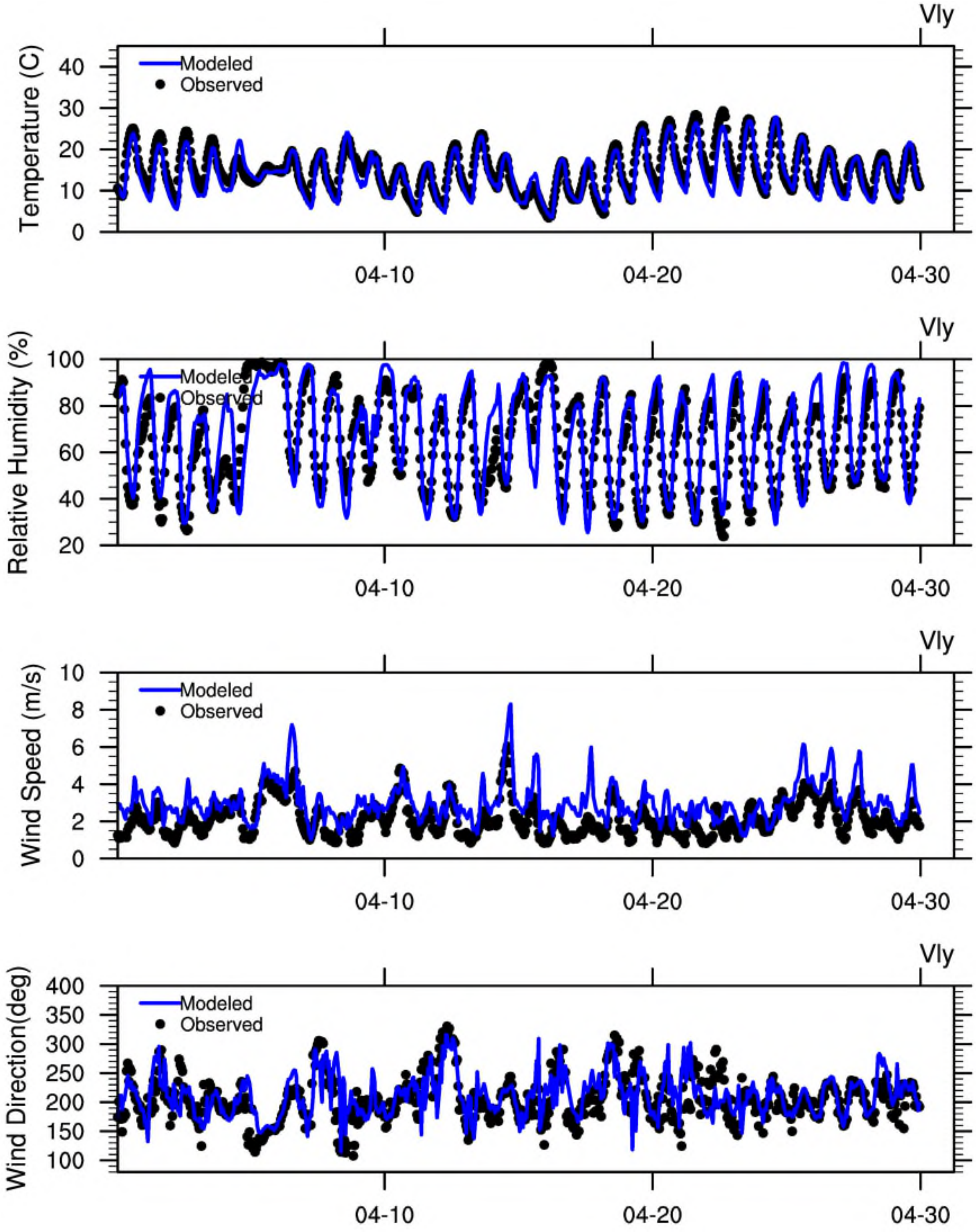

Figure S 2. Time series of average temperature, relative humidity, wind speed, and direction of all mountain sites in April 2018.

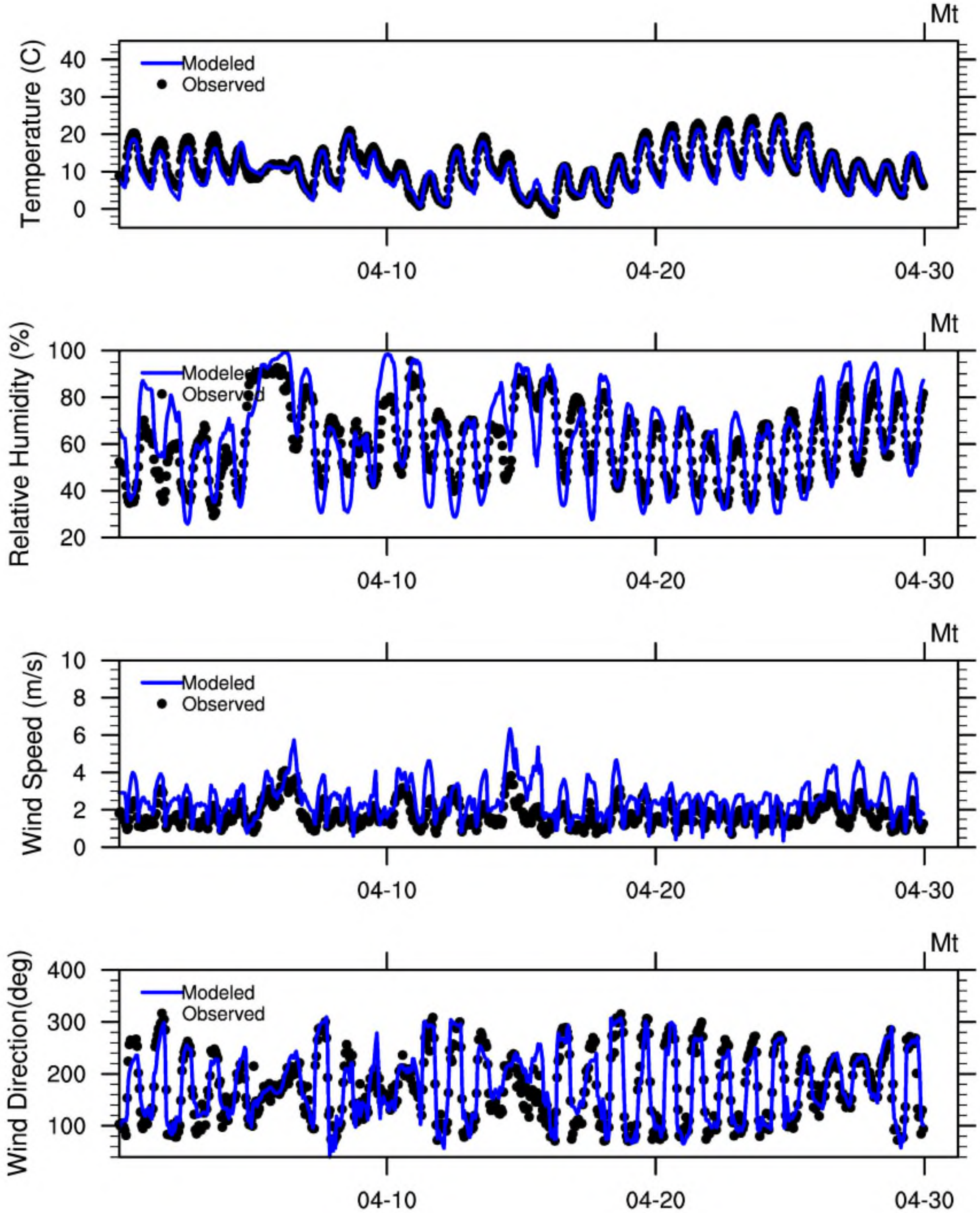

Figure S 3. Time series of average temperature, relative humidity, wind speed, and direction of all valley sites in May 2018.

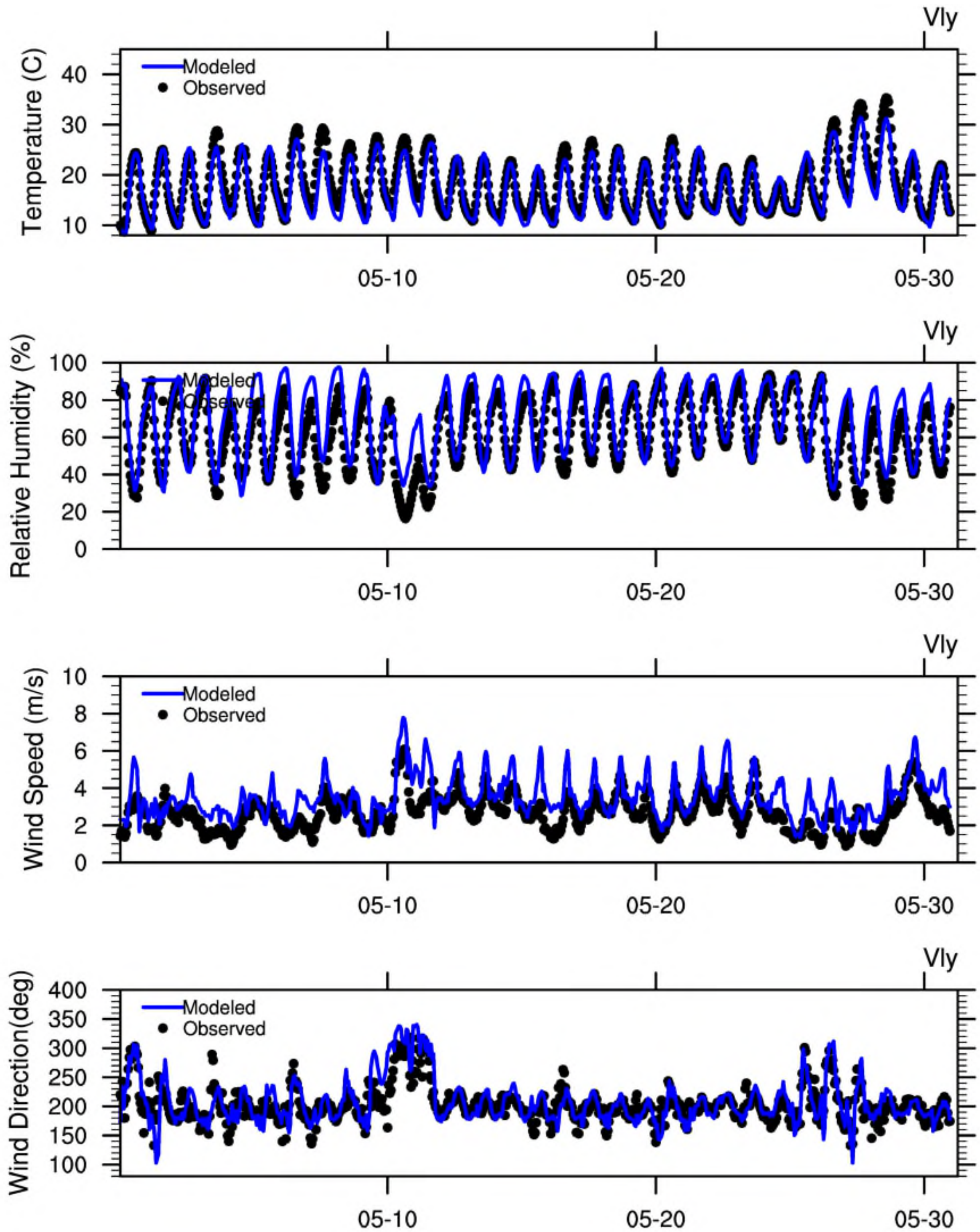

Figure S 4. Time series of average temperature, relative humidity, wind speed, and direction of all mountain sites in May 2018.

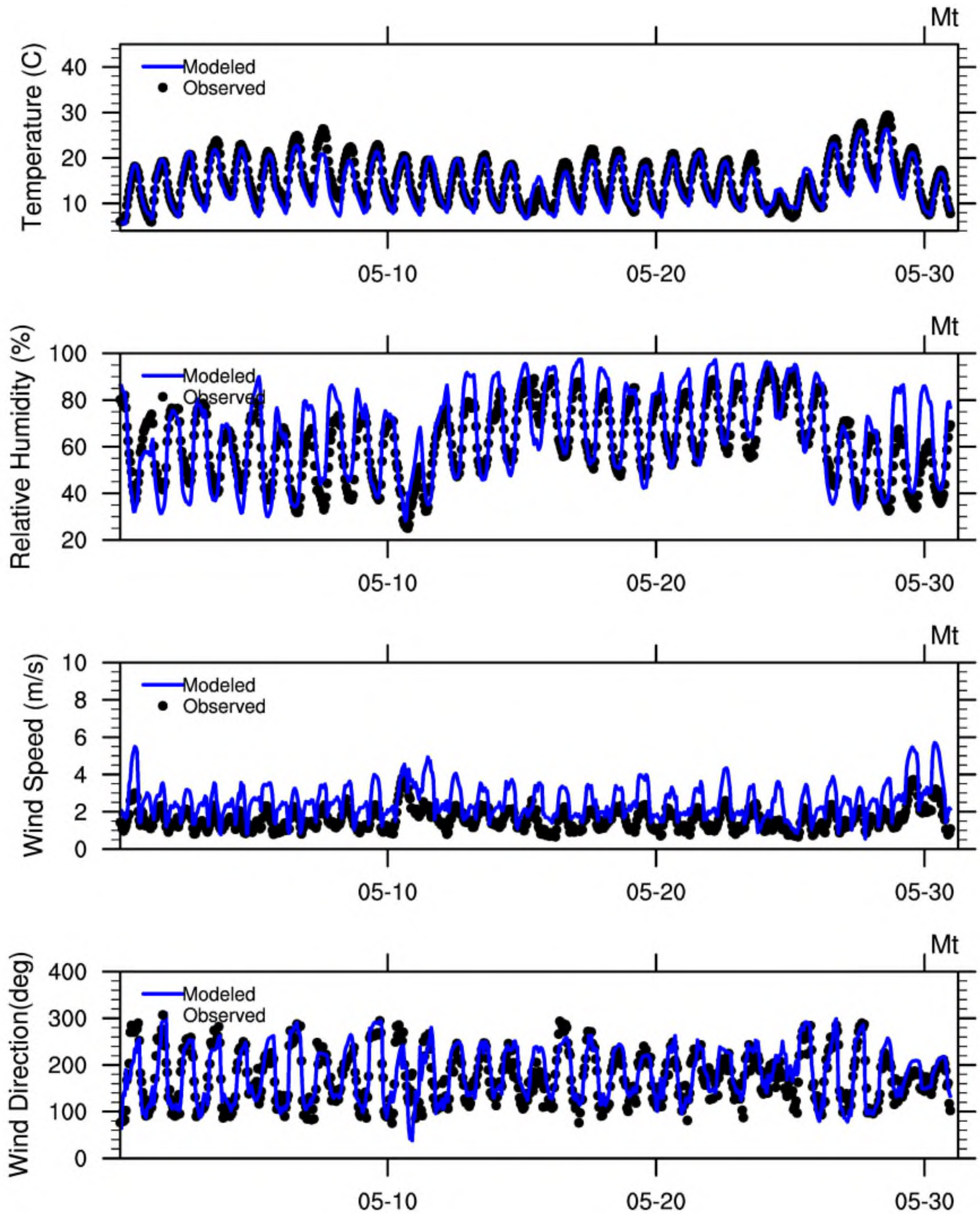

Figure S 5. Time series of average temperature, relative humidity, wind speed, and direction of all valley sites in June 2018.

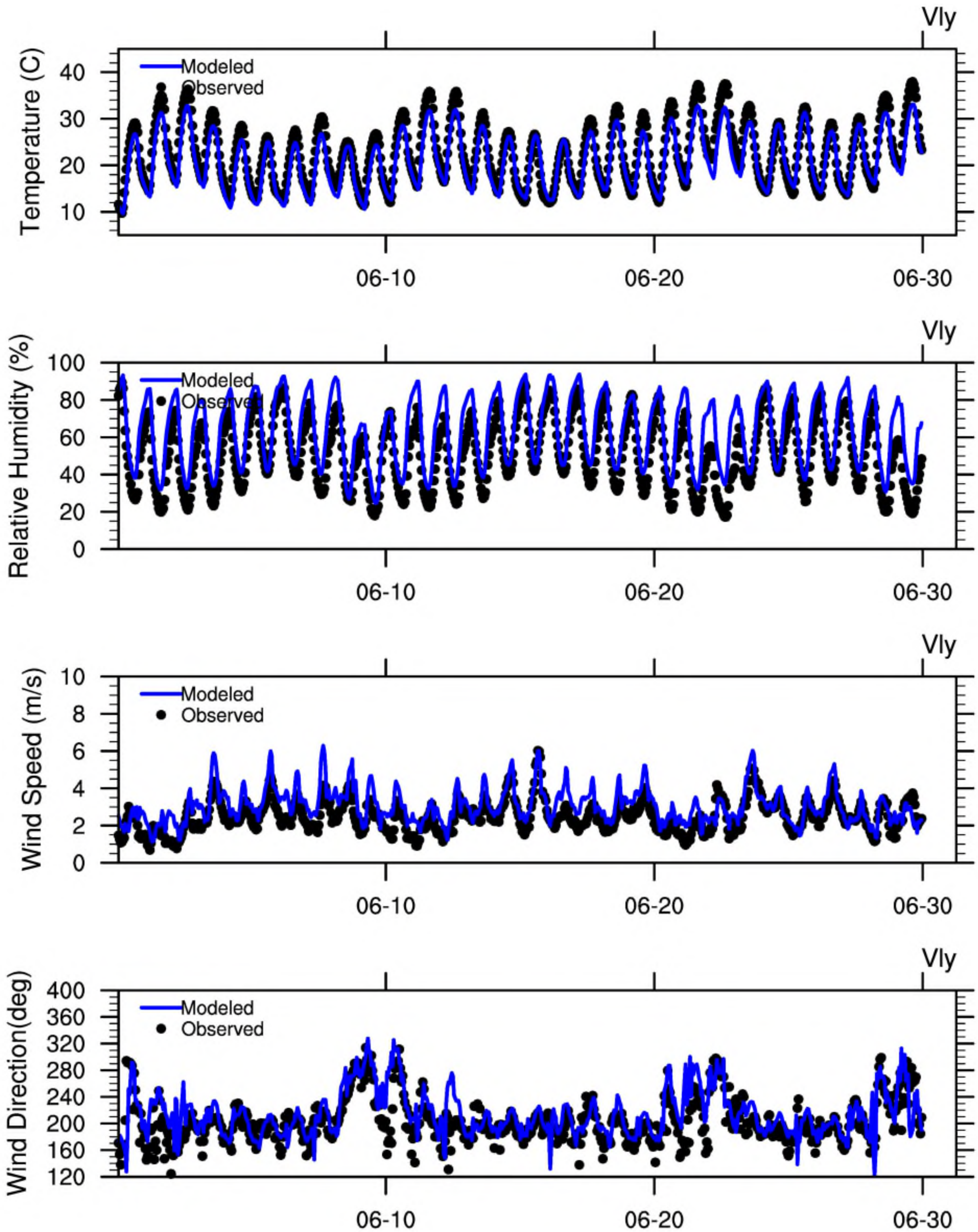

Figure S 6. Time series of average temperature, relative humidity, wind speed, and direction of all mountain sites in June 2018.

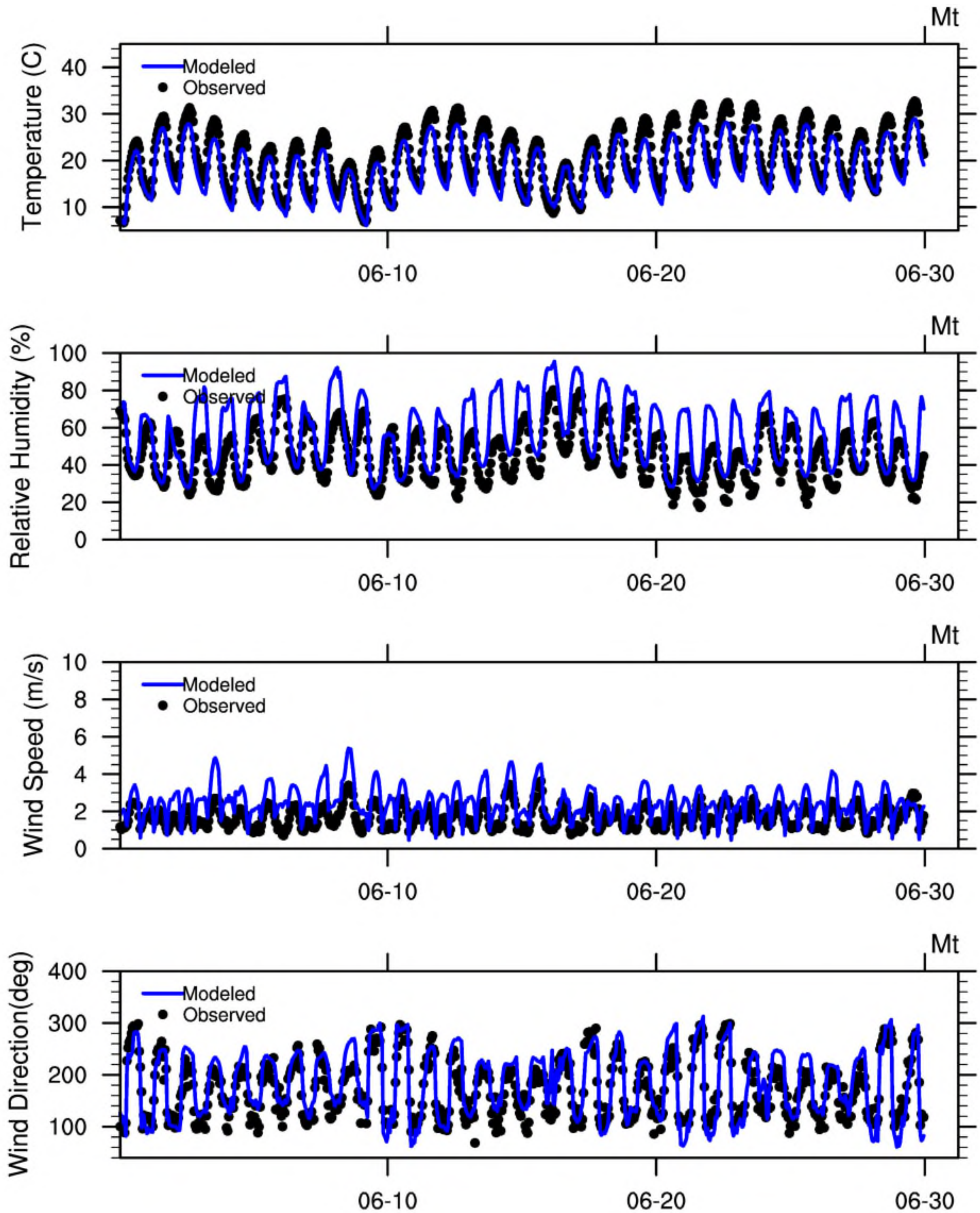

Figure S 7. Time series of average temperature, relative humidity, wind speed, and direction of all valley sites in July 2018.

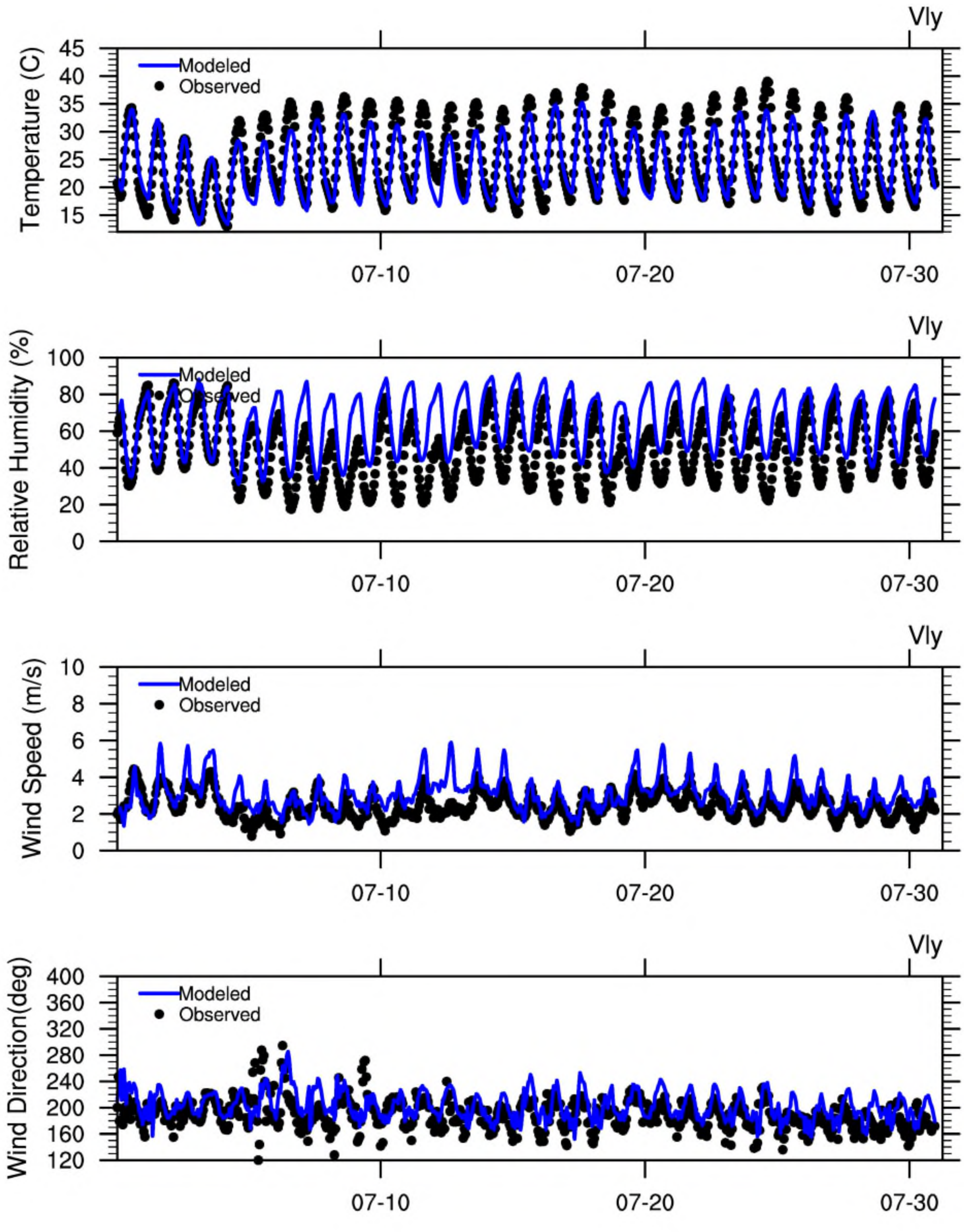

Figure S 8. Time series of average temperature, relative humidity, wind speed, and direction of all mountain sites in July 2018.

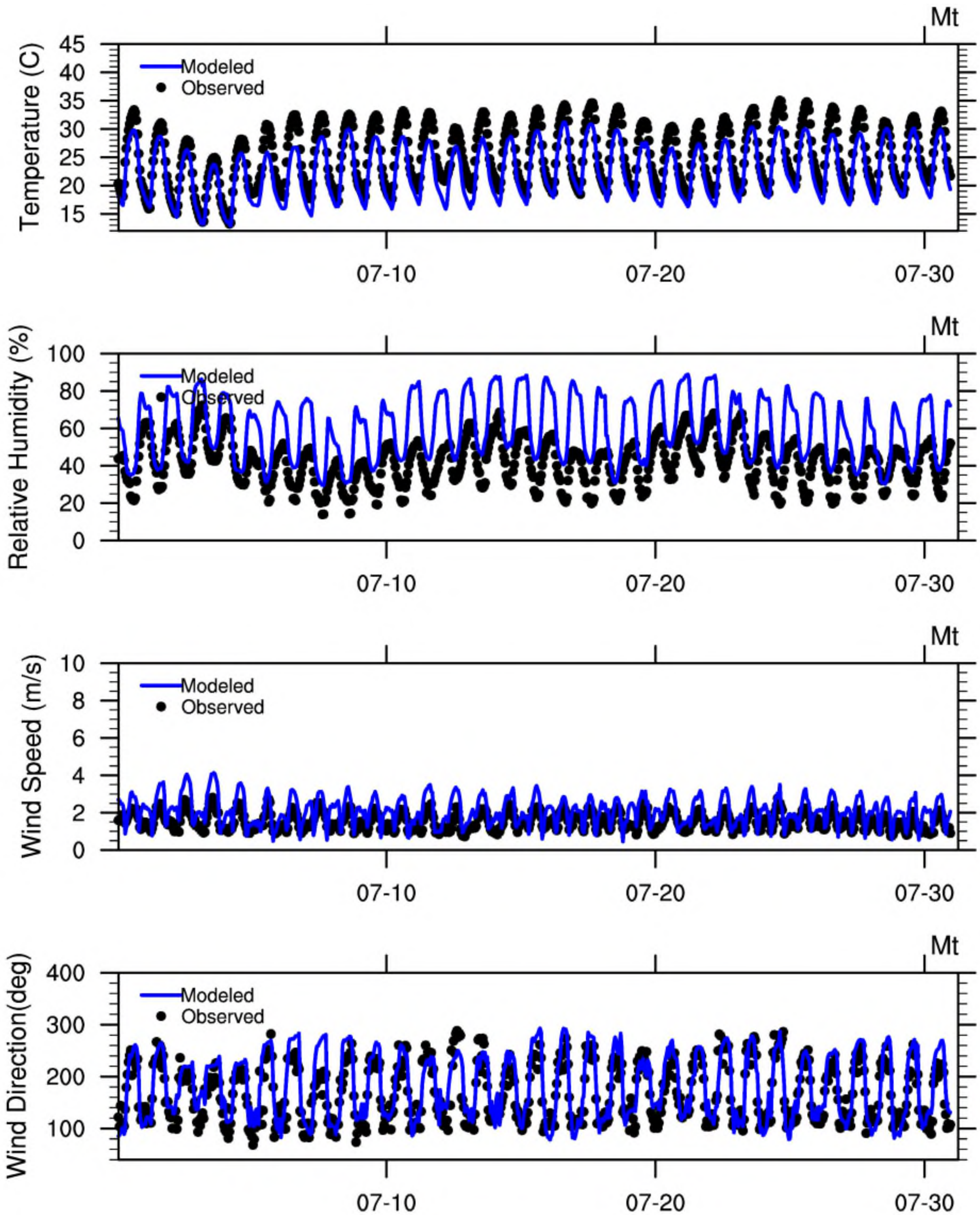

Figure S 9. Time series of average temperature, relative humidity, wind speed, and direction of all valley sites in August 2018.

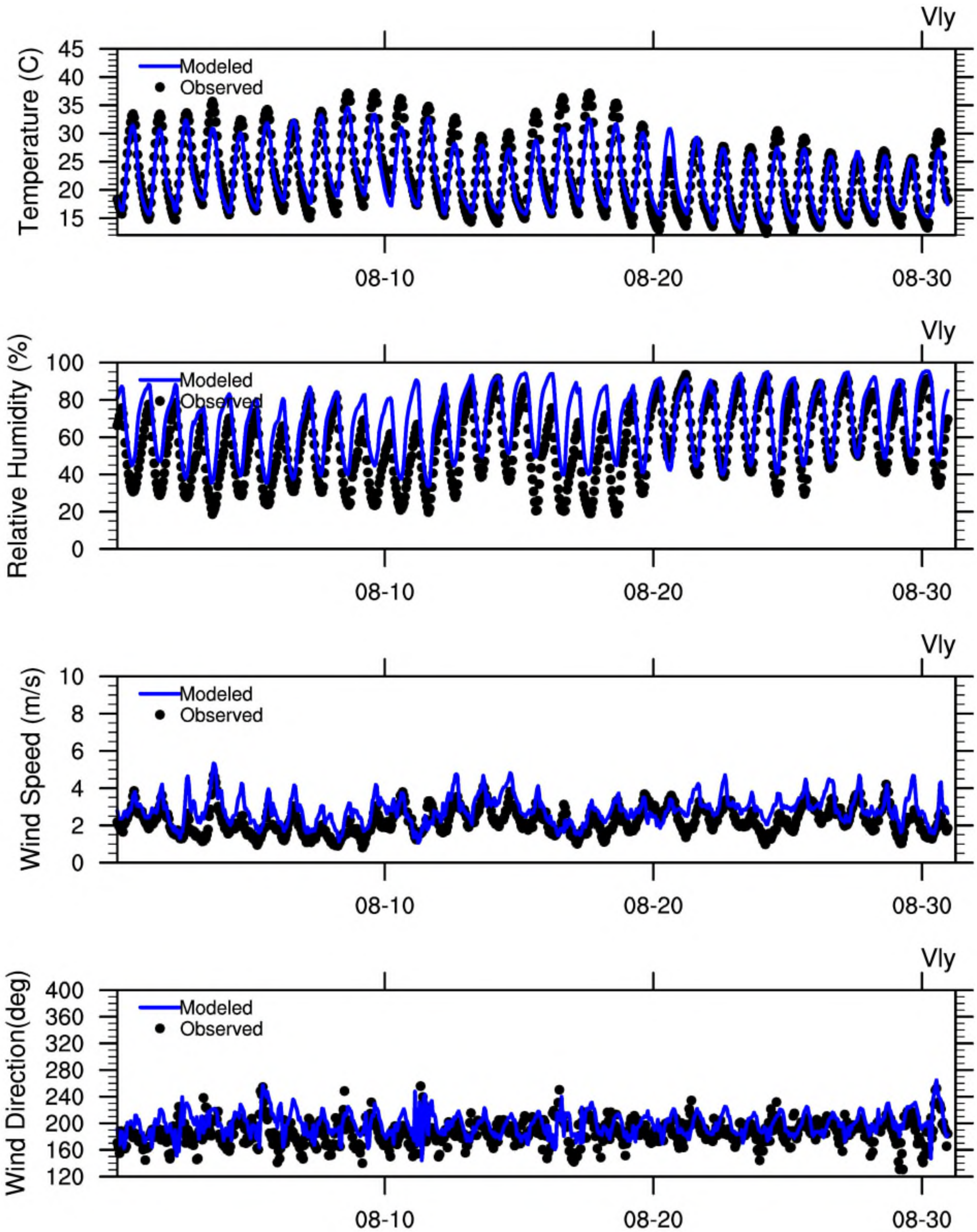

Figure S 10. Time series of average temperature, relative humidity, wind speed, and direction of all mountain sites in August 2018.

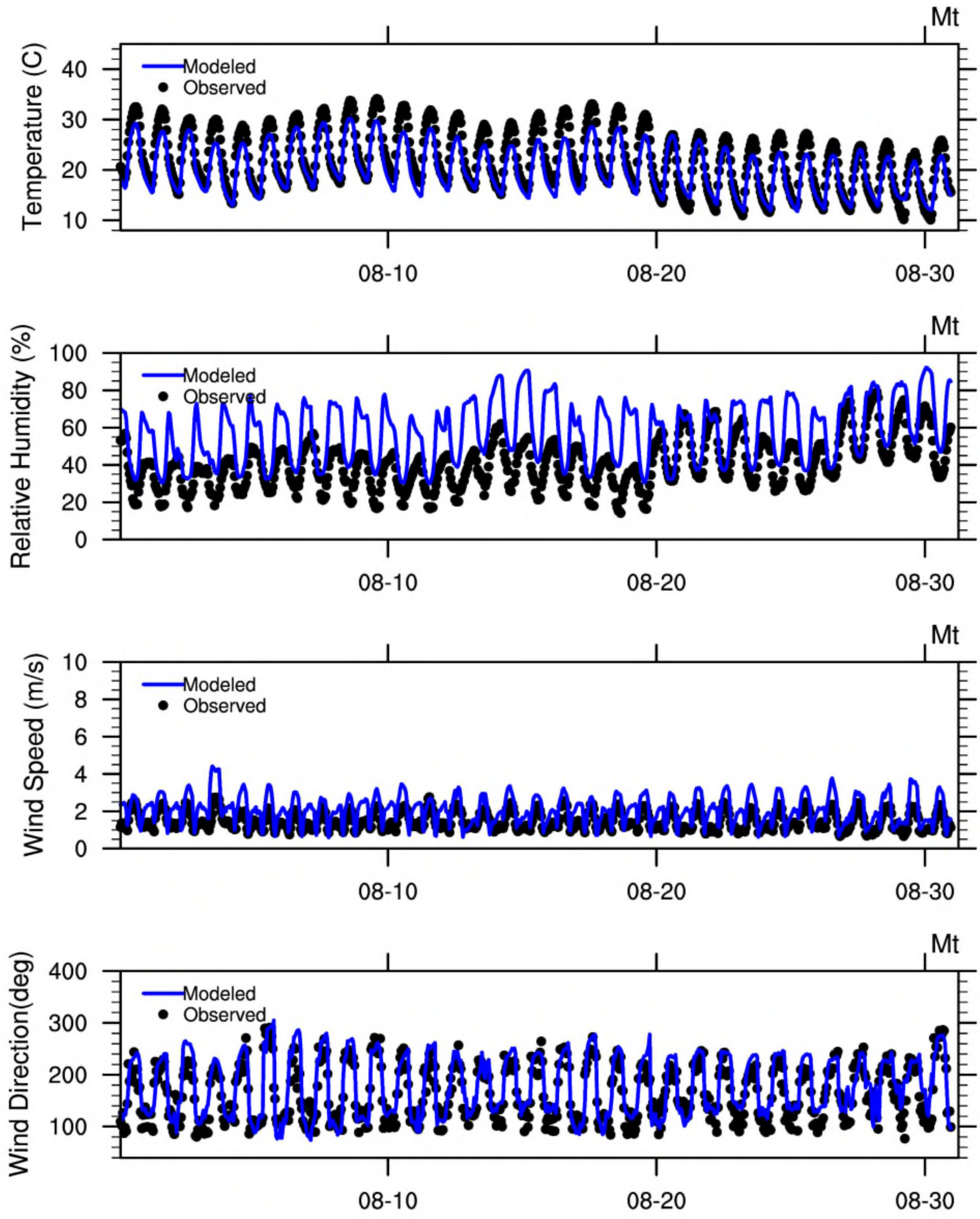

Figure S 11. Time series of average temperature, relative humidity, wind speed, and direction of all valley sites in September 2018.

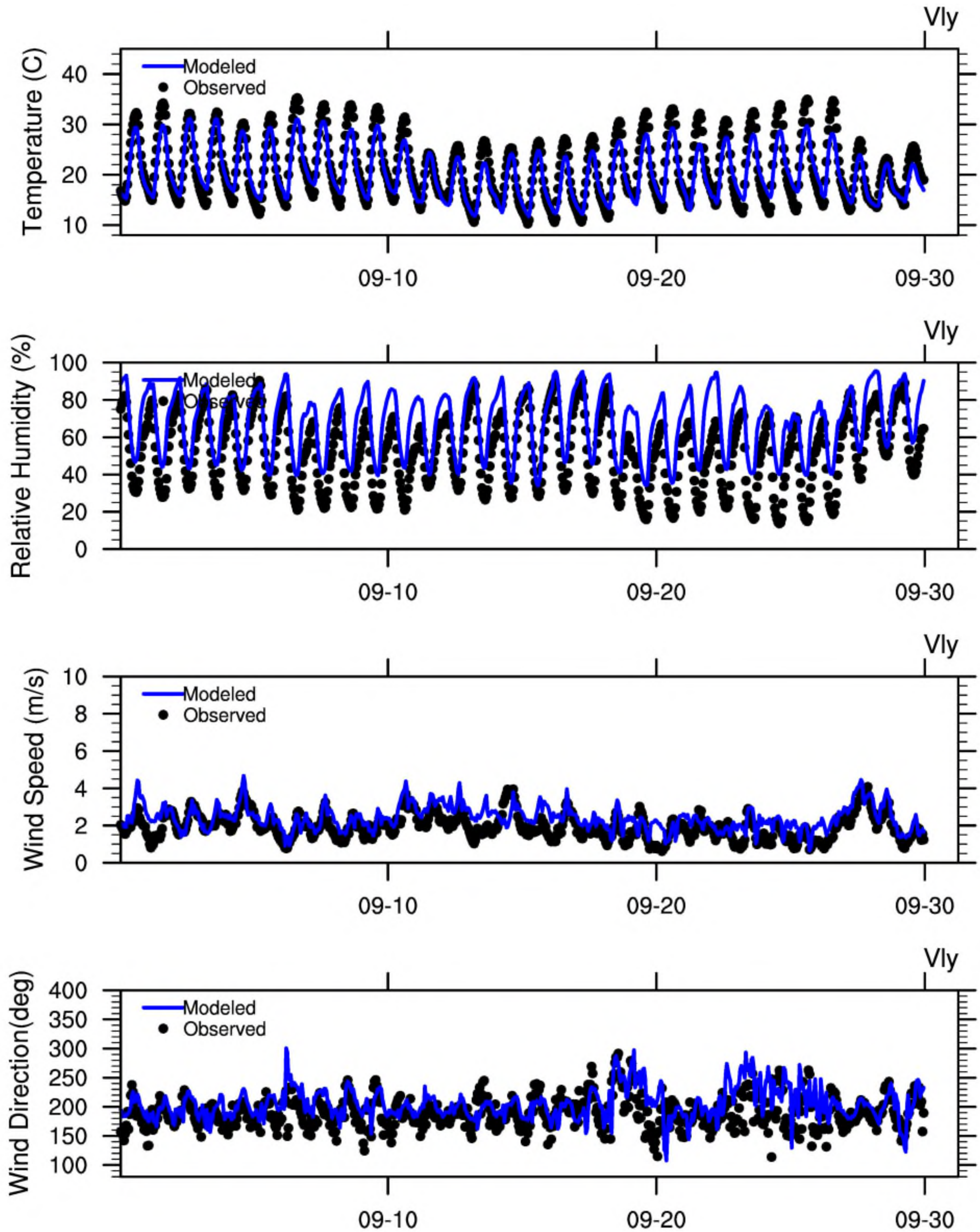

Figure S 12. Time series of average temperature, relative humidity, wind speed, and direction of all mountain sites in September 2018.

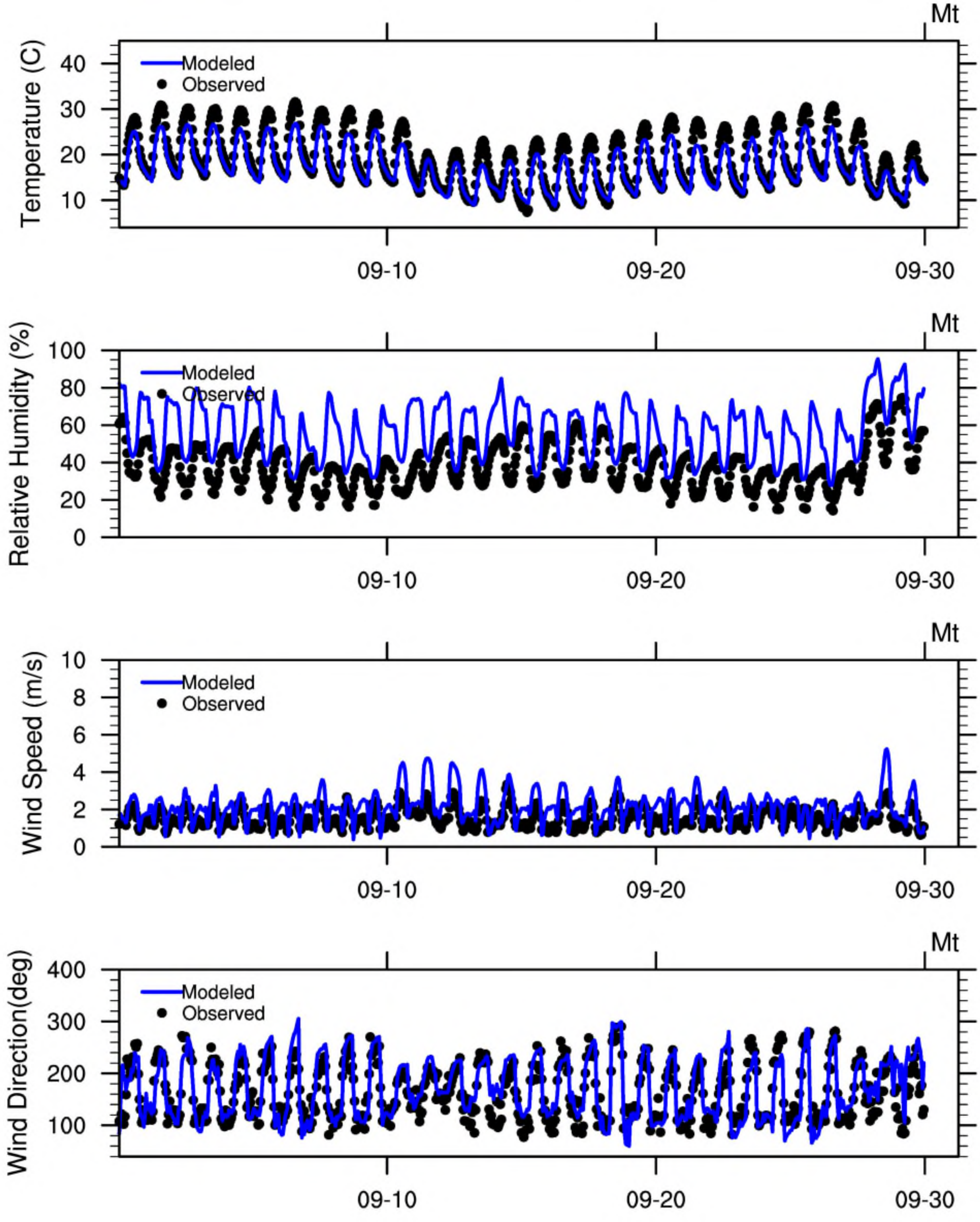

Figure S 13. Time series of average temperature, relative humidity, wind speed, and direction, and temperature of all valley sites in October 2018.

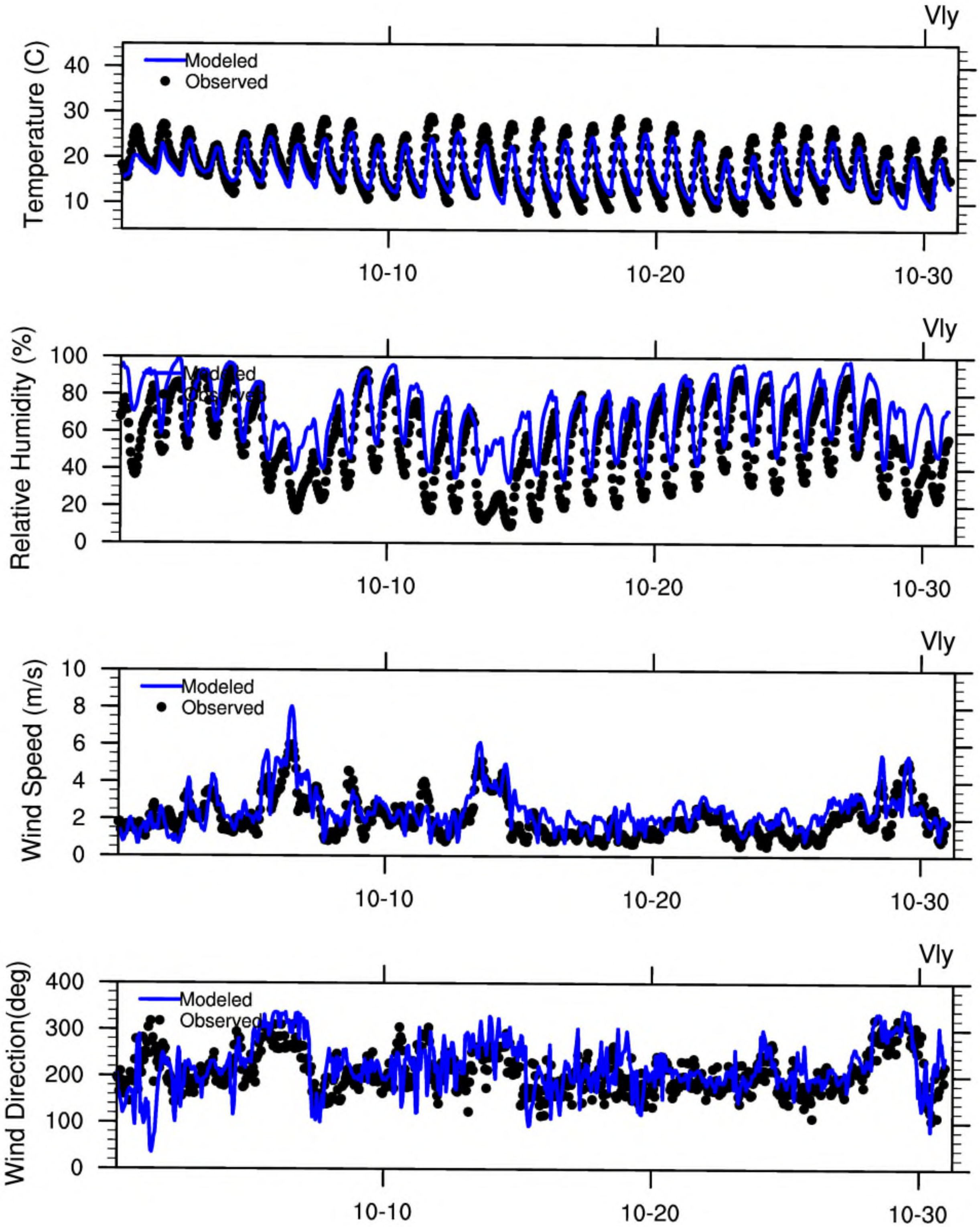

Figure S 14. Time series of average temperature, relative humidity, wind speed, and direction, and temperature of all mountain sites in October 2018.

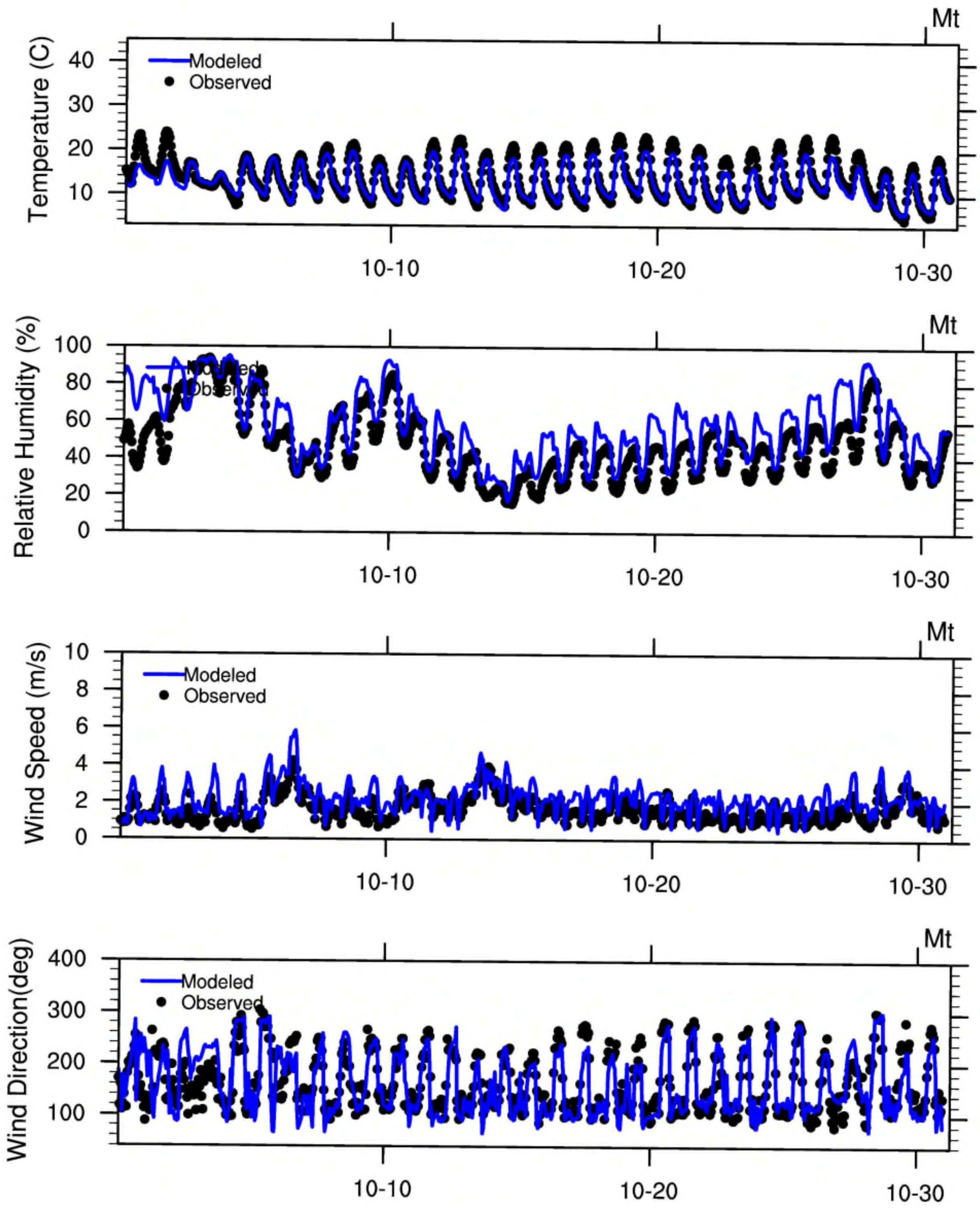

Figure S 15. Observed and modeled ozone frequency distribution for the ozone season in the SFNA (April – October 2018)

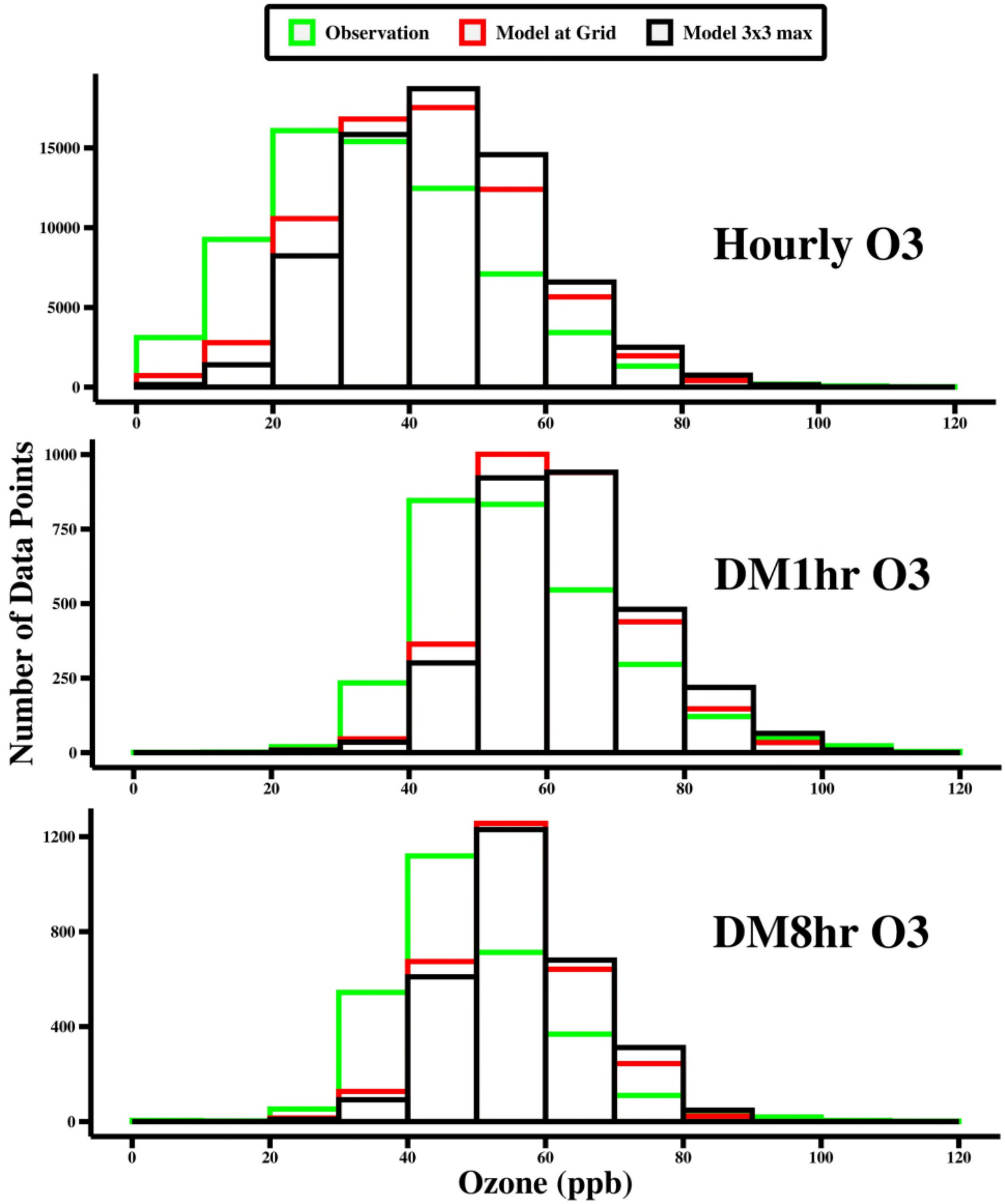

Figure S 16. Observed and modeled ozone frequency distribution for the ozone season in the SFNA (Fire days excluded in April – October 2018)

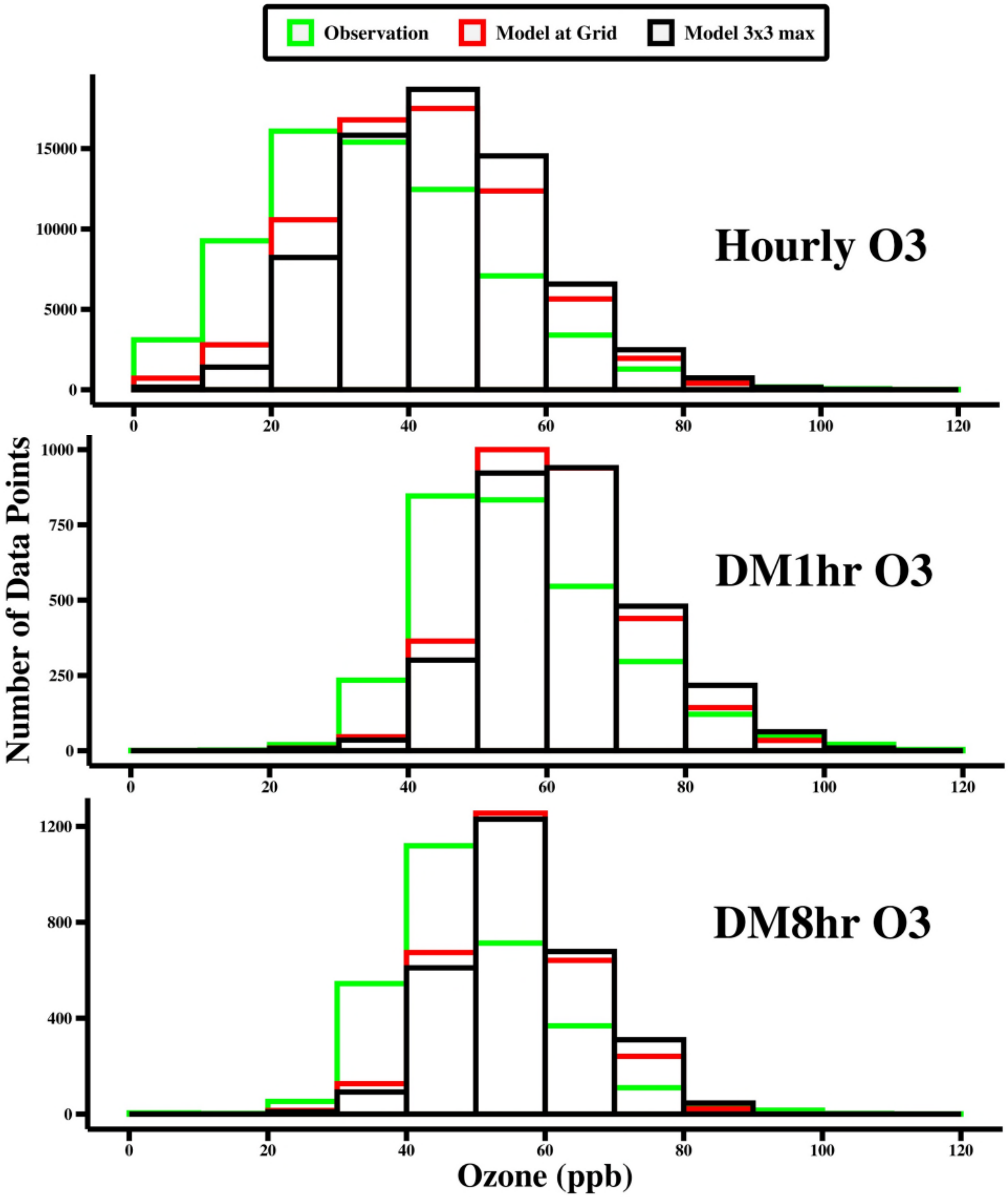

Figure S 17. Observed and modeled ozone scatter plots for the ozone season in the SFNA with fire day values shown in red (April – October 2018)

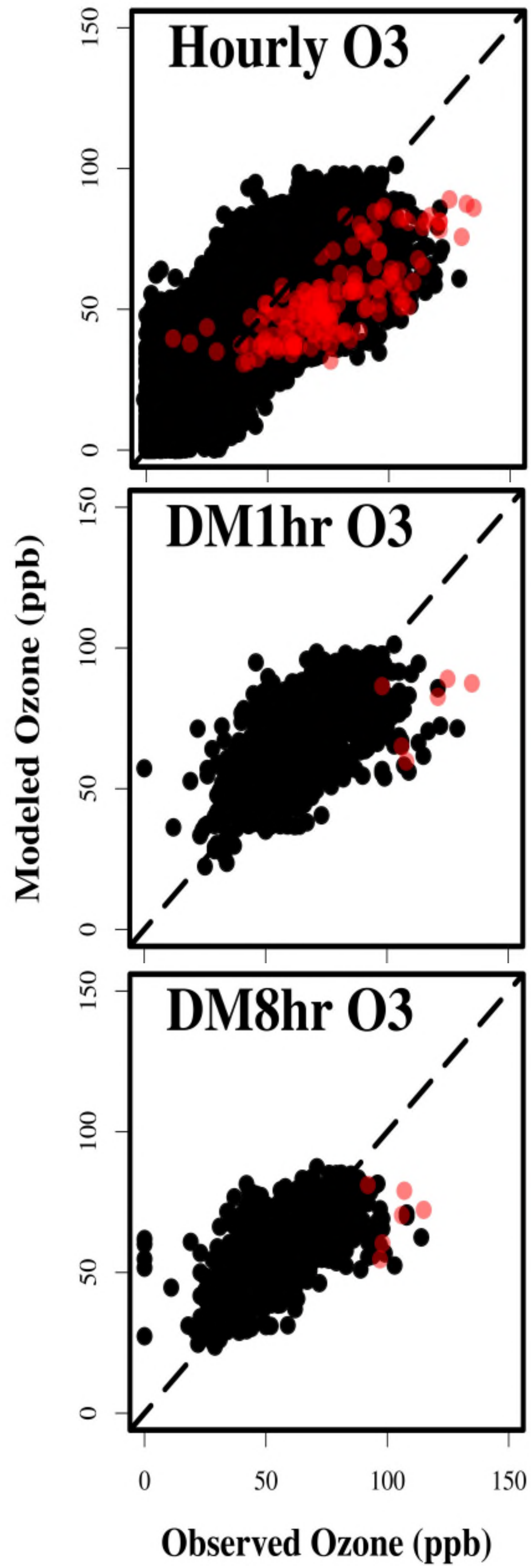

Figure S 18. Time-series of hourly ozone at Placerville-Gold for the ozone season (April – October 2018)

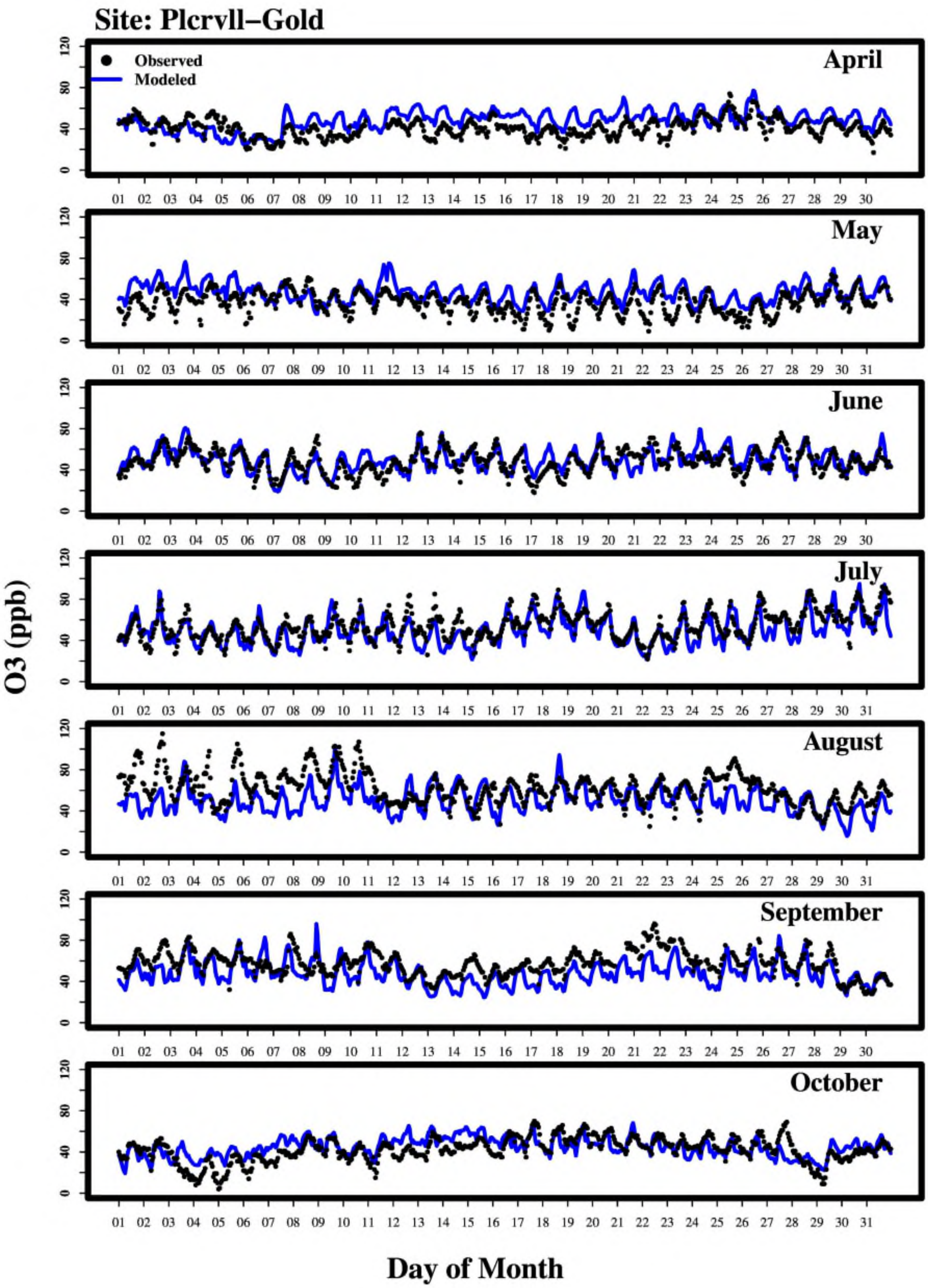

Figure S 19. Time-series of hourly ozone at Colfax-CityHall for the ozone season (April – October 2018)

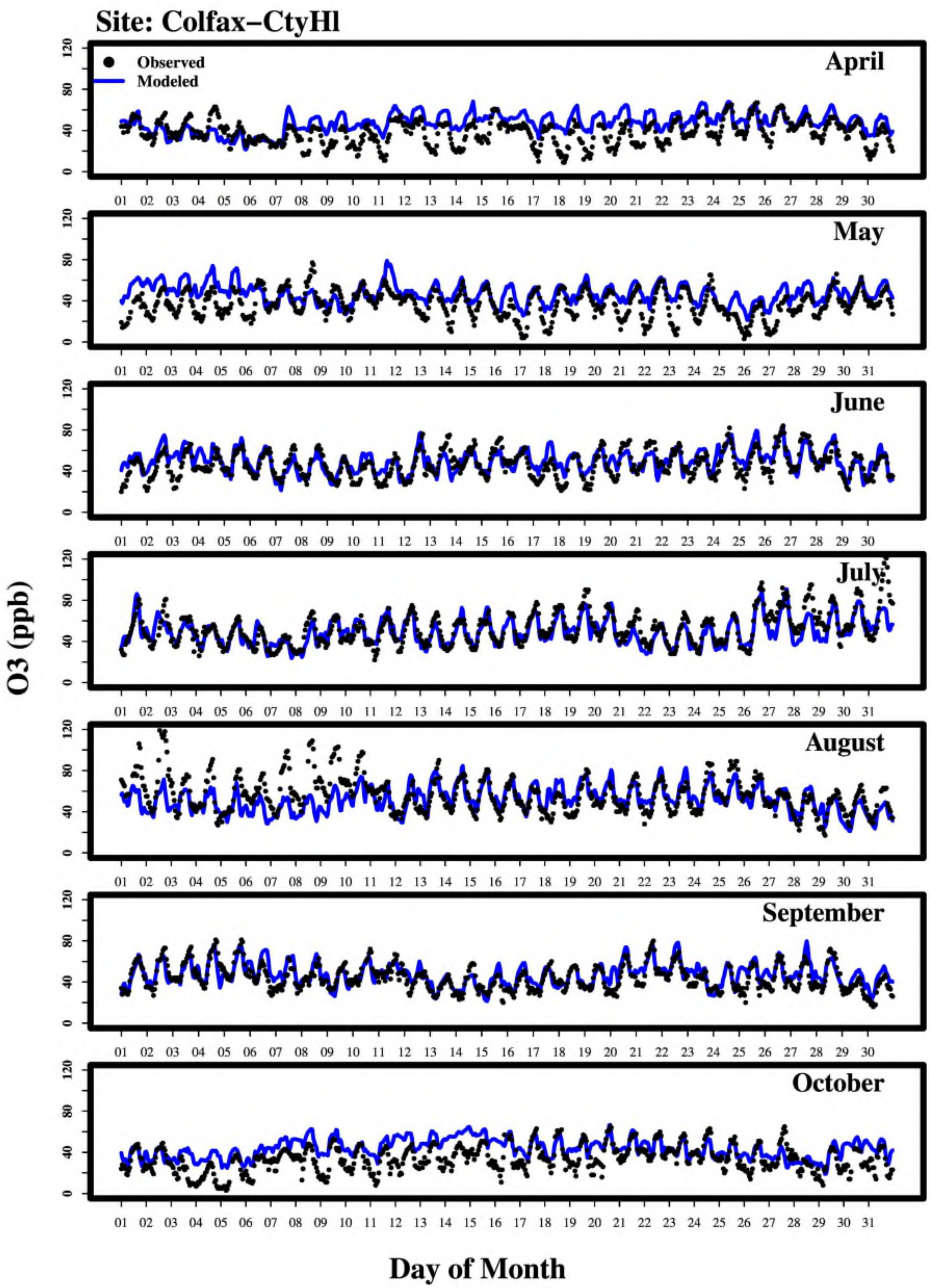

Figure S 20. Time-series of hourly ozone at Cool-Hwy193 for the ozone season (April – October 2018)

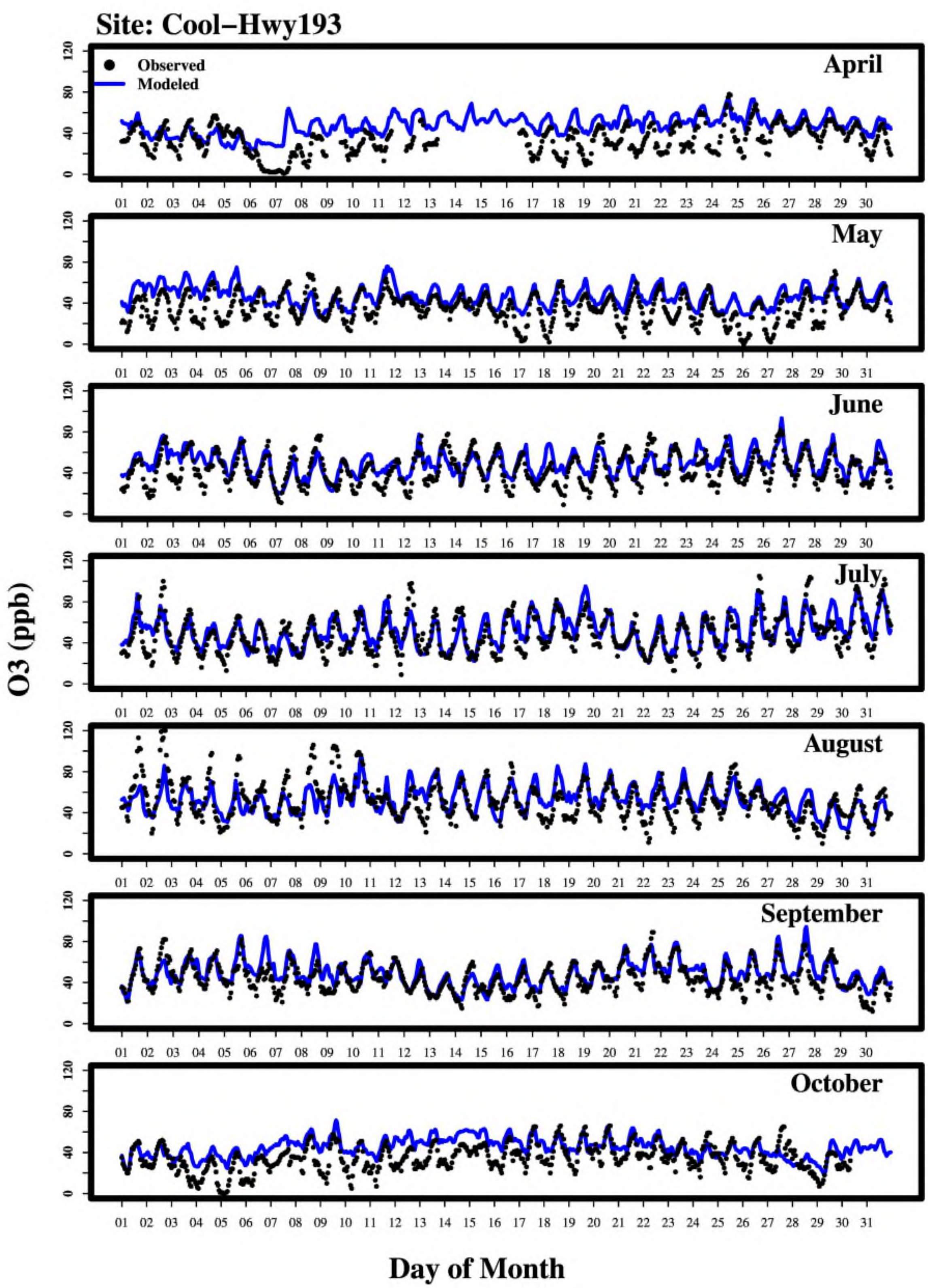

Figure S 21. Time-series of hourly ozone at Auburn-Atwood for the ozone season (April – October 2018)

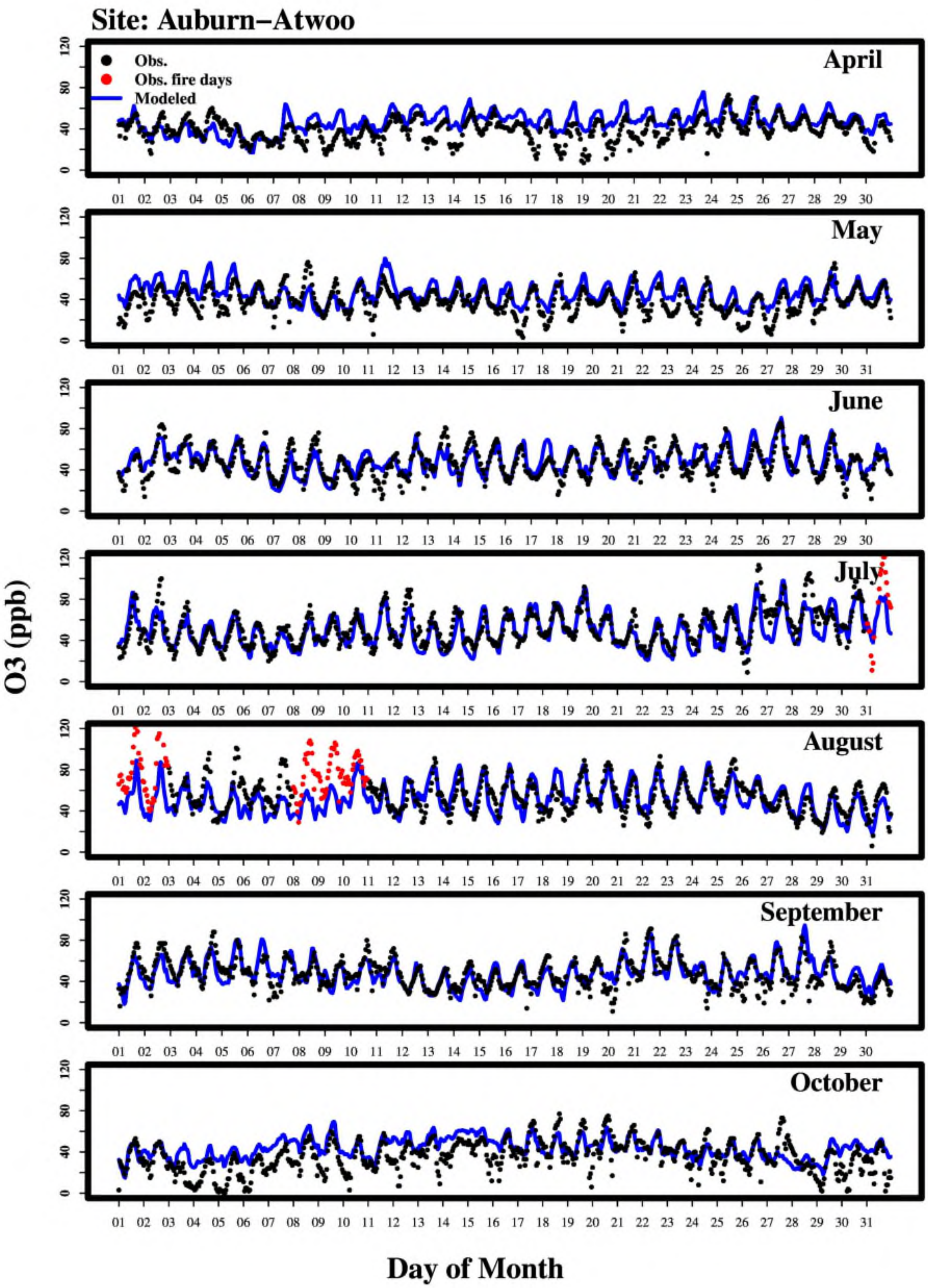

Figure S 22. Time-series of hourly ozone at Folsom-Natomas for the ozone season (April – October 2018)

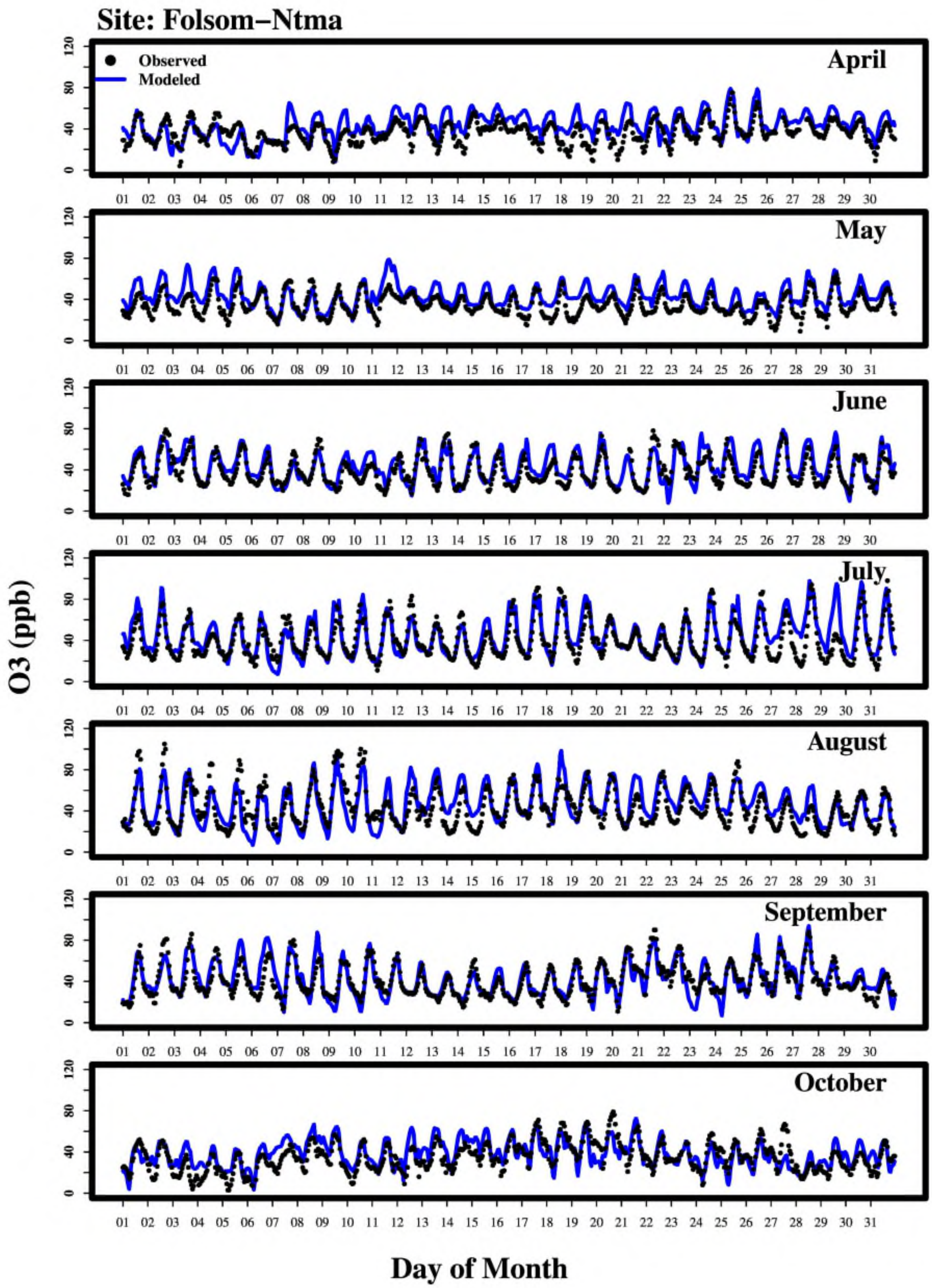

Figure S 23. Time-series of hourly ozone at Roseville-NSunrise for the ozone season (April – October 2018)

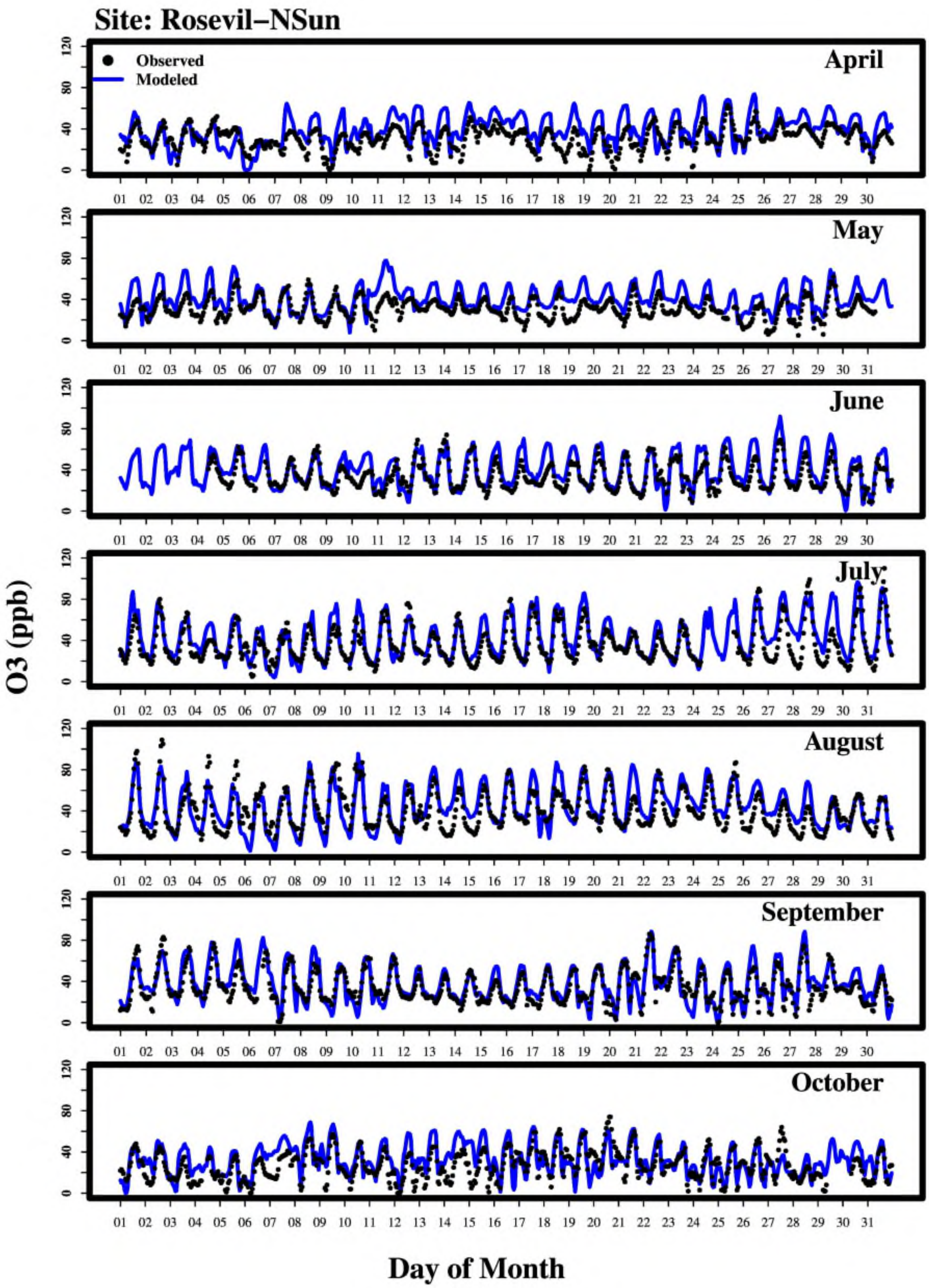

Figure S 24. Time-series of hourly ozone at N_Highlands-Blackfoot for the ozone season (April – October 2018)

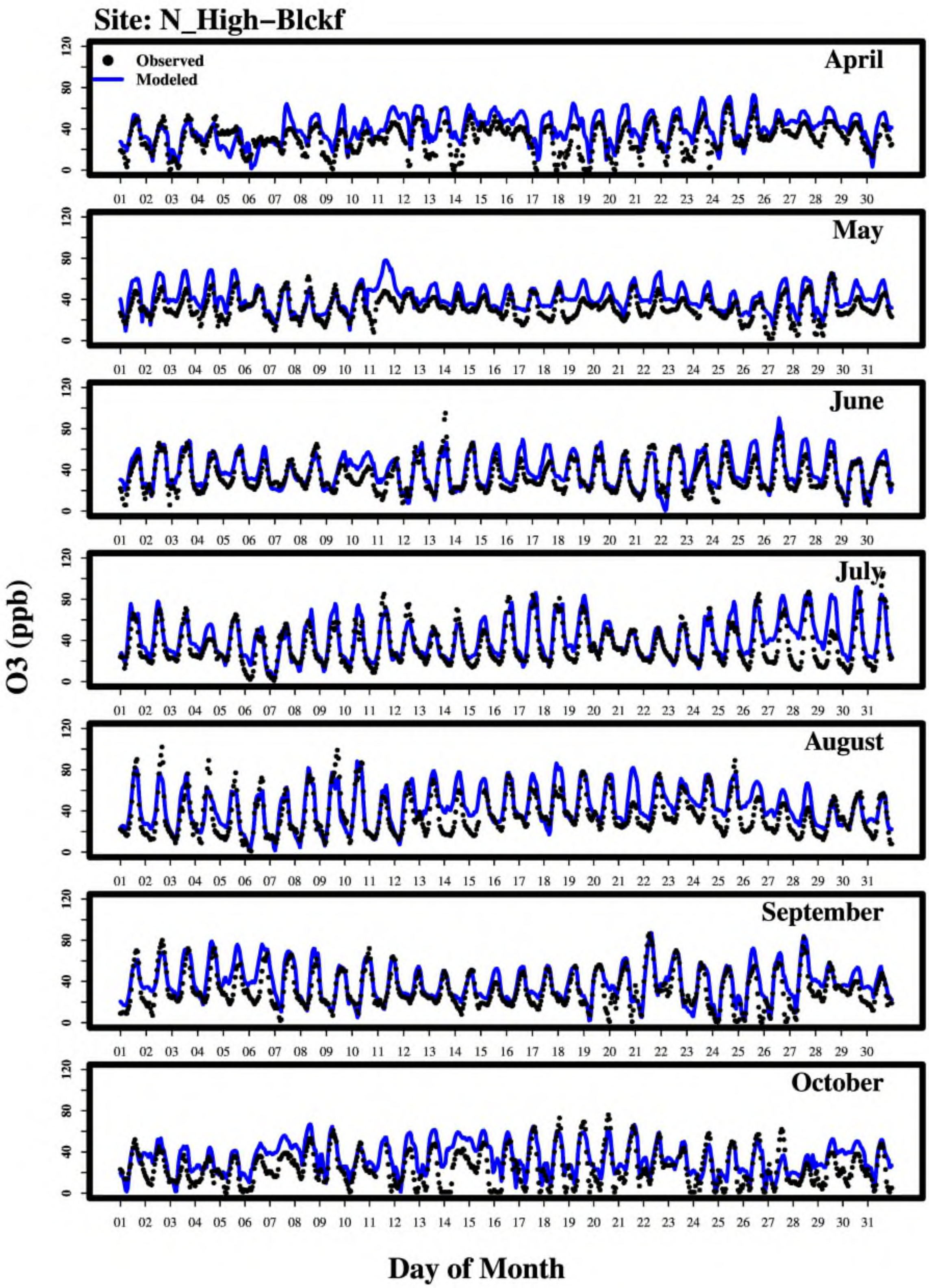

Figure S 25. Time-series of hourly ozone at Sacramento-DelPas for the ozone season (April – October 2018)

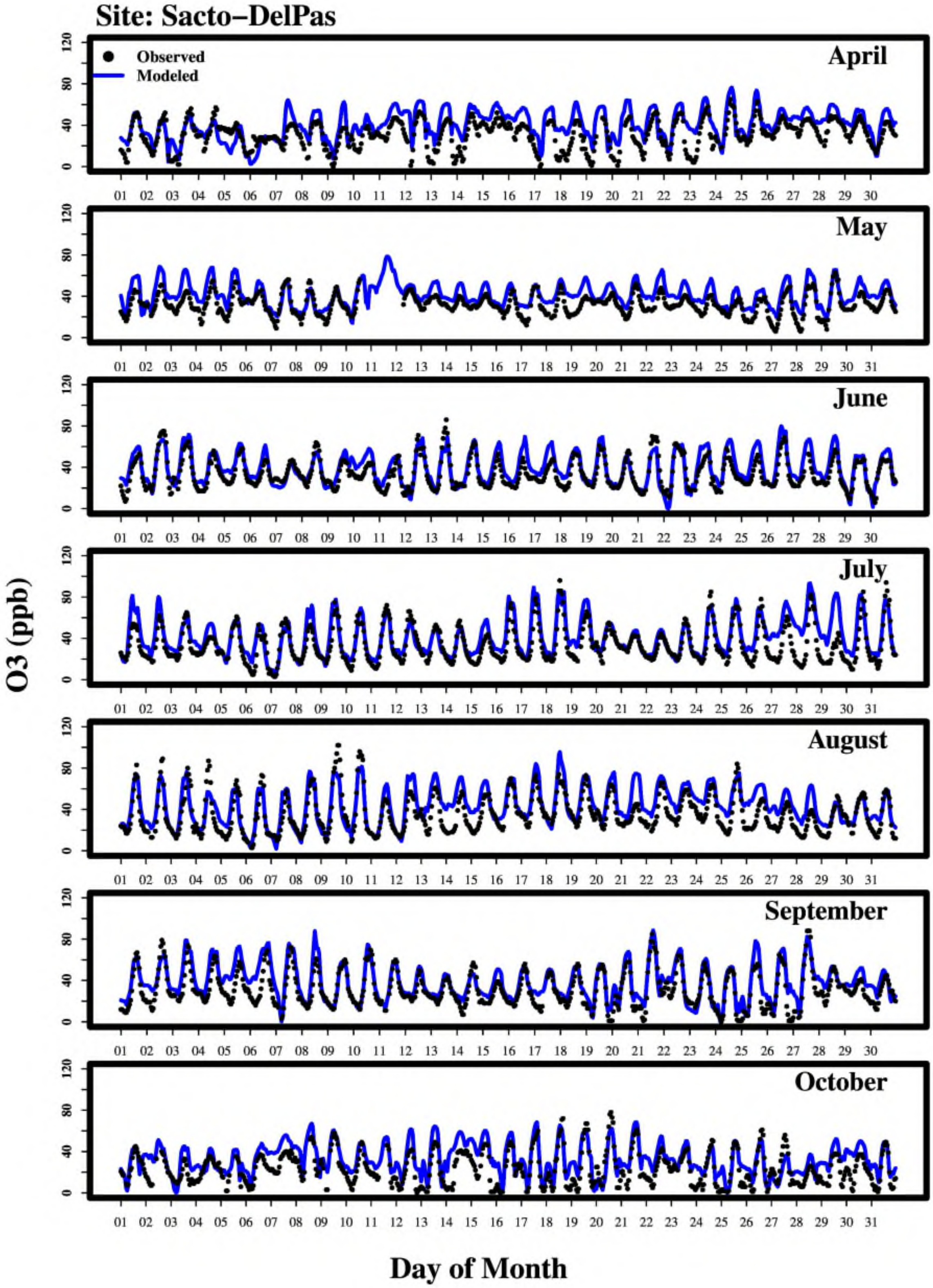

Figure S 26. Time-series of hourly ozone at Sloughouse for the ozone season (April – October 2018)

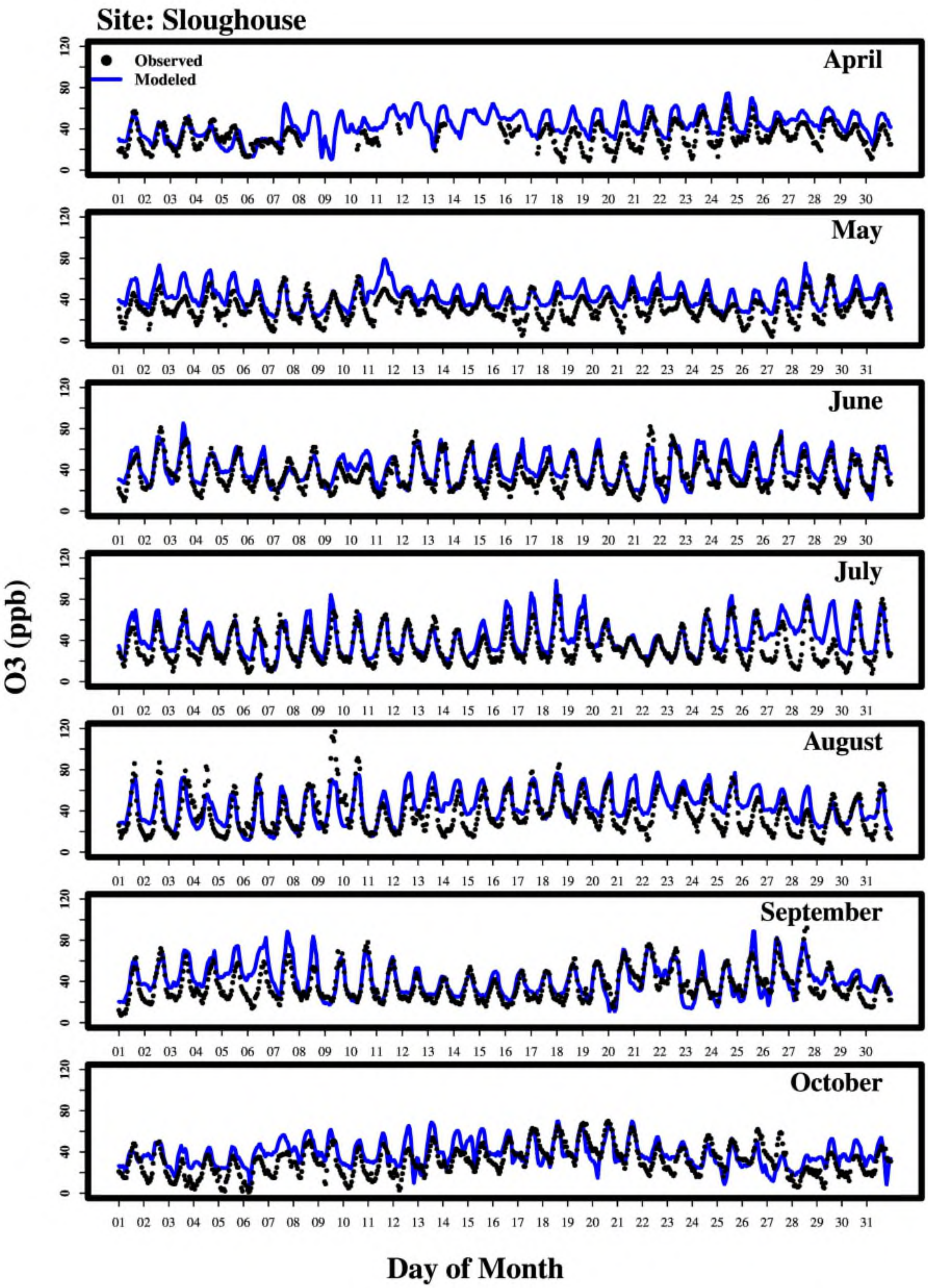

Figure S 27. Time-series of hourly ozone at Sacramento-TStreet for the ozone season (April – October 2018)

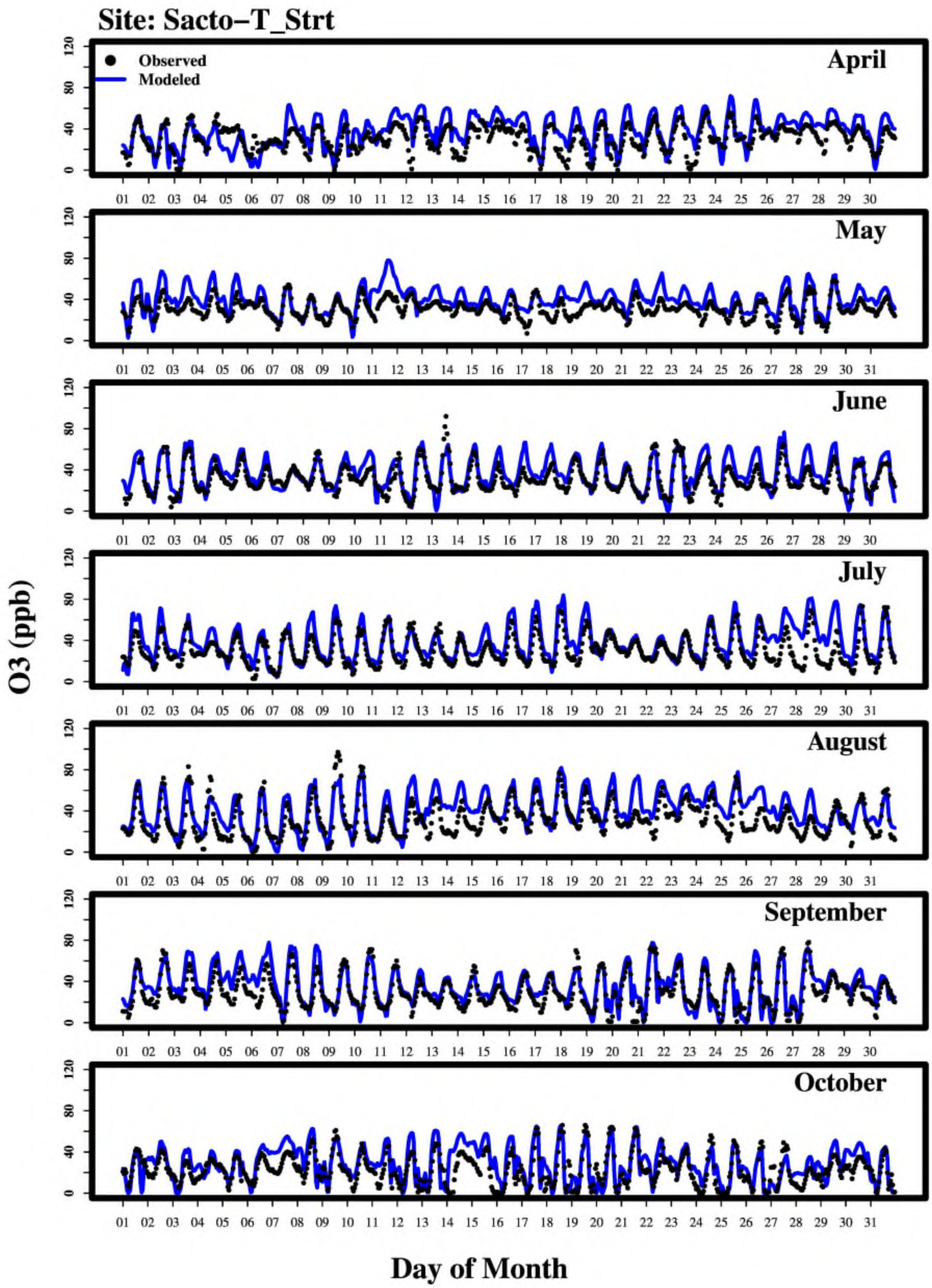

Figure S 28. Time-series of hourly ozone at Elk_Grove-Bruceville for the ozone season (April – October 2018)

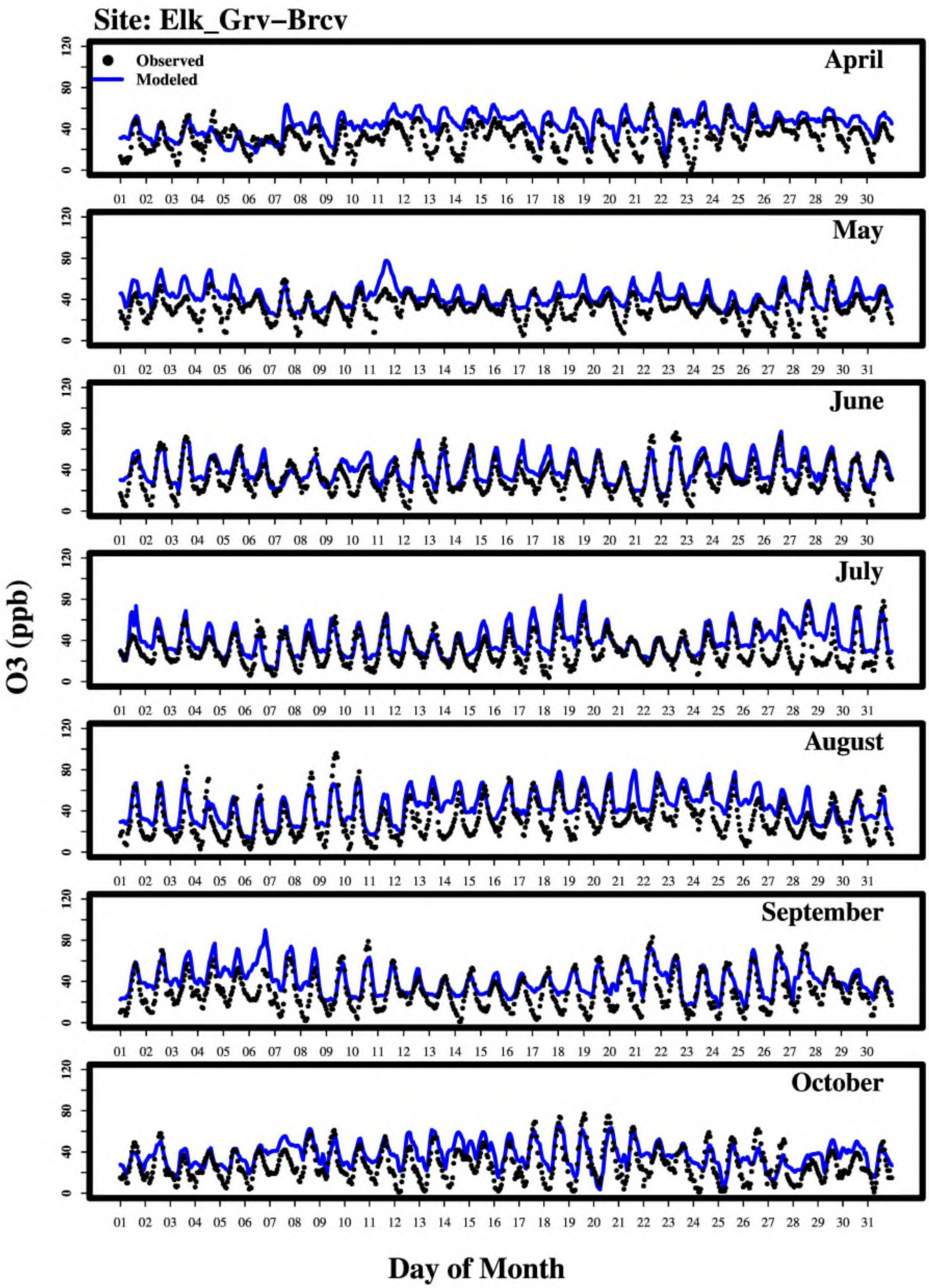

Figure S 29. Time-series of hourly ozone at Woodland-Gibson for the ozone season (April – October 2018)

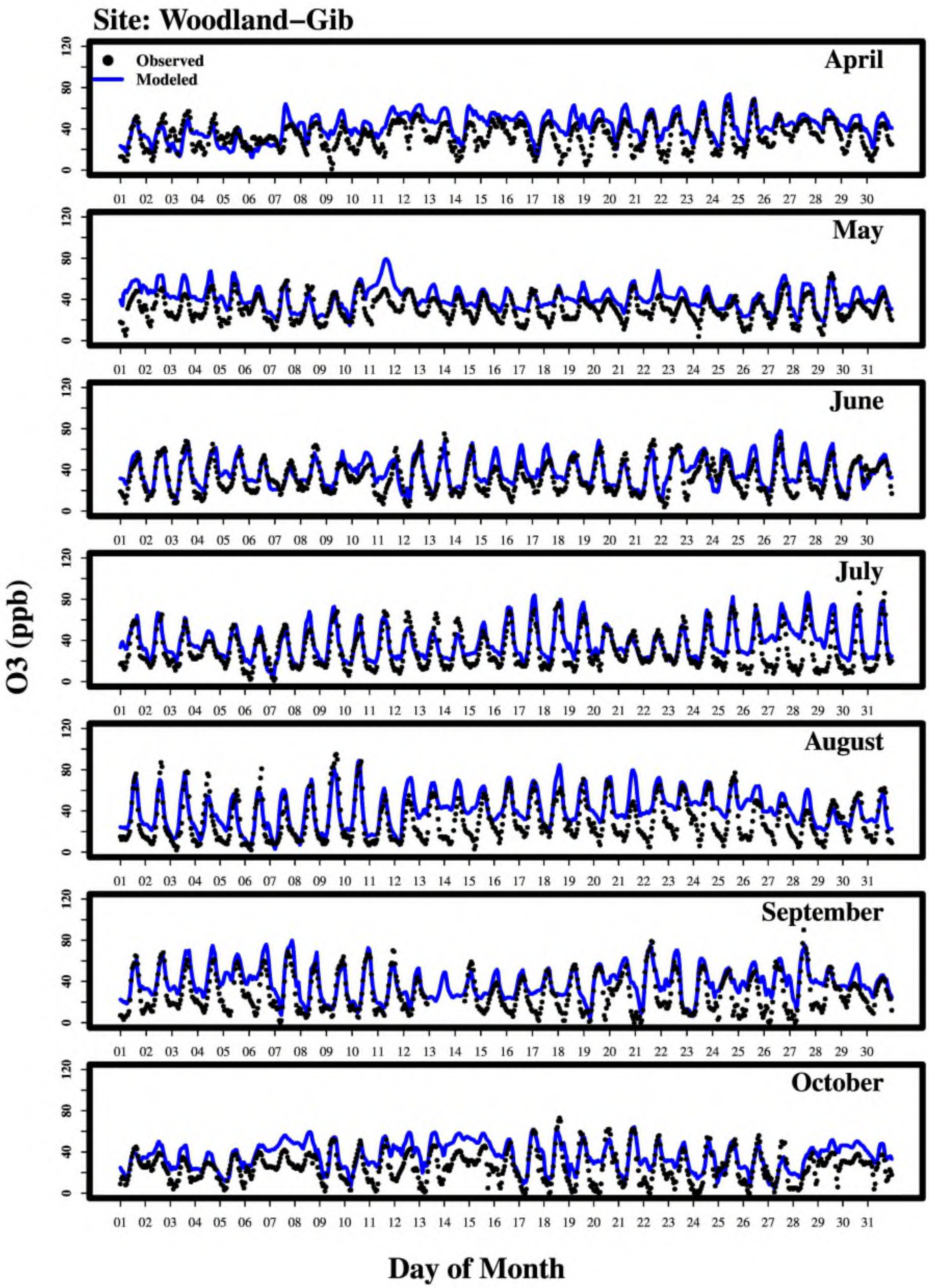

Figure S 30. Time-series of hourly ozone at Vacaville-Ulatis for the ozone season (April – October 2018)

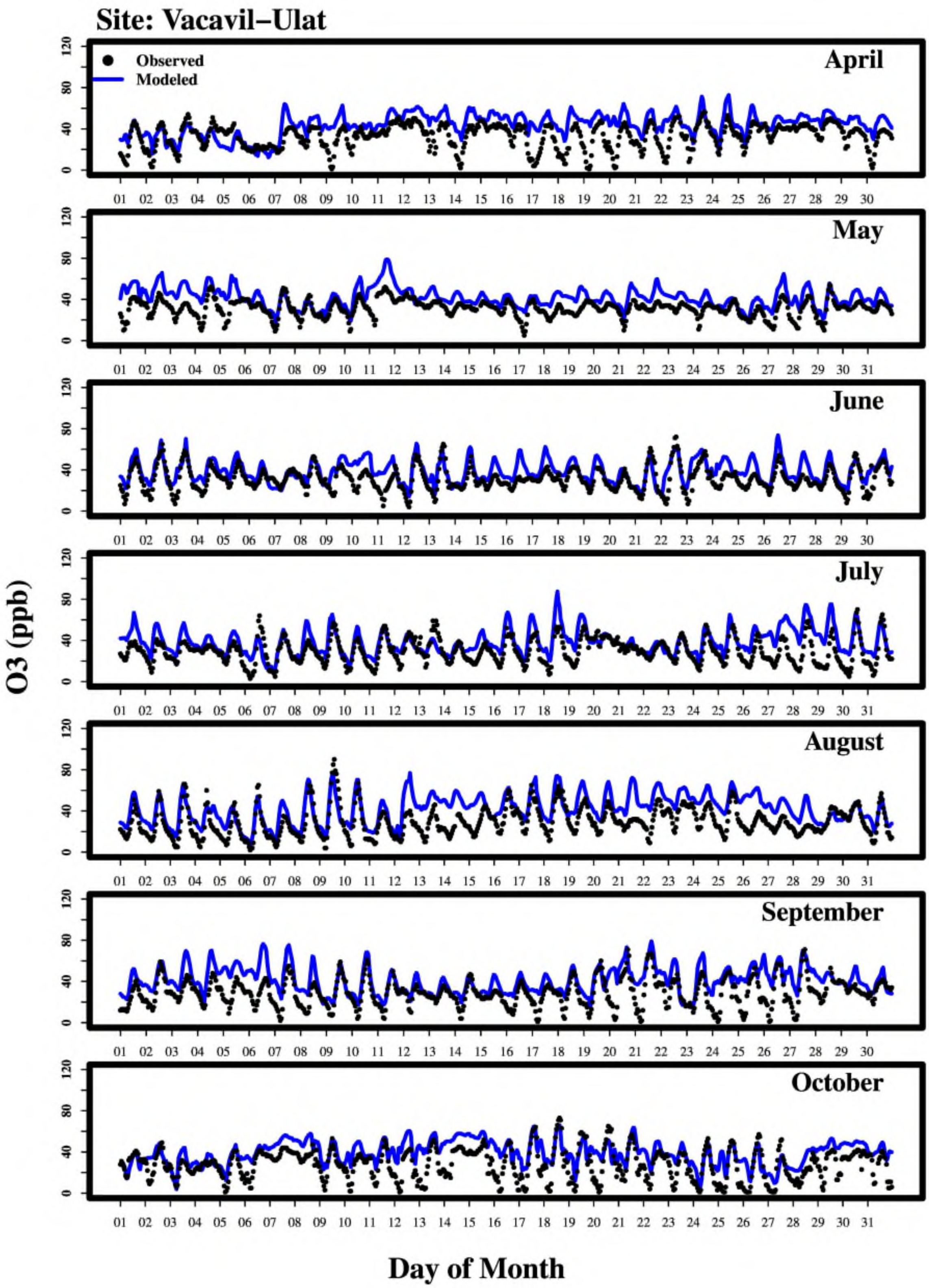

Figure S 31. Time-series of hourly ozone at Davis-UCD for the ozone season (April – October 2018)

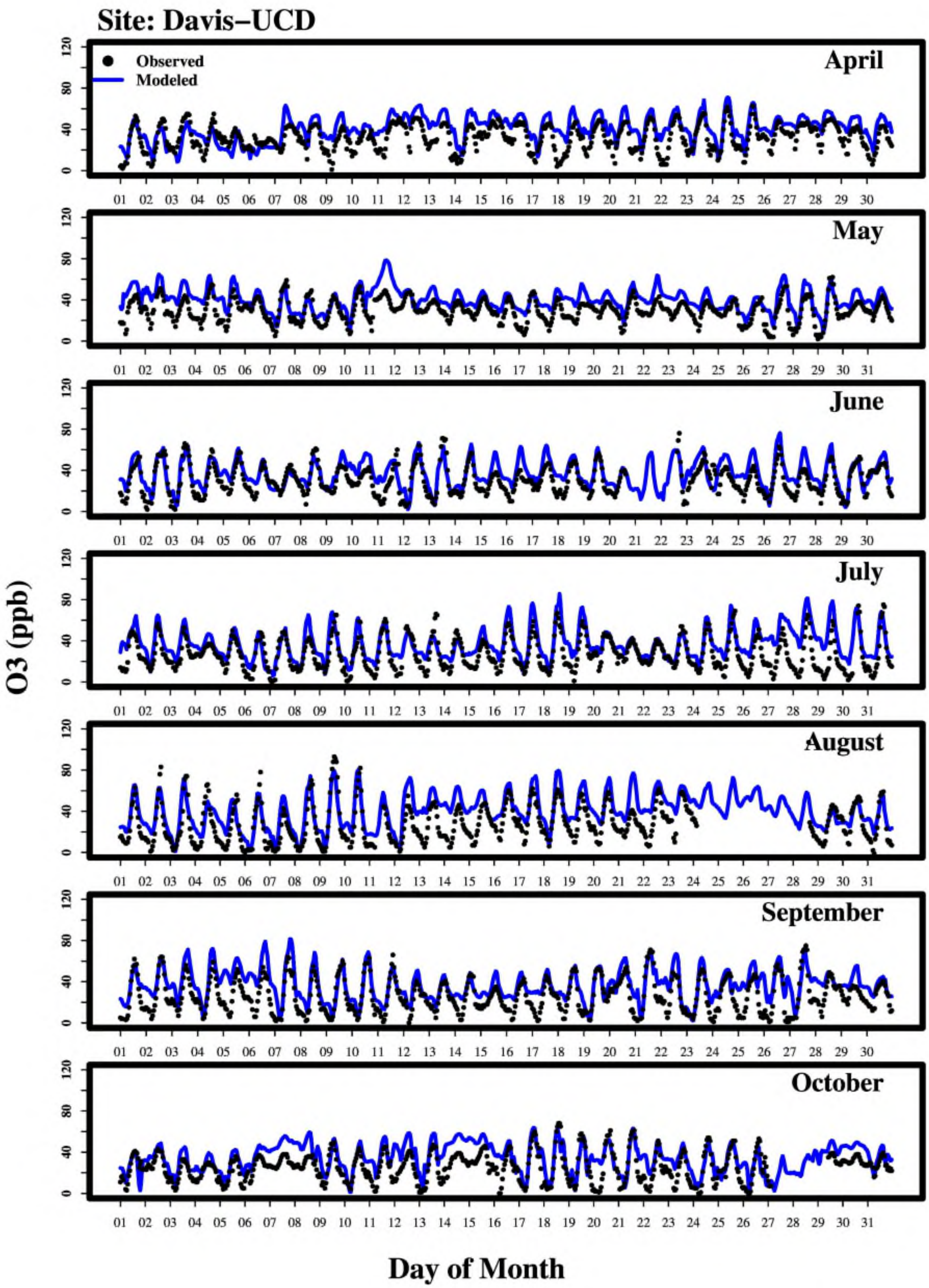

Figure S 32. Time-series of maximum daily 1-hour ozone at Placerville-Gold for the ozone season (April – October 2018)

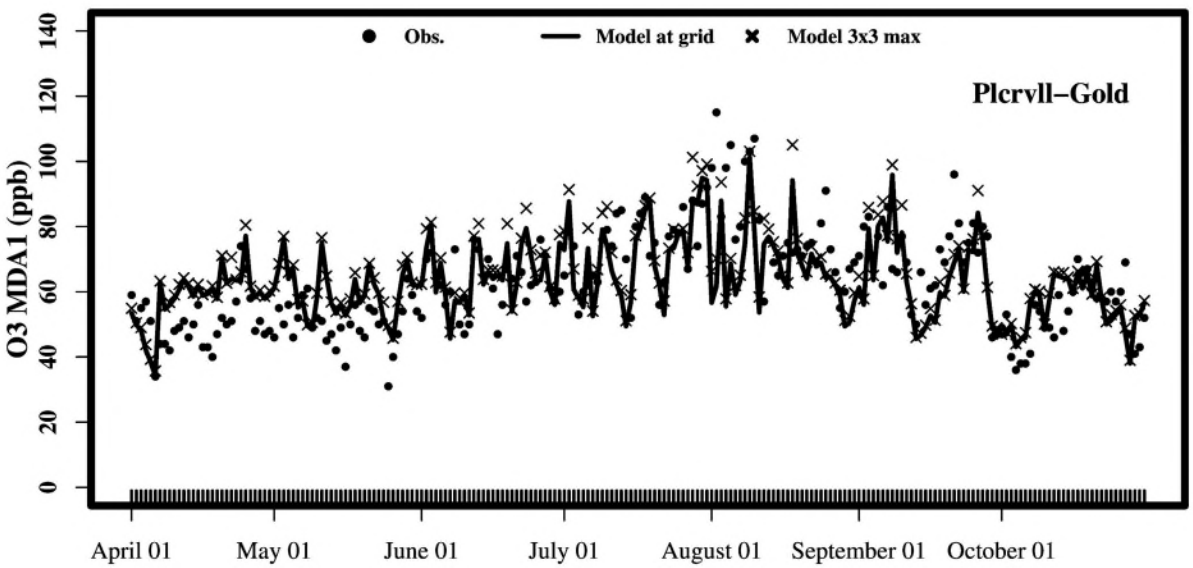

Figure S 33. Time-series of maximum daily 1-hour ozone at Colfax-CityHall for the ozone season (April – October 2018)

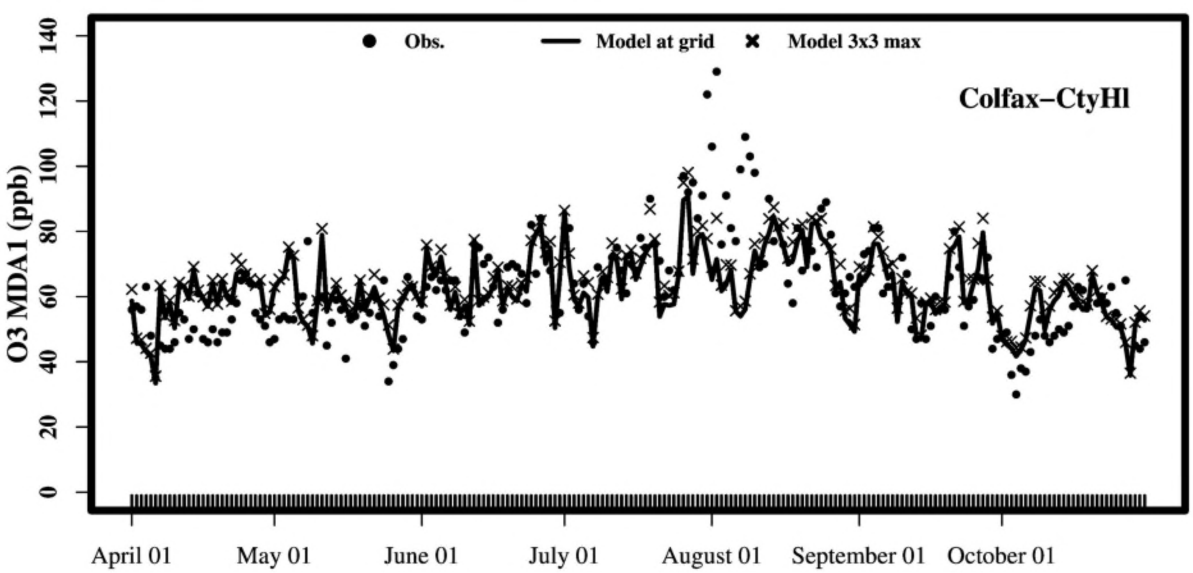

Figure S 34. Time-series of maximum daily 1-hour ozone at Cool-Hwy193 for the ozone season (April – October 2018)

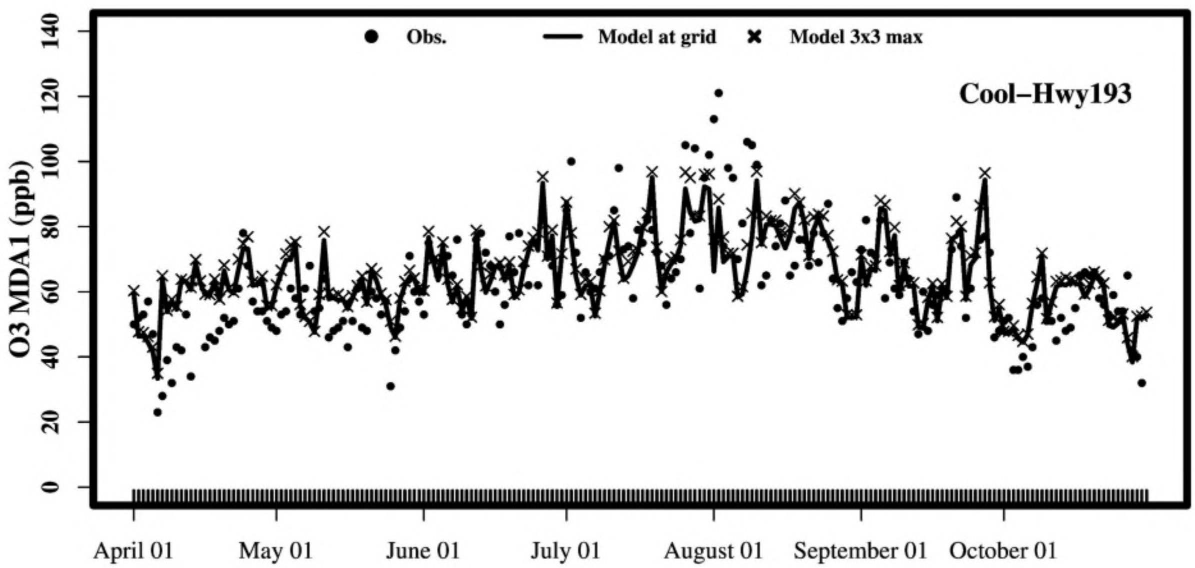

Figure S 35. Time-series of maximum daily 1-hour ozone at Auburn-Atwood for the ozone season (April – October 2018)

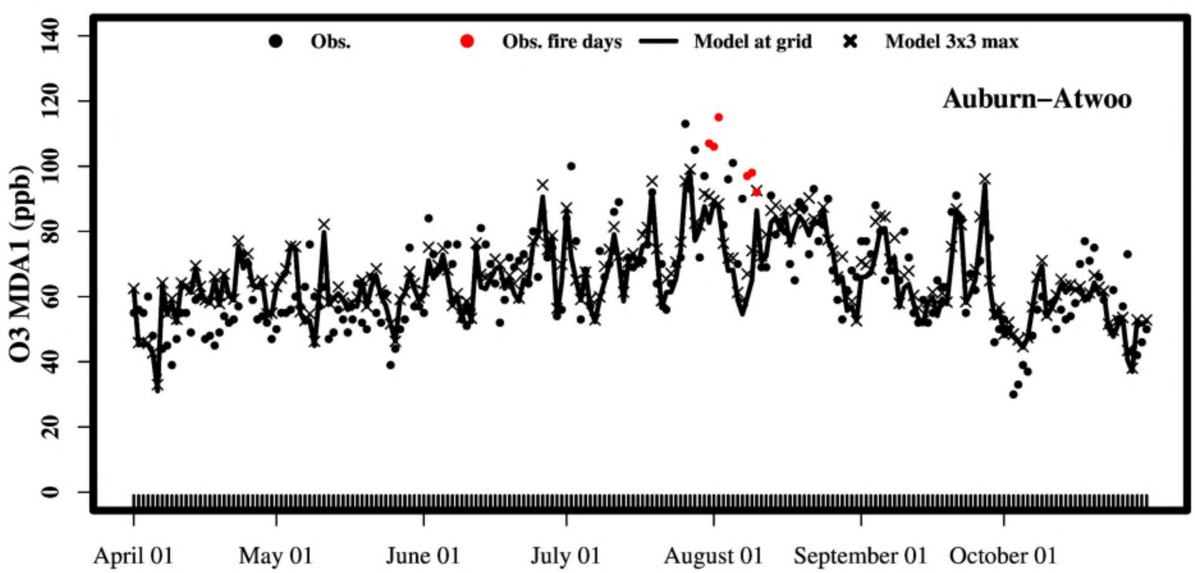

Figure S 36. Time-series of maximum daily 1-hour ozone at Folsom-Natomas for the ozone season (April – October 2018)

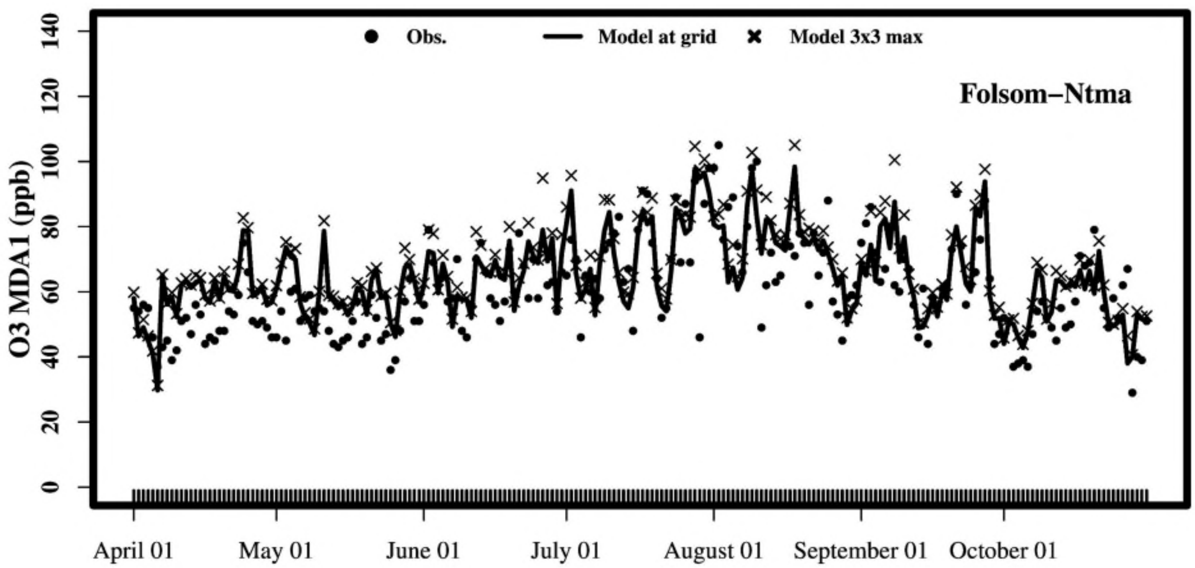

Figure S 37. Time-series of maximum daily 1-hour ozone at Roseville-NSunrise for the ozone season (April – October 2018)

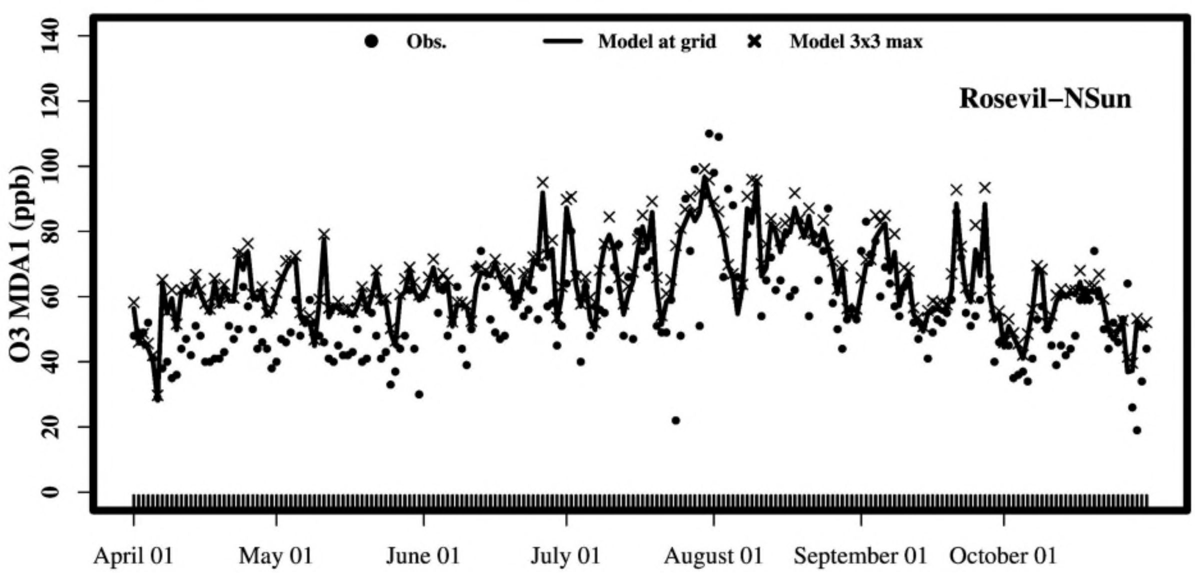

Figure S 38. Time-series of maximum daily 1-hour ozone at N_Highlands-Blackfoot for the ozone season (April – October 2018)

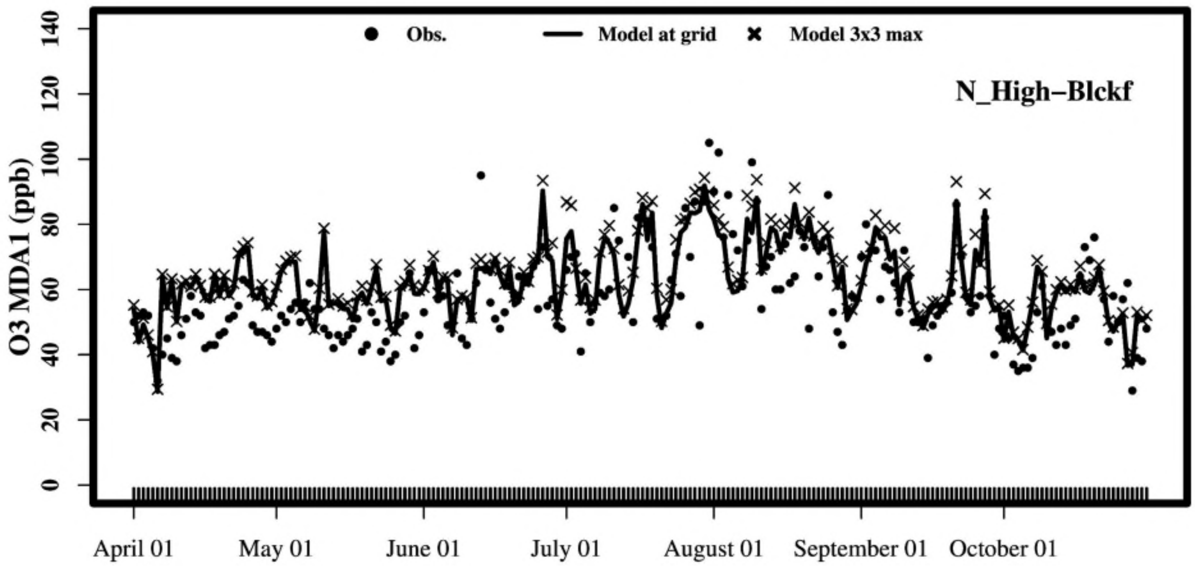

Figure S 39. Time-series of maximum daily 1-hour ozone at Sacramento-DelPas for the ozone season (April – October 2018)

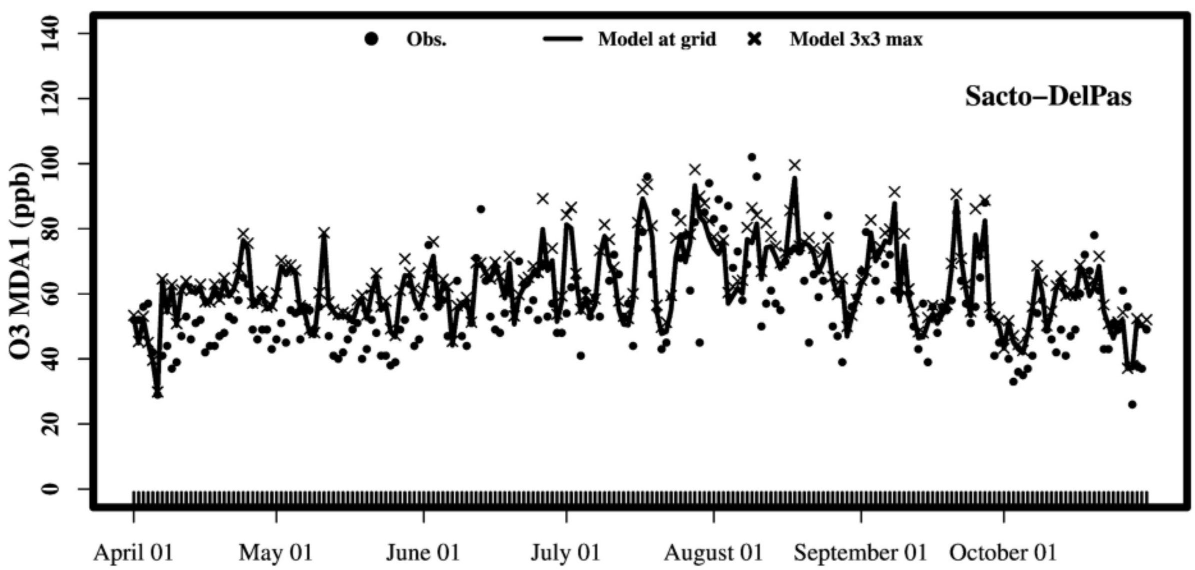

Figure S 40. Time-series of maximum daily 1-hour ozone at Sloughhouse for the ozone season (April – October 2018)

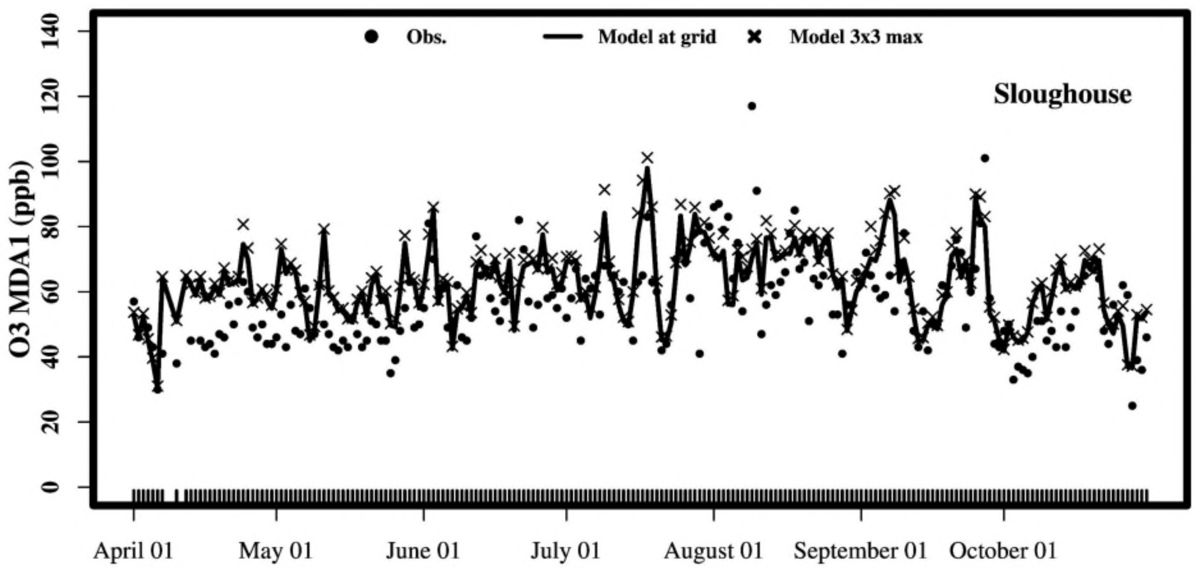

Figure S 41. Time-series of maximum daily 1-hour ozone at Sacramento-TStreet for the ozone season (April – October 2018)

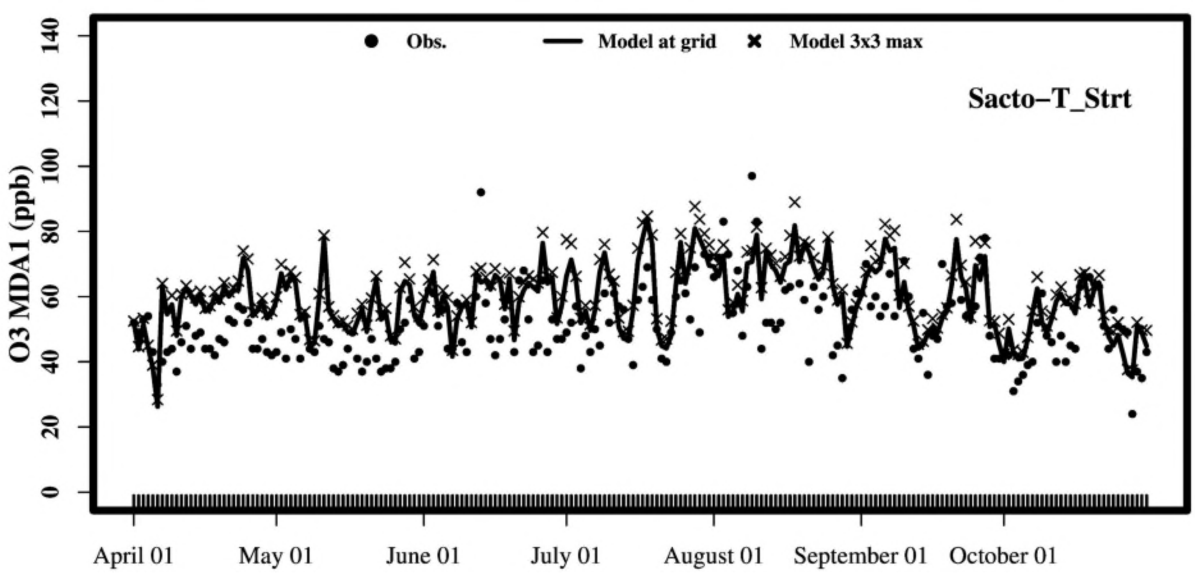

Figure S 42. Time-series of maximum daily 1-hour ozone at Elk_Grove-Bruceville for the ozone season (April – October 2018)

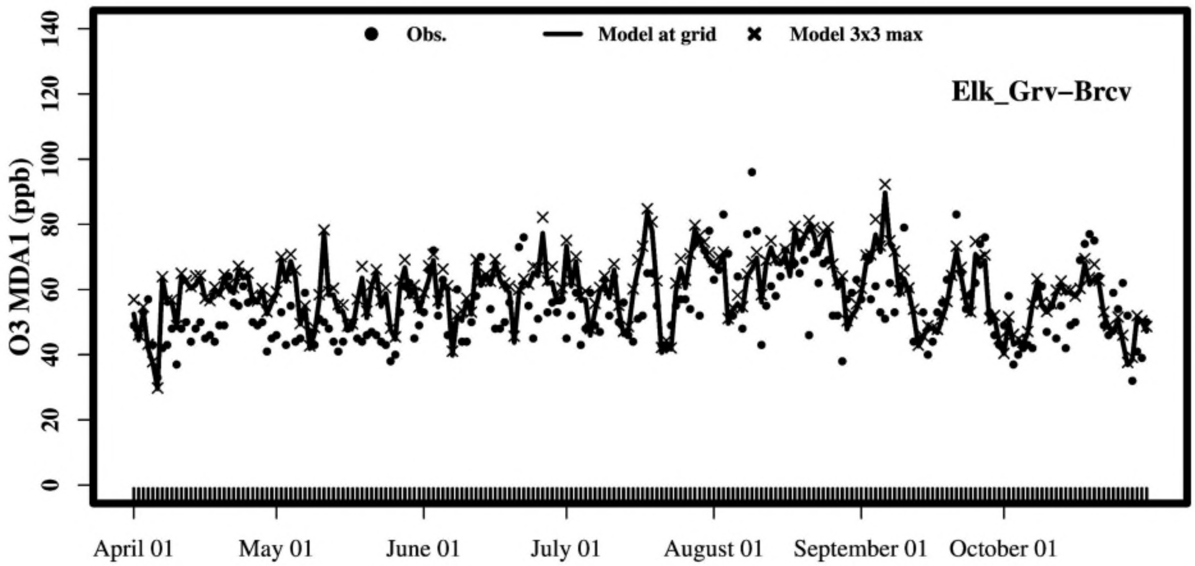

Figure S 43. Time-series of maximum daily 1-hour ozone at Woodland-Gibson for the ozone season (April – October 2018)

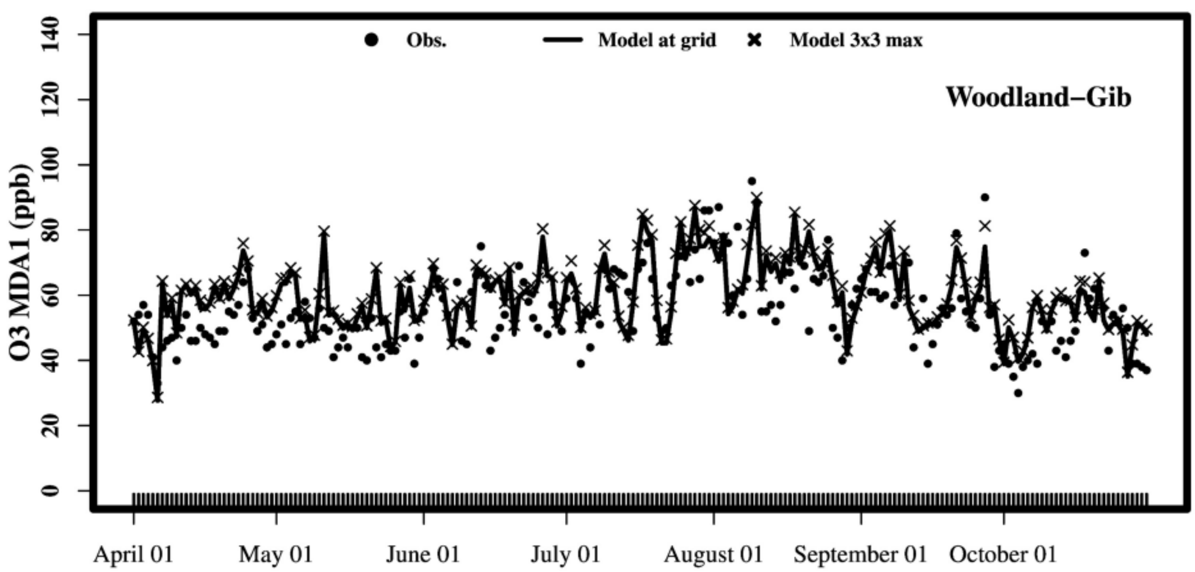

Figure S 44. Time-series of maximum daily 1-hour ozone at Vacaville-Ultatis for the ozone season (April – October 2018)

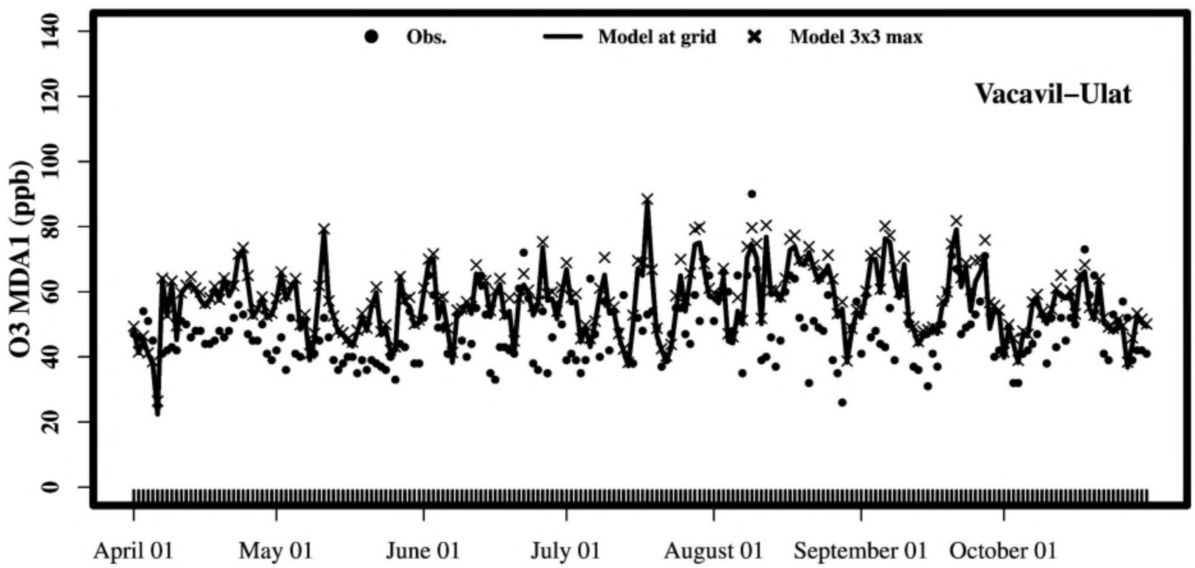

Figure S 45. Time-series of maximum daily 1-hour ozone at Davis-UCD for the ozone season (April – October 2018)

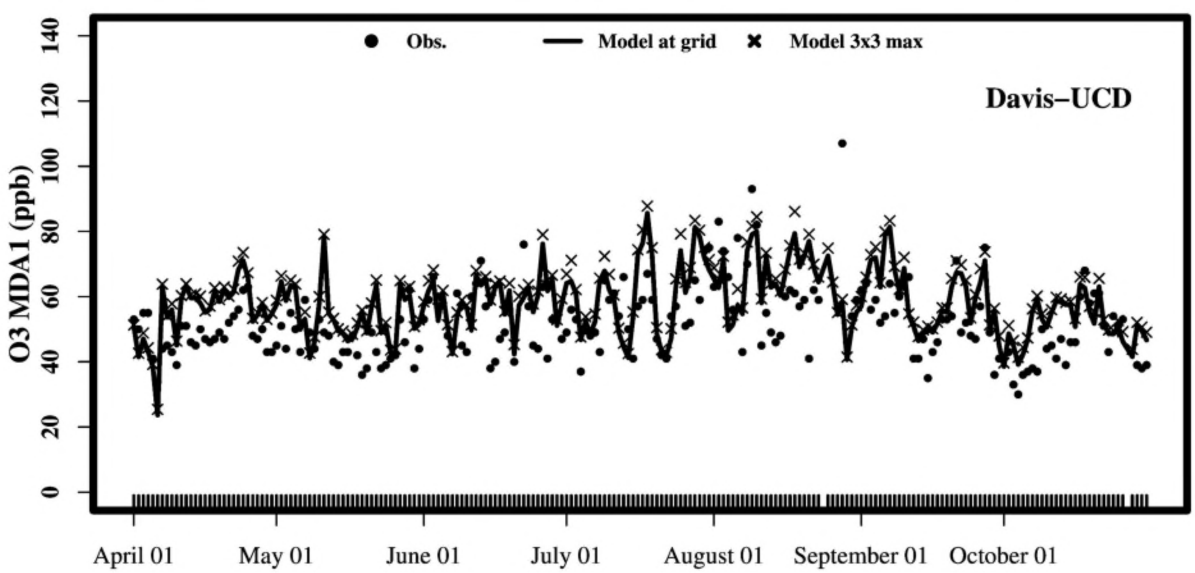

Figure S 46. Time-series of maximum daily average 8-hour ozone at Placerville-Gold for the ozone season (April – October 2018)

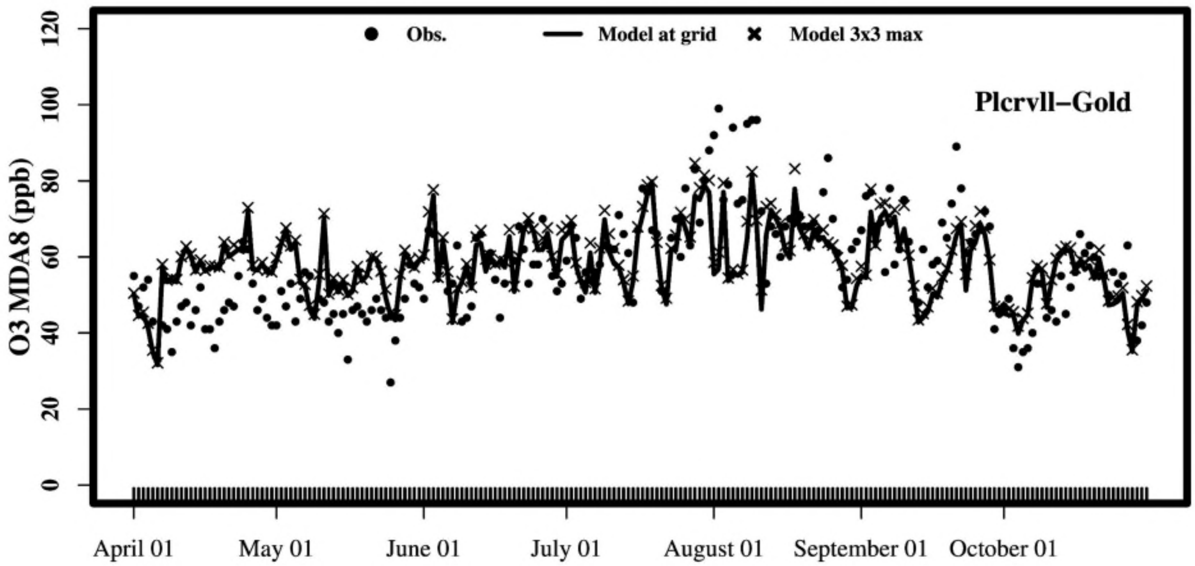

Figure S 47. Time-series of maximum daily average 8-hour ozone at Colfax-CityHall for the ozone season (April – October 2018)

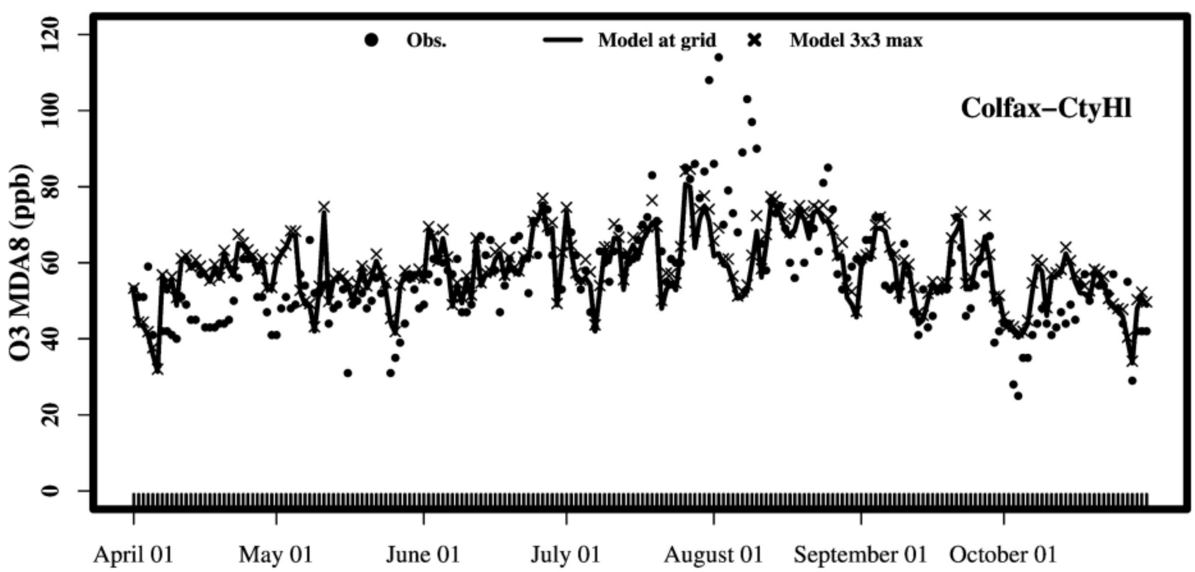

Figure S 48. Time-series of maximum daily average 8-hour ozone at Cool-Hwy193 for the ozone season (April – October 2018)

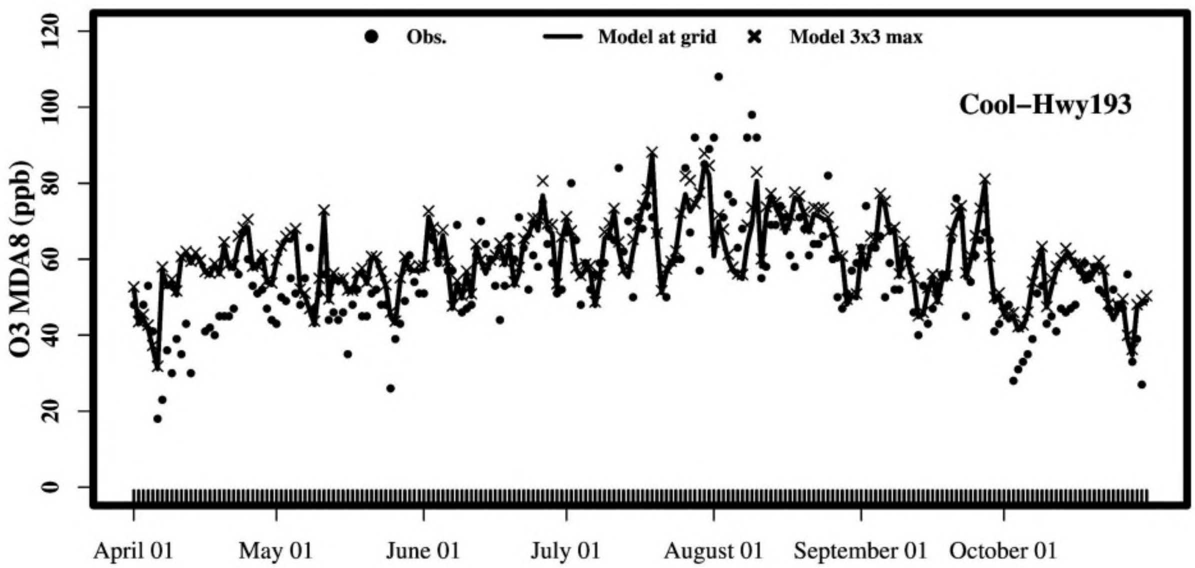

Figure S 49. Time-series of maximum daily average 8-hour ozone at Auburn-Atwood for the ozone season (April – October 2018)

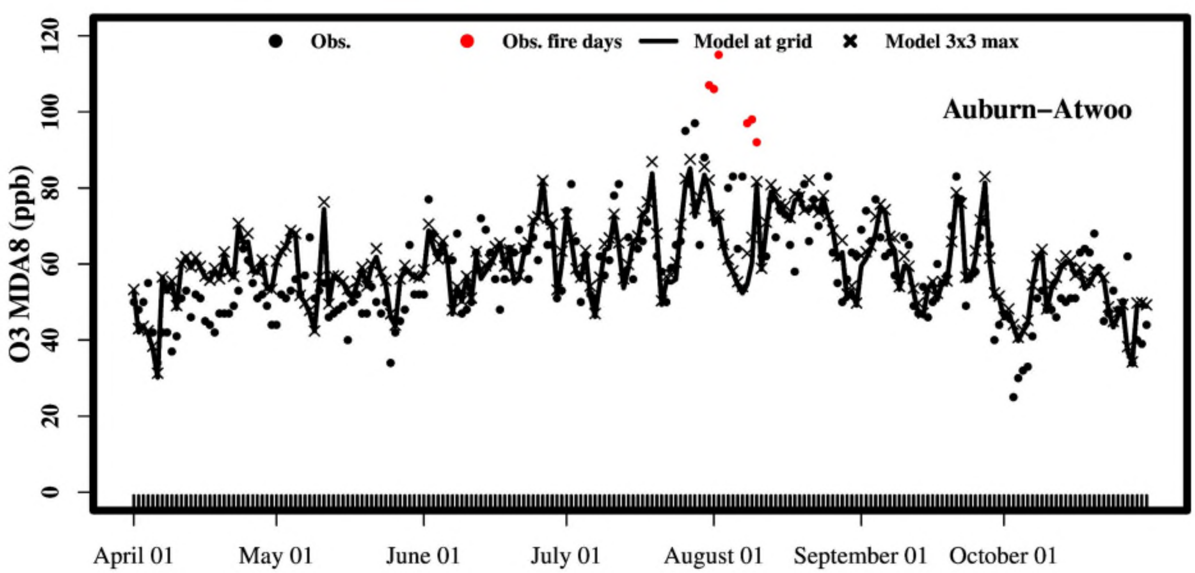

Figure S 50. Time-series of maximum daily average 8-hour ozone at Folsom-Natomas for the ozone season (April – October 2018)

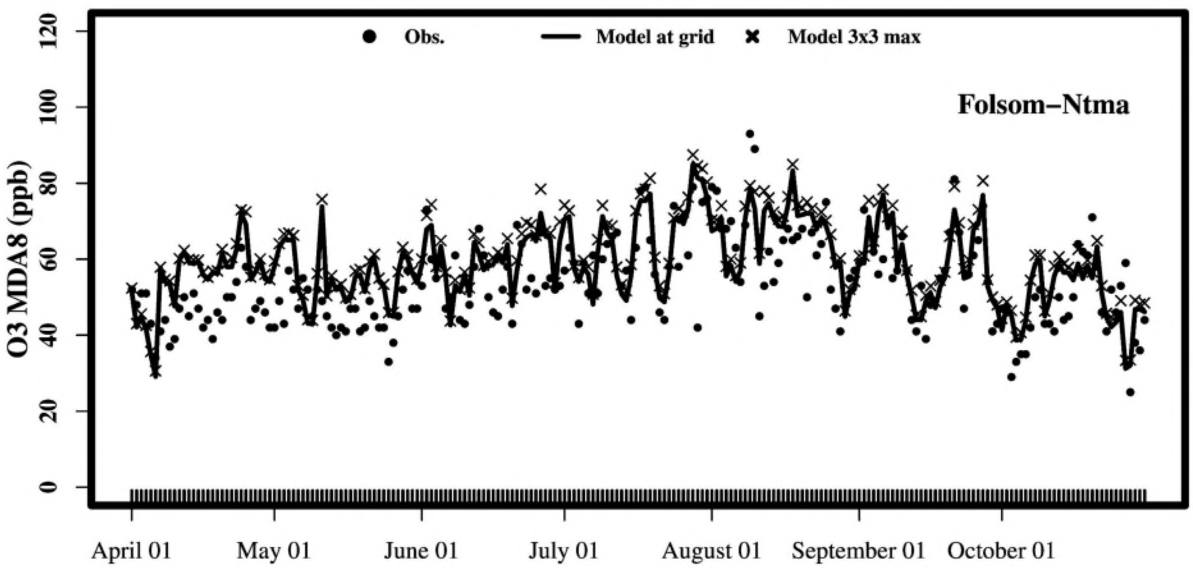

Figure S 51. Time-series of maximum daily average 8-hour ozone at Roseville-NSunrise for the ozone season (April – October 2018)

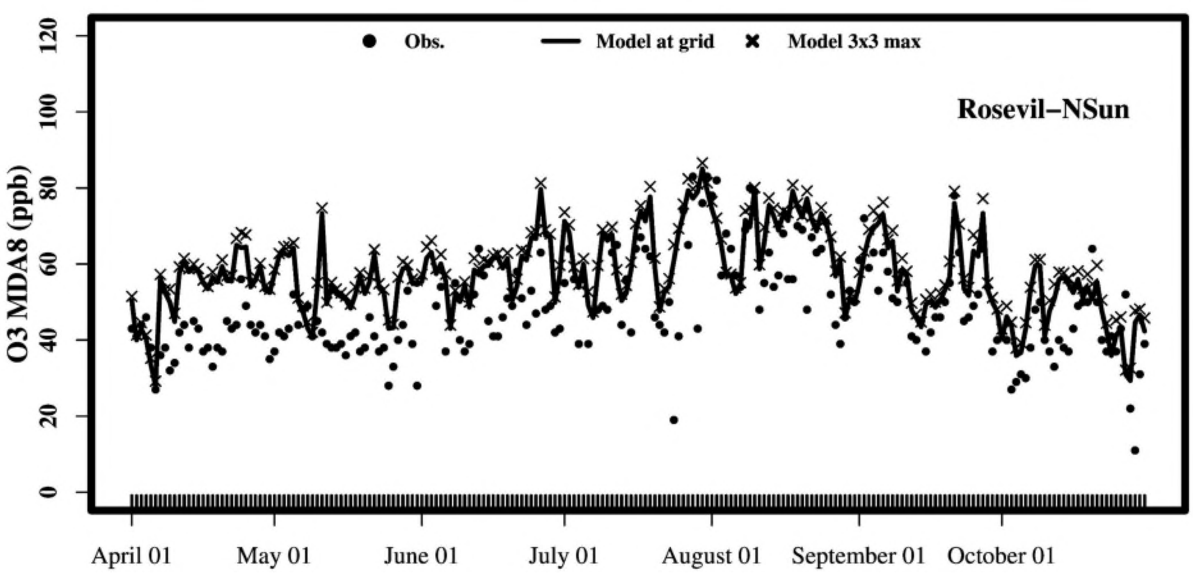

Figure S 52. Time-series of maximum daily average 8-hour ozone at N_Highlands-Blackfoot for the ozone season (April – October 2018)

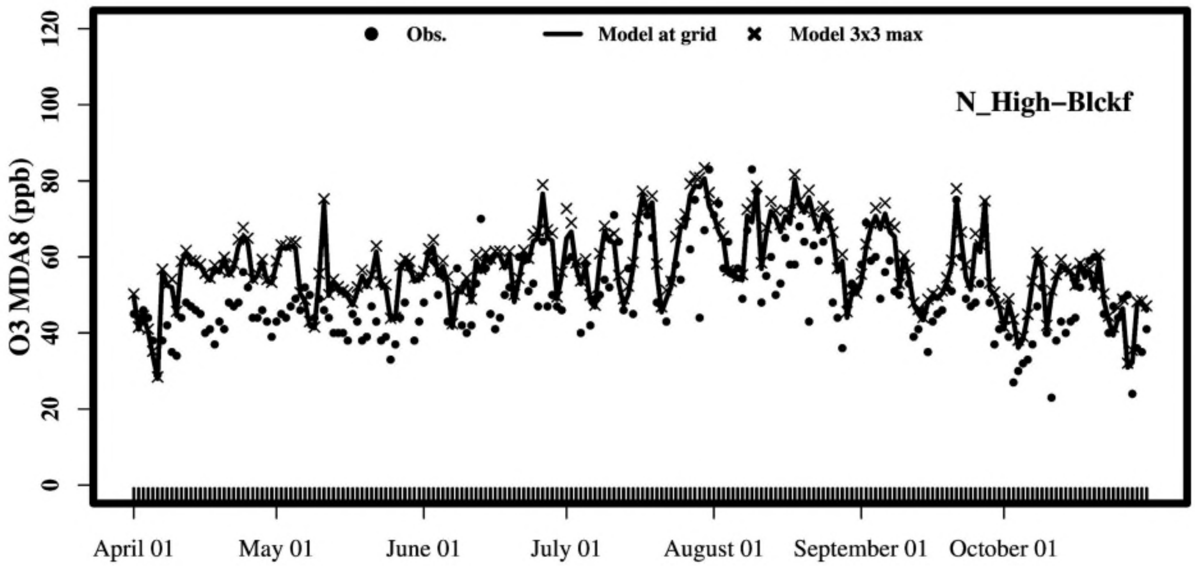

Figure S 53. Time-series of maximum daily average 8-hour ozone at Sacramento-DelPas for the ozone season (April – October 2018)

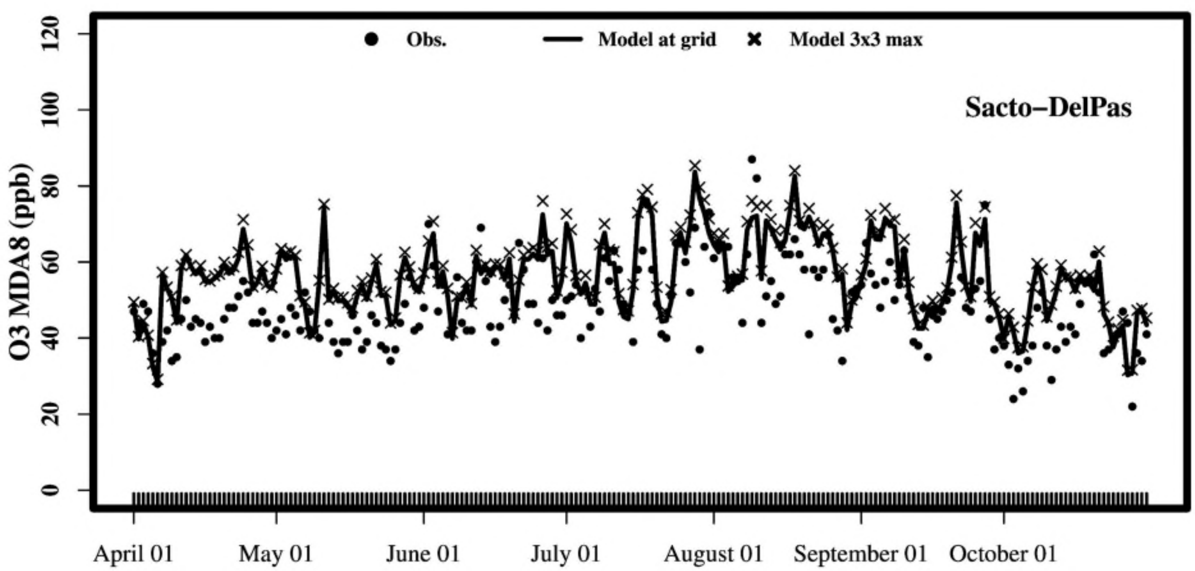

Figure S 54. Time-series of maximum daily average 8-hour ozone at Sloughhouse for the ozone season (April – October 2018)

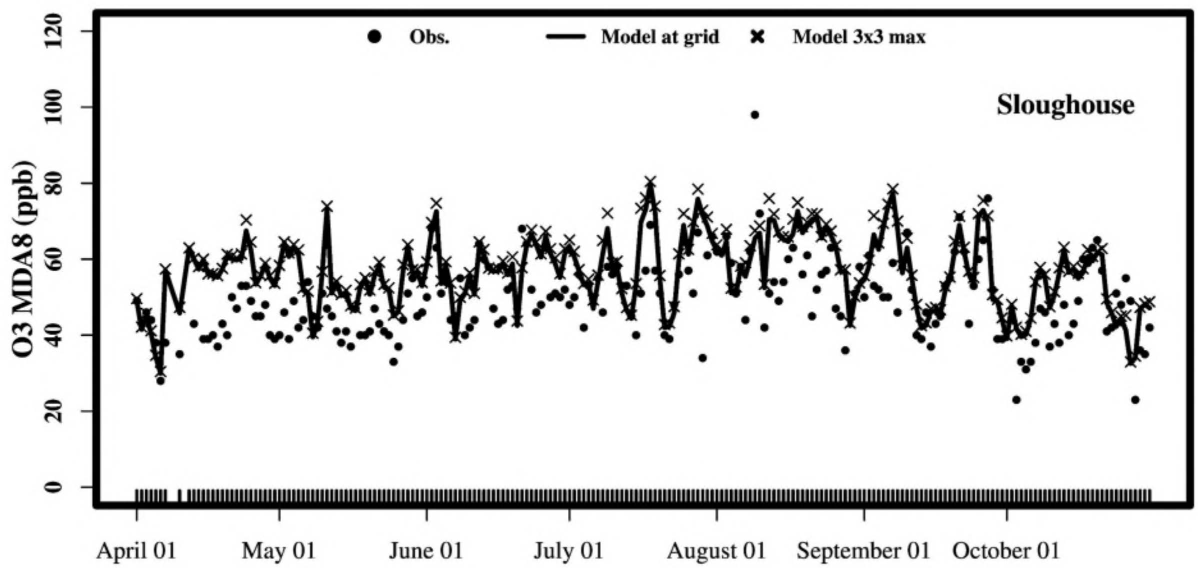

Figure S 55. Time-series of maximum daily average 8-hour ozone at Sacramento-TStreet for the ozone season (April – October 2018)

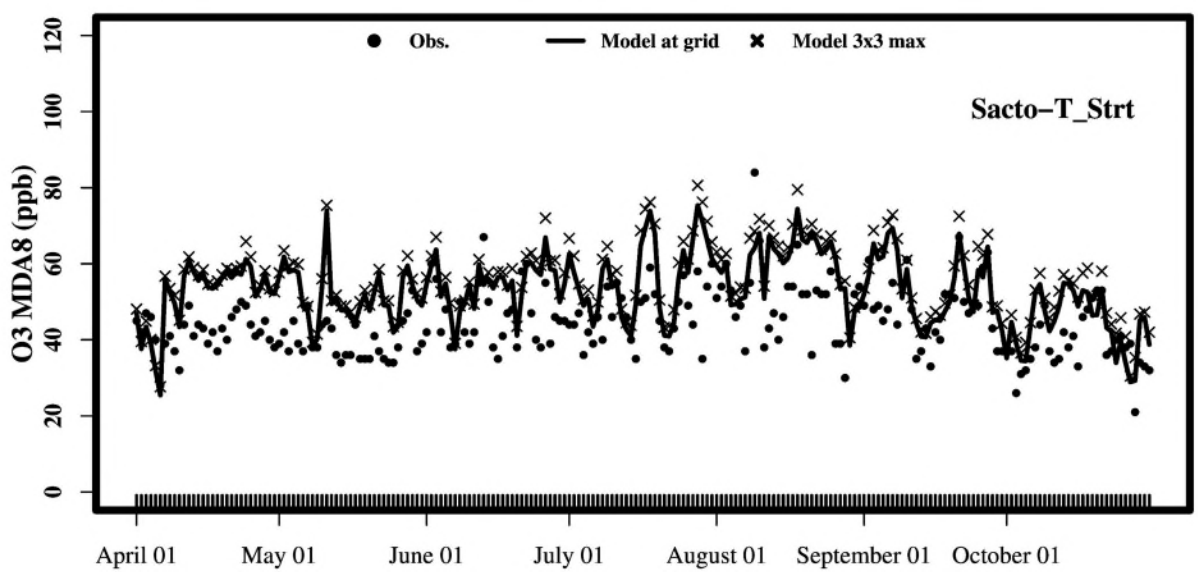

Figure S 56. Time-series of maximum daily average 8-hour ozone at Elk_Grove-Bruceville for the ozone season (April – October 2018)

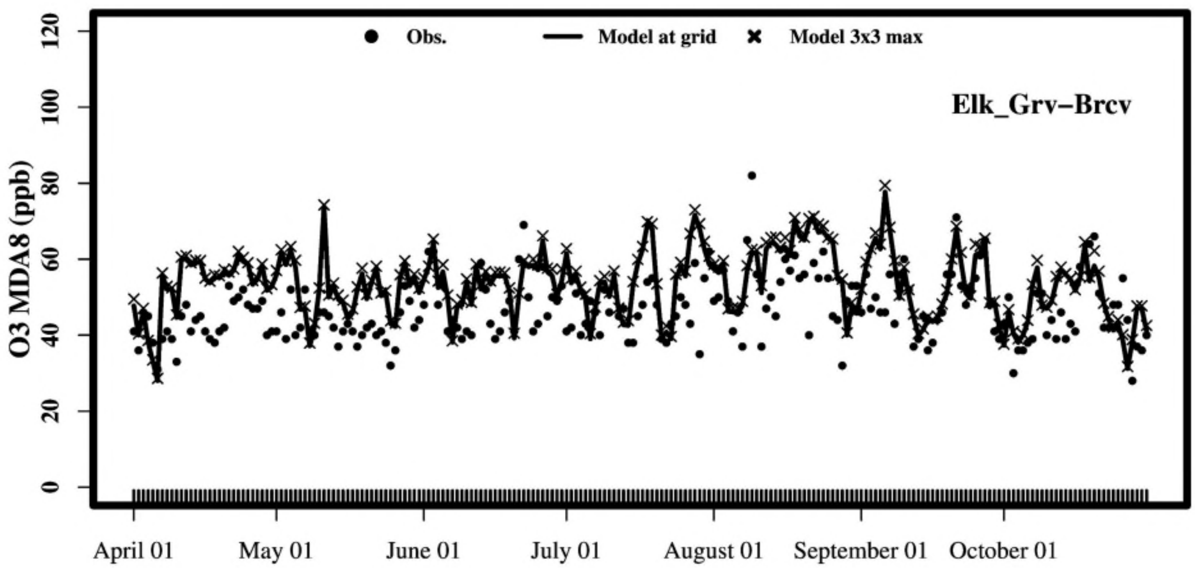

Figure S 57. Time-series of maximum daily average 8-hour ozone at Woodland-Gibson for the ozone season (April – October 2018)

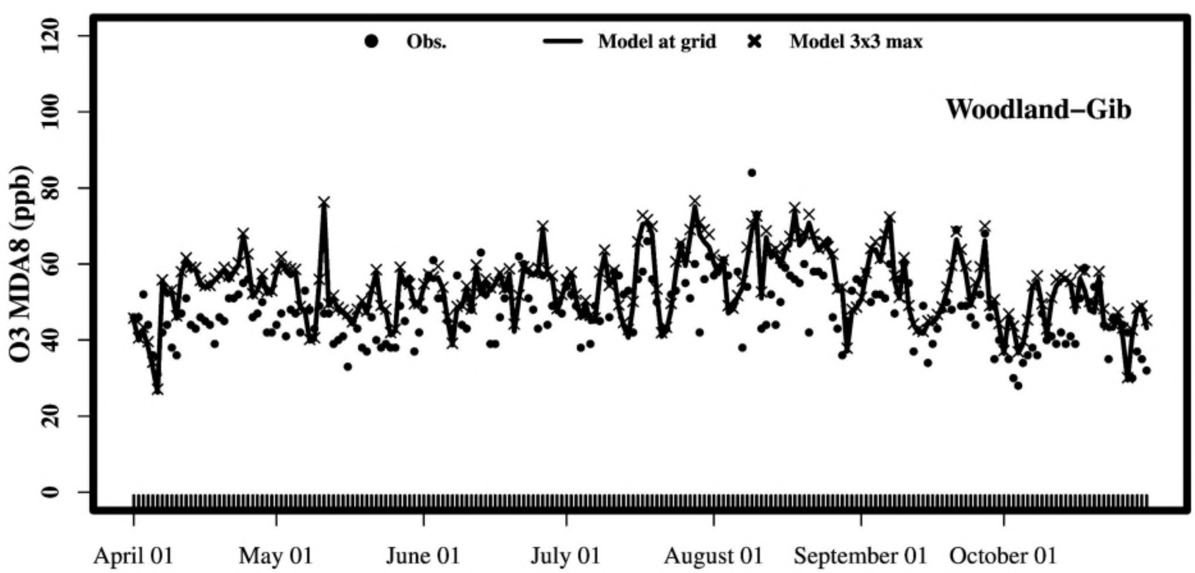

Figure S 58. Time-series of maximum daily average 8-hour ozone at Vacaville-Ulatis for the ozone season (April – October 2018)

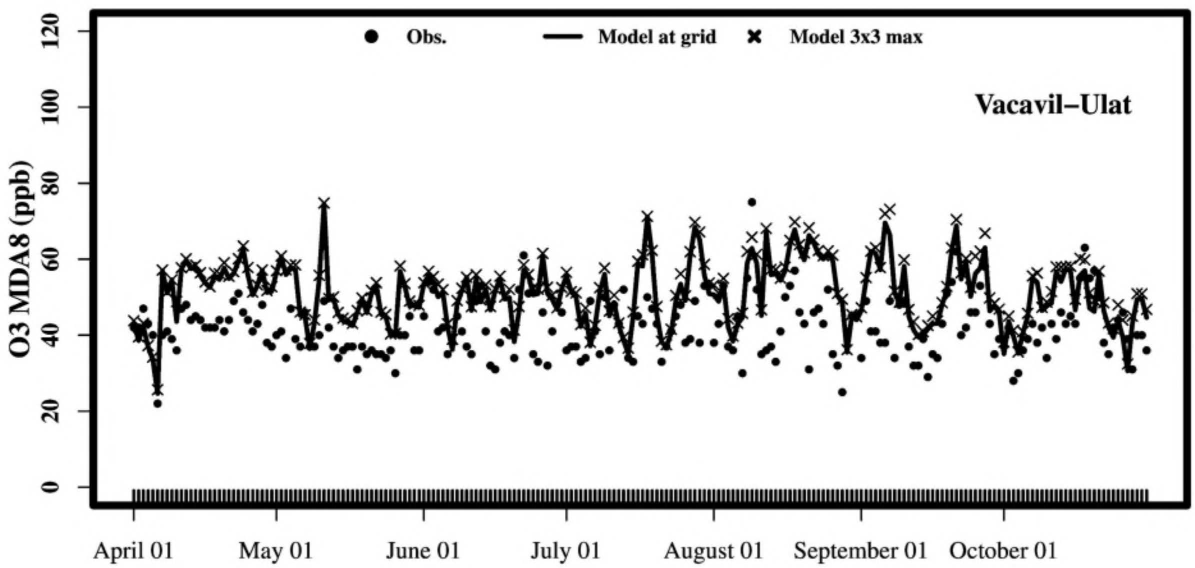

Figure S 59. Time-series of maximum daily average 8-hour ozone at Davis-UCD for the ozone season (April – October 2018)

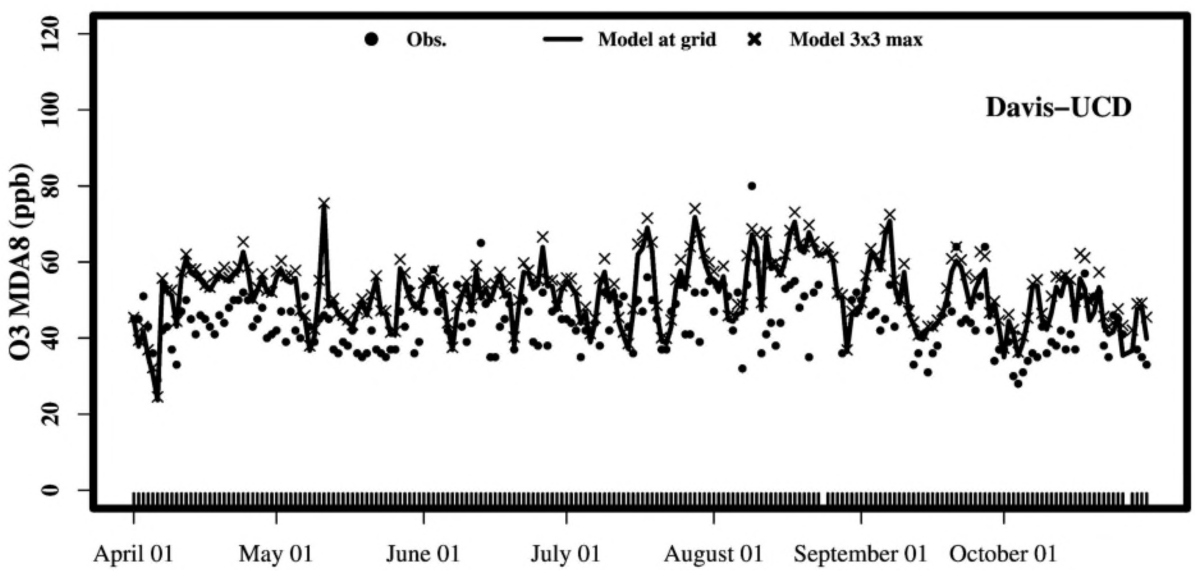

Figure S 60. Observed and modeled daily average NO_X scatter plot for the ozone season in the SFNA (April – October 2018)

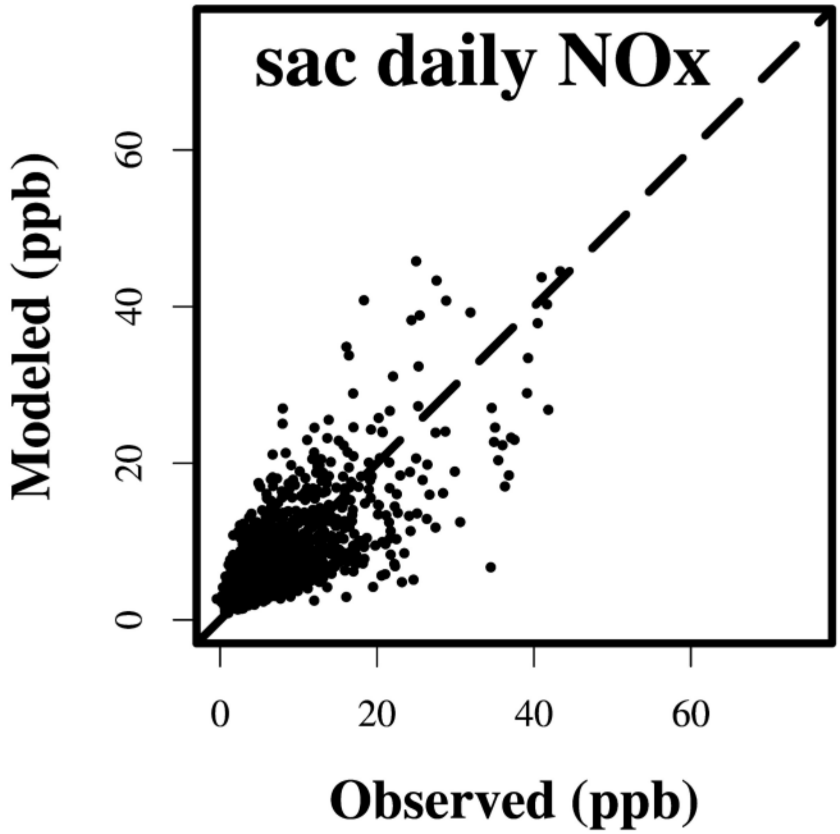

Figure S 61. Curtain plot of monthly averaged 8 hour O_3 concentrations in May 2018 and 2032 along row 127 of modeling domain.

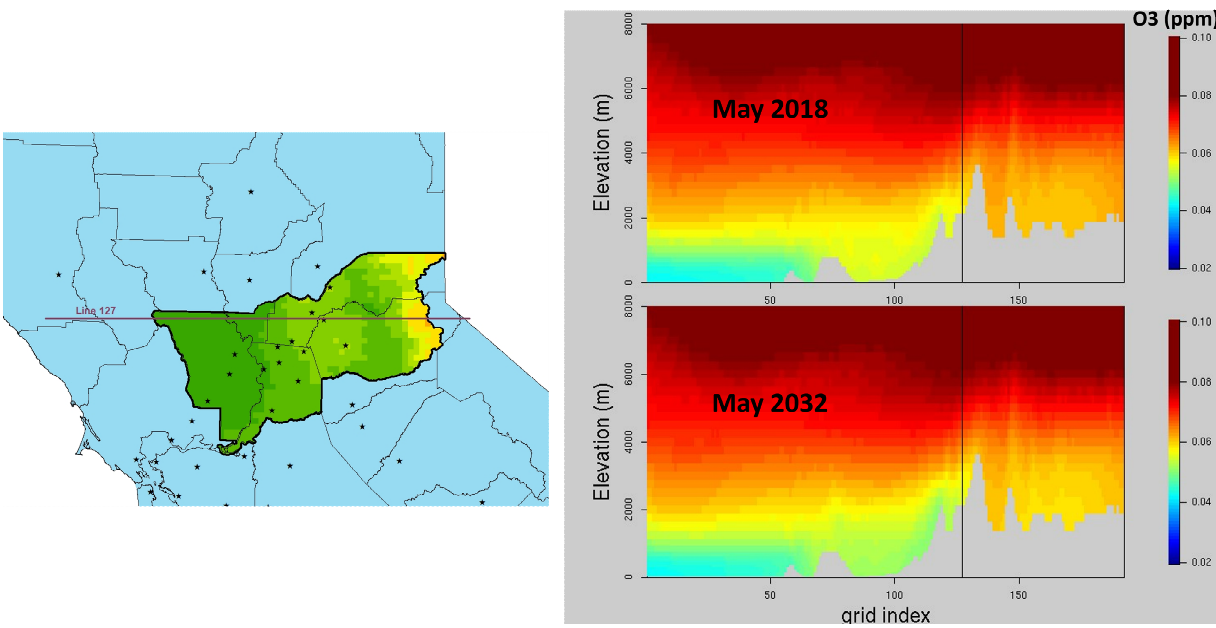

Figure S 62. Curtain plot of monthly averaged 8 hour O_3 concentrations in August 2018 and 2032 along row 127 of modeling domain.

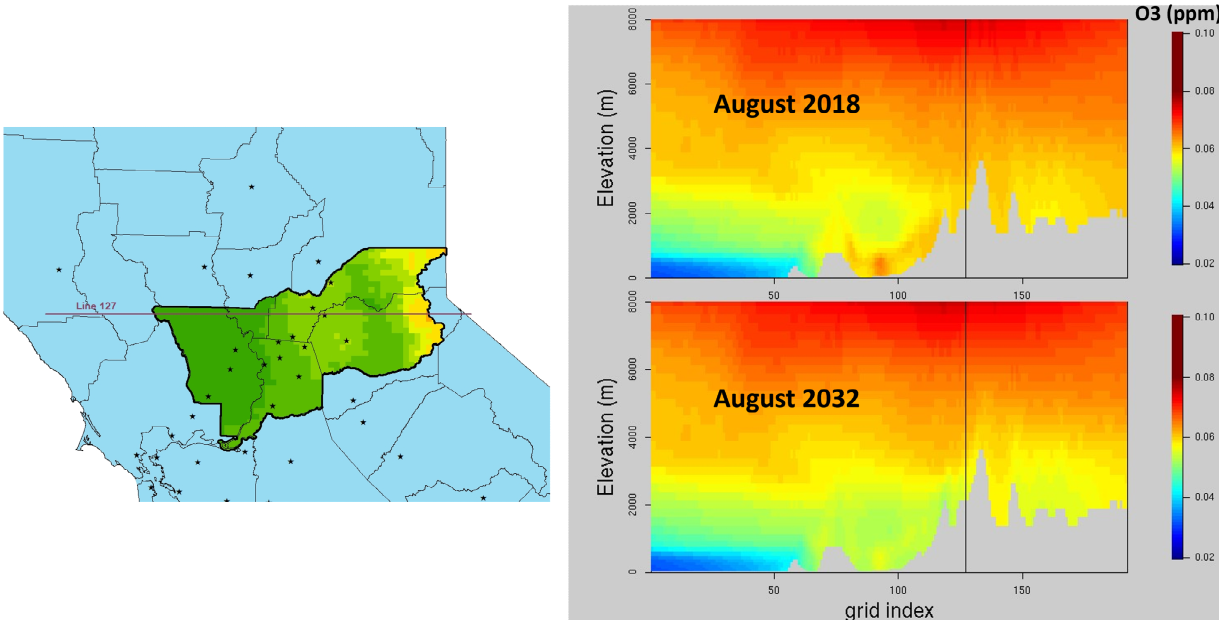

Figure S 63. Time Series of MDA8 O_3 in April to October during 2016 to 2020 at Echo Summit monitor

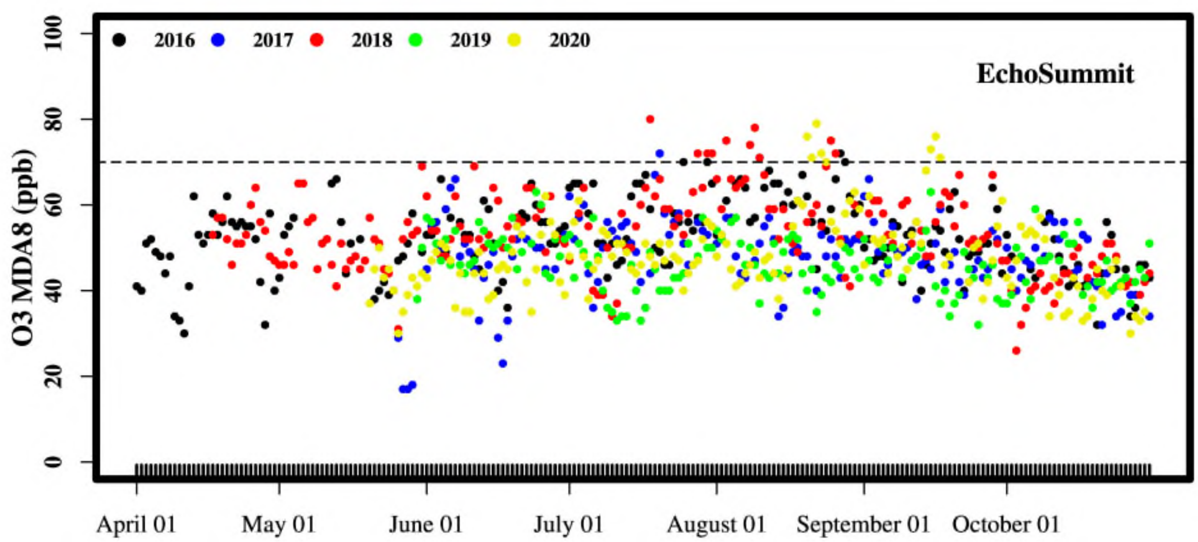

B.2 Modeling Emissions Inventory

Modeling Emission Inventory for the Sacramento Regional 2015 NAAQS 8-Hour Ozone Attainment and Reasonable Further Progress Plan

February 2023

CALIFORNIA
AIR RESOURCES BOARD

Acronyms

APCD – Air Pollution Control District

AQMD – Air Quality Management District

Caltrans – California Department of Transportation

CalVAD – California Vehicle Activity Database

CARB – California Air Resources Board

CCAQS – Central California Air Quality Studies

CCOS – Central California Ozone Study

CEIDARS – California Emission Inventory Development and Reporting System

CEMS – Continuous emissions monitoring system

CEPAM – California Emission Projection Analysis Model

CMAQ – Community Multi-Scale Air Quality

CRPAQS – California Regional PM10/PM25 Air Quality Study

EIC – Emission Inventory Code

EICSUM – EIC SUMmary category, the first three digits of EIC

ERG – Eastern Research Group

HD – Heavy Duty

I&M – Inspection and Maintenance

MPO – Metropolitan Planning Organization

NLCD – National Land Cover Database

NO_X – Oxides of Nitrogen

OGV – Ocean Going Vessel

PM – Particulate Matter

PM_{10} – Particulate Matter 10 micrometers in diameter and smaller

$PM_{2.5}$ – Particulate Matter 2.5 micrometers in diameter and smaller

ROG – Reactive Organic Gases

RRF – Relative Response Factor

RTPA – Regional Transportation Planning Agencies

RWC – Residential Wood Combustion

SAPRC – Statewide Air Pollution Research Center

SCC – Source Classification Code

SIP – State Implementation Plan

SIPIWG – State Implementation Plan Inventory Working Group

SJV – San Joaquin Valley

SMOKE – Sparse Matrix Operator Kernel Emissions

SSS – State SIP Strategy

TOG – Total Organic Gases

B.2.1 Development of Ozone Emissions Inventories

Emission inputs for air quality modeling (commonly and interchangeably referred to as “modeling inventories” or “gridded inventories”) have been developed by the California Air Resources Board (CARB) and staff from multiple air districts. These inventories support multiple State Implementation Plans (SIPs) across California to address nonattainment of the federal ozone (O_3) standards. CARB maintains an electronic database of emissions and other useful information to generate aggregate emission estimates at the county, air basin, and district level, *Criteria Pollutant Emission Inventory Data*. This database is called the California Emission Inventory Development and Reporting System (CEIDARS). CEIDARS provides a foundation for the development of a more refined (hourly, grid cell-specific) set of emission inputs that are required by air quality models. The CEIDARS base year inventory is a primary input to the state’s emission forecasting system, known as the California Emission Projection Analysis Model (CEPAM). CEPAM produces the projected emissions that are then processed to serve as the emission input for air quality models. The following sections of this document describe the methods used to prepare the base and future year emissions inventory estimates.

B.2.1.1 Inventory Coordination

Most of this inventory was developed in direct coordination with staff at the regional Air Pollution Control Districts across the state. In July of 2019, CARB convened the SIP Inventory Working Group (SIPIWG) to provide an opportunity and means for interested parties (CARB, districts, etc.) to discuss issues pertaining to the development and review of base year, future year, planning and gridded inventories to be used in SIP modeling. The group met every four to six weeks since convening into early 2020. Group participants included staff from Bay Area, Butte, Eastern Kern, El Dorado, Feather River, Imperial, Northern Sierra, Placer, Sacramento, San Diego, San Joaquin Valley, San Luis Obispo, South Coast, Ventura, and Yolo-Solano air districts.

Additionally, CARB established the SIPIWG Spatial Surrogate Sub-committee, which focuses on improving input data to spatially disaggregate emissions at a more refined level needed for air quality modeling. Local air districts that participate include San Joaquin Valley, San Diego, Bay Area, Imperial, South Coast, Ventura, and Sacramento.

A great deal of work preceded this modeling effort through the Central California Air Quality Studies (CCAQS). CCAQS consisted of two studies: 1) the Central California Ozone Study (CCOS); and 2) the California Regional PM_{10} (particulate matter 10μm in diameter and smaller) /$PM_{2.5}$ (particulate matter 2.5μm in diameter and smaller) Air Quality Study (CRPAQS).

B.2.1.2 Background

California's emission inventory is an estimate of the amounts and types of pollutants emitted from thousands of industrial facilities, millions of motor vehicles, and myriad emission sources such as consumer products and fireplaces. The development and maintenance of the emission inventory involves several agencies. This multi-agency effort includes: CARB, 35 local air pollution control and air quality management districts (Districts), regional transportation planning agencies (RTPAs), and the California Department of Transportation (Caltrans). CARB is responsible for the compilation of the final statewide emission inventory, and for maintaining this information in CEIDARS. In addition to the statewide emission inventory, emissions from northern Mexico and western United States (Nevada, Arizona, Oregon, Idaho, and Utah) are also incorporated in the final emission inventory used for modeling. The final emission inventory reflects the best information available at the time.

The basic principle for estimating county-wide regulatory emissions is to multiply an estimated, per-unit emission factor by an estimate of typical usage or activity. For example, on-road motor vehicle emission factors are estimated for a specific vehicle type and applied to all applicable vehicles. The estimates are based on dynamometer tests of a small sample for a vehicle type. The activity for any given vehicle type is based on an estimate of typical driving patterns, number of vehicle starts, and typical miles driven. Assumptions are also made regarding typical usage: it is assumed that all vehicles of a certain vehicle type are driven under similar conditions in each region of the state.

Developing emission estimates for stationary sources involves the use of per unit emission factors and activity levels. Under ideal conditions, facility-specific emission factors are determined from emission tests for a particular process at a facility. A continuous emission monitoring system (CEMS) can also be used to determine a gas or particulate matter concentration or emission rate (EPA). More commonly, a generic emission factor is developed by averaging the results of emission tests from similar processes at several different facilities. This generic factor is then used to estimate emissions from similar types of processes when a facility-specific emission factor is not available. Activity levels from stationary sources can be derived from the amount of product produced, solvent used, or fuel used.

The district-reported and CARB-estimated emissions totals are stored in the CEIDARS database for any given pollutant. Both criteria pollutants and their precursors are stored in this complex database. These are typically annual average emissions for each county, air basin, and district. Modeling inventories for reactive organic gases (ROG) are estimated from total organic gases (TOG). Similarly, the modeling inventories for PM_{10} and $PM_{2.5}$ are estimated from total particulate matter (PM). Details about chemical and size resolved speciation of emissions for modeling can be found in Section B.2.2.5. Additional information on CARB emission inventories can be found at *CARB Emission Inventory Activities*.

B.2.1.3 Inventory Years

The emission inventory scenarios used for air quality modeling must be consistent with U.S. EPA's Modeling Guidance (EPA). Since changes in the emissions inventory can affect the calculation of the relative response factors (RRFs) used to project air quality to future years, the terms used in the preparation of the emission inventory scenarios must be clearly defined. In this document, the following inventory definitions will be used.

B.2.1.3.1 Base Case Modeling Inventory (2018)

Base case modeling is intended to evaluate model performance and demonstrate confidence in the modeling system used for the modeled attainment test. The base case modeling inventory is not used as part of the modeled attainment test itself. Model performance is assessed relative to how well model-simulated concentrations match actual measured concentrations. The modeling inputs are developed to represent (as best as possible) actual, day-specific conditions. Emissions for certain sectors are based on day-specific activities, meteorology, and emission adjustments. Actual district-reported point source emissions were gathered for the year 2017 and forecasted to 2018. The year 2018 was selected to coincide with the year selected for baseline design values (described below). The U.S. EPA modeling guidance states that once the model has been shown to perform adequately, the use of day-specific emissions is no longer needed. In preparation for SIP development, both CARB and the local air districts began a comprehensive review and update of the emission inventory resulting in a comprehensive emissions inventory for 2018.

B.2.1.3.2 Reference Year Modeling Inventory (2018)

The reference year inventory is intended to be a representation of emission patterns occurring through the baseline design value period and the emission patterns expected in the future year. U.S. EPA modeling guidance describes the reference year modeling inventory as "a common starting point" that represents average or "typical" conditions that are consistent with the baseline design value period. U.S. EPA guidance also states "using a 'typical' or average reference year inventory provides an appropriate platform for comparisons between baseline and future years." The 2018 reference year inventory represents typical average conditions and emission patterns through the 2018 design value period. This reference emissions inventory is not developed to capture all day-specific emission characteristics; however, this reference inventory does include meteorological effects for 2018 (e.g., temperature, relative humidity, and solar insolation), as well as certain day-specific emission activities, such as agricultural and prescribed burning.

B.2.1.3.3 Future Year Modeling Inventory (2032)

Future year modeling inventories, along with the reference year modeling inventory, are used in the model-derived RRF calculation. Projected inventory year 2032 was chosen to address the modeled attainment year for the 8-hour 2015 ozone standard of 70 ppb.

These inventories maintain the "typical," average patterns of the 2018 reference year modeling inventory. Some sectors of the 2032 inventories include temporal variations that were driven by temperature, relative humidity, and solar insolation effects from reference year (2018) meteorology. Future year point and area source emissions are projected from the 2017 baseline emissions. Future year on-road emission inventories are used as projected by EMFAC.

B.2.1.4 Spatial Extent of Emission Inventories

The emissions model-ready files that are prepared for use as an input for the air quality model conform to the definition and extent of the grids shown in Figure B-23 illustrates an enlarged image of the Sacramento Nonattainment area in California (highlighted in yellow) in the statewide 4 km modeling grid.

Figure B-22. Figure B-23 illustrates an enlarged image of the Sacramento Nonattainment area in California (highlighted in yellow) in the statewide 4 km modeling grid.

Figure B-22. Spatial coverage of emissions grid with nonattainment area highlighted in yellow

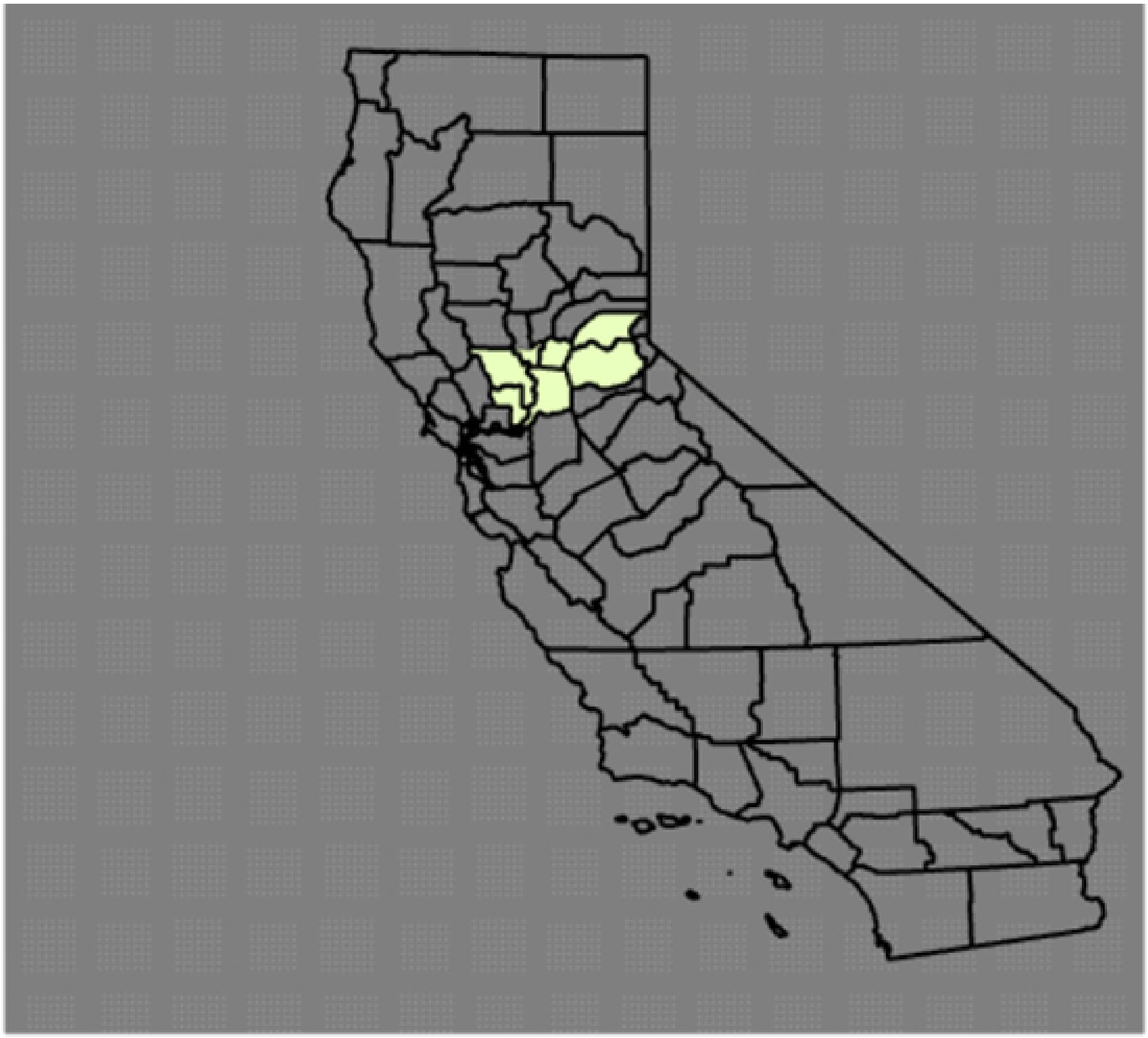

Figure B-23: Sacramento Nonattainment area highlighted in California with statewide 4 km grid overlayed

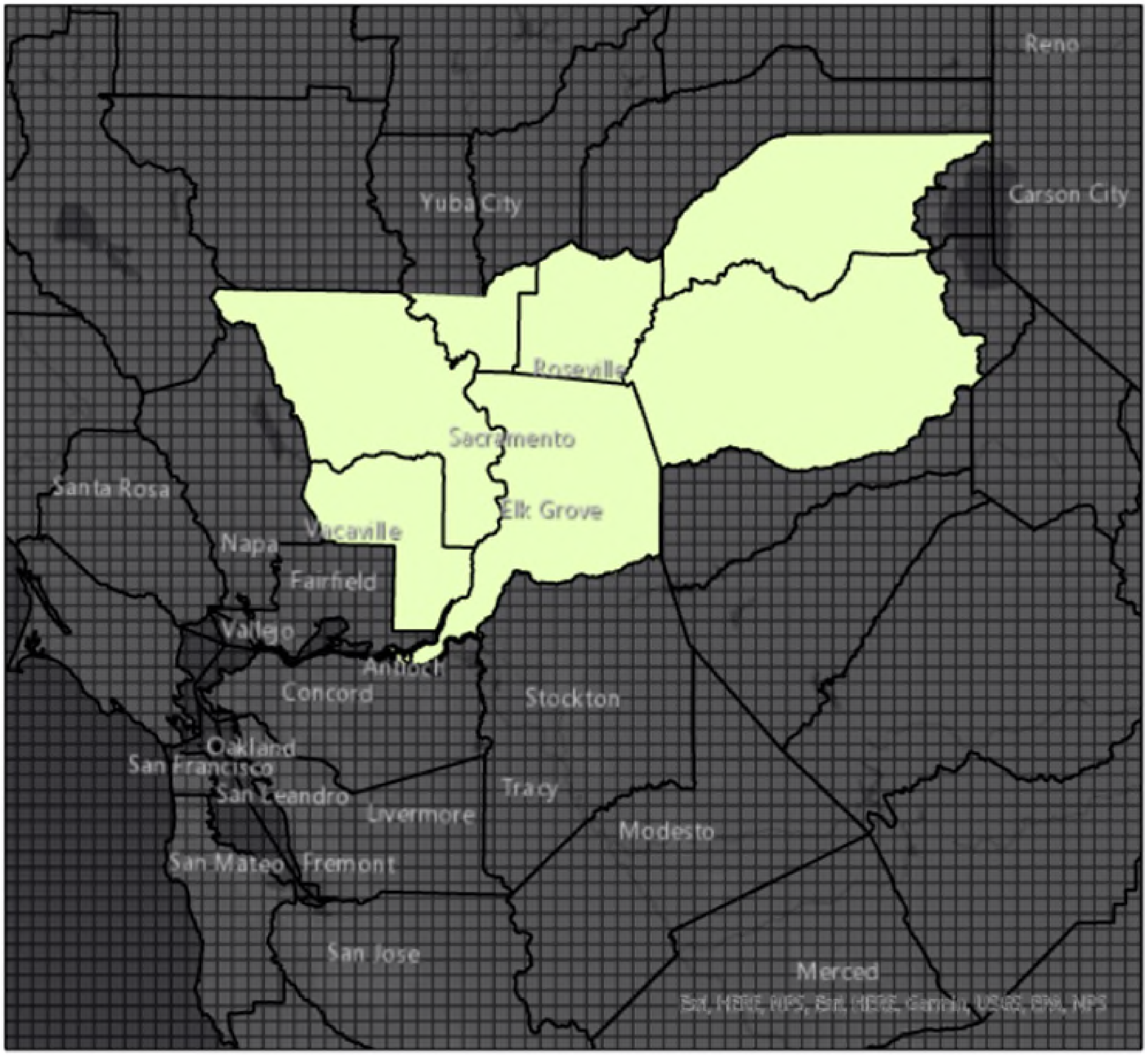

The domain uses a Lambert projection and assumes a spherical Earth. The emissions inventory grid uses a Lambert Conical Projection with two parallels. The parallels are at 30° and 60° N latitude, with a central meridian at 120.5° W longitude. The coordinate system origin is offset to 37° N latitude. The emissions inventory is developed for the gridded statewide domain on a spatial resolution of 4 km x 4 km. The state modeling domain extends entirely over California and 100 nautical miles west over the Pacific Ocean. The specifications for the statewide modeling domain are summarized in Table B-16.

Table B-16: Modeling domain parameters

Parameter	Statewide domain
Map Projection	Lambert Conformal Conic
Datum	None (Clarke 1866 spheroid)
1st Standard Parallel	30.0° N
2nd Standard Parallel	60.0° N
Central Meridian	-120.5° W
Latitude of projection origin	37.0° N
Coordinate system Units	Meters
Semi-major axis	6370 km
Semi-minor axis	6370 km
Grid size	4 km x 4 km
Number of cells	291 x 321 cells
Lambert origin	(-684,000 m, -564,000 m)
Geographic center	-120.5° Lat and 37.0° Lon

B.2.2 Estimation of Base Year Modeling Inventory

As mentioned in Section B.2.1.3.1, base case modeling is intended to demonstrate confidence in the modeling system used for the modeled attainment test. The following sections describe the temporal and spatial distribution of emissions and how each of the sectors within the modeling inventories are prepared.

B.2.2.1 Terminology

The terms "point sources" and "area sources" are often confused. Traditionally, these terms have had different meanings to the developers of planning emissions inventories and the developers of modeling emissions inventories. Table B-17 summarizes the difference in the terms as both sets of terms are used in this document. In modeling terminology, "point sources" traditionally refers to elevated emission sources that exit from a stack and have an associated plume rise. The current inventory includes emissions sources reported by the Air Pollution Control District (APCD). Those sources associated with a facility are treated as either elevated sources or non-elevated. The emissions processor calculates plume rise for elevated sources; non-elevated sources are treated as ground-level sources. Examples of non-elevated emissions sources include landfills and composting facilities. "Area sources" refers collectively to area-wide sources, stationary-aggregated sources, and other mobile sources (including aircraft, trains, ships, and all off-road vehicles and equipment). That is, "area sources" are low-level sources from a modeling perspective.

Table B-17: Inventory terms for emission source types

Modeling Term	Emission Inventory Term	Examples
Point	Stationary – Point Facilities	Stacks at Individual Facilities
Area	Off-road Mobile	Construction Equipment, Farm Equipment, Trains, Recreational Boats
Area	Area-wide	Residential Fuel Combustion, Livestock Waste, Consumer Products, Architectural Coatings
Area	Stationary - Aggregated	Industrial Fuel Use
On-road Motor Vehicles	On-road Mobile	Cars and Trucks
Biogenic	Biogenic	Trees

The following sections describe in more detail the temporal, spatial, and chemical disaggregation of the emissions inventory for point sources and area sources.

B.2.2.2 Emissions Inventory

Modeling emissions are based on the CEPAM inventories for the base year and future year. Since the modeling inventory was processed in parallel to the application of updates to CEPAM the modeling inventory was patched from CEPAM 2019 v1.03 for the following source sectors:

- Off-Road SORE (small off-road engines) rule as adopted by the Board December 2021
- Cargo Handling Equipment (CHE)
- Construction “In Use” Equipment
- Large Spark Ignition (LSI) Forklifts
- Forestry Equipment
- Industrial/Military Rail
- Additional adjustments for Ground Support Equipment (GSE) in South Coast

The resulting modeling inventory matches totals from CEPAM 2019 v1.04.

B.2.2.3 Temporal Distribution of Emissions

The emissions are temporally resolved by month, week, day, and hour to more accurately gauge model performance and ultimately better assess the influence of control measures on attainment. This section covers the temporal distributions of the point, area, and off-road mobile sources. The temporal distribution of the emissions from on-road, biogenic, and ocean-going vessel (OGV) sources are discussed in Sections B.2.3.2, B.2.3.3, and B.2.3.5. The temporal distribution of residential wood combustion (RWC) and agricultural ammonia sectors are described in Section B.2.3.6.4 and Section B.2.3.6.5, respectively.

Temporal data are stored in CARB’s emission inventory database. Each local air district assigns temporal data for all processes at each facility in their district to represent when emissions at each process occur. For example, emissions from degreasing may operate differently than a boiler. CARB or district staff also assign temporal data for each area source category by county/air basin/district.

B.2.2.3.1 Monthly Variation

Emissions are adjusted temporally to represent variations by month. Some emission sources operate the same throughout a year. For example, a process heater at a refinery or a line-haul locomotive likely operates the same month-to-month. Other emission categories, such as a tomato processing plant or use of recreational boats, vary significantly by season. CARB's emission inventory database stores the relative monthly fractional activity for each process, the sum of which is 100. Using an example of emission sources that typically operate the same over each season, emissions from refinery heaters and line-haul locomotives would have a monthly fraction (throughput) of 8.33 for each month (calculated as 100/12 = 8.33). This is considered a flat monthly profile. To apply monthly variations to create a gridded inventory, the annual average day's emissions (yearly emissions divided by 365) is multiplied by the typical monthly throughput. For example, a typical monthly throughput of 15 in July for recreational boats results in emissions about 1.8 times higher (15 / 8.33 = 1.8) than a day in a month with a flat monthly profile.

B.2.2.3.2 Weekly Variation

Emissions are adjusted temporally to represent variations by day of the week. Some operations are the same over a week, such as a utility boiler or a landfill. Many businesses operate only 5 days per week. Other emissions sources are similar on weekdays, but may operate differently on weekend days, such as architectural coatings or off-road motorcycles. To accommodate variations in days of the week, each process or emission category is assigned a days-per-week code or DPWK. Table B-18 shows the current DPWK codes.

Table B-18: Day of week variation factors

Code	WEEKLY CYCLE CODE DESCRIPTION	M	T	W	TH	F	S	S
1	One day per week	1	1	1	1	1	0	0
2	Two days per week	1	1	1	1	1	0	0
3	Three days per week	1	1	1	1	1	0	0
4	Four days per week	1	1	1	1	1	0	0
5	Five days per week - Uniform activity on weekdays, none on Saturday and Sunday	1	1	1	1	1	0	0
6	Six days per week - Uniform activity on weekdays, none on Saturday and Sunday	1	1	1	1	1	1	0
7	Seven days per week – Uniform activity every day of the week	1	1	1	1	1	1	1
20	Uniform activity on Saturday and Sunday, no activity the remainder of the week	0	0	0	0	0	1	1

Code	WEEKLY CYCLE CODE DESCRIPTION	M	T	W	TH	F	S	S
21	Uniform activity on Saturday and Sunday, half as much activity on weekdays	5	5	5	5	5	10	10
22	Uniform activity on weekdays, reduced activity on weekends	10	10	10	10	10	7	4
23	Uniform activity on weekdays, reduced activity on weekends	10	10	10	10	10	8	8
24	Uniform activity on weekdays; half as much activity on Saturday. Little activity on Sunday	10	10	10	10	10	5	1
25	Uniform activity on weekdays, one third as much on Saturday, little on Sunday	10	10	10	10	10	3	1
26	Uniform activity on weekdays, little activity on Saturday, no activity on Sunday	10	10	10	10	10	3	0
27	Uniform activity on weekdays, half as much activity on weekends	10	10	10	10	10	5	5
28	Uniform activity on weekdays, five times as much activity on weekends	2	2	2	2	2	10	10
29	Uniform activity on Monday through Thursday, increased activity on Friday, Saturday, and Sunday	8	8	8	8	10	10	10

B.2.2.3.3 Daily Variation

Emissions are adjusted temporally to represent variations by hour of day. Many emission sources occur 24 hours per day, such as livestock waste or a sewage treatment plant whereas many businesses operate 8 hours per day. Other emissions sources vary significantly over a day, such as residential space heating or pesticide application. Each process or emission category is assigned an hours-per-day (HPDY) code. Table B-19 displays the daily variation factors or current HPDY codes. Code 33 is no longer used for residential fuel combustion in favor of day specific adjustments see Section B.2.3.6.4. Additional temporal profiles are shown in Sub-Appendix B.C.

Table B-19: Daily variation factors

Code	CODE DESCRIPTION	0	1	2	3	4	5	6	7	8	9	10	11	12	13	14	15	16	17	18	19	20	21	22	23
1	1 HOUR PER DAY	0	0	0	0	0	0	0	0	1	0	0	0	0	0	0	0	0	0	0	0	0	0	0	0
2	2 HOURS PER DAY	0	0	0	0	0	0	0	0	1	1	0	0	0	0	0	0	0	0	0	0	0	0	0	0
3	3 HOURS PER DAY	0	0	0	0	0	0	0	0	1	1	1	0	0	0	0	0	0	0	0	0	0	0	0	0
4	4 HOURS PER DAY	0	0	0	0	0	0	0	0	1	1	1	1	0	0	0	0	0	0	0	0	0	0	0	0
5	5 HOURS PER DAY	0	0	0	0	0	0	0	0	1	1	1	1	1	0	0	0	0	0	0	0	0	0	0	0
6	6 HOURS PER DAY	0	0	0	0	0	0	0	0	1	1	1	1	1	1	0	0	0	0	0	0	0	0	0	0
7	7 HOURS PER DAY	0	0	0	0	0	0	0	0	1	1	1	1	1	1	1	0	0	0	0	0	0	0	0	0
8	8 HOURS PER DAY - UNIFORM ACTIVITY FROM 8 A.M. TO 4 P.M. (NORMAL WORKING SHIFT)	0	0	0	0	0	0	0	0	1	1	1	1	1	1	1	1	0	0	0	0	0	0	0	0
9	9 HOURS PER DAY	0	0	0	0	0	0	0	0	1	1	1	1	1	1	1	1	1	0	0	0	0	0	0	0
10	10 HOURS PER DAY	0	0	0	0	0	0	0	1	1	1	1	1	1	1	1	1	1	0	0	0	0	0	0	0
11	11 HOURS PER DAY	0	0	0	0	0	0	0	1	1	1	1	1	1	1	1	1	1	1	0	0	0	0	0	0
12	12 HOURS PER DAY	0	0	0	0	0	0	0	1	1	1	1	1	1	1	1	1	1	1	1	0	0	0	0	0
13	13 HOURS PER DAY	0	0	0	0	0	0	0	0	1	1	1	1	1	1	1	1	1	1	1	1	1	0	0	0
14	14 HOURS PER DAY	0	0	0	0	0	0	0	0	1	1	1	1	1	1	1	1	1	1	1	1	1	1	0	0
15	15 HOURS PER DAY	0	0	0	0	0	0	0	0	1	1	1	1	1	1	1	1	1	1	1	1	1	1	1	0
16	16 HOURS PER DAY - UNIFORM ACTIVITY FROM 8 A.M. TO MIDNIGHT (2 WORKING SHIFTS)	0	0	0	0	0	0	0	0	1	1	1	1	1	1	1	1	1	1	1	1	1	1	1	1
17	17 HOURS PER DAY	0	0	0	0	0	0	0	1	1	1	1	1	1	1	1	1	1	1	1	1	1	1	1	1
18	18 HOURS PER DAY	0	0	0	0	0	0	1	1	1	1	1	1	1	1	1	1	1	1	1	1	1	1	1	1
19	19 HOURS PER DAY	0	0	0	1	1	1	1	1	1	1	1	1	1	1	1	1	1	1	1	1	1	1	0	0
20	20 HOURS PER DAY	0	0	0	1	1	1	1	1	1	1	1	1	1	1	1	1	1	1	1	1	1	1	1	0
21	21 HOURS PER DAY	0	0	1	1	1	1	1	1	1	1	1	1	1	1	1	1	1	1	1	1	1	1	1	0
22	22 HOURS PER DAY	0	1	1	1	1	1	1	1	1	1	1	1	1	1	1	1	1	1	1	1	1	1	1	0
23	23 HOURS PER DAY	0	1	1	1	1	1	1	1	1	1	1	1	1	1	1	1	1	1	1	1	1	1	1	1
24	24 HOURS PER DAY - UNIFORM ACTIVITY DURING THE DAY	1	1	1	1	1	1	1	1	1	1	1	1	1	1	1	1	1	1	1	1	1	1	1	1
31	MAJOR ACTIVITY 5-9 P.M., AVERAGE DURING DAY, MINIMAL IN EARLY A.M.(GAS STATIONS)	3	1	1	1	1	1	1	5	5	5	5	5	5	5	5	5	5	10	10	10	10	7	7	3
33	MAX ACTIVITY 7-9 A.M. & 7-11 P.M.,AVERAGE DURING DAY, LOW AT NIGHT (RESIDENTIAL FUEL COMBUSTION)	2	2	2	2	2	2	2	10	10	6	6	5	5	5	5	5	5	5	5	10	10	10	10	2

Code	CODE DESCRIPTION	0	1	2	3	4	5	6	7	8	9	10	11	12	13	14	15	16	17	18	19	20	21	22	23
34	ACTIVITY 1 TO 9 A.M.; NO ACTIVITY REMAINDER OF DAY (i.e. ORCHARD HEATERS)	0	8	8	8	8	10	10	10	10	0	0	0	0	0	0	0	0	0	0	0	0	0	0	0
35	MAX ACTIVITY 7 A.M. TO 1 A.M., REMAINDER IS LOW (i.e. COMMERCIAL AIRCRAFT)	10	1	1	1	1	1	1	8	8	10	10	10	10	10	10	10	10	10	10	10	10	10	10	10
37	ACTIVITY DURING DAYLIGHT HOURS; LESS CHANCE IN EARLY MORNING AND LATE EVENING	0	0	0	0	0	1	3	6	9	10	10	10	10	10	10	10	10	9	6	3	1	0	0	0
38	ACTIVITY DURING MEAL TIME HOURS (i.e. RESIDENTIAL COOKING)	0	0	0	0	0	2	6	6	2	2	1	2	4	4	2	1	1	3	10	8	7	6	1	0
50	PEAK ACTIVITY AT 7 A.M. & 4 P.M.; AVERAGE DURING DAY (ON-ROAD MOTOR VEHICLES)	1	1	1	1	1	1	6	10	6	5	5	5	5	5	5	6	10	8	6	4	1	1	1	1
51	ACTIVITY FROM 6 A.M. TO 12 P.M. (PETROLEUM DRY CLEANING)	0	0	0	0	0	0	1	1	1	1	1	1	0	0	0	0	0	0	0	0	0	0	0	0
52	MAJOR ACTIVITY FROM 6 A.M.-12 P.M., LESS FROM 12-7 P.M. (PESTICIDES)	0	0	0	0	0	1	6	10	10	10	10	10	6	3	3	3	3	4	4	0	0	0	0	0
53	ACTIVITY FROM 7 A.M. TO 12 P.M. (AGRICULTURAL AIRCRAFT)	0	0	0	0	0	0	0	2	2	2	2	2	1	0	0	0	0	0	0	0	0	0	0	0
54	UNIFORM ACTIVITY FROM 7 A.M. TO 9 P.M. (DAYTIME BIOGENICS)	0	0	0	0	0	0	0	1	1	1	1	1	1	1	1	1	1	1	1	1	1	0	0	0
55	UNIFORM ACTIVITY FROM 9 P.M. TO 7 A.M. (NIGHTIME BIOGENICS)	1	1	1	1	1	1	1	0	0	0	0	0	0	0	0	0	0	0	0	0	0	1	1	1
56	MAX ACTIVITY 8 A.M. TO 5 P.M, MINIMAL AT NIGHT & EARLY MORNING (CAN&COIL/METAL PARTS COATINGS)	0	0	0	0	1	1	2	3	10	10	10	10	10	10	10	10	9	1	1	1	1	1	1	1
57	MAX ACTIVITY 7 A.M. TO 2 P.M., MINIMAL AT EVENING AND MORNING HOURS (CONSTRUCTION EQUIPMENT ON HOT DAYS)	0	0	0	0	0	1	6	10	10	10	10	10	10	9	8	4	2	1	1	0	0	0	0	0
58	MAX ACTIVITY 7 A.M. TO NOON.;REDUCED ACTIVITY NOON TO 6 P.M. (AUTO REFINISHING)	0	0	0	0	0	0	0	10	10	10	10	10	8	8	8	8	8	8	0	0	0	0	0	0
59	MAXIMUM ACTIVITY FROM 7:00 AM TO 3:00 PM; REDUCED ACTIVITY FROM 3:00 TO 6:00 PM.(CONSTRUCTION EQUIPMENT ON NORMAL DAYS)	0	0	0	0	0	0	2	10	10	10	10	10	10	10	10	7	3	1	1	0	0	0	0	0
60	MAXIMUM ACTIVITY FROM NOON TO 7:00 PM; REDUCED ACTIVITY	0	0	0	0	0	0	0	2	4	6	7	9	10	10	10	10	10	10	10	7	5	3	1	0

Code	CODE DESCRIPTION	0	1	2	3	4	5	6	7	8	9	10	11	12	13	14	15	16	17	18	19	20	21	22	23
	EVENING AND MORNING HOURS (RECREATIONAL BOAT EXHAUST)																								
81	MAX ACTIVITY 9 AM TO 3 PM; HALF THE ACTIVITY REMAINING HOURS (WASTE FROM DAIRY CATTLE)	7	6	6	5	4	4	4	5	7	8	9	10	10	10	7	3	3	3	4	4	5	6	7	7
82	ACTIVITY FROM 10 AM TO 9 PM RISING TO PEAK AT 3; NO ACTIVITY REMAINDER OF DAY (WASTE FROM POULTRY)	0	0	0	0	0	0	0	0	0	3	3	7	7	7	10	10	7	3	3	3	3	0	0	0
83	ACTIVITY FROM 9 AM TO 12 AM RISING TO PEAK AT 3; MINIMUM ACTIVITY REMAINDER OF DAY (WASTE FROM SWINE)	0	0	0	0	0	0	0	1	1	2	4	6	8	8	9	10	8	4	3	3	2	1	1	1
84	MAJOR ACTIVITY FROM 11AM TO 6PM; REDUCED OTHER HOURS (EVAP-COASTAL COUNTIES)	7	7	6	6	6	6	6	7	8	8	9	9	10	10	10	10	9	9	8	8	7	7	7	7
85	MAJOR ACTIVITY FROM 11AM TO 6PM; REDUCED OTHER HOURS (EVAP-NON-COASTAL COUNTIES)	5	5	5	5	4	4	5	5	6	7	8	9	9	10	10	10	9	9	8	7	6	6	6	5

B.2.2.4 Spatial Allocation

Once the base case, reference, or future year inventories are developed, the next step of modeling inventory development is to spatially allocate the emissions. Air quality models attempt to replicate the physical (e.g., transport) and chemical processes that occur in the atmosphere within a modeling domain. Therefore, it is important that the physical location of emissions be specified as accurately as possible. Ideally, the actual location of all emissions would be known exactly. However, some categories of emissions would be virtually impossible to determine—for example, the actual amount and location of consumer products (e.g., deodorant) used every day. To the extent possible, the spatial allocation of emissions in a modeling inventory approximates as closely as possible the actual location of emissions.

Spatial allocation is typically accomplished by using spatial surrogates. These spatial surrogates are processed into spatial allocation factors to geographically distribute county-wide area source emissions to individual grid cells. Spatial surrogates are developed based on demographic, land cover, and other data that exhibit patterns geographically. Sonoma Technology, Inc. (STI) (Funk, et al., 2001) under CCOS contract, originally developed many of the spatial surrogates by creating a base year (2000) and various future year surrogate inventories. STI updated the underlying spatial data and developed new surrogates (Reid, et al., 2006), completing the project in 2008. CARB and districts have since continued to update and improve many of the spatial surrogates, adding new ones as more data become available.

Four basic types of data are used to develop the spatial allocation factors: land use and land cover, satellite imagery, facility location, and demographic and socioeconomic data. Land use and land cover data are associated with specific land uses, such as agricultural harvesting or recreational boats. Facility locations are used for sources such as gas stations and dry cleaners. Demographic and socioeconomic data, such as population and housing, are associated with residential, industrial, and commercial activities (e.g., residential fuel combustion). To develop spatial allocation factors of high quality and resolution, local socioeconomic and demographic data were used when available for developing base case, baseline, and future year inventories. These data were available from local Metropolitan Planning Organizations (MPOs) or Regional Transportation Planning Agency (RTPA), where they are used as inputs for travel demand models. In rural regions for which local data were not available, data from Caltrans' Statewide Transportation Model were used.

The current snapshot used for the Sacramento O_3 SIP emission inventory is defined as snapshot October 1st, 2021 (SNP20211001_SORE) with improvements to SORE categories. Detailed methodology for each surrogate can be found in the spatial surrogate methodology document (AMSS, Spatial Surrogate Methodology Document SNP2021-10-01). This working snapshot includes all previous updates noted in surrogate snapshot

2020-10-01 (AMSS), as well as recent improvements outlined below. A summary of the primary spatial surrogates by EICSUM is provided in Sub-Appendix B.D.

- Improvements to small off-road equipment (SORE) surrogates
  - Creation of SNOW-level allocation factors for single family housing and commercial activity related to locations that will only occur with snowfall (snowblowers, etc.).
  - Creation of forest roads spatial surrogate (191) based on the integration of NLCD forest data with the TIGER road network
- Updated to 2016 National Land Cover Database
- Improvements to the Dunn and Bradstreet based surrogates with integration of Digital Maps Products 2017 Parcel data
- Updates to ocean going vessel surrogates based on 2018 Automatic Identification System (AIS)
- Improvement to construction surrogates
  - Creation of a 90:10 ratio split of on-road to offroad construction surrogate
- Improvements to agriculture surrogates
  - Updated input data for Farm Road VMT and inclusion of California Department of Pesticide Regulation (CDPR) data
  - Updated input data to our poultry related surrogate from California Water Board, Southern California Association of Governments (SCAG), and San Diego Association of Governments (SANDAG)
- Creation of a Water bodies and Land mask to remove anomalies caused by AIS satellite bias.

B.2.2.4.1 Spatial Allocation of Area Sources

Area-wide emissions are modeled using a top-down approach where emission totals are estimated for a large geographic area of interest (GAI). Each area source category is assigned a primary spatial surrogate that is used to allocate emissions to a grid cell in CARB's 4 km statewide modeling domain. Examples of surrogates include population, land use, and other data with known geographic distributions for allocating emissions to grid cells, as described above.

B.2.2.4.2 Spatial Allocation of Point Sources

Each point source is allocated to grid cells using the latitude and longitude reported for each stack. If there are no stack latitude and longitude, the facility coordinates are used. There are two types of point sources: elevated and non-elevated sources. Stationary point sources with stacks are regarded as elevated sources. Those without physical stacks that provide only latitude/longitude, such as airports or landfills, are considered non-elevated. Emissions are allocated vertically for elevated sources using the SMOKE (Sparse Matrix Operator Kernel Emissions) modeling system's in-line plume rise calculation within the

CMAQ (Community Multi-scale Air Quality) photochemical model. SMOKE will select the sources that will receive the CMAQ in-line plume rise treatment, and group together sources with nearly identical stack parameters to reduce the number of calculations performed by the CMAQ in-line plume rise module. SMOKE will then output the emissions by grouped sources and the accompanying stack/facility coordinates and stack parameters for CMAQ's in-line plume rise module to handle the vertical allocation of the elevated sources.

B.2.2.4.3 Spatial Allocation of Wildfires, Prescribed Burns, and Wildland Fire Use

Emissions from wildfires, prescribed burns, and wildland fires are event- and location-based. A fire event can last a few hours or span multiple days. Each fire is spatially allocated to grid cells using the final extent of each fire event while the temporal distribution also reflects the actual duration of the fire. The spatial information to allocate the fire emissions comes from a statewide interagency fire perimeters geodatabase maintained by the Fire and Resource Assessment Program (FRAP) of the California Department of Forestry and Fire Protection (CALFIRE). More details on the methodology and estimation of the wildfire emissions can be found in Section B.2.3.6.1.

B.2.2.4.4 Spatial Allocation of Ocean-going Vessels (OGV)

CARB OGV emissions consist of four activity types: hoteling, maneuvering, anchorage, and transit. Since hoteling is stationary in port areas, it was treated as a point source. The remaining activity types are regarded as area sources. Individual berths were identified from a combination of AIS telemetry data, satellite and aerial photography, and detailed port maps where available. The centroids of grid cells on the Statewide domain containing berth locations were then associated with hoteling emissions for each GAI. Transit, spatial surrogates were constructed based on the National Waterway Network and AIS data from 2017. Maneuvering spatial surrogates were drawn to connect the transit lanes with the berth locations for each port. Anchorage locations were determined based on raster data from the National Oceanic and Atmospheric Administration (NOAA) which reflects anchorage locations codified in the Federal Register.

B.2.2.4.5 Spatial Allocation of On-road Motor Vehicles

The spatial allocation of on-road motor vehicles is based on data from the latest travel demand models provided by local Metropolitan Planning Organizations (MPOs). These model outputs are combined into a statewide transportation network using the Integrated Transportation Network (ITN). For areas without a regional travel demand model, data from the California Department of Transportation (Caltrans) California Statewide Travel Demand Model (CSTDM). For more details, see Section B.2.3.2.3.

B.2.2.5 Speciation Profiles

CARB's emission inventory lists the amounts of pollutants discharged into the atmosphere by source in a certain geographical area during a given time period. It currently contains estimates for CO, NH_3, NO_X, SO_X, total organic gases (TOG) and particulate matter (PM). CO and NH_3 each are single species; NO_X emissions are composed of NO, NO_2 and HONO; and SO_X emissions are composed of SO_2 and SO_3. TOG and PM potentially contain over hundreds of different chemical species, and speciation is the process of disaggregating these inventory pollutants into individual chemical species components or groups of species. CARB maintains and updates such speciation profiles for organic gases (OG) and PM for a variety of source categories.

Photochemical models simulate the physical and chemical processes in the lower atmosphere and include all emissions of the important classes of chemicals involved in photochemistry as well as less reactive compounds that are of concern from a health or visibility standpoint. TOG includes all organic compounds that can become airborne (through evaporation, sublimation, as aerosols, etc.), excluding CO, CO_2, carbonic acid, metallic carbides or carbonates, and ammonium carbonate. TOG emissions reported in the CARB's emission inventory are the basis for deriving the reactive organic gas (ROG) emission components, which are also reported in the inventory. ROG is defined as TOG minus CARB's exempt compounds (e.g., methane, ethane, various chlorinated fluorocarbons, acetone, perchloroethylene, volatile methyl siloxanes, etc.). ROG is nearly identical to U.S. EPA's Volatile Organic Compounds (VOC), which is based on EPA's exempt list. For all practical purposes, use of the terms ROG and VOC are interchangeable.

The OG speciation profiles are applied to estimate the amounts of various organic compounds that make up TOG emissions. A speciation profile contains a list of organic compounds and the weight fraction that each compound comprises of the TOG emissions from a particular source type. In addition to the chemical name for each chemical constituent, the file also shows the 5-digit CARB internal identification chemical code. The speciation profiles are applied to TOG to develop both the photochemical model inputs and the emission inventory for ROG. District-reported fractions are not used in developing modeling inventories because the information needed to calculate the amount of each organic compound is not available.

The PM emissions are size-fractionated by using PM size distribution profiles, which contain the total weight fraction for $PM_{2.5}$ and PM_{10} out of total PM. The fine and coarse PM chemical compositions are characterized by applying the PM chemical speciation profiles for each source type, which contain the weight fractions of each chemical species for $PM_{2.5}$, PM_{10}, and total PM. PM chemical speciation profiles may also vary for different PM size fractions even for the same emission source. PM size profiles and speciation profiles are typically generated based on source testing data. In most previous source testing studies aimed at determining PM chemical composition, filter-based sampling techniques were used to collect PM samples for chemical analyses.

The most current OG profiles and PM profiles are available for download from *CARB's speciation profile web page*. Based on these original profiles, a model-ready speciation file, gspro, was generated for a specific chemical mechanism (for example, SAPRC07T) to separate aggregated inventory pollutant emission totals into emissions of model species required by the air quality model.

Each process or product category is keyed to one of the OG profiles and one of the PM profiles. Also available for download from CARB's web site (see link in previous paragraph) is a cross-reference file that indicates which OG profile and PM profile are assigned to each category in the inventory. The inventory source categories are represented by an 8-digit source classification code (SCC) for point sources, or a 14-digit emission inventory code (EIC) for area and mobile sources. Some of the OG profiles and PM profiles related to motor vehicles, ocean going vessels, and fuel evaporative sources vary by the inventory year of interest, due to changes in fuel composition, vehicle fleet composition, and emissions control devices such as diesel particulate filters (DPFs). Details can be found in CARB's references of speciation profile development available on the *Consolidated List for Speciation Profiles site*. Mapping of each category to OG and PM profiles is summarized in rogpm and gsref files.

Research studies are conducted regularly to improve CARB's speciation profiles. These profiles support ozone and PM modeling studies and can also be used for regional toxics modeling. Speciation profiles need to be as complete and accurate as possible. CARB has an ongoing effort to update speciation profiles as data become available through testing of emission sources or surveys of product formulations. New speciation data generally undergo technical and peer review; updates to the profiles are coordinated with end users of the data. The recent additions to CARB's speciation profiles include:

- OG profiles
    - Off-road recreational vehicle exhaust and evaporation
    - Biomass burning
    - Consumer products
    - Architectural coating
    - Gasoline fuel and headspace vapor
    - Gasoline vehicle hot soak and diurnal evaporation
    - Gasoline vehicle start and running exhaust
    - Silage
    - Aircraft exhaust
    - Compressed Natural Gas (CNG) bus running exhaust
- PM profiles
    - Tire burning

- Gasoline vehicle exhaust
- On-road diesel exhaust
- Off-road diesel exhaust
- Ocean going vessel exhaust
- Aircraft exhaust
- Concrete batching
- Commercial cooking
- Residential fuel combustion-natural gas
- Coating/painting
- Cotton ginning
- Stationary combustion
- OGV auxiliary boiler combustion
- Compressed Natural Gas (CNG) vehicle running exhaust

B.2.3 Methodology for Developing Base Case, Baseline, and Future Projected Emissions Inventories

As mentioned in Section B.2.1.3, the base case and reference inventories include temperature, humidity, and solar insolation effects for some emission categories; development of these data is described in Sections B.2.3.6. Sections B.2.3.1 through B.2.3.8 detail how the base case and reference inventories were created for different sectors of the inventory such as point, area, on-road motor vehicles, biogenic, OGV, other day-specific sources, Northern Mexico, and Western States.

B.2.3.1 Estimation of Gridded Area and Point sources

Emissions inventories that are temporally, chemically, and spatially resolved are needed as inputs for the photochemical air quality model. Point sources and area sources (area-wide, off-road mobile, and aggregated stationary) are processed into emissions inventories for photochemical modeling using the SMOKE modeling system (https://www.cmascenter.org/smoke/). The current SIP modeling uses SMOKE v4.8 (referred as Official SMOKE hereafter) following in-house testing of this version of the software.

Inputs for SMOKE are annual emissions totals from CEPAM and information for allocating to temporal, chemical, and spatial resolutions. Temporal inputs for SMOKE are screened for missing or invalid temporal codes as discussed in Section B.2.4.1. Temporal allocation of emissions using SMOKE involves the disaggregation of annual emissions totals into monthly, day-of-week, and hour-of-day emissions totals. The temporal codes from Table B-18 and Table B-19 are reformatted into an input-ready format as explained in the SMOKE user's manual. Chemical speciation profiles, as described in Section B.2.2.5, and emissions source cross-reference files used as inputs for SMOKE are developed by

CARB staff. SMOKE uses the files for the chemical speciation of NO_X, SO_X, TOG, and PM to produce the species needed by photochemical air quality models.

Emissions for area sources are allocated to grid cells defined by the modeling grid domain in Section B.2.1.4. Emissions are spatially disaggregated using spatial surrogates as described in Section B.2.2.4. These spatial surrogates are converted to a SMOKE-ready format as described in the SMOKE user's manual. Emissions for point sources are allocated to grid cells by SMOKE using the latitude and longitude coordinates reported for each stack.

B.2.3.2 Estimation of On-road Motor Vehicle Emissions

B.2.3.2.1 General Methodology

The EMFAC2017 with Metropolitan Planning Organizations specific activity version 10 (MPOv10) emissions are processed into on-road emissions inventories using ESTA developed by CARB. The ESTA model applies spatial and temporal surrogates to emissions to create top-down emission inventory files.

More information on ESTA is available at the following *GitHub repository for Emissions Spatial and Temporal Allocator*.

B.2.3.2.2 Activity Data Updates

Link-based and Traffic Analysis Zone (TAZ)-based travel activity from travel demand models provided by different MPOs, Caltrans and other California RTPAs. Parameters such as vehicle mix and VMT are compared between the default EMFAC and Caltrans databases prior to spatial allocation to ensure values lie within reasonable limits.

B.2.3.2.3 Spatial Adjustment

CARB works with local Metropolitan Planning Organizations (MPOs) to obtain the latest available output from regional travel demand models. The output link networks from these models are combined into a statewide link network using the Integrated Transportation Network (ITN) framework (CARB). For regions where no local travel demand model data are available, data from the Caltrans California Statewide Travel Demand Model (CSTDM) are used (Caltrans). Data are quality assured by checking network/link volume, vehicle miles traveled (VMT), and spatial rendering. Overlapping networks are checked for duplicate links to avoid overallocation in these regions. Model output years vary between all regional data sources for ITN. The networks are normalized into modeling years used for air quality modeling using county level growth factors from EMFAC. Table B-20 contains the data vintages used in the current working version of the statewide ITN.

Spatial allocation of on-road activity surrogates is split into two vehicle groups, light-duty and heavy-duty. Some major MPOs and Caltrans provide vehicle classification splits in their model link outputs. When possible, this information is incorporated into the ITN.

However, when no vehicle splits are provided by the regional models the total network volumes must be used for both light-duty and heavy-duty spatial distribution. Travel demand model output provides network volume information organized by peak and off-peak time periods. This peak period volume information is disaggregated to create 24 hourly surrogates for an average modeling day.

The link networks are processed through the spatial allocator tool to create gridded surrogates weighted by VMT.

Table B-20: Network information for data sources used in current version of ITN

Network	Counties in Network	Data Vintage
Association of Monterey Bay Area Governments (AMBAG)	Monterey, San Benito, Santa Cruz	2018 RTDM
Butte County Association of Governments (BCAG)	Butte	2020 RTP/SCS
California Statewide Travel Demand Model (CSTDM)	Statewide	Version 3.0
Fresno Council of Governments (FCOG)	Fresno	2019 RTP/SCS
Kings County Association of Governments (KCAG)	Kings	2018 RTP/SCS
Kern Council of Governments (KCOG)	Kern	2018 RTP/SCS
Merced County Association of Governments (MCAG)	Merced	2018 RTP/SCS
Madera County Transportation Commission (MCTC)	Madera	2018 RTP/SCS
Metropolitan Transportation Commission (MTC)	Alameda, Contra Costa, Marin, Napa, San Francisco, San Mateo, Santa Clara, Solano, Sonoma	2017 RTP/SCS
Sacramento Area Council of Governments (SACOG)	El Dorado, Placer, Sacramento, Solano, Sutter, Yolo, Yuba	2020 MTP/SCS
San Diego Association of Governments (SANDAG)	San Diego	2018 RTP/SCS
Santa Barbara County Association of Governments (SBCAG)	Santa Barbara	2017 FSTIP
Southern California Association of Governments (SCAG)	Imperial, Los Angeles, Orange, Riverside, San Bernardino, Ventura	2020 RTP/SCS
San Joaquin Council of Governments (SJCOG)	San Joaquin	2018 RTP/SCS
San Luis Obispo Council of Governments (SLOCOG)	San Luis Obispo	2019 RTP
Shasta Regional Transportation Agency (SRTA)	Shasta	2018 RTP
Stanislaus Council of Governments (StanCOG)	Stanislaus	2018 RTP
Tulare County Association of Governments (TCAG)	Tulare	2018 RTP
Tahoe Metropolitan Planning Organization (TMPO)	El Dorado, Placer	2015 FSTIP

Evaporative surrogates were created using registration data from the California Department of Motor Vehicles (DMV). Vehicle registration was provided by census block group for the entire state. Registration data were split into five vehicle types and two fuel types. Table B-21 shows the vehicle type categories used for the evaporative emission surrogates. Registration counts were totaled over a three-year period (2015-2018) and assigned to the corresponding census block group polygons. Data from the NASA Nighttime Lights (Mills, Weiss and Liang) dataset was used to clip the census block group into areas with active population.

Table B-21: Registration data vehicle type classes.

Vehicle Class Group Name	**Description**
MC	Motorcycles
MH_BUS	Motorhomes and Buses
P	Passenger Vehicles
T1_T4	Light-Heavy Duty Trucks
T5_T7	Heavy-Heavy Duty Trucks

B.2.3.2.4 Temporal Adjustment (Day-of-week adjustments for EMFAC daily totals)

EMFAC2017 produces average day-of-week (DOW) estimates that represent Tuesday, Wednesday, and Thursday. To more accurately represent daily emissions, DOW adjustments are made to all emissions estimated on a Friday, Saturday, Sunday or Monday. The DOW adjustment factors were developed using California Vehicle Activity Database (CalVAD) data. The CalVAD, developed by UC Irvine for CARB, is a system that fuses available data sources to produce a "best estimate" of vehicle activity by class. The latest activity from the CalVAD database was released in 2012. There are no expected upcoming updates. The CalVAD data set includes actual daily measurements of VMT on the road network for 43 of the 58 counties in California. However, there are seven counties that can't be used because the total vehicle miles traveled are less than the sum of the heavy heavy-duty truck vehicle miles traveled and trucks excluding heavy heavy-duty vehicle miles traveled. Furthermore, two more counties that have high vehicle miles traveled on Sunday are also excluded. Therefore, only 34 of these counties had useful data. To fill the missing 24 counties' data to cover all of California, a county which is nearby and similar in geography is selected to represent each of the missing counties. The CalVAD fractions were developed for three categories of vehicles: passenger cars (LD), light- and medium-duty trucks (LM), and heavy-heavy duty trucks (HHDT). Table B-22 also shows the corresponding assignment to each vehicle type. Furthermore, the CalVAD fractions are scaled so that a typical workday (Tuesday, Wednesday, or Thursday) gets a scaling factor of 1.0. All other days of the week receive a scaling factor where their VMT is related back to the typical workday. This means there are a total of five weekday scaling factors. Lastly, the CalVAD data were used to create a typical holiday, because the traffic patterns for holidays are quite different than a typical weekday. Thus, in the end, there are six daily fractions for each of the three vehicle classes, for all 58 counties. The DOW factors and vehicle type can be found in Sub-Appendix B.A.

Heavy-heavy duty vehicle fractions were updated using 2018 Performance Measurement System (PeMS) data. Truck volumes were pulled for each county. Day of year specific fractions were calculated relative to an average weekday for each county. Fractions were manually reviewed by staff to check data integrity. Counties without data or poor data quality were screened out and replaced with an older version of fractions from CalVAD.

Table B-22: Vehicle classification and type of adjustment

Vehicle Class	Vehicle type	Type of adjustment
1	LDA	LD
2	LDT1	LD
3	LDT2	LD
4	MDV	LD
5	LHDT1	LM
6	LHDT2	LM
7	T6	LM
8	T7 HHDT	HHDT
9	Other Bus	LM
10	School Bus	Unadjusted on weekdays, zeroed on weekends
11	Urban Bus	LD
12	Motorhomes	LD
13	Motorcycles	LD

B.2.3.2.5 Temporal Adjustment (Hour-of-day profiles for EMFAC daily totals)

EMFAC produces emission estimates for an average weekday and lacks the day-of-week hour-of-day temporal variations that are known to occur on specific days of the week. To rectify this, the CalVAD data were used to develop hour-of-day profiles for Friday through Monday, a typical weekday, and a typical holiday. Heavy-heavy duty hourly vehicle fractions were updated using 2018 Performance Measurement System (PeMS) data from Caltrans in counties where data were available. The hour-of-day profiles for passenger cars (LD), light- and medium-duty trucks (LM), and heavy heavy-duty trucks (HH) can be found in Sub-Appendix B.B.

B.2.3.2.6 Summary of On-road Emissions Processing Steps

The six steps to process on-road emissions for regional air quality modeling with CMAQ are represented below in Figure B-24. Step 1 reads daily emissions input data from EMFAC. Step 2 reads SMOKE-ready spatial surrogates files. Step 3 reads day of week and diurnal temporal activity profiles from CALVAD. Step 4 applies both the spatial surrogates and temporal allocations to the daily emissions from EMFAC. Step 5 creates the gridded, hourly NETCDF files for each day of the year being modeled. Lastly, step 6 produces text files for use in quality assurance and quality checks of the emissions data.

Figure B-24: Workflow for spatial and temporal allocation of on-road emissions

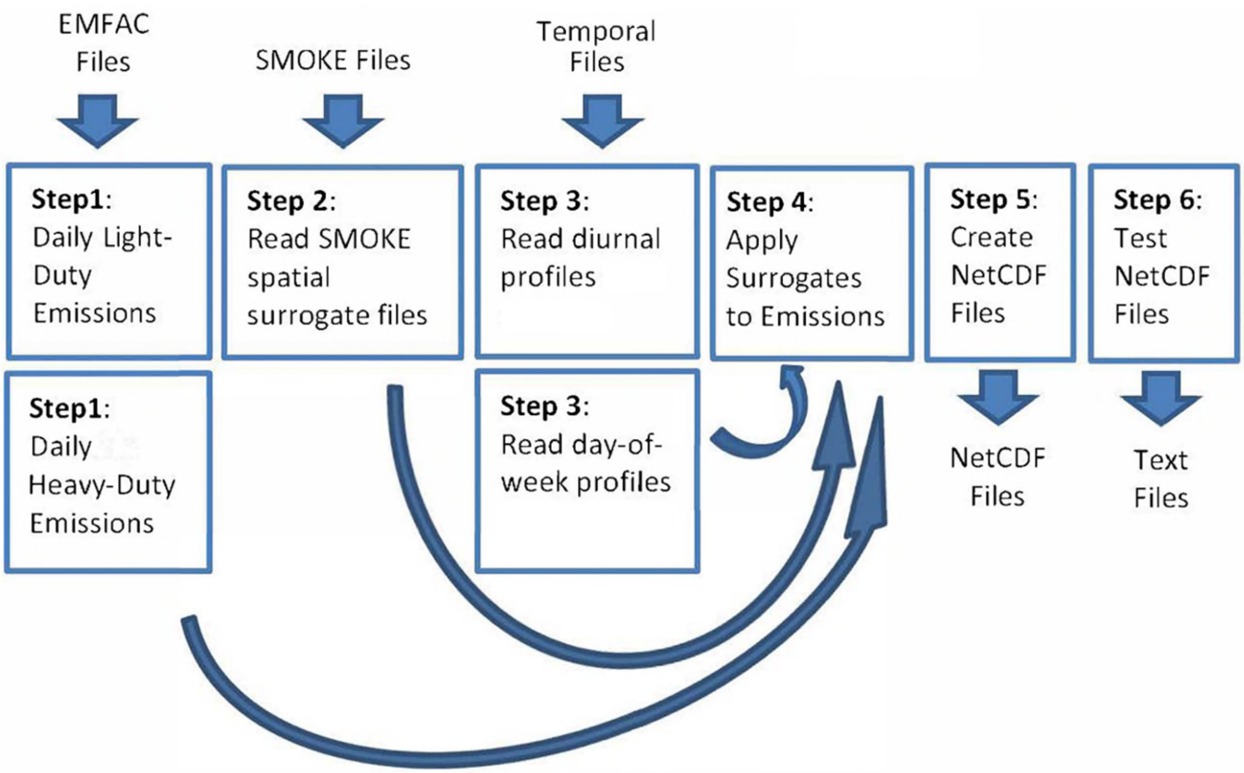

B.2.3.2.7 Adjustment to the Future Year On-road Emissions

The future year on-road mobile source emissions were adjusted to incorporate emission reduction programs for heavy duty vehicles. The reductions applied to the inventory reflect the Low NO_X Standard (CARB, Heavy-Duty Low NOx), Advanced Clean Truck (ACT) (CARB, Advanced Clean Trucks), and Heavy Duty Inspection and Maintenance Regulation (CARB, Heavy-Duty Inspection and Maintenance Regulation). The combined factors for 2026 are shown in Table B-23.

Table B-23: NO_X reductions (TPD) by Air Basin for 2026 and 2032

Region	2026 Reductions (Tpd)	2032 Reductions (Tpd)
El Dorado	0.16	0.27
Placer	0.75	1.46
Sacramento	1.66	2.82
Solano	0.96	2
Sutter	0.08	0.18
Yolo	0.5	1
Total Statewide reductions	65.8	117.29

B.2.3.3 Estimation of Gridded Biogenic Emissions

Biogenic emissions were generated using the MEGAN3.0 biogenic emissions model (https://bai.ess.uci.edu/megan/versions). MEGAN3.0 incorporates a new pre-processor (MEGAN-EFP) for estimating biogenic emission factors based on available landcover and emissions data. The MEGAN3.0 default datasets for plant growth form, ecotype, and emissions were utilized. Leaf Area Index (LAI) for non-urban grid cells was based on the 8-day 500-m resolution MODIS Terra/AQUA combined product (MCD15A2H) for 2018 (https://earthdata.nasa.gov/). The LAI data was converted to LAIv, which represents the LAI for the vegetated fraction within each grid cell, by dividing the gridded MODIS LAI values by the Maximum Green Vegetation Fraction (MGVF) for each grid cell (https://archive.USGS.gov/archive/sites/landcover.USGS.gov/green_veg.html). The MODIS LAI product does not provide information on LAI in urban regions, so urban LAIv was estimated from the US Forest Service's Forest Inventory and Analysis (FIA) urban tree plot data, processed through the i-Tree v6 software (https://www.itreetools.org/tools/i-tree-eco). Hourly meteorology was provided by 4-km WRF simulations for 2018, and all stress factor adjustments were turned off.

B.2.3.4 Aircraft Emissions

Aircraft emissions were generated using the Gridded Aircraft Trajectory Emissions Model (GATE) developed by CARB (AQPSD CARB, 2019). The GATE model distributes aircraft emissions in three dimensions. The GATE model takes annual aircraft emissions during landing, taxiing, and take-off, and converts this data into gridded, hourly emissions as follows:

- Read aircraft emissions from an annual inventory
- Split the emissions into hourly components
- Split any county-wide emissions into individual runways
- Geometrically model the 3D flight paths at each runway
- Intersect the above 3D paths with the 3D modeling grid
- Distribute the hourly aircraft emissions into the 3D grid

More information on GATE is available at the following *GitHub repository for GATE*.

B.2.3.5 Estimation of Ocean-going Vessel (OGV) Emissions

Annual emissions are provided through CEPAM for commercial and military OGV. The Mobile Source Analysis Branch compiled port activity data for 2016 reported for Long Beach, Port of Los Angeles, Bay Area, and San Diego. The activity data consisted of daily visits by vessel types for the full calendar year. This data was used to derive monthly and weekly temporal profiles for OGV sources. No activity data was available to create temporal profiles for the military sector; default SMOKE temporal profiles were assumed.

After applying the port activity factors mentioned above, emissions were separated by at-berth and everything else. At-berth emissions are processed through SMOKE and plume rise is calculated for every day of the year (Kwok). For transit, maneuvering, and anchorage, emissions are distributed evenly in two vertical layers (2 and 3) (Kwok).

B.2.3.6 Estimation of Other Day-specific Sources

Day-specific data were used for preparing base case inventories when data were available. CARB and district staff were able to gather hourly/daily emission information for 1) wildfires and prescribed burns, 2) paved and unpaved road dust, and 3) agricultural burns in six districts (more details highlighted below).

For the reference and future year inventories, day-specific emissions for wildfires, prescribed burns, and wildland fires use (WFU) are left out of the inventory. All other day-specific data are included in both reference and future year modeling inventories.

B.2.3.6.1 Wildfires and Prescribed Burns

Day-specific, base case estimates of emissions from wildfires and prescribed fires were developed in a two-part process. The first part consisted of estimating micro-scale, fire-specific emissions (i.e. at the fire polygon scale, which can be at a smaller spatial scale than the grid cells used in air quality modeling). The second part consisted of several steps of post-processing fire polygon emission estimates into gridded, hourly emission estimates that were formatted for use in air quality modeling.

Fire event-specific emissions were estimated using a combination of geospatial databases and a federal wildland fire emission model (Clinton, Gong and Scott). A series of pre-processing steps were performed using GIS to develop fuel loading and fuel moisture inputs to the First Order Fire Effects (FOFEM) fire emission model (Lutes, et al., 2012). Polygons from a statewide interagency fire perimeters geodatabase (Fire17_1.zip, downloaded May 8, 2018) maintained by the Fire and Resource Assessment Program (FRAP) of the California Department of Forestry and Fire Protection (CALFIRE) provided georeferenced information on the location, size (area), spatial shape, and timing of wildfires and prescribed burns. Under interagency Memorandums of Understanding, federal, state, and local agencies report California wildfire and prescribed burning activity data to FRAP. Using GIS software, fire polygons were overlaid upon a vegetation fuels raster dataset called the Fuel Characteristic Classification System (FCCS) (Ottmar, et al., 2007). The FCCS maps vegetation fuels at a 30-meter spatial resolution, and is maintained and distributed by LANDFIRE.GOV, a state and federal consortium of wildland fire and natural resource management agencies. With spatial overlay of fire polygons upon the FCCS raster, fuel model codes were retrieved and component areas within each fire footprint tabulated. For each fuel code, loadings (tons/acre) for fuel categories were retrieved from a FOFEM look-up table. Fuel categories included dead woody fuel size classes, overstory live tree crown, understory trees, shrubs, herbaceous vegetation, litter, and duff. Fuel moisture values for each fire were estimated by overlaying fire polygons on year- and month-specific 1 km spatial resolution fuel moisture raster files generated from the national Wildland Fire Assessment System (WFAS.net) and retrieving moisture values from fire polygon centroids. Fire event-specific fuel loads and fuel moisture values were compiled and formatted to a batch input file and run through FOFEM.

A series of post-processing steps were performed on the FOFEM batch output to include emission estimates (pounds/acre) for three supplemental pollutant species (NH_3, TNMHC, and N_2O) in addition to the seven species native to FOFEM (CO, CO_2, $PM_{2.5}$, PM_{10}, CH_4, NO_X, and SO_2), and to calculate total emissions (tons) by pollutant species for each fire. Emission estimates for NH_3, TNMHC, and N_2O were based on mass ratios to emitted CO and CO_2 (Gong, Clinton and Pu).

Fire polygon emissions were apportioned to CMAQ model grid cells using area fractions, developed using GIS software, by intersecting fire polygons to the grid domain.

Another set of post-processing steps were applied to allocate fire polygon emissions by date and hour of the day. Fire polygon emissions were allocated evenly between fire start and end dates, taken from the fire perimeters geodatabase. Daily emissions were then allocated to hour of day and to the model grid cells by using a script developed by CARB. A stack file and a 2-D hourly emissions file are generated for each day that has fire emissions. The stack file includes the fire locations, stack parameters and the number of acres burned for a fire in one day. The 2-D hourly emissions file includes the emissions for each specie and the heat flux (BTU/hr). CMAQ's in-line plume rise module will handle the vertical allocation of the fire emissions.

B.2.3.6.2 Paved and Unpaved Road Dust

Statewide emissions of total particulate matter from both paved and unpaved road dust are also a part of the CEPAM inventory. However, the sectors that have been embedded in any CEPAM version are already pre-adjusted. The unadjusted emissions are what is required before making any adjustment. Therefore, the unadjusted paved road dust is based upon CEPAM SIP2019v1.02-v1.01, while the unadjusted unpaved road dust uses an older CEPAM version with 20161130 snapshot. To adjust for precipitation, daily precipitation data for 2018 were used, provided by an in-house database maintained by CARB staff that stores meteorological data collected from outside sources. The specific data sources for these data include Remote Automated Weather Stations (RAWS), Atmospheric Infrared Sounder (AIRS), California Irrigation Management Information System (CIMIS) networks, and Federal Aviation Administration (FAA). FAA data provide precipitation data collected from airports in California.

When the precipitation reaches or exceeds 0.01 inches (measured anywhere within a county or county/air basin boundary on a particular day), the uncontrolled emissions are reduced on that day only: 25% for paved road dust, and total removal for the unpaved. The reductions can be achieved by running SMOKE with control matrices.

B.2.3.6.3 Agricultural Burning

Agricultural burn 2018 data processed were reported by air districts. The tons burned provided by the air districts were converted to acres using fuel loading data. With date of the burns, the location of the burns (latitude and longitude coordinates), crop type, and burn duration, the agricultural burn data were processed and then projected onto a statewide grid for each hour of a specific day.

B.2.3.6.4 Residential Wood Combustion Curtailment

Emissions were reduced to reflect residential wood curtailment (RWC) in San Joaquin Valley APCD and Sacramento Metropolitan AQMD.

A pre-SMOKE utility program called GenTpro is used to generate county-specific temporal profiles based on average temperature by grid cell (UNC Chapel Hill - The Institute for the Environment). Emissions for any given county are only allocated whenever the daily average temperature by grid cell is below 50 °F based on WRF simulated meteorology.

San Joaquin Valley APCD provided areas of curtailment, which are used to mask the spatial surrogates for woodstoves and fireplaces. The masked surrogates were used to apply day-specific curtailment. The corresponding complimentary surrogates were also constructed by subtracting the masked surrogates from the original spatial surrogates. These complimentary surrogates apply to areas without curtailment. For winter months (January, February, November, December) SJVAPCD provided no-burn days by county, from which day-specific CNTLMAT curtailment files were constructed. With these settings, processing of winter months using SMOKE is enabled by merging the outputs of two separate runs. The first run is for the portion with masked surrogates with curtailment via CNTLMAT, and the second run is for the portion that includes complimentary surrogates without curtailment. For non-winter months, SMOKE is only run once with the original spatial surrogates without any curtailment. When curtailment is applied to any county in SJV, wood burning emissions are reduced by 51%.

Areas under Sacramento Metropolitan AQMD (SMAQMD) have their RWC emissions reduced by 70% (i.e. 30% remaining) whenever no-burn days are designated. Curtailment is applied to the full spatial surrogates without exceptions.

B.2.3.6.5 Estimation of Agricultural Ammonia Emissions

Ammonia emissions from fertilizers/pesticides and livestock are separated from the aggregated area source inventory as they are affected by local meteorology. For fertilizers/pesticides, emissions vary by hour based on WRF’s two-meter temperature and ten-meter wind speed. For livestock, WRF’s ground temperature and aerodynamic resistance drive hourly variations in emissions. Through GenTpro these meteorological factors are averaged by county before creating year-long hourly profiles for each of the respective sectors. All algorithms are described in the SMOKE Manual 4. (UNC Chapel Hill - The Institute for the Environment), while the results of CARB in-house tests were summarized in an internal report (Kwok, Meteorology-adjusted Temporal Profiles for Agricultural and Residential Wood Combustion Sectors Using Smoke Gentpro Utility Program). In general, higher temperature and/or wind speeds favor ammonia emissions. Monthly surrogates based upon the frequency of pesticides applications were also applied to fertilizer NH_3. The sector also has emissions reported by a few individual facilities whose latitudes/longitudes are known.

Thus, the facility-reported livestock were represented as point sources. Another hourly GenTpro file was created just for them. To preserve the spatial distribution, emissions were apportioned to those individual facilities by GAI. SMOKE runs with these spatio-temporal allocations covered criteria pollutants NH_3, PM and TOG.

B.2.3.7 Northern Mexico Emissions

Transboundary flow of pollutants between California and Mexico must be considered and accounted for in air quality simulations of Southern California. Affected areas in California include the border regions of San Diego, Imperial and given the right meteorological conditions, more northern counties such as Riverside, Orange, and Los Angeles. As a result, emissions within the five municipal districts of Mexico's State of Baja California and one municipal district in Sonora must be included when running regional air quality models on the California Statewide Domain.

CARB's Mexico emissions inventory for area, point and non-road emission sources have been processed using an updated inventory developed by Eastern Research Group Inc. (ERG). This inventory is based on the 2014 Mexico National Emissions Inventory (MNEI) with additional improvements made by ground truthing agricultural burning, brick kilns and improving methods to calculate idling mobile emissions at the border entries (ERG). Base year 2017 emission estimates were developed by projecting the 2014 emissions to 2017. Future year 2037 emissions estimates were developed by interpolating 2014, 2020 and 2025 emission estimates to 2037.

For mobile sources, the U.S. EPA on-road emissions model SMOKE-MOVES (Sparse Matrix Operator Kernel Emissions – Motor Vehicle Emission Simulator) Mexico was used to produce an on-road emissions inventory. The on-road sector is reflective of true 2017 emissions. Future year 2037 emission estimates used the U.S. EPA on-road emissions model SMOKE-MOVES Mexico for future year 2028. SMOKE-MOVES is more comprehensive than the data provided for the on-road sector in the 2014 MNEI, and after discussions with U.S. EPA it was suggested to use SMOKE-MOVES over the 2014 MNEI estimates.

Figure B-25: Outline of Mexico municipalities included in California air quality simulations. The grey box outlines the boundaries of the CAState_4km modeling domain

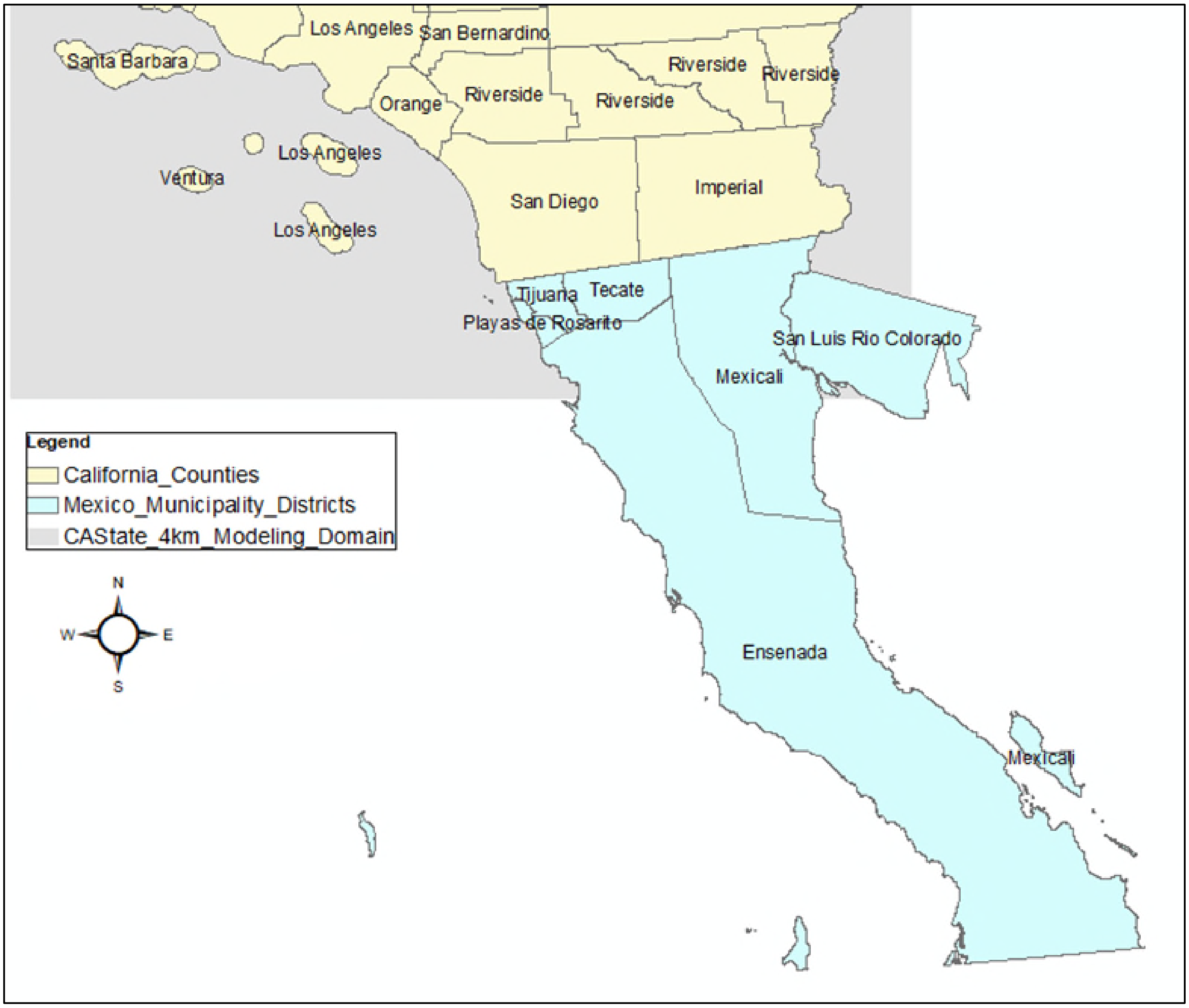

Under contract to CARB, ERG recently completed an update to the spatial distribution of Mexico's area, non-road, and on-road emissions (ERG). These updates include additional spatial surrogates such as the location of brick kilns, bakeries, ports, airports etc. for the state of Baja California. In addition, the project supports large improvements on emission estimates at two major border crossings (ERG). These updates have been included in the base and future year inventories and the surrogates used are listed in Table B-24.

EPA's National Emission Inventory (NEI) has been used by ARB as a foundation for identifying spatial surrogates that will aid in allocating emissions in the northern part of Mexico. While searching for improved surrogates, different online databases were investigated to find shapefiles relevant to established source sectors. The updated population surrogate was pulled from Instituto Nacional de Estadística y Geografía

(INEGI) using information from Mexico's 2010 Population and Housing Census. INEGI provides spatial information about Mexico such as resources, population, and land use. The population surrogate was also used to update the following residential heating sources: wood, distillate oil, coal, and LP gas. The total road miles surrogate that is used to spatially allocate on-road emissions was also updated using data provided by INEGI's dataset containing information on urban and rural roads and highways. Agriculture and forests spatial surrogates were updated using the same dataset from Comisión Nacional Forestal (CONAFOR). Using satellite images taken by the MODIS sensor (Moderate Resolution Imaging Spectroradiometer), the resulting vector data set from CONAFOR was produced to characterize Mexico's land. The border crossings surrogate was updated using statistics from the U.S. Bureau of Transportation, which provided points of entry along California and Mexico's border. Once the shapefiles were collected, they were converted to the standard projection used in CARB's modelling. These EPA-based surrogates are used within the state of Sonora, which was not covered in the ERG contract, and as secondary spatial allocation for the state of Baja CA. Table B-25 lists the EPA-based Mexico surrogates dated as of May 2018.

Table B-24: List indicating ERG developed spatial surrogates for the state of Baja California

Spatial Surrogate ID	Description	Year
100	Mexicali Agriculture	2014
110	Mexicali Agburn	2014
111	Mexicali Agburn Asparagus	2014
112	Mexicali Agburn Bermuda	2014
113	Mexicali Agburn Wheat	2014
120	Airports	2014
130	Autoshop	2014
140	Bakeries	2014
150	Border Crossing	2014
160	Brick Kilns	2014
170	Charbroiling	2014
180	Feedlots	2014
190	Gas Stations	2014
200	Graphic Arts	2014
210	Hospitals	2014
220	Landfills	2014
230	Total Population	2014
231	Rural Population	2014
232	Urban Population	2014
240	Ports	2014
250	Railroads	2014

Spatial Surrogate ID	Description	Year
260	Wastewater	2014
270	Windblown Dust	2014

Table B-25: List of EPA's Mexico surrogates as of May 2018

#	Surrogate	Year	Shapefile	Weight field
10	Population	2010	north_mexico_population.shp	population
12	Housing	2010	north_mexico_population.shp	population
14	Residential Heating Wood	2010	north_mexico_population.shp	population
16	Residential Heating Distillate Oil	2010	north_mexico_population.shp	population
18	Residential Heating Coal	2010	north_mexico_population.shp	population
20	Residential Heating LP Gas	2010	north_mexico_population.shp	population
22	Total Road Miles	2011	MEX_roads.shp	WEIGHT
24	Total Railroad Miles	2000	mexico_rr_MM5.shp	LENGTH
26	Total Agriculture	2015	MEX_agriculture.shp	WEIGHT
28	Forest Land	2015	MEX_Forests.shp	WEIGHT
30	Land Area	2000	REPMEX_ES_HEAT1_MM5.shp	P001
32	Commercial Land	1999	com_ind_viv_MM5.shp	A500_2000
34	Industrial Land	1999	com_ind_viv_MM5.shp	A505_2000
36	Commercial Plus Industrial	1999	com_ind_viv_MM5.shp	A510_2000
38	Commercial plus Industrial Land	1999	com_ind_viv_MM5.shp	A515_2000
40	Residential Commercial Industrial Institutional	1999	com_ind_viv_MM5.shp	a535_2000
42	Personal Repair	1999	REP_CRUCES_MM5.shp	a545_1999
44	Airports Area	1999	mexico_air_MM5.shp	WEIGHT
46	Marine Ports	1999	mexico_ports_MM5.shp	VALUE
48	Brick Kilns	1999	BOSQUE_LAD_MM5.shp	LAD_2000
50	Mobile Sources Border Crossing	2014	Border_Crossing_Years_MM5.shp	Y20**

B.2.3.8 Western States Emissions

In addition to transboundary flow from Mexico into California cities, pollutants can travel between various bordering states such as Nevada, Arizona, Oregon, Idaho, and Utah. The current statewide modeling domain includes grid cells that cover these regions and therefore emission estimates from the four major source sectors (area, point, non-road, and on-road) need to be included for a complete California State modeling domain inventory. As CARB or California air districts are not responsible for the development of emission estimates in those geographic regions, the national emission inventory developed by the U.S. EPA was used.

CARB's Western US emissions inventory has been developed using the U.S. Environmental Protection Agency (EPA) 2011 National Emissions Inventory (NEI) platform version 3 with future year projections for 2017and 2028[1].

Base year 2017 emissions were developed with "2011v3 NEI 2017ek_cb6v2_v6_11g" which are 2017 projections from the 2011 national emissions inventory version three, while the future year 2032 emissions were processed from "2011v3 NEI 2028el_cb6v2_v6_11g" 2028 projections based on the 2011 National Emissions Inventory version three. Spatial and temporal allocations were applied using the EPA ancillary files however, all spatial surrogates were processed through the spatial allocator tool with the California statewide map projection applied.

B.2.3.9 Application of Control Measure Reduction Factors

Future year onroad vehicle emissions were adjusted to reflect statewide reduction commitments for CARB's Low NO_X, ACT, and HD I&M for 2032. SSS adjustments for onroad were applied to the 2032 projected inventory. The onroad adjustments are summarized in Section B.2.3.2.7.

B.2.3.10 Application of Emission Reduction Credits

The Sacramento Federal Nonattainment Area modeling inventory incorporated emission reduction credit (ERC) adjustments to the projected future year (FY) 2032 inventories. Quarterly ERCs for VOC and NO_X in tons per day were received from the SMAQMD for the Sac Metro, Placer, Feather River, and Yolo-Solano districts. The ERC adjustments were applied at the COABDIS level to stationary area and point sources. The annual average daily NO_X and ROG ERCs for 2032 are show in Table B-26.

Table B-26: Annual average ERCs for Sacramento Nonattainment Area

Year	NO_X (TPD)	ROG (TPD)
2032	2.80	3.80

B.2.4 Quality Assurance of Modeling Inventories

As mentioned in Section B.2.1.3.1., base case modeling is intended to demonstrate confidence in the modeling system. Quality assurance of the data is necessary to detect outliers and potential problems with emission estimates. The most important quality assurance checks of the modeling emissions inventory are summarized in the following sections.

1 All inventory and ancillary files for spatial and temporal allocation are available for download at: ftp://newftp.epa.gov/air/emismod/2011/v3platform/ (U.S. EPA, 2018).

B.2.4.1 Area and Point Sources

All SMOKE inputs are subject to extensive quality assurance procedures performed by CARB staff. Annual and forecasted emissions are carefully reviewed prior to running SMOKE. CARB and district staff review data used to calculate emissions along with other ancillary data, such as temporal profiles and the location of facilities and assignment of SCC to each process. Growth and control information are reviewed and updated as needed.

We also compare annual average emissions from CEPAM with planning inventory totals to ensure data integrity. The planning and modeling inventories start with the same annual average emissions. The planning inventory is developed for an average summer day and an average winter day, whereas the modeling inventory processes daily emissions. Both inventory types use the same temporal data described in Section B.2.2.2. The summer planning inventory uses the monthly throughputs from May through October. Similarly, the winter planning inventory uses the monthly throughputs from November through April. The modeling inventory produces emissions for every day of the year.

Annual, gridded emissions totals are plotted on the statewide modeling domain and visually inspected to check the spatial allocation of emissions. Spatial plots by source category like the one shown in Figure B-26 are carefully screened for proper spatial distribution of emissions.

Figure B-26: Example of an ROG spatial plot by source category (Consumer Products)

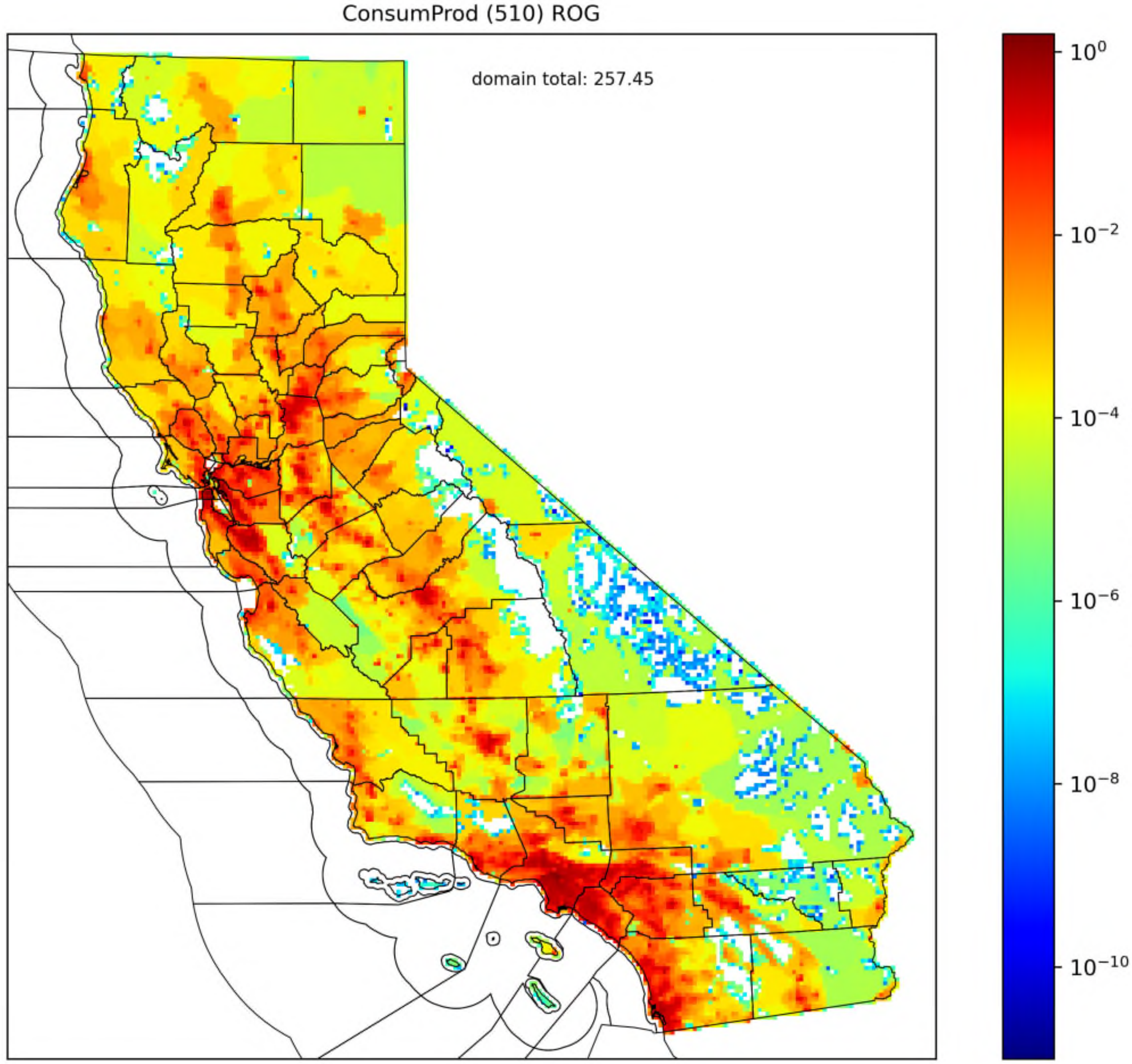

Before air quality model-ready emissions files are generated by SMOKE, the run configurations and parameters set within the SMOKE environment are checked for consistency for both the reference and future years.

To aid in the quality assurance process, SMOKE is configured to generate inventory reports of temporally, chemically, and spatially-resolved emissions inventories. CARB staff utilize the SMOKE reports by checking emissions totals by source category and region. Staff also create and analyze time series plots, and compare aggregate emissions totals with the pre-SMOKE emissions totals obtained from CEPAM.

Checks for missing or invalid temporal assignments are conducted to ensure accurate temporal allocation of emissions. Special attention is paid to checking monthly throughputs and appropriate monthly temporal distribution of emissions for each source category. In addition, checks for time-invariant temporal assignments are done for certain source categories and suitable alternate temporal assignments are determined and applied.

Further improvements to temporal profiles used in the allocation of area source emissions are performed using suitable alternate temporal assignments determined by CARB staff. Select sources from manufacturing and industrial, degreasing, petroleum marketing, mineral processes, consumer products, residential fuel combustion, farming operations, aircraft, off-road equipment, and commercial harbor craft sectors are among the source categories included in the application of adjustments to temporal allocation.

B.2.4.2 On-road Emissions

There are several processes to conduct quality assurance of the on-road mobile source modeling inventory at various stages of the inventory processing. The specific steps taken are described below.

- Plot MPO provided data spatially to find any missing or incomplete links.
- Compare spatial distribution of VMT between on and off-peak periods for each MPO.
- Generate time series plots for the on-road emissions files to check the diurnal pattern.
- Compare the daily total emissions for the on-road emissions files and the EMFAC 2017 emissions files for each county to ensure that the emissions are the same.
- Generate the spatial plot for the on-road emissions files to check if there were any missing emissions.

B.2.4.3 Aircraft Emissions

There are two steps to conduct quality assurance of the aircraft emissions.

- Compare the daily total emissions for the aircraft emissions files and the raw emissions files for each county to ensure that the emissions are the same.
- Generate the spatial plot for the aircraft emissions files to check if there were any missing emissions.

B.2.4.4 Day-specific Sources

B.2.4.4.1 Wildfires

GIS records for 413 wildfires, 166 prescribed wildland burn events, and 28 wildland fires use reported for 2018 were downloaded from *The California Department of Forestry and Fire Protection's Fire and Resource Assessment Program (FRAP)* and imported to a geodatabase. Data fields included wildfire or burn project name, burned area, and start and end dates. A series of geoprocessing steps were used to map and overlay wildfire and prescribed burn footprint polygons on the statewide vegetation fuels (FCCS) and moisture raster datasets, to retrieve associated fuel loadings and moisture values for use as input to FOFEM. Wildfire and prescribed burn footprint polygons were also overlaid on the statewide 4-km modeling grid to assign grid cell IDs to each wildfire and prescribed burn. Emission estimates for each wildfire and prescribed burn event were generated by FOFEM and summarized in an Access database. To check the location of the fires and the daily total emissions, a script is used to make a netCDF file from the stack file and the 2-D hourly emissions file for each day. The spatial plot and the daily total emissions from processing the netCDF file are then compared to the raw fire emissions data to check for accuracy.

B.2.4.4.2 Agricultural Burning

Checks were done to verify the quality of the agricultural burn data. The day-specific emissions from agricultural burning were compared to the emissions from CEPAM for each county to check for agreement between the planning and modeling inventories. Time series plots were reviewed for each county to see that days when burning occurred matched the days provided by the local air district. For each county, a few individual fires were calculated by hand starting from the raw data through all the steps to the final model-ready emissions files to make sure the calculations were done correctly. Spatial plots were made to verify the location of each burn.

B.2.4.5 Additional Quality Assurance

In addition to the quality assurance described above, comparisons are made between annual average inventories from CEPAM and modeling inventories. The modeling inventory shows emissions by month and subsequently calculates the annual average for comparison with CEPAM emissions. Annual average inventories and modeling inventories can be different, but differences should be well understood. For example, modeling inventories are adjusted to reflect different days of the week for on-road motor vehicles as detailed in Section B.2.3.2; since weekend travel is generally less than weekday travel, modeling inventory emissions are usually lower when compared to annual average inventories from CEPAM. Figure B-27 is an example of a QA report that summarizes NO_X emissions by category for EIC3 10 through 499 for Sacramento Nonattainment Area. The report compares the monthly and annual processed emissions totals against CEPAM. Please note that this report is only an example since emissions have been updated from what is displayed here.

Figure B-27: Comparison of inventories report

2018 Ozone SIP, Base Year 2018 -- CEPAM 2019 Ozone SIP Ver 1.03 With Off-Road Patch (CEPAM2022v1.01) And Zero Out 430-995-7000-0000 NOx in E. Kern BYr:2018 MYr:2018

Basin:*SV* Spec:*NOx*

EIC	Description	Jan	Feb	Mar	Apr	May	Jun	Jul	Aug	Sep	Oct	Nov	Dec	Annual	RF3064_19v1.02	RF3084_19v1.03	RF3108_19v1.04	RF3089_22v1.01
10	Electric Utilities	2.04	1.91	1.88	1.77	1.65	1.92	2.15	2.18	2.12	2.76	1.94	2.28	2.05	1.86	2.05	2.05	1.96
20	Cogeneration	1.48	1.43	1.48	0.99	1.43	1.55	1.61	1.58	1.49	1.52	1.48	1.35	1.45	1.63	1.45	1.45	0.99
30	Oil And Gas Production (Combustion)	2.16	2.16	2.16	2.16	2.16	2.16	2.16	2.16	2.16	2.16	2.16	2.18	2.16	2.16	2.16	2.16	2.16
40	Petroleum Refining (Combustion)	0.00	0.00	0.00	0.00	0.00	0.00	0.00	0.00	0.00	0.00	0.00	0.00	0.00	0.00	0.00	0.00	0.00
50	Manufacturing And Industrial	4.02	4.20	4.60	4.99	5.38	5.40	5.37	5.39	5.35	5.35	4.92	4.39	4.95	4.88	4.95	4.95	5.05
52	Food And Agricultural Processing	1.09	1.08	1.09	2.68	2.69	2.79	3.50	3.87	4.07	1.96	1.39	1.12	2.28	2.21	2.28	2.28	2.23
60	Service And Commercial	10.07	9.67	8.19	6.50	3.62	3.61	3.58	3.65	3.61	3.69	4.06	8.82	5.74	5.61	5.75	6.04	6.30
99	Other (Fuel Combustion)	0.39	0.39	0.39	0.39	0.41	0.41	0.41	0.41	0.41	0.41	0.39	0.39	0.40	0.43	0.40	0.40	0.66
110	Sewage Treatment	0.00	0.00	0.00	0.00	0.00	0.00	0.00	0.00	0.00	0.00	0.00	0.00	0.00	0.00	0.00	0.00	0.00
120	Landfills	0.06	0.06	0.06	0.06	0.06	0.06	0.06	0.06	0.06	0.06	0.06	0.06	0.06	0.06	0.06	0.06	0.06
130	Incinerators	0.05	0.05	0.05	0.05	0.05	0.05	0.05	0.05	0.05	0.05	0.05	0.04	0.05	0.05	0.05	0.05	0.04
140	Soil Remediation	0.03	0.03	0.03	0.03	0.03	0.03	0.03	0.03	0.03	0.03	0.03	0.03	0.03	0.03	0.03	0.03	0.01
199	Other (Waste Disposal)	0.00	0.00	0.00	0.00	0.00	0.00	0.00	0.00	0.00	0.00	0.00	0.00	0.00	0.00	0.00	0.00	0.00
210	Laundering	0.00	0.00	0.00	0.00	0.00	0.00	0.00	0.00	0.00	0.00	0.00	0.00	0.00	0.00	0.00	0.00	0.00
220	Degreasing	0.00	0.00	0.00	0.00	0.00	0.00	0.00	0.00	0.00	0.00	0.00	0.00	0.00	0.00	0.00	0.00	0.00
230	Coatings And Related Process Solvents	0.01	0.01	0.01	0.01	0.01	0.01	0.01	0.01	0.01	0.01	0.01	0.01	0.01	0.01	0.01	0.01	0.01
240	Printing	0.00	0.00	0.00	0.00	0.00	0.00	0.00	0.00	0.00	0.00	0.00	0.00	0.00	0.00	0.00	0.00	0.00
250	Adhesives And Sealants	0.00	0.00	0.00	0.00	0.00	0.00	0.00	0.00	0.00	0.00	0.00	0.00	0.00	0.00	0.00	0.00	0.00
299	Other (Cleaning And Surface Coatings)	0.00	0.00	0.00	0.00	0.00	0.00	0.00	0.00	0.00	0.00	0.00	0.00	0.00	0.00	0.00	0.00	0.00
310	Oil And Gas Production	1.78	1.78	1.78	1.78	1.78	1.78	1.78	1.78	1.78	1.78	1.78	1.78	1.78	1.78	1.78	1.78	1.79
320	Petroleum Refining	0.00	0.00	0.00	0.00	0.00	0.00	0.00	0.00	0.00	0.00	0.00	0.00	0.00	0.00	0.00	0.00	0.00
330	Petroleum Marketing	0.01	0.01	0.01	0.01	0.01	0.01	0.01	0.01	0.01	0.01	0.01	0.01	0.01	0.01	0.01	0.01	0.09
399	Other (Petroleum Production And Marketing)	0.00	0.00	0.00	0.00	0.00	0.00	0.00	0.00	0.00	0.00	0.00	0.00	0.00	0.00	0.00	0.00	0.00
410	Chemical	0.04	0.05	0.06	0.07	0.06	0.06	0.05	0.08	0.07	0.07	0.09	0.08	0.06	0.06	0.06	0.06	0.06
420	Food And Agriculture	0.02	0.02	0.02	0.02	0.02	0.03	0.03	0.04	0.06	0.08	0.06	0.04	0.04	0.04	0.04	0.04	0.03
430	Mineral Processes	2.64	2.68	2.74	2.76	2.77	2.81	2.79	2.84	2.73	2.79	2.69	2.66	2.74	2.78	2.76	2.76	2.96
440	Metal Processes	0.01	0.01	0.01	0.01	0.01	0.01	0.01	0.01	0.01	0.01	0.01	0.01	0.01	0.01	0.01	0.01	0.01
450	Wood And Paper	0.10	0.10	0.10	0.10	0.10	0.11	0.10	0.11	0.10	0.11	0.10	0.10	0.10	0.11	0.11	0.11	0.11
460	Glass And Related Products	0.00	0.00	0.00	0.00	0.00	0.00	0.00	0.00	0.00	0.00	0.00	0.00	0.00	0.00	0.00	0.00	0.00
470	Electronics	0.00	0.00	0.00	0.00	0.00	0.00	0.00	0.00	0.00	0.00	0.00	0.00	0.00	0.00	0.00	0.00	0.00
499	Other (Industrial Processes)	0.02	0.02	0.02	0.02	0.02	0.02	0.02	0.02	0.02	0.02	0.02	0.02	0.02	0.04	0.02	0.02	0.03

Notes:

- CEPAM refers to annual average emissions from 2019 SIP Baseline Emission Inventory Tool with external adjustments: *CEPAM External Adjustment Reporting Tool*
- Monthly gridded emissions come from GeoVAST mo-yr/avg tabular summary - gid 657

Staff also review how modeling emissions vary over a year. Figure B-28 provides an example of a modeling inventory time series plot for Sacramento Valley Air Basin for area-wide sources, on-road sources, and off-road sources. Again, this figure is only an example.

Figure B-28: Daily variation of NO_X emissions for sources in Sacramento Valley Air Basin in 2018

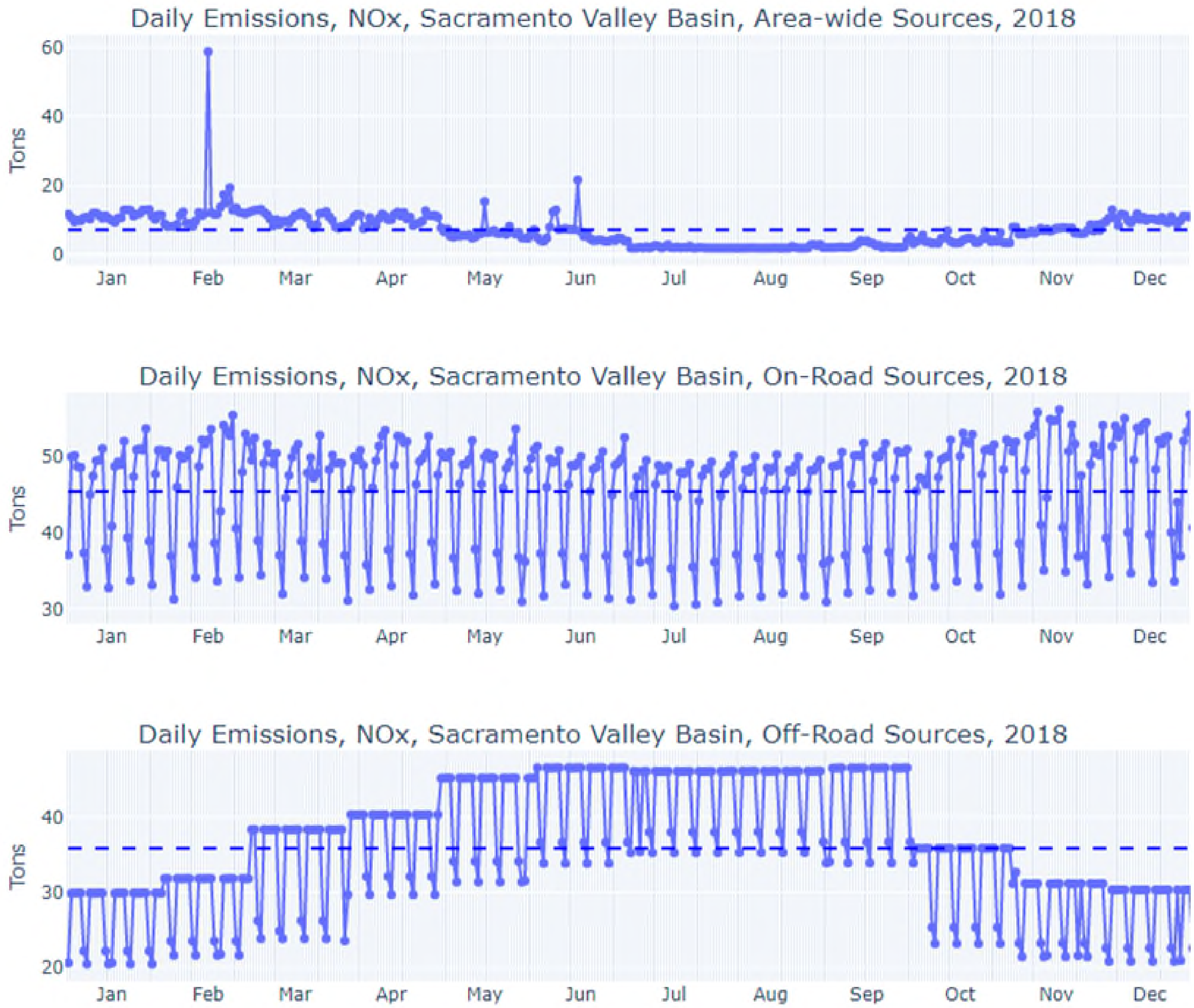

B.2.4.6 Model-ready Files Quality Assurance

Prior to developing the modeling inventory emissions files used in the photochemical models, the same model-ready emissions files developed for the individual source categories (e.g., on-road, area, point, day-specific sources) are checked for quality assurance. Extensive quality assurance procedures are already performed by CARB staff on the intermediate emissions files (e.g., SMOKE-generated reports); however, further checks are needed to ensure data integrity is preserved when the model-ready emissions files are generated from those intermediate emissions files. Figure B-29 shows the share of area, on-road, and point sources contribution to annual NO_X emissions are shown for the Sacramento Nonattainment Area in 2018. These same sources are shown as a daily timeseries for the Sacramento Nonattainment Area in Figure B-30. These figures are only examples and do not reflect the inventory totals used for SIP attainment modeling.

Figure B-29: Annual processed emissions example for 2018 Sacramento Nonattainment Area NO_X for area, on-road, and point sources

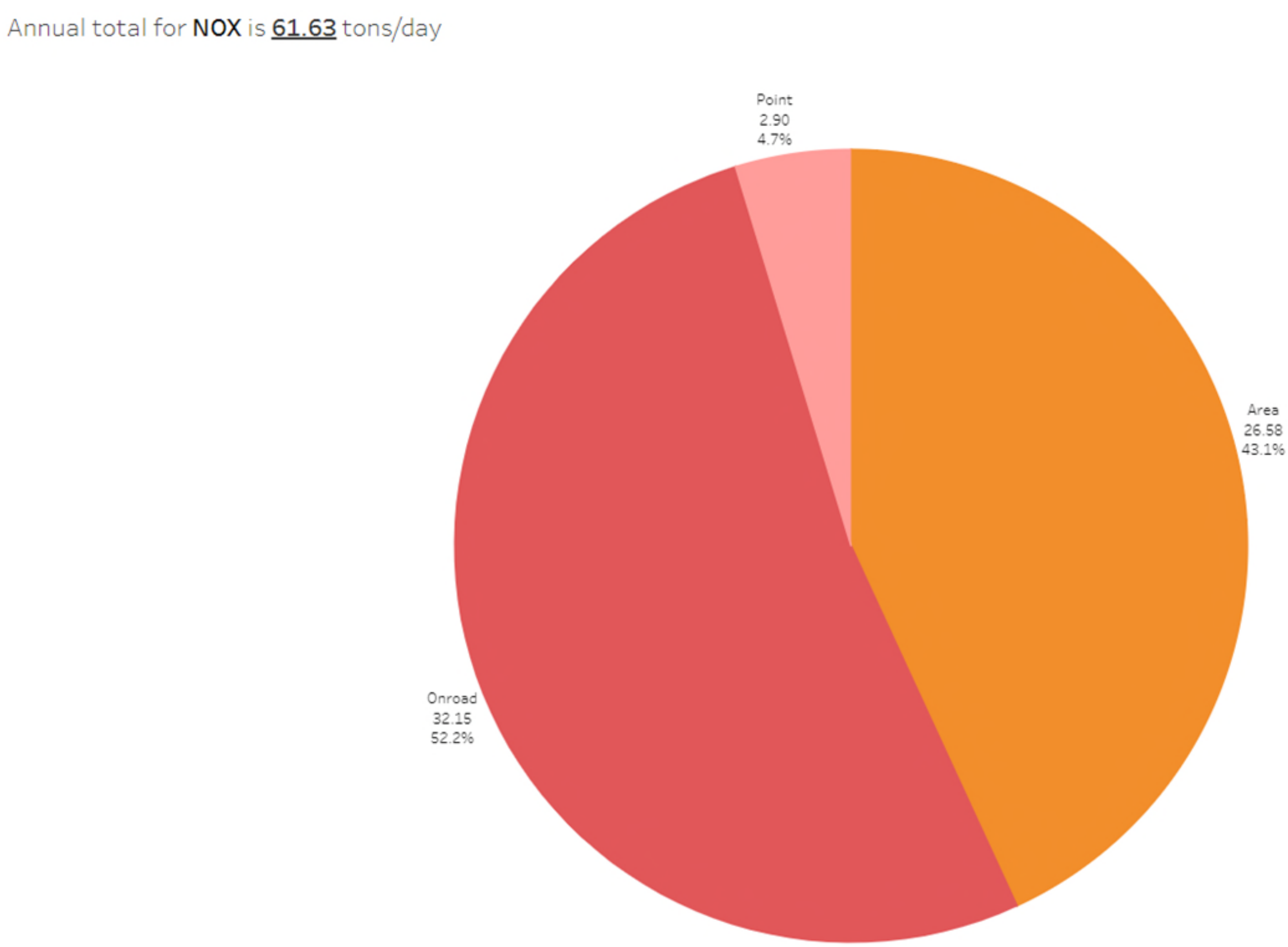

Figure B-30: Example timeseries plot for daily 2018 NO_X emissions from area, on-road, and point sources for Sacramento Nonattainment Area

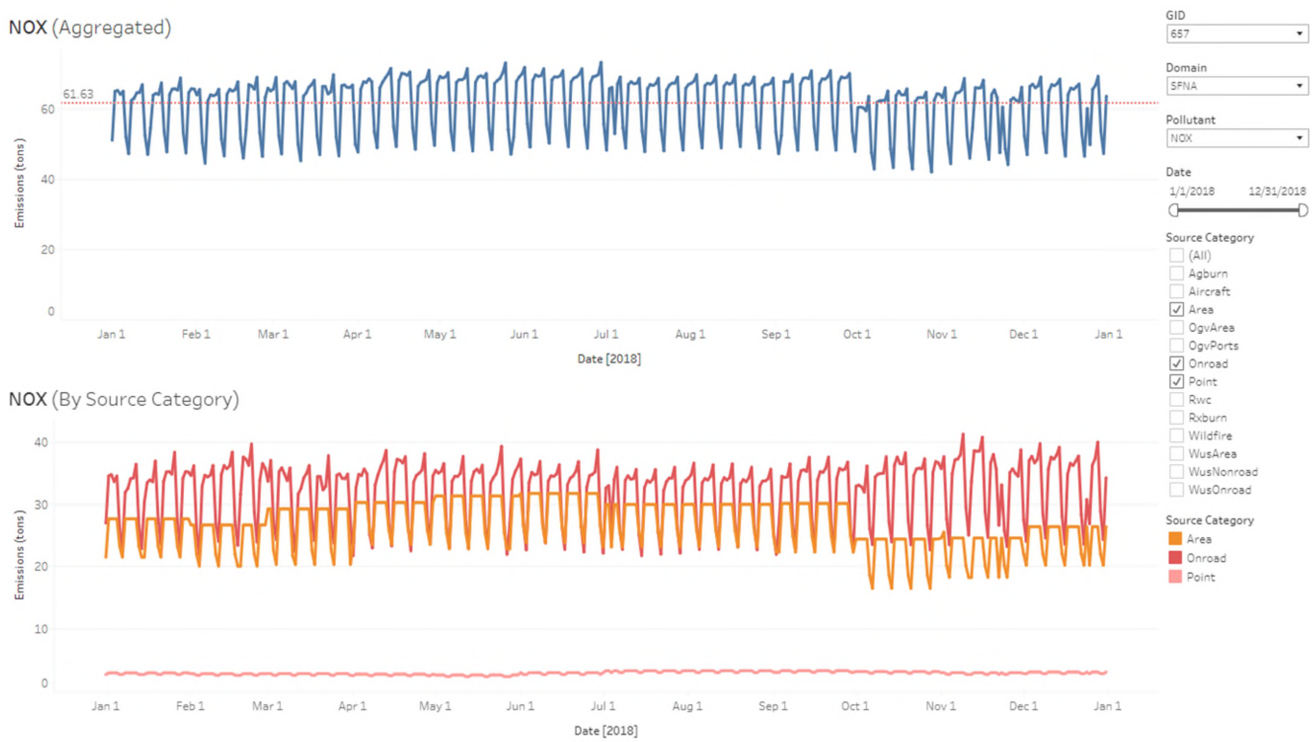

Comparisons of the totals for both the intermediate and model-ready emissions files are made. Emissions totals are aggregated spatially, temporally, and chemically to single-layer, statewide, daily values by inventory pollutant. Spatial plots are also generated for both the intermediate and model-ready emissions files using the same graphical utilities and aggregated to the same spatial, temporal, and chemical resolution to allow equal comparison of emissions. Any discrepancies in the emissions totals are reconciled before proceeding with the development of the model-ready inventory emissions files.

Before combining the model-ready emissions files of the individual source category inventories into a single model-ready inventory, they are checked for completeness. Most sources should have emissions for every day in the modeling period. Exceptions to this apply to sources like fires since burning (natural or planned) does not occur every day. It is important that during these checks source inventories with missing files are identified and resolved. Once all constituent source inventories are complete, they are used to develop the model-ready inventory used in photochemical modeling. When the modeling inventory files are generated, log files are also generated documenting the constituents of each daily model-ready emissions file as an additional means of verifying that each daily model-ready inventory is complete.

B.2.5 References

AMSS. *Spatial Surrogate Methodology Document SNP2020-10-01*. Sacramento: INTERNAL DRAFT CARB, 2020.

—. *Spatial Surrogate Methodology Document SNP2021-10-01*. Sacramento: INTERNAL DRAFT CARB, 2021.

Angevine, W. M., et al. "Meteorological model evaluation for CalNex 2010." *Monthly Weather Review* 140 (2012): 3885-3906.

Atsuyuki, O., et al. *Spatial tessellations: concepts and applications of Voronoi diagrams*. Second. John Wiley & Sons, 2009.

Baker, K. R., et al. "Evaluation of surface and upper air fine scale WRF meteorological modeling of the May and June 2010 CalNex period in California." *Atmospheric Environment* 80 (2013): 299-309.

Bao, J.W., et al. "Observed and WRF-simulated low-level winds in a high-ozone episode during the Central California ozone study." *Journal of Applied Meteorology and Climatology* 47 (2008): 2372-2394.

Beaver, S. and A. Palazoglu. "Influence of synoptic and mesoscale meteorology on ozone pollution potential for San Joaquin Valley of California." *Atmospheric Environment* 43.10 (2009).

Blanchard, C.L., et al. "Understanding Relationships between Changes in Ambient Ozone and Precursor Concentrations and Changes in VOC and NOx Emissions from 1990 to 2004 in Central California." Report prepared for the California Air Resources Board. 2008.

Buchholz, R. R., et al. "CESM2.1/CAM-chem Instantaneous Output for Boundary Conditions." UCAR/NCAR - Atmospheric Chemistry Observations and Modeling Laboratory, 2019. <https://doi.org/10.5065/NMP7-EP60>.

Cai, C., et al. "Simulating Reactive Nitrogen, Carbon Monoxide, and Ozone in California During ARCTAS-CARB 2008 with High Wildfire Activity." *Atmospheric Environment* (2016): 28-44.

—. "Simulating the Weekly Cycle of NOx-VOC-HOx-O3Photochemical System in the South Coast ofCalifornia During CalNex-2010 Campaign." *Journal of Geophysical Research: Atmospheres* (2019): 3532–3555.

Caltrans. *Statewide Modeling*. 2020. <https://dot.ca.gov/programs/transportation-planning/multi-modal-system-planning/statewide-modeling>.

CARB. 1990. *Assessment and Mitigation of the Impacts of Transported Pollutants on Ozone Concentrations within California, Staff Report prepared by the Technical Support Division and the Office of Air Quality Planning and Liaison of the California Air Resources Board.* <available at https://www.arb.ca.gov/aqd/transport/assessments/1990.pdf>.

—. *2017 Baseline Inventory and Vehicle Miles Traveled Offset Demonstration for the 2015 70 ppb 8-hour Ozone Standard available at https://ww2.arb.ca.gov/resources/documents/2017-baseline-inventory-and-vehicle-miles-traveled-offset-demonstration-2015-70*. 2020. Jan 2022.

—. "2018 Western Nevada County Planning Area Ozone Attainment Plan available at https://ww3.arb.ca.gov/planning/sip/planarea/wnc/carb_staff_report.pdf." Staff Report. 2018. Jan 2022.

—. *Advanced Clean Trucks*. 07 02 2020. <https://ww2.arb.ca.gov/our-work/programs/advanced-clean-trucks>.

—. *Heavy-Duty Inspection and Maintenance Regulation*. 2021. <https://ww2.arb.ca.gov/rulemaking/2021/hdim2021>.

—. "Heavy-Duty Low NOx." 07 February 2020. <https://ww2.arb.ca.gov/our-work/programs/heavy-duty-low-nox>.

—. "Report on Updates to the California Integrated Transportation Network (ITN)." 2021.

Carter, W.P.L. "Development of a condensed SAPRC-07 chemical mechanism." *Atmospheric Environment* (2010b): 5336-5345.

—. "Development of the SAPRC-07 chemical mechanism." *Atmospheric Environment* (2010a): 5324-5335.

Chen, J., et al. "Modeling air quality in the San Joaquin Valley of California during the 2013 DISCOVER-AQ field campaign." *Atmospheric Environment* 5 (2020): 100067.

Clinton, N., P. Gong and K. Scott. "Quantification of pollutants emitted from very large wildland fires in Southern California." *Atmospheric Environment* (2006): Volume 40, pp. 3686-3695.

Deligiorgi, D. and K. Philippopoulos. "Spatial Interpolation Methodologies in Urban Air Pollution Modeling: Application for the Greater Area of Metropolitan Athens, Greece." *Advanced Air Pollution*. 2011.

EasternKern. "2017 Ozone Attainment Plan, available at: http://www.kernair.org/Documents/Announcements/Attainment/2017%20Ozone%20Plan_EKAPCD_Adopted_7-27-17.pdf." 2017.

EKAPCD. "East Kern County Ozone Attainment Demonstration, Maintenance Plan, and Redesignation Request." 2003. <available at https://www.arb.ca.gov/planning/sip/planarea/easternkern/2003kernplan.pdf>.

Emery, C., et al. "Recommendations on statistics and benchmarks to assess photochemical model performance." *Journal of the Air & Waste Management Association* (2017): 582-598.

Emmons, L. K., et al. "The Chemistry Mechanism in the Community Earth System Model version 2 (CESM2)." *Journal of Advances in Modeling Earth Systems* (2020). <https://doi.org/10.1029/2019MS001882>.

EPA. *Draft Modeling Guidance for Demonstrating Attainment of Air Quality Goals for Ozone, PM2.5, and RegionalHaze*. Modeling guidance. United States Environmental Protection Agency. North Carollina: U.S. EPA, 2014. 10 July 2015. <http://www.epa.gov/ttn/scram/guidance/guide/Draft_O3-PM-RH_Modeling_Guidance-2014.pdf>.

—. *https://www3.epa.gov/ttn/emc/cem.html*. 2016. 16 August 2016. <https://www3.epa.gov/ttn/emc/cem.html>.

—. *Modeling Guidance for Demonstrating Attainment of Air Quality Goals for Ozone, PM2.5, and Regional Haze*. 29 11 2018. <https://www.epa.gov/scram/sip-modeling-guidance-documents>.

—. "NOx Substitution Guidance, available at https://www3.epa.gov/ttn/naaqs/aqmguide/collection/cp2/19931201_oaqps_nox_substitution_guidance.pdf." 1993.

—. "Technical Support Document for 2008 Ozone NAAQS Designation." 2008. <https://19january2017snapshot.epa.gov/www3/region9/air/ozone/pdf/R9_CA_NevadaCounty_FINAL.pdf>.

EPA, U.S. "Ozone Designations - 2015 Standards accessible at https://www.epa.gov/sites/default/files/2018-05/documents/ca_tsd_combined_final_0.pdf." 2017. Jan 2022. <https://www.epa.gov/sites/default/files/2018-05/documents/ca_tsd_combined_final_0.pdf>.

ERG. "2014 Northern Baja California Emissions Inventory Project." 2019.

Fast, J. D., et al. "Transport and mixing patterns over Central California during the carbonaceous aerosol and radiative effects study (CARES)." *Atmospheric Chemistry and Physics* 12 (2012): 1759-1783.

Fosberg, M.A. and M.J. Schroeder. "Marine air penetration in Central California." *Journal of Applied Meteorology* 5 (1966): 573-589.

Fujita, E. M., et al. *Field study plan for the Central California Ozone Study*. 1999.

Gkatzelis, G, et al. "Identifying Volatile Chemical Product Tracer Compounds in U.S. Cities." *Environmental Science & Technology* 55.1 (2021): 188-199.

Gong, P., N. Clinton and R. T. Y. a. S. J. Pu. *Extension and input refinement to the ARB wildland fire emissions estimation model Final report, contract number 00-729*. Sacramento, CA: Air Resources Board, 2003.

He, H., X-Z. Liang and D. J. Wuebbles. "Effects of emissions change, climate change and long-range transport on regional modeling of future U.S. particulate matter pollution and speciation." *Atmospheric Environment* 2018: 166-176. <https://www.sciencedirect.com/science/article/pii/S135223101830092X>.

Heuss, J. M., D. F. Kahlbaum and G. T. Wolff. "Weekday/Weekend Ozone Differences: What Can We Learn from Them?" *Journal of the Air & Waste Management Association* 53.7 (2003): 772-788.

Hu, J., et al. "Mobile Source and Livestock Feed Contributions to Regional Ozone Formation in Central California." *Environmental Science and Technology* 46 (2012): 2781-2789.

Imperial. " Imperial County 2017 State Implementation Plan for the 2008 8-Hour Ozone Standard, available at: https://ww3.arb.ca.gov/planning/sip/planarea/imperial/2017o3sip_final.pdf ." 2017.

—. " Imperial County 2018 Annual Particulate Matter Less than 2.5 Microns in Diameter State Implementation Plan, available at: https://ww3.arb.ca.gov/planning/sip/planarea/imperial/final_2018_ic_pm25_sip.pdf ." 2018.

Jeanne, P., Saah, D., Esperanza, A., Bytnerowicz, A., Fraczek, W., and Cisneros, R. "Ozone Distribution in Remote Ecologically Vulnerable Terrain of the Southern Sierra Nevada, Ca." *Environmental Pollution* 182 (2013): 343-56.

Jin, L., et al. "Seasonal versus episodic performance evaluation for an Eulerian photochemical air quality model." *Journal of Geophysical Research: Atmospheres* (2010): 115, D09302.

—. "Sensitivity analysis of ozone formation and transport for a central California air pollution episode." *Environmental Science and Technology* (2008): 3683-3689.

Kelly, J. T., et al. "Fine-scale simulation of ammonium and nitrate over the South Coast Air Basin and San Joaquin Valley of California during CalNex-2010." *Journal of Geophysical Research* 119 (2014): 3600-3614.

Kelly, J.T., et al. "Fine-scale simulation of ammonium and nitrate over the South Coast Air Basin and San Joaquin Valley of California during CalNex-2010." *Journal of Geophysical Research: Atmosphere* (2014): 3600–3614.

—. "Simulating particle size distributions over California and impact on lung deposition fraction." *Aerosol Science and Technology* (2010): 148-162.

Kulkarni, S., et al. "An extended approach to calculate the ozone relative response factors used in the attainment demonstration for the National Ambient Air Quality Standards." *Journal of the Air and Waste Management Association* (2014): 1204-1213.

Kwok, Roger. *Meteorology-adjusted Temporal Profiles for Agricultural and Residential Wood Combustion Sectors Using Smoke Gentpro Utility Program*. Sacramento: INTERNAL DRAFT CARB, 2016.

—. *Modeling Plume Rise of Ocean-going Vessel Emissions*. Sacramento: INTERNAL DRAFT CARB, 2015.

LaFranchi, B. W., A. H. Goldstein and R. C and Cohen. "Observations of the temperature dependent response of ozone to NOx reductions in the Sacramento, CA urban plume." *Atmospheric Chemistry and Physics* (2011): 6945-6960.

Lamarque, J.-F., et al. "CAM-chem: description and evaluation of interactive atmospheric chemistry in the Community Earth System Model." *Geoscientific Model Development* (2012): 369-411.

Lehrman, D. "Characterization of the 2000 Measurement Period." Interim Report prepared for California Air Resources Board. 2001.

Lehrman, D., et al. "Characterization of the CCOS 2000 measurement period." Final Report prepared for California Air Resources Board. 2004.

Lin, M., et al. "Springtime high surface ozone events over the western United States: Quantifying the role of stratospheric." *Journal of Geophysical Research* (2012): D00V22, doi:10.1029/2012JD018151.

Livingstone, P.L., et al. "Simulating PM concentration during a winter episode in a subtropical valley: Sensitivity simulations and evaluation methods." *Atmospheric Environment* (2009): 5971-5977.

Mills, S., S. Weiss and C. Liang. "VIIRS day/night band (DNB) stray light characterization and correction." *SPIE Proceedings* (2013): Vol. 8866.

Pun, B. K., J. F. Loius and C. Seigneur. "A conceptual model of ozone formation in the San Joaquin Valley." CP049-1-98. 2008.

Pun, B.K., R.T.F. Balmori and C. Seigneur. "Modeling wintertime particulate matter formation in central California." *Atmospheric Environment* (2009): 402-409.

Pusede, S. E. and R. C. Cohen. "On the observed response of ozone to NOx and VOC reactivity reductions in San Joaquin Valley California 1995–present." *Atmospheric Chemistry and Physics* (2012): 8323-8339.

Pusede, S. E., et al. "On the temperature dependence of organic reactivity, nitrogen oxides, ozone production, and the impact of emission controls in San Joaquin Valley, California." *Atmospheric Chemistry and Physics* (2014): 3373-3395.

Ricardo, C., et al. "Ozone, Nitric Acid, and Ammonia Air Pollution Is Unhealthy for People and Ecosystems in Southern Sierra Nevada, California." *Environmental Pollution* 158.10 (2010): 3261-71.

Sacramento. "Sacramento Regional 2008 NAAQS 8-Hour Ozone Attainment And Reasonable Further Progress Plan, available at http://www.airquality.org/ProgramCoordination/Documents/Sac%20Regional%202008%20NAAQS%20Attainment%20and%20RFP%20Plan.pdf." 2017.

Seinfeld, J. H. and S. N. Pandis. *Atmospheric Chemistry and Physics: From Air Pollution to Climate Change*. Ed. 1. New York: J. Wiley, 1998.

Sen, Zekai. "2.8.1 Delaney, Varoni, and Thiessen Polygons." *Spatial Modeling Principles in Earth Sciences*. Springer, 2016. 57.

Shahrokhishahraki, N., et al. "High-resolution modeling of gaseous air pollutants over Tehran and validation with surface and satellite data." *Atmospheric Environment* 2022. <https://www.sciencedirect.com/science/article/pii/S1352231021007032>.

Shearer, S.M, et al. "Comparison of SAPRC99 and SAPRC07 mechanisms in photochemical modeling for central California." *Atmospheric Environment* (2012): 205-216.

Sillman, S. "The relation between ozone, NOx and hydrocarbons in urban and polluted rural environments." *Atmospheric Environment* 33.12 (1999): 1821-1845.

Simon, H., K. R. Baker and S. Phillips. "Compilation and interpretation of photochemical model performance statistics published between 2006 and 2012." *Atmospheric Environment* 61 (2012): 124-139.

SJV. " 2018 PM2.5 Plan for the San Joaquin Valley, available at: http://valleyair.org/pmplans/ ." 2018.

—. "2008 PM2.5 Plan, available at: http://www.valleyair.org/Air_Quality_Plans/AQ_Proposed_PM25_2008.htm." 2008.

—. "2012 PM2.5 Plan, available at: http://www.valleyair.org/Air_Quality_Plans/PM25Plans2012.htm ." 2012.

—. "2013 Plan for the Revoked 1-Hour Ozone Standard, available at: http://valleyair.org/Air_Quality_Plans/Ozone-OneHourPlan-2013.htm ." 2013.

—. "2016 Moderate Area Plan for the 2012 PM2.5 Standard, available at: http://www.valleyair.org/Air_Quality_Plans/docs/PM25-2016/2016-Plan.pdf ." 2016a.

—. "2016 Plan for the 2008 8-Hour Ozone Standard, available at: http://valleyair.org/Air_Quality_Plans/Ozone-Plan-2016.htm ." 2016b.

Skamarock, W. C., et al. *Description ofthe Advanced Research WRF version 4,Rep. NCAR/TN-475++STR,Natl. Cent. for Atmos. Res.* Boulder, Colo., 2008.

SouthCoast. "Final 2012 Air Quality Management Plan, available at: http://www.aqmd.gov/home/air-quality/clean-air-plans/air-quality-mgt-plan/final-2012-air-quality-management-plan ." 2012.

—. "Final 2016 Air Quality Management Plan, available at: http://www.aqmd.gov/docs/default-source/clean-air-plans/air-quality-management-plans/2016-air-quality-management-plan/final-2016-aqmp/cover-and-opening.pdf?sfvrsn=6." 2016.

Stein, A.F., et al. " NOAA's HYSPLIT atmospheric transport and dispersion modeling system." *Bulletin of the American Meteorological Society* (2015): 2059-2077.

Tonse, S. R., et al. "A process-analysis based study of the ozone weekend effect." *Atmospheric Environment* (2008): 7728-7736.

UNC Chapel Hill - The Institute for the Environment. "SMOKE v4.0 User’s Manual." 30 September 2016. 07 02 2020. <https://www.cmascenter.org/smoke/documentation/4.0/manual_smokev40.pdf>.

Van Ooy, D.J. and J.J. Carroll. "The spatial variation of ozone climatology on the western slope of the Sierra Nevada." *Atmospheric Environment* (1995): 1319-1330.

Ventura. "Final 2016 Ventura County Air Quality Management Plan, available at: http://www.vcapcd.org/pubs/Planning/AQMP/2016/Final/Final-2016-Ventura-County-AQMP.pdf ." 2016.

Vijayaraghavan, K., P. Karamchadania and C. Seigneur. "Plume-in-grid modeling of summer air pollution in Central California." *Atmospheric Environment* (2006): 5097-5109.

Wang, P., et al. "Ground-level ozone simulation using ensemble WRF/Chem predictions over the Southeast United States." *Chemosphere* 2022. <https://www.sciencedirect.com/science/article/pii/S0045653521029003>.

WesternMojave. "2016 8-Hour Ozone SIP: Western Mojave Desert Nonattainment Area, available at: https://ww3.arb.ca.gov/planning/sip/planarea/mojavesedsip.htm#2016." 2016.

WesternNevada. "Western Nevada County 8-hour Ozone Attainment Plan, available at: https://ww3.arb.ca.gov/planning/sip/planarea/wncsip.htm." 2018.

Wu, Shenglun, et al. "Direct measurements of ozone response to emissions perturbations in California." *Atompheric Chemistry and Phtsics* (2022): 4929-4949. <https://acp.copernicus.org/articles/22/4929/2022/acp-22-4929-2022.pdf>.

Yan, F., et al. "Revealing the modulation of boundary conditions and governing processes on ozone formation over northern China in June 2017." *Environmental Pollution* 272 (2021). <https://www.sciencedirect.com/science/article/pii/S0269749120366884>.

Yienger, J. J. and H. Levy II. "Empirical model of global soil-biogenic NOχ emissions." *Journal of Geophysical Research: Atmospheres* (1995): 11447-11464.

Zhang, Y., et al. "Fine scale modeling of wintertime aerosol mass, number, and size distributions in Central California." *Journal of Geophysical Research* (2010): D15207, doi:10.1029/2009JD012950.

Zhu, S., Horne, J. R., Kinnon, M. M., Samuelsen, G. S., Dabdub, D. "Comprehensively assessing the drivers of future air quality in California." *Environment International* (2019): 386-398.

Sub-Appendix B.A: Day-of-week Redistribution Factors by Vehicle Type and County

The factors shown in Table B-27 and Table B-28 represent the “day-of-week” factors for a broad vehicle class: LD is Light-Duty, LM is Light- and Medium-Duty Trucks, and HH is Heavy Heavy-Duty Trucks.

Table B-27: Day-of-week adjustment for LD and LM vehicle class by county

County	Day of Week	LD	LM
El Dorado	Sunday	1.04	0.68
El Dorado	Monday	1.00	0.97
El Dorado	Tues/Wed/Thurs	1.00	1.00
El Dorado	Friday	1.20	1.01
El Dorado	Saturday	1.15	0.76
El Dorado	Holiday	1.05	1.05
Placer	Sunday	1.07	0.55
Placer	Monday	1.05	1.00
Placer	Tues/Wed/Thurs	1.00	1.00
Placer	Friday	1.17	0.92
Placer	Saturday	1.16	0.62
Placer	Holiday	1.12	1.03
Sacramento	Sunday	0.77	0.49
Sacramento	Monday	0.96	0.95
Sacramento	Tues/Wed/Thurs	1.00	1.00
Sacramento	Friday	1.06	1.04
Sacramento	Saturday	0.88	0.62
Sacramento	Holiday	0.81	0.83
Solano	Sunday	1.01	0.59
Solano	Monday	0.98	0.95
Solano	Tues/Wed/Thurs	1.00	1.00
Solano	Friday	1.13	1.03
Solano	Saturday	1.09	0.72
Solano	Holiday	0.91	0.90
Sutter	Sunday	0.97	0.67
Sutter	Monday	0.99	0.98
Sutter	Tues/Wed/Thurs	1.00	1.00
Sutter	Friday	1.18	1.10
Sutter	Saturday	1.04	0.79
Sutter	Holiday	0.97	0.93
Yolo	Sunday	0.90	0.56
Yolo	Monday	0.97	0.95

County	Day of Week	LD	LM
Yolo	Tues/Wed/Thurs	1.00	1.00
Yolo	Friday	1.10	1.05
Yolo	Saturday	0.99	0.67
Yolo	Holiday	0.89	0.88

Table B-28: Day-of-week adjustment excerpt from July 1st to 7th for HH vehicle class by county

Date	Day of Week	El Dorado	Placer	Sacramento	Solano	Sutter	Yolo
7/1/2018	Sunday	0.56	0.89	0.68	0.57	0.60	0.40
7/2/2018	Monday	0.90	1.21	1.03	0.96	0.94	0.87
7/3/2018	Tuesday	1.00	1.14	0.91	1.02	1.00	0.74
7/4/2018	Holiday	0.98	0.85	0.68	0.61	0.92	0.59
7/5/2018	Thursday	1.00	1.13	1.01	0.90	1.00	0.95
7/6/2018	Friday	0.88	1.19	1.06	0.94	0.96	0.98
7/7/2018	Saturday	0.59	0.88	0.78	0.64	0.58	0.67

Sub Appendix B.B: Hour-of-day Profiles by Vehicle Type and County

The factors shown in the table below represent the different hourly profiles for different days of the week for each county for a broad vehicle class: LD is Light-Duty, LM is Light- and Medium-Duty Trucks, and HH is Heavy Heavy-Duty Trucks. Hourly profiles for LD, LM, and HH by day of week are shown in Table B-29, Table B-30, and Table B-31.

Table B-29: Hour-of-day profiles for LD and LM vehicle classes in El Dorado, Placer, and Sacramento Counties

Day of Week	Hour	El Dorado LD	El Dorado LM	Placer LD	Placer LM	Sacramento LD	Sacramento LM
Sunday	0	0.009	0.017	0.002	0.009	0.019	0.031
Sunday	1	0.005	0.012	0.001	0.002	0.013	0.025
Sunday	2	0.003	0.009	0.000	0.001	0.009	0.021
Sunday	3	0.002	0.008	0.000	0.000	0.007	0.019
Sunday	4	0.002	0.007	0.001	0.001	0.008	0.020
Sunday	5	0.003	0.010	0.002	0.007	0.011	0.023
Sunday	6	0.009	0.017	0.011	0.019	0.017	0.027
Sunday	7	0.023	0.028	0.031	0.035	0.025	0.033
Sunday	8	0.040	0.041	0.056	0.059	0.035	0.042
Sunday	9	0.062	0.060	0.075	0.072	0.049	0.052
Sunday	10	0.082	0.078	0.089	0.088	0.060	0.060
Sunday	11	0.094	0.089	0.099	0.104	0.066	0.063
Sunday	12	0.093	0.090	0.098	0.096	0.072	0.066
Sunday	13	0.091	0.085	0.093	0.093	0.074	0.067
Sunday	14	0.086	0.079	0.090	0.081	0.074	0.064
Sunday	15	0.081	0.074	0.088	0.076	0.072	0.061
Sunday	16	0.076	0.069	0.079	0.072	0.071	0.059
Sunday	17	0.067	0.061	0.066	0.059	0.068	0.056
Sunday	18	0.054	0.048	0.047	0.040	0.061	0.049
Sunday	19	0.043	0.038	0.033	0.031	0.053	0.042
Sunday	20	0.032	0.029	0.021	0.021	0.048	0.038
Sunday	21	0.022	0.023	0.012	0.015	0.040	0.032
Sunday	22	0.014	0.016	0.005	0.012	0.029	0.027
Sunday	23	0.007	0.011	0.002	0.006	0.019	0.023
Monday	0	0.003	0.010	0.000	0.001	0.009	0.018
Monday	1	0.001	0.006	0.000	0.000	0.005	0.015
Monday	2	0.000	0.004	0.000	0.000	0.004	0.015
Monday	3	0.000	0.004	0.000	0.000	0.006	0.018
Monday	4	0.001	0.006	0.000	0.000	0.013	0.026
Monday	5	0.003	0.013	0.002	0.008	0.029	0.040
Monday	6	0.015	0.029	0.025	0.038	0.052	0.057
Monday	7	0.044	0.052	0.060	0.065	0.071	0.066
Monday	8	0.055	0.061	0.078	0.083	0.066	0.064
Monday	9	0.066	0.068	0.077	0.079	0.056	0.059
Monday	10	0.073	0.073	0.079	0.080	0.052	0.057
Monday	11	0.082	0.078	0.084	0.086	0.053	0.058

Day of Week	Hour	El Dorado LD	El Dorado LM	Placer LD	Placer LM	Sacramento LD	Sacramento LM
Monday	12	0.085	0.080	0.084	0.086	0.056	0.059
Monday	13	0.083	0.080	0.085	0.082	0.057	0.059
Monday	14	0.083	0.078	0.086	0.086	0.062	0.060
Monday	15	0.085	0.077	0.091	0.083	0.070	0.064
Monday	16	0.085	0.075	0.095	0.080	0.076	0.063
Monday	17	0.077	0.066	0.074	0.063	0.073	0.057
Monday	18	0.055	0.048	0.042	0.035	0.056	0.044
Monday	19	0.040	0.034	0.020	0.021	0.040	0.031
Monday	20	0.029	0.024	0.011	0.014	0.032	0.024
Monday	21	0.018	0.017	0.005	0.007	0.028	0.019
Monday	22	0.011	0.011	0.002	0.003	0.021	0.015
Monday	23	0.005	0.007	0.000	0.001	0.014	0.011
Tues/Wed/Thurs	0	0.002	0.008	0.000	0.000	0.008	0.018
Tues/Wed/Thurs	1	0.001	0.005	0.000	0.000	0.005	0.015
Tues/Wed/Thurs	2	0.000	0.003	0.000	0.000	0.004	0.015
Tues/Wed/Thurs	3	0.000	0.002	0.000	0.000	0.006	0.017
Tues/Wed/Thurs	4	0.001	0.004	0.000	0.000	0.012	0.024
Tues/Wed/Thurs	5	0.002	0.009	0.000	0.002	0.027	0.038
Tues/Wed/Thurs	6	0.014	0.027	0.020	0.040	0.052	0.057
Tues/Wed/Thurs	7	0.044	0.053	0.060	0.066	0.071	0.066
Tues/Wed/Thurs	8	0.053	0.061	0.077	0.079	0.066	0.063
Tues/Wed/Thurs	9	0.062	0.067	0.070	0.080	0.056	0.059
Tues/Wed/Thurs	10	0.068	0.071	0.072	0.078	0.051	0.057
Tues/Wed/Thurs	11	0.076	0.076	0.079	0.082	0.052	0.057
Tues/Wed/Thurs	12	0.081	0.081	0.082	0.083	0.054	0.058
Tues/Wed/Thurs	13	0.081	0.080	0.080	0.082	0.056	0.059
Tues/Wed/Thurs	14	0.082	0.079	0.085	0.082	0.061	0.061
Tues/Wed/Thurs	15	0.085	0.078	0.092	0.081	0.070	0.064
Tues/Wed/Thurs	16	0.087	0.077	0.099	0.083	0.075	0.063
Tues/Wed/Thurs	17	0.082	0.070	0.082	0.067	0.073	0.057
Tues/Wed/Thurs	18	0.058	0.049	0.047	0.039	0.059	0.046
Tues/Wed/Thurs	19	0.044	0.036	0.025	0.025	0.041	0.033
Tues/Wed/Thurs	20	0.032	0.026	0.015	0.016	0.034	0.026
Tues/Wed/Thurs	21	0.023	0.019	0.009	0.009	0.030	0.021
Tues/Wed/Thurs	22	0.014	0.012	0.004	0.004	0.022	0.016
Tues/Wed/Thurs	23	0.007	0.008	0.001	0.002	0.015	0.012
Friday	0	0.003	0.009	0.000	0.000	0.009	0.019
Friday	1	0.001	0.006	0.000	0.000	0.005	0.016
Friday	2	0.000	0.004	0.000	0.000	0.004	0.016

Day of Week	Hour	El Dorado LD	El Dorado LM	Placer LD	Placer LM	Sacramento LD	Sacramento LM
Friday	3	0.000	0.003	0.000	0.000	0.006	0.017
Friday	4	0.001	0.005	0.000	0.000	0.011	0.024
Friday	5	0.002	0.009	0.000	0.002	0.024	0.036
Friday	6	0.011	0.024	0.014	0.035	0.045	0.053
Friday	7	0.035	0.047	0.048	0.059	0.063	0.063
Friday	8	0.044	0.056	0.064	0.074	0.059	0.061
Friday	9	0.054	0.063	0.065	0.077	0.052	0.058
Friday	10	0.061	0.068	0.068	0.081	0.050	0.057
Friday	11	0.070	0.075	0.075	0.084	0.053	0.059
Friday	12	0.075	0.079	0.079	0.083	0.056	0.060
Friday	13	0.078	0.078	0.079	0.081	0.058	0.060
Friday	14	0.081	0.079	0.085	0.082	0.063	0.062
Friday	15	0.084	0.079	0.090	0.087	0.070	0.063
Friday	16	0.084	0.076	0.091	0.080	0.072	0.060
Friday	17	0.078	0.067	0.079	0.063	0.069	0.055
Friday	18	0.063	0.053	0.054	0.040	0.060	0.046
Friday	19	0.052	0.039	0.035	0.025	0.046	0.035
Friday	20	0.042	0.030	0.026	0.017	0.038	0.026
Friday	21	0.035	0.023	0.021	0.013	0.035	0.022
Friday	22	0.027	0.017	0.016	0.010	0.029	0.018
Friday	23	0.018	0.011	0.010	0.007	0.020	0.013
Saturday	0	0.008	0.017	0.003	0.008	0.016	0.027
Saturday	1	0.004	0.011	0.000	0.001	0.011	0.022
Saturday	2	0.002	0.007	0.000	0.000	0.008	0.020
Saturday	3	0.001	0.006	0.000	0.000	0.007	0.019
Saturday	4	0.001	0.006	0.000	0.000	0.009	0.022
Saturday	5	0.002	0.008	0.001	0.004	0.014	0.027
Saturday	6	0.009	0.018	0.009	0.021	0.023	0.035
Saturday	7	0.023	0.030	0.031	0.044	0.034	0.044
Saturday	8	0.037	0.042	0.053	0.059	0.045	0.052
Saturday	9	0.054	0.058	0.066	0.071	0.054	0.059
Saturday	10	0.070	0.071	0.076	0.081	0.061	0.063
Saturday	11	0.081	0.079	0.083	0.083	0.066	0.065
Saturday	12	0.085	0.081	0.086	0.085	0.068	0.065
Saturday	13	0.084	0.080	0.085	0.084	0.068	0.064
Saturday	14	0.082	0.075	0.086	0.081	0.068	0.061
Saturday	15	0.080	0.075	0.090	0.081	0.067	0.059
Saturday	16	0.079	0.072	0.086	0.081	0.067	0.056
Saturday	17	0.072	0.068	0.074	0.063	0.064	0.052

Day of Week	Hour	El Dorado LD	El Dorado LM	Placer LD	Placer LM	Sacramento LD	Sacramento LM
Saturday	18	0.062	0.054	0.054	0.045	0.057	0.045
Saturday	19	0.050	0.043	0.039	0.031	0.048	0.037
Saturday	20	0.040	0.034	0.029	0.026	0.042	0.031
Saturday	21	0.032	0.027	0.022	0.020	0.040	0.029
Saturday	22	0.024	0.021	0.016	0.016	0.036	0.026
Saturday	23	0.016	0.016	0.009	0.013	0.026	0.020
Holiday	0	0.007	0.013	0.001	0.003	0.013	0.023
Holiday	1	0.004	0.010	0.000	0.000	0.008	0.019
Holiday	2	0.002	0.006	0.000	0.000	0.006	0.018
Holiday	3	0.001	0.005	0.000	0.000	0.006	0.019
Holiday	4	0.001	0.006	0.000	0.000	0.010	0.023
Holiday	5	0.002	0.010	0.001	0.004	0.019	0.032
Holiday	6	0.010	0.022	0.012	0.026	0.031	0.041
Holiday	7	0.031	0.040	0.039	0.050	0.042	0.049
Holiday	8	0.049	0.052	0.068	0.077	0.048	0.054
Holiday	9	0.066	0.067	0.076	0.088	0.052	0.057
Holiday	10	0.079	0.079	0.088	0.084	0.057	0.060
Holiday	11	0.087	0.087	0.095	0.089	0.063	0.065
Holiday	12	0.086	0.086	0.093	0.086	0.067	0.065
Holiday	13	0.084	0.087	0.089	0.093	0.068	0.066
Holiday	14	0.084	0.081	0.087	0.083	0.069	0.065
Holiday	15	0.082	0.073	0.090	0.081	0.070	0.063
Holiday	16	0.081	0.073	0.090	0.089	0.069	0.060
Holiday	17	0.073	0.066	0.073	0.061	0.066	0.054
Holiday	18	0.056	0.050	0.044	0.038	0.058	0.046
Holiday	19	0.042	0.033	0.025	0.020	0.049	0.036
Holiday	20	0.031	0.024	0.015	0.015	0.043	0.030
Holiday	21	0.021	0.016	0.009	0.007	0.037	0.024
Holiday	22	0.012	0.010	0.004	0.003	0.029	0.019
Holiday	23	0.007	0.006	0.002	0.001	0.020	0.014

Table B-30: Hour-of-day profiles for LD and LM vehicle classes in Solano, Sutter, and Yolo Counties

Day of Week	Hour	Solano LD	Solano LM	Sutter LD	Sutter LM	Yolo LD	Yolo LM
Sunday	0	0.017	0.037	0.013	0.020	0.016	0.026
Sunday	1	0.011	0.032	0.008	0.016	0.011	0.019
Sunday	2	0.009	0.030	0.006	0.013	0.008	0.017

Day of Week	Hour	Solano LD	Solano LM	Sutter LD	Sutter LM	Yolo LD	Yolo LM
Sunday	3	0.007	0.027	0.005	0.012	0.006	0.015
Sunday	4	0.007	0.028	0.005	0.012	0.007	0.016
Sunday	5	0.010	0.029	0.008	0.015	0.011	0.020
Sunday	6	0.016	0.032	0.013	0.020	0.016	0.025
Sunday	7	0.021	0.035	0.022	0.028	0.023	0.031
Sunday	8	0.031	0.041	0.034	0.041	0.034	0.041
Sunday	9	0.046	0.048	0.048	0.055	0.048	0.054
Sunday	10	0.059	0.053	0.064	0.068	0.060	0.063
Sunday	11	0.067	0.055	0.075	0.075	0.067	0.067
Sunday	12	0.069	0.055	0.082	0.079	0.071	0.070
Sunday	13	0.070	0.055	0.084	0.079	0.072	0.070
Sunday	14	0.071	0.053	0.084	0.077	0.073	0.069
Sunday	15	0.071	0.052	0.082	0.073	0.073	0.067
Sunday	16	0.071	0.051	0.079	0.068	0.072	0.063
Sunday	17	0.070	0.051	0.072	0.062	0.070	0.059
Sunday	18	0.066	0.048	0.060	0.052	0.063	0.051
Sunday	19	0.060	0.046	0.050	0.043	0.057	0.044
Sunday	20	0.055	0.043	0.041	0.035	0.051	0.038
Sunday	21	0.045	0.039	0.031	0.026	0.042	0.032
Sunday	22	0.032	0.033	0.021	0.019	0.030	0.025
Sunday	23	0.020	0.028	0.013	0.015	0.019	0.020
Monday	0	0.010	0.026	0.008	0.014	0.010	0.018
Monday	1	0.006	0.025	0.005	0.012	0.006	0.015
Monday	2	0.005	0.024	0.004	0.012	0.005	0.014
Monday	3	0.006	0.026	0.006	0.014	0.007	0.016
Monday	4	0.015	0.032	0.011	0.019	0.016	0.025
Monday	5	0.037	0.043	0.023	0.030	0.032	0.040
Monday	6	0.050	0.051	0.042	0.047	0.048	0.052
Monday	7	0.061	0.058	0.060	0.061	0.066	0.065
Monday	8	0.056	0.057	0.059	0.062	0.064	0.064
Monday	9	0.054	0.056	0.056	0.061	0.057	0.062
Monday	10	0.055	0.058	0.058	0.064	0.055	0.061
Monday	11	0.056	0.057	0.062	0.066	0.056	0.062
Monday	12	0.057	0.058	0.066	0.068	0.058	0.062
Monday	13	0.058	0.057	0.067	0.067	0.059	0.061
Monday	14	0.064	0.057	0.070	0.069	0.062	0.062
Monday	15	0.069	0.056	0.073	0.069	0.068	0.063
Monday	16	0.071	0.054	0.075	0.067	0.073	0.062
Monday	17	0.070	0.050	0.073	0.061	0.072	0.057

Day of Week	Hour	Solano LD	Solano LM	Sutter LD	Sutter LM	Yolo LD	Yolo LM
Monday	18	0.054	0.041	0.056	0.046	0.053	0.043
Monday	19	0.042	0.032	0.040	0.031	0.039	0.030
Monday	20	0.035	0.026	0.031	0.022	0.032	0.023
Monday	21	0.029	0.022	0.025	0.017	0.027	0.018
Monday	22	0.023	0.018	0.017	0.012	0.021	0.014
Monday	23	0.016	0.016	0.012	0.009	0.014	0.011
Tues/Wed/Thurs	0	0.009	0.025	0.008	0.014	0.009	0.017
Tues/Wed/Thurs	1	0.005	0.023	0.004	0.011	0.006	0.014
Tues/Wed/Thurs	2	0.004	0.023	0.004	0.011	0.005	0.014
Tues/Wed/Thurs	3	0.005	0.025	0.005	0.013	0.006	0.016
Tues/Wed/Thurs	4	0.013	0.030	0.010	0.018	0.014	0.023
Tues/Wed/Thurs	5	0.035	0.042	0.022	0.029	0.029	0.037
Tues/Wed/Thurs	6	0.050	0.050	0.042	0.047	0.046	0.051
Tues/Wed/Thurs	7	0.061	0.057	0.060	0.061	0.066	0.065
Tues/Wed/Thurs	8	0.056	0.056	0.060	0.062	0.065	0.064
Tues/Wed/Thurs	9	0.053	0.056	0.055	0.060	0.057	0.062
Tues/Wed/Thurs	10	0.052	0.057	0.056	0.061	0.053	0.061
Tues/Wed/Thurs	11	0.052	0.057	0.059	0.064	0.054	0.061
Tues/Wed/Thurs	12	0.054	0.057	0.061	0.065	0.056	0.061
Tues/Wed/Thurs	13	0.057	0.057	0.064	0.066	0.058	0.061
Tues/Wed/Thurs	14	0.064	0.058	0.068	0.068	0.062	0.062
Tues/Wed/Thurs	15	0.070	0.058	0.073	0.069	0.069	0.063
Tues/Wed/Thurs	16	0.073	0.056	0.075	0.067	0.074	0.062
Tues/Wed/Thurs	17	0.072	0.052	0.074	0.063	0.073	0.058
Tues/Wed/Thurs	18	0.058	0.043	0.059	0.048	0.056	0.045
Tues/Wed/Thurs	19	0.046	0.034	0.043	0.034	0.041	0.032
Tues/Wed/Thurs	20	0.038	0.028	0.035	0.025	0.034	0.025
Tues/Wed/Thurs	21	0.032	0.023	0.029	0.019	0.029	0.020
Tues/Wed/Thurs	22	0.025	0.018	0.020	0.013	0.022	0.015
Tues/Wed/Thurs	23	0.016	0.015	0.013	0.009	0.015	0.011
Friday	0	0.009	0.025	0.007	0.014	0.009	0.017
Friday	1	0.006	0.024	0.005	0.011	0.006	0.014
Friday	2	0.005	0.024	0.004	0.011	0.005	0.014
Friday	3	0.005	0.025	0.005	0.012	0.006	0.015
Friday	4	0.011	0.030	0.008	0.016	0.012	0.022
Friday	5	0.027	0.040	0.017	0.026	0.024	0.034
Friday	6	0.039	0.047	0.033	0.040	0.038	0.047
Friday	7	0.050	0.053	0.049	0.054	0.054	0.059
Friday	8	0.048	0.054	0.051	0.057	0.055	0.059

Day of Week	Hour	Solano LD	Solano LM	Sutter LD	Sutter LM	Yolo LD	Yolo LM
Friday	9	0.048	0.055	0.050	0.057	0.051	0.059
Friday	10	0.052	0.056	0.054	0.061	0.052	0.060
Friday	11	0.056	0.058	0.060	0.066	0.056	0.062
Friday	12	0.059	0.058	0.063	0.067	0.059	0.063
Friday	13	0.063	0.058	0.066	0.068	0.062	0.064
Friday	14	0.067	0.058	0.070	0.070	0.066	0.064
Friday	15	0.069	0.057	0.073	0.070	0.070	0.063
Friday	16	0.070	0.054	0.074	0.067	0.071	0.061
Friday	17	0.067	0.050	0.072	0.063	0.069	0.057
Friday	18	0.061	0.044	0.063	0.051	0.060	0.047
Friday	19	0.054	0.037	0.050	0.039	0.049	0.036
Friday	20	0.047	0.031	0.041	0.029	0.041	0.028
Friday	21	0.039	0.025	0.037	0.023	0.036	0.023
Friday	22	0.030	0.020	0.030	0.017	0.029	0.018
Friday	23	0.021	0.016	0.019	0.011	0.019	0.013
Saturday	0	0.014	0.031	0.013	0.019	0.014	0.024
Saturday	1	0.009	0.028	0.008	0.015	0.009	0.019
Saturday	2	0.007	0.027	0.006	0.014	0.008	0.017
Saturday	3	0.006	0.026	0.006	0.013	0.007	0.016
Saturday	4	0.008	0.028	0.007	0.014	0.009	0.019
Saturday	5	0.014	0.031	0.011	0.018	0.014	0.025
Saturday	6	0.022	0.037	0.019	0.026	0.023	0.033
Saturday	7	0.032	0.042	0.032	0.038	0.034	0.044
Saturday	8	0.044	0.049	0.045	0.051	0.046	0.055
Saturday	9	0.056	0.054	0.057	0.062	0.057	0.064
Saturday	10	0.065	0.057	0.067	0.071	0.065	0.070
Saturday	11	0.068	0.058	0.074	0.076	0.069	0.071
Saturday	12	0.067	0.057	0.075	0.075	0.069	0.068
Saturday	13	0.066	0.056	0.075	0.074	0.069	0.065
Saturday	14	0.066	0.055	0.074	0.071	0.068	0.063
Saturday	15	0.066	0.054	0.072	0.068	0.067	0.060
Saturday	16	0.066	0.053	0.070	0.064	0.066	0.056
Saturday	17	0.065	0.050	0.066	0.057	0.063	0.052
Saturday	18	0.058	0.046	0.056	0.047	0.057	0.045
Saturday	19	0.050	0.040	0.046	0.037	0.048	0.035
Saturday	20	0.045	0.036	0.040	0.030	0.042	0.030
Saturday	21	0.041	0.033	0.035	0.025	0.039	0.027
Saturday	22	0.035	0.029	0.028	0.019	0.034	0.023
Saturday	23	0.026	0.023	0.020	0.014	0.024	0.018

Day of Week	Hour	Solano LD	Solano LM	Sutter LD	Sutter LM	Yolo LD	Yolo LM
Holiday	0	0.013	0.029	0.010	0.016	0.012	0.022
Holiday	1	0.008	0.027	0.006	0.013	0.008	0.017
Holiday	2	0.005	0.025	0.004	0.012	0.006	0.015
Holiday	3	0.005	0.026	0.005	0.013	0.006	0.017
Holiday	4	0.008	0.028	0.008	0.016	0.011	0.021
Holiday	5	0.018	0.034	0.014	0.023	0.019	0.030
Holiday	6	0.025	0.040	0.025	0.033	0.027	0.038
Holiday	7	0.032	0.045	0.036	0.044	0.037	0.046
Holiday	8	0.041	0.050	0.046	0.053	0.046	0.054
Holiday	9	0.051	0.055	0.054	0.059	0.053	0.059
Holiday	10	0.062	0.060	0.065	0.069	0.061	0.065
Holiday	11	0.068	0.063	0.074	0.074	0.067	0.069
Holiday	12	0.070	0.061	0.077	0.074	0.069	0.068
Holiday	13	0.071	0.062	0.076	0.074	0.069	0.068
Holiday	14	0.072	0.060	0.075	0.073	0.070	0.066
Holiday	15	0.068	0.056	0.074	0.070	0.069	0.065
Holiday	16	0.066	0.054	0.072	0.066	0.067	0.060
Holiday	17	0.064	0.050	0.068	0.059	0.064	0.055
Holiday	18	0.058	0.042	0.057	0.049	0.057	0.046
Holiday	19	0.051	0.037	0.047	0.036	0.050	0.036
Holiday	20	0.047	0.031	0.039	0.029	0.044	0.029
Holiday	21	0.042	0.026	0.030	0.020	0.039	0.023
Holiday	22	0.033	0.022	0.023	0.015	0.030	0.018
Holiday	23	0.022	0.018	0.015	0.010	0.020	0.014

Table B-31: Hour-of-day profiles excerpt from July 1st to 7th for HH vehicle class by county

Date	Hour	El Dorado	Placer	Sacramento	Solano	Sutter	Yolo
7/1/2018	0	0.025	0.019	0.023	0.018	0.031	0.025
7/1/2018	1	0.016	0.012	0.018	0.011	0.028	0.017
7/1/2018	2	0.012	0.009	0.015	0.010	0.026	0.015
7/1/2018	3	0.009	0.009	0.013	0.007	0.025	0.015
7/1/2018	4	0.009	0.010	0.016	0.010	0.025	0.018
7/1/2018	5	0.016	0.016	0.020	0.013	0.027	0.023
7/1/2018	6	0.029	0.028	0.028	0.020	0.030	0.028
7/1/2018	7	0.038	0.039	0.035	0.029	0.034	0.037
7/1/2018	8	0.045	0.052	0.044	0.038	0.040	0.043
7/1/2018	9	0.054	0.067	0.053	0.051	0.046	0.053
7/1/2018	10	0.064	0.068	0.062	0.061	0.052	0.059

Date	Hour	El Dorado	Placer	Sacramento	Solano	Sutter	Yolo
7/1/2018	11	0.071	0.078	0.064	0.067	0.055	0.059
7/1/2018	12	0.072	0.071	0.066	0.069	0.058	0.062
7/1/2018	13	0.069	0.069	0.068	0.070	0.058	0.069
7/1/2018	14	0.064	0.063	0.063	0.065	0.057	0.063
7/1/2018	15	0.062	0.061	0.062	0.067	0.057	0.057
7/1/2018	16	0.060	0.059	0.060	0.066	0.055	0.057
7/1/2018	17	0.056	0.055	0.054	0.062	0.053	0.056
7/1/2018	18	0.050	0.051	0.052	0.062	0.049	0.051
7/1/2018	19	0.044	0.048	0.048	0.052	0.045	0.052
7/1/2018	20	0.039	0.041	0.044	0.047	0.042	0.043
7/1/2018	21	0.038	0.034	0.037	0.043	0.039	0.039
7/1/2018	22	0.032	0.024	0.031	0.035	0.036	0.030
7/1/2018	23	0.026	0.018	0.025	0.026	0.033	0.027
7/2/2018	0	0.009	0.012	0.013	0.011	0.027	0.013
7/2/2018	1	0.004	0.010	0.012	0.009	0.025	0.011
7/2/2018	2	0.002	0.012	0.012	0.010	0.025	0.011
7/2/2018	3	0.002	0.014	0.015	0.014	0.027	0.018
7/2/2018	4	0.003	0.018	0.024	0.028	0.030	0.030
7/2/2018	5	0.014	0.030	0.038	0.041	0.036	0.047
7/2/2018	6	0.038	0.043	0.052	0.052	0.043	0.061
7/2/2018	7	0.050	0.050	0.059	0.057	0.048	0.064
7/2/2018	8	0.054	0.052	0.060	0.064	0.050	0.058
7/2/2018	9	0.059	0.061	0.059	0.067	0.050	0.062
7/2/2018	10	0.063	0.069	0.059	0.070	0.051	0.060
7/2/2018	11	0.066	0.074	0.062	0.069	0.053	0.060
7/2/2018	12	0.067	0.068	0.062	0.050	0.054	0.058
7/2/2018	13	0.068	0.065	0.061	0.059	0.054	0.056
7/2/2018	14	0.068	0.067	0.062	0.061	0.055	0.055
7/2/2018	15	0.070	0.060	0.060	0.054	0.055	0.057
7/2/2018	16	0.069	0.055	0.056	0.057	0.054	0.062
7/2/2018	17	0.066	0.052	0.052	0.052	0.052	0.055
7/2/2018	18	0.057	0.047	0.044	0.044	0.045	0.040
7/2/2018	19	0.051	0.040	0.035	0.037	0.039	0.034
7/2/2018	20	0.043	0.032	0.031	0.031	0.035	0.029
7/2/2018	21	0.037	0.028	0.028	0.025	0.032	0.022
7/2/2018	22	0.026	0.024	0.025	0.020	0.030	0.019
7/2/2018	23	0.014	0.018	0.020	0.017	0.030	0.019
7/3/2018	0	0.007	0.015	0.015	0.012	0.029	0.018
7/3/2018	1	0.003	0.013	0.012	0.010	0.027	0.011

Date	Hour	El Dorado	Placer	Sacramento	Solano	Sutter	Yolo
7/3/2018	2	0.002	0.012	0.012	0.012	0.027	0.012
7/3/2018	3	0.001	0.013	0.015	0.015	0.029	0.018
7/3/2018	4	0.002	0.019	0.023	0.028	0.031	0.029
7/3/2018	5	0.007	0.029	0.035	0.042	0.037	0.041
7/3/2018	6	0.038	0.042	0.052	0.053	0.044	0.055
7/3/2018	7	0.055	0.049	0.059	0.058	0.050	0.057
7/3/2018	8	0.060	0.052	0.059	0.058	0.051	0.050
7/3/2018	9	0.064	0.057	0.056	0.065	0.050	0.050
7/3/2018	10	0.065	0.063	0.057	0.064	0.051	0.050
7/3/2018	11	0.068	0.064	0.059	0.066	0.052	0.054
7/3/2018	12	0.070	0.067	0.059	0.066	0.053	0.053
7/3/2018	13	0.069	0.064	0.059	0.059	0.053	0.054
7/3/2018	14	0.069	0.065	0.059	0.055	0.053	0.057
7/3/2018	15	0.069	0.062	0.063	0.055	0.053	0.062
7/3/2018	16	0.068	0.057	0.061	0.051	0.052	0.076
7/3/2018	17	0.064	0.054	0.058	0.052	0.050	0.066
7/3/2018	18	0.054	0.045	0.048	0.042	0.044	0.051
7/3/2018	19	0.047	0.042	0.036	0.038	0.038	0.037
7/3/2018	20	0.041	0.033	0.031	0.031	0.034	0.034
7/3/2018	21	0.035	0.031	0.028	0.027	0.031	0.028
7/3/2018	22	0.027	0.029	0.025	0.023	0.029	0.020
7/3/2018	23	0.016	0.023	0.020	0.017	0.028	0.017
7/4/2018	0	0.015	0.025	0.025	0.020	0.028	0.027
7/4/2018	1	0.010	0.018	0.021	0.017	0.027	0.025
7/4/2018	2	0.006	0.015	0.019	0.015	0.026	0.021
7/4/2018	3	0.005	0.016	0.018	0.015	0.027	0.022
7/4/2018	4	0.003	0.018	0.022	0.018	0.029	0.028
7/4/2018	5	0.008	0.022	0.028	0.025	0.032	0.031
7/4/2018	6	0.029	0.035	0.036	0.036	0.036	0.041
7/4/2018	7	0.045	0.046	0.041	0.046	0.042	0.043
7/4/2018	8	0.052	0.059	0.047	0.050	0.048	0.050
7/4/2018	9	0.059	0.060	0.056	0.055	0.050	0.058
7/4/2018	10	0.066	0.065	0.060	0.058	0.053	0.063
7/4/2018	11	0.071	0.072	0.063	0.063	0.057	0.068
7/4/2018	12	0.074	0.079	0.065	0.063	0.056	0.064
7/4/2018	13	0.074	0.070	0.063	0.061	0.058	0.059
7/4/2018	14	0.071	0.065	0.060	0.059	0.056	0.054
7/4/2018	15	0.067	0.056	0.057	0.057	0.055	0.053
7/4/2018	16	0.069	0.052	0.053	0.053	0.054	0.043

Date	Hour	El Dorado	Placer	Sacramento	Solano	Sutter	Yolo
7/4/2018	17	0.065	0.044	0.047	0.051	0.051	0.044
7/4/2018	18	0.056	0.042	0.042	0.051	0.045	0.039
7/4/2018	19	0.045	0.037	0.039	0.049	0.041	0.039
7/4/2018	20	0.040	0.029	0.036	0.043	0.037	0.033
7/4/2018	21	0.033	0.023	0.032	0.037	0.033	0.030
7/4/2018	22	0.023	0.028	0.041	0.032	0.031	0.036
7/4/2018	23	0.015	0.022	0.030	0.025	0.029	0.027
7/5/2018	0	0.007	0.014	0.015	0.011	0.029	0.016
7/5/2018	1	0.003	0.009	0.011	0.008	0.027	0.012
7/5/2018	2	0.002	0.008	0.011	0.009	0.027	0.012
7/5/2018	3	0.001	0.011	0.013	0.013	0.029	0.018
7/5/2018	4	0.002	0.017	0.021	0.024	0.031	0.028
7/5/2018	5	0.007	0.028	0.035	0.038	0.037	0.040
7/5/2018	6	0.038	0.042	0.051	0.049	0.044	0.052
7/5/2018	7	0.055	0.054	0.058	0.057	0.050	0.052
7/5/2018	8	0.060	0.049	0.057	0.060	0.051	0.058
7/5/2018	9	0.064	0.063	0.059	0.064	0.050	0.060
7/5/2018	10	0.065	0.072	0.063	0.066	0.051	0.058
7/5/2018	11	0.068	0.069	0.063	0.067	0.052	0.059
7/5/2018	12	0.070	0.070	0.065	0.066	0.053	0.061
7/5/2018	13	0.069	0.068	0.063	0.063	0.053	0.064
7/5/2018	14	0.069	0.065	0.062	0.060	0.053	0.057
7/5/2018	15	0.069	0.059	0.059	0.058	0.053	0.062
7/5/2018	16	0.068	0.055	0.055	0.053	0.052	0.060
7/5/2018	17	0.064	0.048	0.050	0.051	0.050	0.057
7/5/2018	18	0.054	0.045	0.045	0.045	0.044	0.041
7/5/2018	19	0.047	0.044	0.038	0.037	0.038	0.036
7/5/2018	20	0.041	0.036	0.033	0.032	0.034	0.030
7/5/2018	21	0.035	0.028	0.029	0.027	0.031	0.026
7/5/2018	22	0.027	0.024	0.025	0.024	0.029	0.023
7/5/2018	23	0.016	0.019	0.020	0.018	0.028	0.019
7/6/2018	0	0.010	0.016	0.016	0.014	0.032	0.016
7/6/2018	1	0.004	0.012	0.014	0.012	0.030	0.013
7/6/2018	2	0.003	0.012	0.013	0.011	0.030	0.015
7/6/2018	3	0.002	0.014	0.016	0.015	0.030	0.020
7/6/2018	4	0.003	0.017	0.023	0.027	0.033	0.030
7/6/2018	5	0.008	0.028	0.034	0.039	0.038	0.038
7/6/2018	6	0.038	0.040	0.050	0.048	0.045	0.049
7/6/2018	7	0.054	0.046	0.056	0.056	0.050	0.053

Date	Hour	El Dorado	Placer	Sacramento	Solano	Sutter	Yolo
7/6/2018	8	0.059	0.056	0.054	0.062	0.052	0.056
7/6/2018	9	0.062	0.062	0.057	0.064	0.052	0.057
7/6/2018	10	0.065	0.068	0.059	0.067	0.054	0.059
7/6/2018	11	0.067	0.072	0.063	0.065	0.055	0.064
7/6/2018	12	0.070	0.070	0.061	0.068	0.055	0.063
7/6/2018	13	0.068	0.067	0.065	0.064	0.054	0.059
7/6/2018	14	0.067	0.064	0.063	0.056	0.054	0.060
7/6/2018	15	0.068	0.057	0.059	0.053	0.052	0.055
7/6/2018	16	0.065	0.052	0.055	0.053	0.050	0.057
7/6/2018	17	0.059	0.057	0.052	0.049	0.047	0.056
7/6/2018	18	0.051	0.047	0.044	0.044	0.042	0.044
7/6/2018	19	0.044	0.039	0.038	0.036	0.035	0.037
7/6/2018	20	0.038	0.031	0.033	0.030	0.030	0.032
7/6/2018	21	0.035	0.027	0.028	0.027	0.028	0.026
7/6/2018	22	0.031	0.025	0.026	0.023	0.026	0.023
7/6/2018	23	0.029	0.021	0.021	0.018	0.024	0.020
7/7/2018	0	0.032	0.022	0.024	0.019	0.038	0.028
7/7/2018	1	0.020	0.017	0.019	0.015	0.034	0.018
7/7/2018	2	0.010	0.012	0.016	0.014	0.032	0.018
7/7/2018	3	0.007	0.012	0.016	0.013	0.031	0.019
7/7/2018	4	0.006	0.016	0.020	0.017	0.032	0.024
7/7/2018	5	0.013	0.024	0.027	0.024	0.034	0.031
7/7/2018	6	0.039	0.041	0.037	0.031	0.039	0.038
7/7/2018	7	0.046	0.050	0.043	0.040	0.046	0.047
7/7/2018	8	0.052	0.057	0.049	0.048	0.052	0.049
7/7/2018	9	0.061	0.065	0.058	0.054	0.056	0.055
7/7/2018	10	0.067	0.067	0.063	0.060	0.060	0.055
7/7/2018	11	0.070	0.074	0.063	0.065	0.061	0.058
7/7/2018	12	0.071	0.074	0.064	0.064	0.060	0.061
7/7/2018	13	0.067	0.074	0.062	0.060	0.057	0.065
7/7/2018	14	0.065	0.068	0.062	0.062	0.055	0.060
7/7/2018	15	0.062	0.058	0.060	0.058	0.051	0.056
7/7/2018	16	0.060	0.053	0.054	0.058	0.048	0.056
7/7/2018	17	0.054	0.047	0.050	0.055	0.044	0.051
7/7/2018	18	0.046	0.041	0.047	0.056	0.038	0.044
7/7/2018	19	0.038	0.034	0.041	0.049	0.033	0.041
7/7/2018	20	0.034	0.027	0.035	0.040	0.028	0.038
7/7/2018	21	0.029	0.027	0.035	0.038	0.025	0.032
7/7/2018	22	0.027	0.023	0.031	0.034	0.023	0.032

Date	Hour	El Dorado	Placer	Sacramento	Solano	Sutter	Yolo
7/7/2018	23	0.025	0.016	0.024	0.024	0.021	0.023

Sub-Appendix B.C: Additional Temporal Profiles

OGV temporal profiles were constructed based on 2016 port activities of all vessels, compiled by an in-house section in CARB. Fractions for the ports of Long Beach, Los Angeles, Oakland, and San Diego were updated using aggregated AIS data from 2015 through 2019. All vessel types were grouped by port area boundary and divided into day of week and monthly activity fractions (Table B-32 and Table B-33). Some profiles are either area- or inline specific, others will be used by both area and inline sources. Activity data was not available for all ports; a flat (emissions are spread evenly across the time period) monthly and daily profile was used for those ports. A flat profile was also used to represent the hourly variation for all OGV vessels at every port area/waters. The temporal profiles do not apply to OGV military, which assumes a flat at monthly, days of week, and hours of day intervals (see the profile labeled Elsewhere in the tables below). The areas labeled with a "+" received area source profile updates and "*" received inline only updates.

Hourly temporal profiles were updated for consumer products Table B-34 and Table B-35. The new profiles were developed by the Consumer Products and Air Quality Assessment Branch based on research on identifying volatile chemical product tracer compounds in U.S. cities (Gkatzelis, Coggon and McDonald).

Table B-32: OGV monthly profiles

Port areas/waters	Profile ID	Jan	Feb	Mar	Apr	May	Jun	Jul	Aug	Sep	Oct	Nov	Dec
Eureka	M_EKA	0.000	0.000	0.000	0.000	0.167	0.167	0.167	0.000	0.167	0.167	0.167	0.000
Hueneme	M_NTD	0.065	0.088	0.090	0.093	0.095	0.083	0.083	0.075	0.078	0.080	0.088	0.085
Carquinez	M_CAR	0.068	0.076	0.080	0.076	0.087	0.093	0.090	0.085	0.085	0.090	0.075	0.095
Oakland	M_OAK	0.084	0.088	0.081	0.078	0.081	0.084	0.084	0.090	0.081	0.090	0.080	0.079
Redwood City	M_RWC	0.055	0.018	0.091	0.091	0.127	0.073	0.055	0.127	0.091	0.091	0.036	0.145
Richmond	M_RCH	0.083	0.092	0.086	0.081	0.086	0.095	0.083	0.097	0.075	0.062	0.084	0.076
Sacramento	M_SAC	0.018	0.036	0.018	0.054	0.054	0.089	0.036	0.036	0.054	0.071	0.482	0.054
San Diego	M_SGQ	0.081	0.078	0.077	0.086	0.088	0.093	0.085	0.075	0.088	0.086	0.082	0.082
San Francisco	M_SFO	0.070	0.071	0.074	0.080	0.095	0.093	0.071	0.087	0.080	0.087	0.091	0.100
Stockton	M_SCK	0.083	0.088	0.083	0.074	0.111	0.101	0.060	0.101	0.055	0.083	0.092	0.069
Elsewhere	1	0.083	0.083	0.083	0.083	0.083	0.083	0.083	0.083	0.083	0.083	0.083	0.083
Waters of LA County+	M_6059	0.093	0.071	0.084	0.088	0.084	0.075	0.080	0.091	0.074	0.087	0.081	0.092
El Segundo*	M_ELS	0.104	0.055	0.084	0.093	0.086	0.066	0.075	0.104	0.066	0.090	0.075	0.104
Port of Los Angeles*	M_LAX	0.087	0.088	0.087	0.087	0.084	0.083	0.081	0.082	0.081	0.079	0.081	0.081

Port areas/waters	Profile ID	Jan	Feb	Mar	Apr	May	Jun	Jul	Aug	Sep	Oct	Nov	Dec
Port of Long Beach*	M_LGB	0.084	0.086	0.082	0.083	0.081	0.087	0.084	0.082	0.086	0.084	0.081	0.080

Table B-33: OGV Weekly Profiles

Port Areas/Waters	Profile ID	Mon	Tue	Wed	Thu	Fri	Sat	Sun
Eureka	W_EKA	0.500	0.000	0.333	0.000	0.000	0.000	0.167
Hueneme	W_NTD	0.113	0.145	0.205	0.160	0.108	0.115	0.155
Carquinez	W_CAR	0.178	0.131	0.146	0.163	0.136	0.126	0.121
Oakland	W_OAK	0.150	0.151	0.161	0.151	0.135	0.121	0.130
Redwood City	W_RWC	0.109	0.127	0.200	0.091	0.218	0.109	0.145
Richmond	W_RCH	0.167	0.153	0.142	0.126	0.161	0.129	0.122
Sacramento	W_SAC	0.179	0.250	0.089	0.143	0.161	0.071	0.107
San Diego	W_SGQ	0.150	0.162	0.169	0.142	0.129	0.117	0.131
San Francisco	W_SFO	0.155	0.138	0.153	0.137	0.127	0.143	0.146
Stockton	W_SCK	0.152	0.147	0.106	0.157	0.161	0.106	0.171
Elsewhere	7	0.143	0.143	0.143	0.143	0.143	0.143	0.143
Waters of LA County+	W_6059	0.143	0.132	0.152	0.150	0.139	0.148	0.135
El Segundo*	W_ELS	0.137	0.137	0.154	0.148	0.137	0.145	0.143
Port of Los Angeles*	W_LAX	0.142	0.145	0.153	0.155	0.150	0.135	0.121
Port of Long Beach*	W_LGB	0.138	0.140	0.148	0.147	0.152	0.144	0.132

Table B-34: Consumer products diurnal profile assignment codes and descriptions

Tracer Diurnal Profile Assignment	CEIDARS HPDY	HPDYN
PCBTF	86	INCREASING ACTIVITY FROM 9AM TO 2PM AND DECREASING UNTIL 10PM. PCBTF TRACER (CP)
D-4 Siloxane	87	MINOR PEAK AT 5 AM, PEAK ACTIVITY AT 2PM AND 6PM. D4-SILOXANE TRACER (CP)
Monoterpenes	88	ACTIVITY STARTS AT 6AM, 12PM PEAK, OSCILLATES TO 8PM. MONOTERPENE TRACER (CP)
PDCB	89	PEAK ACTIVITY FROM 6PM TO 9PM. MINOR PEAKS AT 5AM AND 12PM.
D-5 Siloxane	90	PRIMARY PEAK ACTIVITY AT 12PM AND SECONDARY AT 8PM. D5-SILOXANE TRACER (CP)

Table B-35: Consumer products hourly temporal profiles

HOUR	PCBTF TRACER (CP)"	D4-SILOXANE TRACER (CP)"	MONOTERPENE TRACER (CP)"	PDCB Tracer (CP)	D5-SILOXANE TRACER (CP)"
0	0.009	0.015	0.015	0.019	0.016
1	0.011	0.017	0.015	0.022	0.018
2	0.012	0.018	0.014	0.023	0.016

HOUR	PCBTF TRACER (CP)"	D4-SILOXANE TRACER (CP)"	MONOTERPENE TRACER (CP)"	PDCB Tracer (CP)	D5-SILOXANE TRACER (CP)"
3	0.012	0.020	0.012	0.026	0.015
4	0.017	0.032	0.013	0.041	0.022
5	0.020	0.038	0.013	0.046	0.027
6	0.017	0.031	0.016	0.036	0.025
7	0.014	0.024	0.025	0.028	0.026
8	0.016	0.026	0.042	0.027	0.034
9	0.026	0.037	0.061	0.033	0.058
10	0.048	0.048	0.074	0.040	0.081
11	0.072	0.055	0.083	0.041	0.088
12	0.097	0.063	0.074	0.038	0.077
13	0.121	0.075	0.069	0.030	0.055
14	0.108	0.070	0.062	0.022	0.039
15	0.079	0.053	0.063	0.024	0.039
16	0.074	0.047	0.064	0.042	0.047
17	0.076	0.073	0.054	0.080	0.050
18	0.061	0.085	0.061	0.097	0.057
19	0.043	0.068	0.063	0.102	0.068
20	0.031	0.049	0.051	0.088	0.063
21	0.016	0.026	0.025	0.049	0.042
22	0.011	0.017	0.014	0.027	0.021
23	0.009	0.015	0.015	0.019	0.016

Sub-Appendix B.D: Spatial Surrogate Assignments

The primary spatial surrogate for each EICSUM and the corresponding data source are listed in Table B-36 below.

Table B-36: Primary surrogate assignment at the EICSUM level, description, and data source

EICSUM	EICSUM Name	Primary Surrogate ID	Primary Surrogate Name	Data Source of Primary Surrogate
10	Electric Utilities	302	UCD Industrial	Longitudinal Employer-Household Dynamics (LEHD)
20	Cogeneration	302	UCD Industrial	Longitudinal Employer-Household Dynamics (LEHD)
30	Oil and Gas Production (Combustion)	211	Gas Well	California Department of Conservation, Division of Oil, Gas and Geothermal Resources

EICSUM	EICSUM Name	Primary Surrogate ID	Primary Surrogate Name	Data Source of Primary Surrogate
30	Oil and Gas Production (Combustion)	431	Oil well	Division of Oil, Gas, And Geothermal Resources
50	Manufacturing and Industrial	302	UCD Industrial	Longitudinal Employer-Household Dynamics (LEHD)
52	Food and Agricultural Processing	720	Farm Road Vehicle Miles Traveled	Department of Pesticide Regulation
60	Service and Commercial	621	UCD Service, Commercial, Employment	Metropolitan Planning Organization (MPO)/Council of Government (COG) Data /California Statewide Travel Demand Model (CSTDM) Data
99	Other (Fuel Combustion)	302	UCD Industrial	Longitudinal Employer-Household Dynamics (LEHD)
110	Sewage Treatment	470	Publicly Owned Treatment Works	State Water Resources Control Board
120	Landfills	341	Landfills	Calrecyle - Solid Waste Information System (Swis) Dataset
130	Incinerators	302	UCD Industrial	Longitudinal Employer-Household Dynamics (LEHD)
140	Soil Remediation	302	UCD Industrial	Longitudinal Employer-Household Dynamics (LEHD)
199	Other (Waste Disposal)	343	Compost	Calrecyle - Solid Waste Information System (SWIS) Dataset
199	Other (Waste Disposal)	390	Nonirrigated Pastureland	National Land Cover Database (NLCD)
199	Other (Waste Disposal)	470	Publicly Owned Treatment Works	State Water Resources Control Board
210	Laundering	150	Drycleaners	Dun & Bradstreet's Market Insight Database
220	Degreasing	120	Autobody Shops	Dun & Bradstreet's Market Insight Database
220	Degreasing	302	UCD Industrial	Longitudinal Employer-Household Dynamics (LEHD)
230	Coatings and Related Process Solvents	120	Autobody Shops	Dun & Bradstreet's Market Insight Database
230	Coatings and Related Process Solvents	743	Wood Furniture	Dun & Bradstreet's Market Insight Database
230	Coatings and Related Process Solvents	302	UCD Industrial	Longitudinal Employer-Household Dynamics (LEHD)

EICSUM	EICSUM Name	Primary Surrogate ID	Primary Surrogate Name	Data Source of Primary Surrogate
240	Printing	731	Print	Dun & Bradstreet's Market Insight Database
250	Adhesives and Sealants	302	UCD Industrial	Longitudinal Employer-Household Dynamics (LEHD)
299	Other (Cleaning and Surface Coatings)	302	UCD Industrial	Longitudinal Employer-Household Dynamics (LEHD)
310	Oil and Gas Production	211	Gas well	California Department of Conservation, Division of Oil, Gas and Geothermal Resources
310	Oil and Gas Production	431	Oilwell	California Department of Conservation, Division of Oil, Gas and Geothermal Resources
330	Petroleum Marketing	460	Ports	(US DOT)/Bureau of Transportation Statistics' (BTS's) National Transportation Atlas Database (NTAD)
330	Petroleum Marketing	200	Gas Stations	Dun & Bradstreet's Market Insight Database
330	Petroleum Marketing	520	Refineries and Tank Farms	FEMA and the ARB CEIDAR Database
330	Petroleum Marketing	214	Gas Distribution	U.S. Energy Information Administration
399	Other (Petroleum Production and Marketing)	200	Gas Stations	Dun & Bradstreet's Market Insight Database
410	Chemical	741	Plastic	Dun & Bradstreet's Market Insight Database
420	Food and Agriculture	680	Wineries	Dun & Bradstreet's Market Insight Database
420	Food and Agriculture	320	Irrigated Cropland	National Land Cover Database (NLCD)
430	Mineral Processes	590	Sand and Gravel Mines	National Atlas
440	Metal Processes	738	Metal Parts	Dun & Bradstreet's Market Insight Database
450	Wood And Paper	732	Wood	Dun & Bradstreet's Market Insight Database
499	Other (Industrial Processes)	302	UCD Industrial	Longitudinal Employer-Household Dynamics (LEHD)
500	Solvent Evaporation Unspecified	441	UCD Population	Metropolitan Planning Organization (MPO)/Council of Government (COG) Data /California Statewide Travel Demand Model (CSTDM) Data

EICSUM	EICSUM Name	Primary Surrogate ID	Primary Surrogate Name	Data Source of Primary Surrogate
510	Consumer Products	550	Residential and Nonresidential Change Industrial Employment	Council of Government (Cog) Housing and Employment
510	Consumer Products	252	UCD Total Housing	Metropolitan Planning Organization (MPO)/Council of Government (COG) Data /California Statewide Travel Demand Model (CSTDM) Data
510	Consumer Products	280	Housing and Restaurants	Combo: Metropolitan Planning Organization (MPO)/Council of Government (COG) Data /California Statewide Travel Demand Model (CSTDM) Data and Dun & Bradstreet Market Insight
510	Consumer Products	260	Housing and Autobody	Combo: Metropolitan Planning Organization (MPO)/Council of Government (COG) Data /California Statewide Travel Demand Model (CSTDM) Data and Dun & Bradstreet Market Insight
510	Consumer Products	120	Autobody Shops	Dun & Bradstreet's Market Insight Database
510	Consumer Products	739	Other Coatings	Dun & Bradstreet's Market Insight Database
510	Consumer Products	270	Housing and Commercial Employment	Metropolitan Planning Organization (MPO)/Council of Government (COG) Data /California Statewide Travel Demand Model (CSTDM) Data
510	Consumer Products	651	UCD Single Family Housing	Metropolitan Planning Organization (MPO)/Council of Government (COG) Data /California Statewide Travel Demand Model (CSTDM) Data
510	Consumer Products	450	Population, Commercial Employment and Hospitals	Metropolitan Planning Organization (MPO)/Council of Government (COG) Data /California Statewide Travel Demand Model (CSTDM) Data and ESRI
510	Consumer Products	672	Developed Land High Density	National Land Cover Database (NLCD)
520	Architectural Coatings and Related Process Solvents	230	HE Square Feet	Council of Government (COG) Housing and Employment

EICSUM	EICSUM Name	Primary Surrogate ID	Primary Surrogate Name	Data Source of Primary Surrogate
520	Architectural Coatings and Related Process Solvents	270	Housing and Commercial Employment	Metropolitan Planning Organization (MPO)/Council of Government (COG) Data /California Statewide Travel Demand Model (CSTDM) Data
520	Architectural Coatings and Related Process Solvents	110	All Paved Roads	Tiger Geodatabases from U.S. Census Bureau
530	Pesticides/Fertilizers	230	HE Square Feet	Council of Government (COG) Housing and Employment
530	Pesticides/Fertilizers	512	Pesticides No Methyl Bromide	Department of Pesticide Regulation
530	Pesticides/Fertilizers	514	Pesticides Methyl Bromide	Department of Pesticide Regulation
530	Pesticides/Fertilizers	732	Wood	Dun & Bradstreet's Market Insight Database
540	Asphalt Paving / Roofing	588	UCD On-road Construction	Caltrans Highway Construction Projects Dataset (Line)
610	Residential Fuel Combustion	573	Fireplaces	Digital Map Products 2017 Parcel Data
610	Residential Fuel Combustion	572	Residential Liquid Petroleum Gas Heating	US Census American Community Survey (ACS)
620	Farming Operations	356	Horse Ranches	CARB Green House Gas Inventory Group
620	Farming Operations	320	Irrigated Cropland	National Land Cover Database (NLCD)
620	Farming Operations	690	Land Prep	Department of Pesticide Regulation
630	Construction and Demolition	588	UCD On-road Construction	Caltrans Highway Construction Projects Dataset (Line)
630	Construction and Demolition	587	UCD Offroad Construction	Storm Notice of Intent (NOI) Dataset
640	Paved Road Dust	590	Sand and Gravel Mines	National Atlas
640	Paved Road Dust	610	Secondary Paved Roads	Tiger Geodatabases from U.S. Census Bureau
645	Unpaved Road Dust	384	Military Tactical	Federal Aviation Administration / National Transportation Atlas Database (NTAD) And ESRI
645	Unpaved Road Dust	190	Forestland	National Land Cover Database (NLCD)

EICSUM	EICSUM Name	Primary Surrogate ID	Primary Surrogate Name	Data Source of Primary Surrogate
645	Unpaved Road Dust	720	Farm Road Vehicle Miles Traveled	Department of Pesticide Regulation
645	Unpaved Road Dust	660	Unpaved Roads	Tiger Geodatabases from U.S. Census Bureau
650	Fugitive Windblown Dust	391	Pasture	National Land Cover Database (NLCD)
650	Fugitive Windblown Dust	660	Unpaved Roads	Tiger Geodatabases from U.S. Census Bureau
650	Fugitive Windblown Dust	160	Dry Lake Beds	U.S. Geological Survey (USGS)
660	Fires	441	UCD Population	Metropolitan Planning Organization (MPO)/Council of Government (COG) Data /California Statewide Travel Demand Model (CSTDM) Data
660	Fires	480	Primary Roads	Tiger Geodatabases from U.S. Census Bureau
670	Managed Burning and Disposal	674	Developed Land Low Density	National Land Cover Database (NLCD)
670	Managed Burning and Disposal	190	Forestland	National Land Cover Database (NLCD)
670	Managed Burning and Disposal	720	Farm Road Vehicle Miles Traveled	Department of Pesticide Regulation
680	Utility Equipment	651	UCD Single Family Housing	Metropolitan Planning Organization (MPO)/Council of Government (COG) Data /California Statewide Travel Demand Model (CSTDM) Data
690	Cooking	561	Charbroiling	SJV APCD & Dun and Bradstreet Insight Market
699	Other (Miscellaneous Processes)	441	UCD Population	Metropolitan Planning Organization (MPO)/Council of Government (COG) Data /California Statewide Travel Demand Model (CSTDM) Data
810	Aircraft	382	Military Aircraft	Federal Aviation Administration / National Transportation Atlas Database (NTAD) And ESRI
810	Aircraft	100	Airports	Federal Aviation Administration and ESRI
810	Aircraft	140	Commercial Airports	Federal Aviation Administration, National Transportation Atlas Database (NTAD)
810	Aircraft	320	Irrigated Cropland	National Land Cover Database (NLCD)

EICSUM	EICSUM Name	Primary Surrogate ID	Primary Surrogate Name	Data Source of Primary Surrogate
820	Trains	491	Linehaul	ARB In-House Rail Modeling
820	Trains	360	Metrolink Lines	Federal Railroad Administration / National Transportation Atlas Database (NTAD)
820	Trains	490	Rail Lines	Federal Railroad Administration / National Transportation Atlas Database (NTAD)
820	Trains	361	Passenger Rail	Offroad Diesel Analysis Section, AQPSD
820	Trains	501	Switcher Railyards	Off-Road Diesel Analysis Section, AQPSD: Union Pacific Railroad (Up) And Burlington Northern Santa Fe Railway (BNSF)
830	Ships and Commercial Boats	460	Ports	(US DOT)/Bureau of Transportation Statistics' (BTS's) National Transportation Atlas Database (NTAD)
830	Ships and Commercial Boats	431	Oilwell	Division of Oil, Gas, And Geothermal Resources
830	Ships and Commercial Boats	640	Ship Lanes	Marine Cadastre Automatic Identification System
833	Ocean Going Vessels	460	Ports	(US DOT)/Bureau of Transportation Statistics' (BTS's) National Transportation Atlas Database (NTAD)
833	Ocean Going Vessels	383	Military Ships	Marine Cadastre - Military Vessel
833	Ocean Going Vessels	640	Ship Lanes	Marine Cadastre Automatic Identification System
833	Ocean Going Vessels	642	Tanker	Marine Cadastre Automatic Identification System
833	Ocean Going Vessels	643	Passenger	Marine Cadastre Automatic Identification System
835	Commercial Harbor Craft	460	Ports	(US DOT)/Bureau of Transportation Statistics' (BTS's) National Transportation Atlas Database (NTAD)
835	Commercial Harbor Craft	332	Ferries	Ferry Company Websites and Google Maps
835	Commercial Harbor Craft	383	Military Ships	Marine Cadastre - Military Vessel
835	Commercial Harbor Craft	641	Crew Supply	Marine Cadastre Automatic Identification System

EICSUM	EICSUM Name	Primary Surrogate ID	Primary Surrogate Name	Data Source of Primary Surrogate
835	Commercial Harbor Craft	339	Dredge	Marine Cadastre Coastal Maintained Channels
840	Recreational Boats	338	Ocean Recreation Boats	Marine Cadastre Automatic Identification System - Pleasure Craft
840	Recreational Boats	651	UCD Single Family Housing	Metropolitan Planning Organization (MPO)/Council of Government (COG) Data /California Statewide Travel Demand Model (CSTDM) Data
840	Recreational Boats	336	Ocean, Lakes and Recreation Boats	U.S. Geological Survey (USGS)
840	Recreational Boats	335	Lakes, Rivers, Recreation Boats	U.S. Geological Survey (USGS)
850	Off-Road Recreational Vehicles	220	Golf Courses	ESRI
850	Off-Road Recreational Vehicles	651	UCD Single Family Housing	Metropolitan Planning Organization (MPO)/Council of Government (COG) Data /California Statewide Travel Demand Model (CSTDM) Data
850	Off-Road Recreational Vehicles	660	Unpaved Roads	Tiger Geodatabases from U.S. Census Bureau
850	Off-Road Recreational Vehicles	170	Elevation over 1500 m	U.S. Geological Survey (USGS)
860	Off-Road Equipment	580	Residential Nonresidential Change	Council of Government (COG) Housing and Employment
860	Off-Road Equipment	630	Service and Commercial Employment, Schools, Golf Courses and Cemeteries	Council of Government (COG) Service and Commercial Employment & Esri
860	Off-Road Equipment	460	Ports	(US DOT)/Bureau of Transportation Statistics' (BTS's) National Transportation Atlas Database (NTAD)
860	Off-Road Equipment	431	Oilwell	Division of Oil, Gas, And Geothermal Resources
860	Off-Road Equipment	384	Military Tactical	Federal Aviation Administration / National Transportation Atlas Database (NTAD) and ESRI

EICSUM	EICSUM Name	Primary Surrogate ID	Primary Surrogate Name	Data Source of Primary Surrogate
860	Off-Road Equipment	100	Airports	Federal Aviation Administration and Esri
860	Off-Road Equipment	500	Railyards	Federal Railroad Administration / National Transportation Atlas Database (NTAD)
860	Off-Road Equipment	485	TRU	Integrated Transportation Network and Caltrans Truck Network And Digital Map Products 2017 Parcel Data
860	Off-Road Equipment	302	UCD Industrial	Longitudinal Employer-Household Dynamics (LEHD)
860	Off-Road Equipment	339	Dredge	Marine Cadastre Coastal Maintained Channels
860	Off-Road Equipment	651	UCD Single Family Housing	Metropolitan Planning Organization (MPO)/Council of Government (COG) Data /California Statewide Travel Demand Model (CSTDM) Data
860	Off-Road Equipment	190	Forestland	National Land Cover Database (NLCD)
860	Off-Road Equipment	191	Forestland Roads	NLCD in conjunction with TIGER road network
860	Off-Road Equipment	587	UCD Offroad Construction	Storm Notice of Intent (NOI) Dataset
870	Farm Equipment	720	Farm Road Vehicle Miles Traveled	Department of Pesticide Regulation
890	Fuel Storage And Handling	651	UCD Single Family Housing	Metropolitan Planning Organization (MPO)/Council of Government (COG) Data /California Statewide Travel Demand Model (CSTDM) Data
890	Fuel Storage and Handling	335	Lakes, Rivers, Recreation boats	U.S. Geological Survey (USGS)
910	Biogenic Sources	672	Developed Land High Density	National Land Cover Database (NLCD)
910	Biogenic Sources	190	Forestland	National Land Cover Database (NLCD)
920	Geogenic Sources	190	Forestland	National Land Cover Database (NLCD)
920	Geogenic Sources	212	Gas Seep	U.S. Geological Survey (USGS)
920	Geogenic Sources	432	Oil Seep	U.S. Geological Survey (USGS) – Pacific Coastal & Marine Science
930	Wildfires	190	Forestland	National Land Cover Database (NLCD)

EICSUM	EICSUM Name	Primary Surrogate ID	Primary Surrogate Name	Data Source of Primary Surrogate
930	Wildfires	391	Pasture	Sierra Research Agtool Contract
940	Windblown Dust	412	Fugitive Dust	National Land Cover Database (NLCD)